Doctoral Dissertation

Tectonic Evolution of South Sulawesi, Indonesia:

Reconstructed by Analysis of Deformation Structures

Asri Jaya

9510201

Department of Engineering and Resource Science
Graduate School of Engineering and Resource Science
Akita University

2014

平成 25 年度博士論文
［博士（資源学)］

Tectonic Evolution of South Sulawesi, Indonesia: Reconstructed by Analysis of Deformation Structures
インドネシア南スラウェシの構造発達: 変形構造解析による復元

2014

アスリ　ジャヤ
Asri Jaya
博士工 9510201

秋田大学大学院
工学資源学研究科博士後期課程
資源学専攻

Tectonic Evolution of South Sulawesi, Indonesia:

Reconstructed by Analysis of Deformation Structures

A dissertation submitted in partial fulfillment of the requirements of the Department of Engineering and Resource Science, Graduate School of Engineering and Resource Science, Akita University for the degree of

Doctoral of Engineering

By

ASRI JAYA

February 2014

DECLARATION

I, thereby, declare that except for references to other people's work which have been duly cited, this work is result of study conducted by myself in the area, and this dissertation has neither nor in part been submitted for a degree either in this University or elsewhere.

……………………..

Asri Jaya

DEDICATION

I dedicate this thesis to my parent, Mr. Abdul Samad Mappe and Mrs. Millo who have supported me since childhood and still do. “My father rest in peace in heaven, right sorry I did not get to meet you while you want to leave to go on forever”.

ABSTRACT

Tectonic Evolution of South Sulawesi, Indonesia: Reconstructed by Analysis of Deformation Structures

By Asri Jaya

On the basis of metamorphic and structural analyses, the Biru Metamorphic Complex exposed in southern part of the West Divide Mountain Range was assessed as a main part of the basement of South Sulawesi with the Bantimala Metamorphic Complex and Barru Metamorphic Block. The metamorphic complex is composed of metamorphic rocks of epidote-amphibolite and amphibolites facies. Major and trace elements characterize the plotolith of the Biru metamorphic rocks as mid-oceanic ridge basalts (MORB), calc-alkali basalts and island-arc tholeiites (IAT). The Early Cretaceous K-Ar age (109 ± 2.4 Ma) indicated that the metamorphism of the Biru Complex was coeval with those in Bantimala Complex and Barru Block. The common general trends of structural elements such as NE-SW striking and south dipping schistosities also indicates similar tectonic environment with Barru Blocks, although diverse of lithologic association are quite different, particularly in Bantimala Complex. The schistosity (S0) defined by preferred orientation of mineral inclusions in the core of garnet, epidote and plagioclase porphyroblasts and main schistosity (S1) parallel to isoclinals fold axial plane (F1, F2) were formed during the plastic deformation (D1) simultaneous with a regional metamorphism (M1). The evidence of D1 deformation is commonly very limited in the quartz texture, it is seemingly caused by a contact metamorphism in association with the emplacement of the Biru granodiorite rocks (M2) in Middle Miocene, although array of elongated subgrains and seriated boundaries still be preserved as a relic of D1. *C*-axis LPO pattern of quartz suggests the non-coaxial flow under the dominant operation of basal<a> slip system. In some areas, metamorphic rocks show an overprint of cataclastic texture (D2). Annealing of plastic deformation structures and superimposed cataclastic deformation were probably resulted from the

Middle Miocene uplifting of the West Divide Mountain Range associated with formation of Walanae Fault System.

The Walanae Fault Zone is a major tectonic structure and its activity is thought to have played a major role in Neogene and Quaternary structural development in the South Sulawesi. In order to clarify stress states associated with the activity of East Walanae Fault and their contribution to the tectonics in South Sulawesi during Neogene and Quaternary, paleostress states around Walanae Fault System were determined using the multiple-inverse method from fault slip and calcite twin data collected from Oligocene-Pliocene volcano-sedimentary rocks. Fault slip data of the Biru area adjacent to the West Walanae fault Zone shows σ_1-axis ranging from NNW-SSE to NNE-SSW and σ_3-axis nearly vertical. Along the East Walanae Fault zone, both fault slip and calcite twin data yield consistent stress states over the studied area and reliable stress tensors (maximum and minimum principal stresses: σ_1 and σ_3, and stress ratio:Φ) as well as fault-slip data, a predominance of NE-SW-to-E-W trending σ_1 and vertical to moderately-south-plunging σ_3 with generally low Φ. These stress states could activate the EWF as a reverse fault with a dextral shear component and account for constructional deformation structures and landform around the trace of the fault. Most of the calcite twins and mesoscale faults were activated during the latest stage of folding or later. Based on the morphology and width of twin lamellae in the carbonate rocks, twinning of calcite in the deformation zone along the EWF may have occurred under the temperature around 200^{o}C. Inferred paleostress states around the EWF were most likely generated under the tectonic conditions influenced by the collision of Sulawesi with the Australian fragments since the Late Miocene. The Late Quaternary radiocarbon ages (3050 cal BP and 3990 cal BP) of sheared soils collected from the outcrop near the EWF trace indicated that the deformation associated with the activity of the EWF is still continued. Present crustal deformation under the E-W to NE-SW compression stress states is also inferred from the N-S trending geomorphological sequence, among which further morphostructural differentiation is proceeded.

Keywords: Biru metamorphic rocks, Deformation, K-Ar dating, Paleostress, Multiple inverse, Fault slip, Calcite twin, Radiocarbon dating, Walanae fault, South Sulawesi, Indonesia.

CONTENTS

LIST OF FIGURES

LIST OF TABLES

CHAPTER 1. INTRODUCTION

1.1 Background of Research

Sulawesi Island: one of main island of Indonesia separated by the strait of Makassar from Borneo island and has a distinct shape, mainly consisted by four arms: the north Minahasa Peninsula; the East Peninsula; the South Peninsula; and the South-east Peninsula. It has been in very complicated tectonic condition since Cretaceous age, and therefore their tectonic evolution has not been established.

In the south arm Sulawesi: a relatively developed area with a large population in the Sulawesi Island, particularly in Makassar area, abundant geological survey and research have been performed and outline of tectonic history has been proposed.

The pre-Tertiary basement of the South Sulawesi is limitedly exposed in the core of the Western mountain range of the South Sulawesi. Numbers of study on the basement rocks in South Sulawesi have been done in two main locations, Bantimala and Barru area. The metamorphic rocks assemblages from these two area show that both metamorphic blocks were accreted slices in origin from a wide range of tectonic environments (Wakita et al., 1994, 1996; Miyazaki et al., 1996; Parkinson et al., 1998; Maulana et al., 2010) and suffered high to intermediate pressure type metamorphisms in the subduction zone probably developed at the south eastern margin of Sundaland. A small exposure of metamorphic rocks (Biru metamorphic rocks) occurs in the Biru area, southeast of the Bantimala and Barru complex in the Western mountain range. The Biru metamorphic rock has been described as contact metamorphic rocks associated with the Cretaceous or Jurassic and Miocene plutonium (Leeuwen, 1981; Sukamto and Supriatna, 1982), although both of adequate petrographic investigations on them have not been yet performed. Analysis of deformation microstructure and dating of metamorphic rocks would provide new convincing information for understanding the characteristics and belonging of this basement rock.

The Neogene tectonic history of Sulawesi is represented by arc continent-continent collision that occurred between the Australian Craton-derived block (Eastern arc) and Sundaland (Western arc) (Hamilton, 1979; Bergman et al., 1996; Hall and Wilson, 2000), resulting in the development of large-scale strike–slip faults, a fold and thrust-belt, and magmatism related to extensive lithospheric melting (Coffield et al., 1993; Bergman et al., 1996). There are a number of N−S to NW−SE trending large faults in Sulawesi Island, such as Palu-Koro fault in west-central Sulawesi and Matano fault in the east arm (Ahmad, 1975; Katili, 1978; Bellier et al., 2006; Watkinson, 2011). The Walanae fault zone is also a major tectonic structure with prominent linear geomorphic features extending over 150 km throughout the south arm of Sulawesi (Fig. 1.1b; van Leeuwen, 1981; Sukamto, 1982; Sukamto and Supriatna, 1982; Grainge and Davies, 1985; Barry and Grady, 1987; Mayall and Cox, 1988; Coffield et al., 1993; Guritno et al., 1996; van Leeuwen et al., 2010). The Walanae fault system is comprised of two parallel faults with a narrow depression zone in between, West Walanae fault (WWF) and East Walanae fault (EWF), which develop along the eastern margin of the Western Mountain Range and the western margin of Bone Mountains, respectively (van Leeuwen, 1981; Grainge and Davies, 1985) (Fig. 1.1). It is thought that the Walanae fault system occurred at the end of the Middle Miocene, involving the development of Walanae Graben filled with Miocene-Pliocene Walanae Formation (Sukamto, 1982; van Leeuwen et al., 2010). The activity of the Walanae fault zone is thought to have played a major role in Neogene and Quaternary structural development in this region. The geomorphic trace of EWF can be recognized as a distinct line of slope transformation between Bone Mountains and Walanae Depression, around which an intensive deformation zone characterized by various scales of faults, folds and associated deformation structures is developed (van Leeuwen et al., 2010). The predominance of a sinistral strike−slip motion of EWF has been assumed on the basis of the shear sense of neighboring major faults, represented by Masupu fault (Coffield et al., 1993; Guritno et al., 1996; Bergman et al., 1996; van Leeuwen et al., 2010) and Sadang fault (Hamilton, 1979). However, the timing and sense of fault motion and associated deformation in Neogene and Quaternary strata have not been sufficiently investigated (Hall and Wilson, 2000; van Leeuwen et al., 2010). Furthermore, the status of recent activity of EWF has not been established, despite segments of EWF being documented as a source of seismicity in a hazard map of Indonesia.

Determination of the paleostress state is very important for reconstruction of the tectonic history, since fault activity, related deformation structures and also geomorphology are strongly controlled by orientation, ratio and magnitude of regional stress.

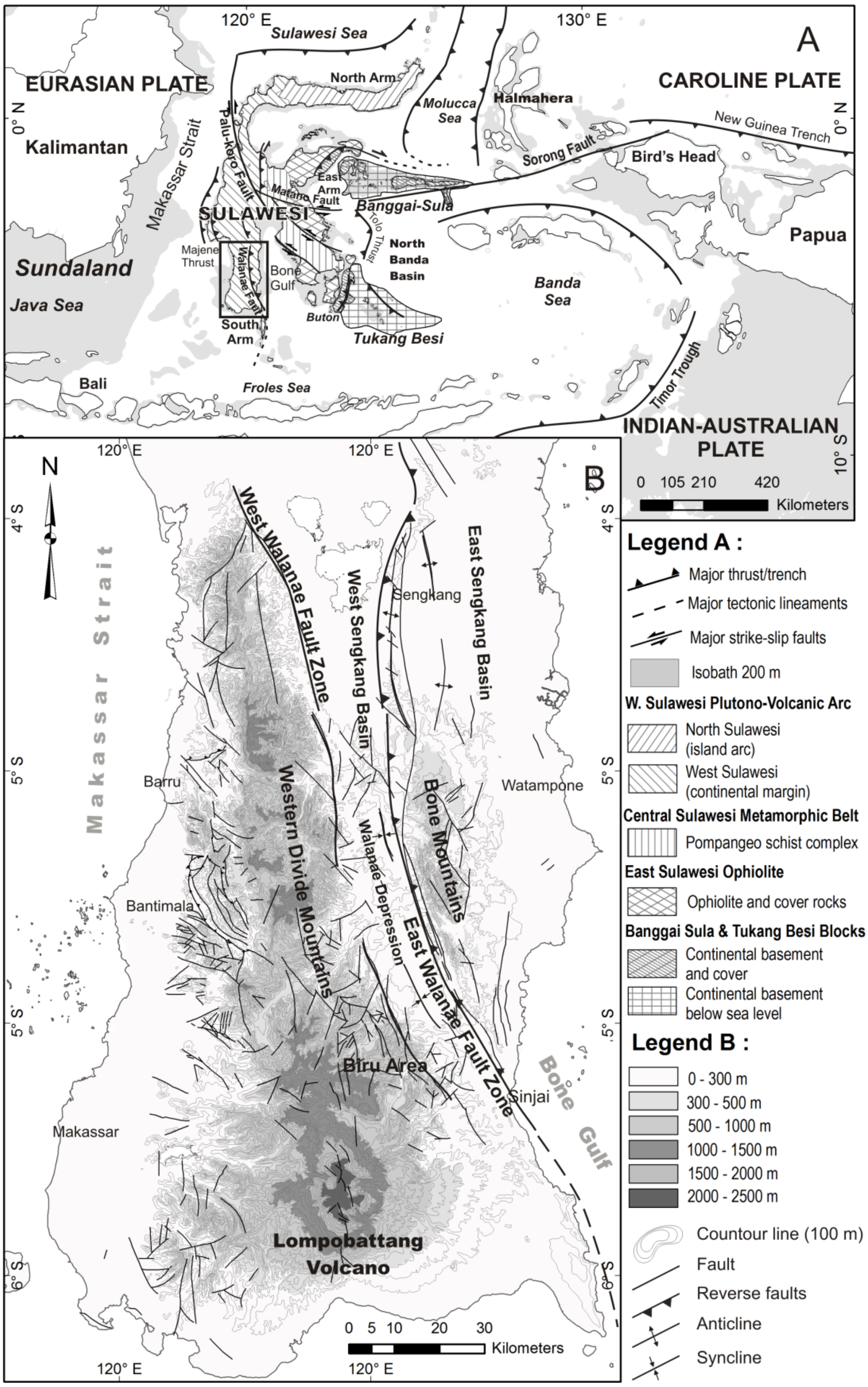

Figure 1.1 (a) Situation of structural elements of South Sulawesi in the tectonic map of Eastern Indonesia (after Hamilton, 1979, Hall and Wilson, 2000). (b) Study area (yellow dashed) on the fault pattern and topographic elevation map of South Arm Sulawesi (after Sukamto 1982; Sukamto and Supriatna, 1982; Berry and Grady, 1987).

A number of mesoscale faults and limestones containing abundant calcite twins are found widely in the Cenozoic volcano-sedimentary strata around EWF trace (van Leeuwen et al., 2010). Lacombe and Laurent (1996) confirmed that both fault slip and calcite twin data generally yielded the same stress state and also pointed out differences in resolution and recorded timing of stress states between the two methods. Inferred paleostress fields would be fundamental for investigation of Neogene and Quaternary tectonics in South Sulawesi.

1.2 Objectives

The aim of this study is to reconstruct tectonic evolution of the South Sulawesi since Cretaceous age as a representative convergent zone with continent–microcontinent collision. On the basis of structural analysis, I have studied several specific subjects as follows.

- To clarify the characteristics of the Biru metamorphic rocks and the effect of later tectonic events such as intrusion of plutonic rocks and activity of WWF, as well as comparison with the Bantimala and Barru metamorphic complex in south Sulawesi, by combination of petrographic and microstructural observation, mineral chemistry and K–Ar dating.
- To determine paleostress states associated with the activity of EWF and WWF, which have contributed to the tectonics in South Sulawesi during Neogene and Quaternary by using the multiple inverse method from the data of both the fault slips and calcite twins.
- To estimate the possibility of recent activity of EWF by radiocarbon dating of soil deformed on the trace of EWF.

1.3 Methods

1.3.1 Basement Rocks

For examining the distribution and observing the occurrence, texture and deformation structure of the plutonic and metamorphic basement rocks, field survey and sampling were performed in the Biru region, particularly along branch of Bila River, Bulubuluk River and Biru River (Fig. 1.1 and 3.1). Petrography and deformation microstructures were investigated under an optical microscope. In this study, an orthogonal reference frame was defined in a deformed rock such that X is parallel to lineation, Y is parallel to foliation and perpendicular to lineation and Z is perpendicular to foliation. Observations of microstructures were performed on XZ, YZ and XY planes. Measurement of bulk rock chemistry was performed using X−ray fluorescence spectrometer (XRF: Rigaku 3270) in Faculty of education and culture, Akita University. Powdered samples were ignited in a measured muffle furnace for two hours at 1100°C before the preparation of fused glass beads containing 1.8 g of sample and 3.6 g of alkali flux (1: 2). The alkali flux was a mixture of lithium metaborate (LiBO2) and lithium tetra borate (Li2B4O7) in a ratio of 1 : 4 (Kimura and Yamada, 1996). Determination of some kinds of minerals and included in metamorphic rocks was performed by X−ray diffractometer (XRD: Rigaku Multi Flex) at 30 kV, 20mA, Cu-Kα radiation with λ = 1.5418 Å in Graduate school of resource and technology, Akita University. Chemistry of minerals included in the metamorphic rocks was measured using electron probe micro-analyzer (EPMA: JEOL JXA-8800 R (RL) Super Probe) at the operating condition of 15kV accelerating voltage, a beam current of 12*n*A, with probe diameter of 2μm in Graduate school of resource and technology, Akita University. Crystallographic preferred orientations of quartz in the metamorphic rocks were measured using electron backscatter diffraction (EBSD) in Graduate school of science, Tohoku University. Each thin sections were polished with colloidal silica suspension to minimize surface damage. EBSD measurement, analysis and mapping were performed using conventional computer software, Oxford HKL Channel 5. At measurement, SEM (Hitachi S−3400N) was operated at an accelerating voltage of 20kV, a probe current of 70nA and working distance of 18mm, with the thin section tilted at an angle of 70° with respect to the beam for EBSD.

K-Ar dating was performed for muscovite in a garnet-amphibolite sample. Mineral separation and measurement were performed in the Hiruzen Institute for Geology and Chronology. The rock samples (~1 kg) were crushed with a stamp mill and then sieved. Muscovite was separated to 60-150 mesh-size fractions. The technique for concentration of muscovite was that described by Itaya and Takasugi (1988) and Itaya and Fujino (1999). Analyses of potassium and argon and calculations of ages and errors were carried out using the method described by Nagao et al. (1984) and Itaya et al., (1991). Potassium was analyzed by flame photometry using a 2000 ppm Cs buffer and has an analytical error within 2% at 2-sigma confidence level. Argon was analyzed on a 15 cm radius sector type mass spectrometer with a single collector system using an isotopic dilution method and an argon 38 spike (Itaya et al., 1991).

1.3.2 Walanae Fault Zone

Cenozoic tectonics in the South Sulawesi has been significantly influenced by activity of the Walanae fault. Observation of deformation structures such as mesoscale folds and faults and associated deformation structures, measurement of fault−slip data and sampling of calcareous rocks for paleostresss analysis using calcite twin were carried out along the East Walanae fault zone (EWFZ) is running and areas from Sengkang to Sinjai (Fig. 1.1b), and also sampling on Langi Volcanics and Biru Granodiorite along Bulubuluk and Biru Rivers in the Biru area where West Walanae fault zone (WWFZ). For paleostress analysis, fault−slip data were measured from 135 outcrops of the basaltic lava of the Salokalupang Group and the sedimentary rocks of the Walanae Formation along EWF, and 52 outcrops of granodiorite and basaltic lava of the Langi Volcanics in Biru area (Fig. 4.1). Bedding attitude in each measurement site is stable including no antlicline and syncline. A dataset for each fault includes strike and dip of fault plane, trend and plunge of striation on the fault plane, sense of shear (either of reverse, normal, dextral or sinistral). 30-45 fault−slip data were collected in each site.

Calcite *e*-twins were also used for stress analysis. 9 limestones and calcareous mudstones samples were collected from the Salokalupang Group and Walanae Formation in the western margin of Bone Mountains and Taccipi Formation in the northern margin of Bone Mountains and on the Sengkang anticline (Fig. 4.7). Geometry of *e*-twining of calcite referred by Lacombe et al., 1990, glide direction and sense of shear as well as plane of twining are crystallographically fixed. There are three equivalent plane on which twining can occur (*e*1, *e*2, *e*3) in a calcite crystal. Pole of twin lamellae and *c*-axis orientation of calcite were measured under an optical microscope using universal stage (U−Stage). The *e*-planes on which twining have not yet occurred in a twined grain were also determined as well as orientations of *c*-axis and one or two sets of twin lamellae. Twin data is collected from three mutually perpendicular thin sections for each sample. Determination of paleostress tensor was performed by multiple inverse method (Yamaji, 2000) computed by MIM Software version 6.02 (Yamaji et al., 2010).

For geomorphological analysis, orthophotos and digital elevation models (DEM) were used. Twenty sheets of black-and-white imagery of orthophotos 1:25.000 in scale and 10”x10” in sheet size, recorded in 1992 by National Coordinating Agency for Surveys and Mapping of Indonesia “BAKOSURTANAL”. Topographic analysis was also conducted combining with DEM by USGS 7.5 minute topographic quadrangles and shaded relief maps produced from 30 m.

In order to constrain the age of the latest activity of EWF, radiocarbon dating was performed for two samples of organic matter included in soils sheared by accelerator mass spectroscopy (AMS). Samples were dated at Beta Analytic Inc., Miami, Florida. The root and plant debris were removed by sieving and then the samples were treated with hydrochloric acid (>3N) wash to remove carbonate minerals from organic matter. The radiocarbon ages measured were converted to conventional radiocarbon ages (Stuiver and Polach, 1977), and calibrated by IntCal04 calibration curve (Reimer et al., 2004).

CHAPTER II. GEOLOGICAL SETTING

2.1 Tectonic Setting and History of Sulawesi Island

Sulawesi Island is located in an area with one of the most complex tectonic conditions under the interaction of three major lithospheric plates, namely, the Eurasian Plate to the west, the Pacific Plate to the east, and the Australian–Indian Plate to the south (Fig. 1.1a). Subduction, rifting and collision around the Southeast margin of Sundaland since Late Cretaceous age have caused multiple phases of tectonic events with thrusting, strike–slip faulting and blocks rotation, which resulted in the development of complexity of geological structure of Sulawesi (Hall and Wilson, 2000).

Sulawesi island has been divided into several tectonic provinces (Sukamto, 1975; Hamilton, 1979), the west Sulawesi plutono-volcanic arc, the central Sulawesi metamorphic belt, the east Sulawesi ophiolite and the microcontinental blocks of Banggai-Sula and Buton-Tukang Besi (Fig. 2.1 and 2.2). The west Sulawesi plutono-volcanic arc is divided into a continental margin segment (Western Sulawesi) and a pre-Cenozoic island arc segment underlain by oceanic crust (Northern Sulawesi) (Leeuwen and Muhardjo, 2005).

Tectonic history of Sulawesi, particularly that of South arm will be overviewed briefly in bellow.

Accretionary complex; The tectonic history of Sulawesi have been began in the Late Jurassic-Early Cretaceous with the development of a continental arc in south-central Kalimantan associated with northeasterly subduction of Meso-Tethys (e.g. Hamilton, 1979; Parkinson et al., 1998; Guntoro, 1999; Hall, 1996; van Leeuwen et al., 2010). The accretionary complexes are represented by the Bantimala-Barru Complexes in the western Sulawesi and the Pompangeo Complex in the central Sulawesi. Pre-Cenozoic accretionary complex in Bantimala represent northeast-dipping imbricate slices, comprises of crystalline schist which had experienced high-pressure type metamorphism, schist breccia unconformably overlain by Late Cretaceous rocks (the radiolarian cherts of Wakita et al., 1996), undeformed rocks of Jurassic shallow marine clastic deposits (the Paremba sandstone of Sukamto and Westermann, 1993) and peridotite separated by thin zones of tectonic mélange (Wakita et al., 1996; Miyazaki et al., 1996; Parkinson, 1998a; Parkinson et al., 1998).

West dipping subduction; In the upper Cretaceous (Late Aptian-Cenomanian) represent a northwest-dipping subduction zone, at Meratus Range in the Southeast Kalimantan suggest an island arc where volcanoclastics are intruded by dykes and stocks which yield K/Ar ages from 87 ± 4 to 72 ± 4 Ma (Yuwono et al., 1988b). In the west Sulawesi, upper Cretaceous turbidity sediments of the Balangbaru, Marada and Latimojong Formations represent development of a deep marine fore-arc basin (van Leeuwen, 1981; Hasan, 1991; Parkinson et al., 1998). Some authors proposed that subduction shifted again southeastward at the beginning of the Paleocene (e.g. van Leeuwen, 1981; Polve´ et al., 1997; Yuwono et al., 1988a). However, the only rocks identified from this period in south arm Sulawesi are calc-alkaline volcanics at Bantimala (Alla/BuaVolcanics) and Langi Volcanics at Biru area. During Paleocene and Early Eocene, Kalimantan and western Sulawesi was largely emerged (Wilson and Moss, 1999).

Sundaland active margin and opening of Makassar Strait; Sundaland active margin is likely took place during the Middle Eocene, there was widespread extension around the area (Wilson and Moss, 1999). Makassar Strait was the site of extension (Fig. 2.2d), block-faulting and subsidence (Guntoro, 1999), which had been deepened in Late Eocene (van Leeuwen et al., 2010). In west Sulawesi, terrestrial to marginal marine silisiclastics containing coal bed of Mallawa Formation (Sukamto, 1982) and platform carbonate of Tonasa Formation were developed at the present Western Divide Mountains (Wilson and Bosence, 1996; Wilson et al., 2000). On the eastern side of the South Sulawesi, large amount of volcanoclastic materials of Matajang Formation were deposited in a shallow marine in Bone Mountains (van Leeuwen et al., 2010).

West Sulawesi passive margin; By the end of the Eocene, the west Sulawesi became a passive margin, paleomagnetic investigations suggest an about 40° of anticlockwise rotation of the west Sulawesi possibly during19-13 Ma (Sasajima et al., 1980), which changed the characteristics of the margin from a convergence to a transform boundary (Polvé et al., 1997; Hall, 1996; van Leeuwen and Muhardjo, 2005).

East Sulawesi ophiolite obduction; East ophiolite complex was obducted in Late Oligocene-Early Miocene or at 30 Ma on Sundaland margin (Bergman et al., 1996; Parkinson, 1998b; Kadarusman et al., 2004) (Fig. 2.2e), some authors have suggested that it started somewhat later at 25 Ma (Hall, 1996; Simandjuntak and Barber, 1996) followed by folding and thrusting and magmatism related to extensive lithospheric melting in Late Miocene (Bergman et al., 1996). The Lamasi ophiolite and Bone Group segments in the south arm Sulawesi has been suggested as constitute fragments of the east Sulawesi ophiolite (Yuwono et al., 1988a; Bergman et al., 1996; Polvé et al., 1997; Kadarusman et al., 2004; Leeuwen et al., 2010). Environment, age and subsequently tectonic history are still not clear and in debate.

Regional Extension and magmatism in west Sulawesi; Around 14– 13 Ma, tectonic condition had been stable, widespread blocks faulting of western divide mountains and the onset of potassic volcanism (van Leeuwen et al., 2010). The end of the Early Miocene volcanic activity which gave rise to the onset of the formation Walanae Graben which later evolved to a basin in which sediment took place of the Walanae Formation (Sukamto, 1982). Bone basin (termed Sengkang Basin in this study) may formed around this time (Hamilton, 1979), it clearly rimmed by major N– S trending marginal fault of Walanae fault (Yulihanto, 2004). The tectonic event culminated around 13–12 Ma (Middle Miocene) with the juxtaposition of the Bone Group segment against the continental margin of Sundaland composed of the Salokalupang Group, along the Walanae fault zone. The Salokalupang rocks were tilted, sliced into tectonic lenses of variable size, and locally folded (van Leeuwen et al., 2010).

Collision of Sula platform; The continental fragments of the Buton-Tukang Besi and Sula collided with the east arm Sulawesi at 13–11 Ma and Sula at 5 Ma, respectively (Fig. 2.2f) (Smith and Silver, 1991; Hall, 1996). The impact of these tectonics induced voluminous granitoid magmatism and uplifting in northern part south arm Sulawesi (Bergman et al., 1996; van Leeuwen and Muhardjo, 2005). The Neogene sediments of the Sengkang Basin have been largely subjected to the folding. Consequently, series of NS-trending anticlines and synclines (van Bemmelen, 1949) and a general uplift of the southwest Sulawesi region occurred during the Pliocene (van Leeuwen, 1981). Lompobattang volcano, which is characterized by high potassium took place. There may be no linkages to a subduction, but it may be developed under distentional intraplate contex (Yuwono et al., 1988a).

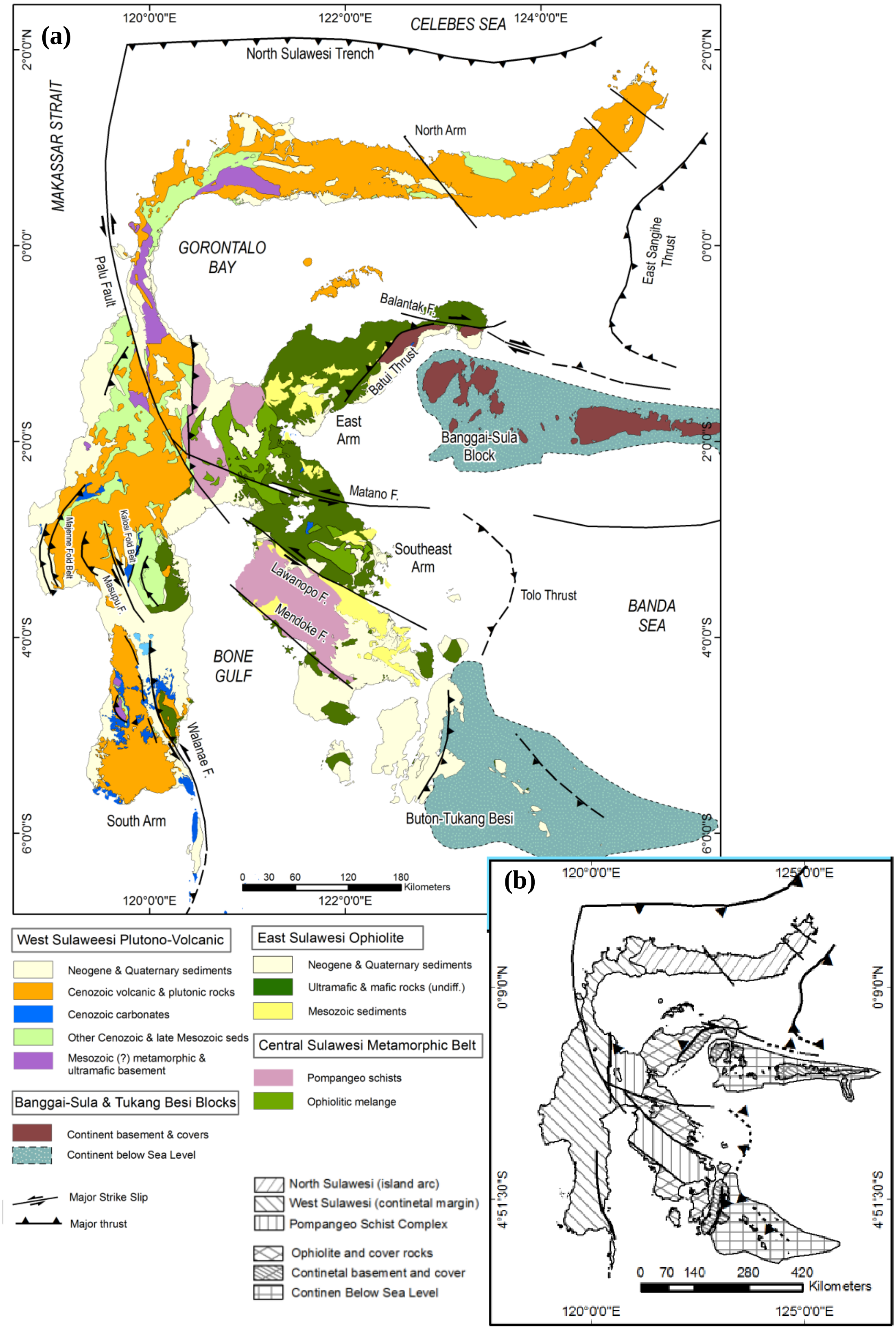

Figure 2.1 (a) Summary of the geology of Sulawesi, showing lithotectonics and principal structures. (b) Tectonic province of Sulawesi island (after Hamilton 1979; Bergman et al., 1996; Hall and Wilson, 2000; van Leeuwen et al., 2010; Watkinson, 2011).

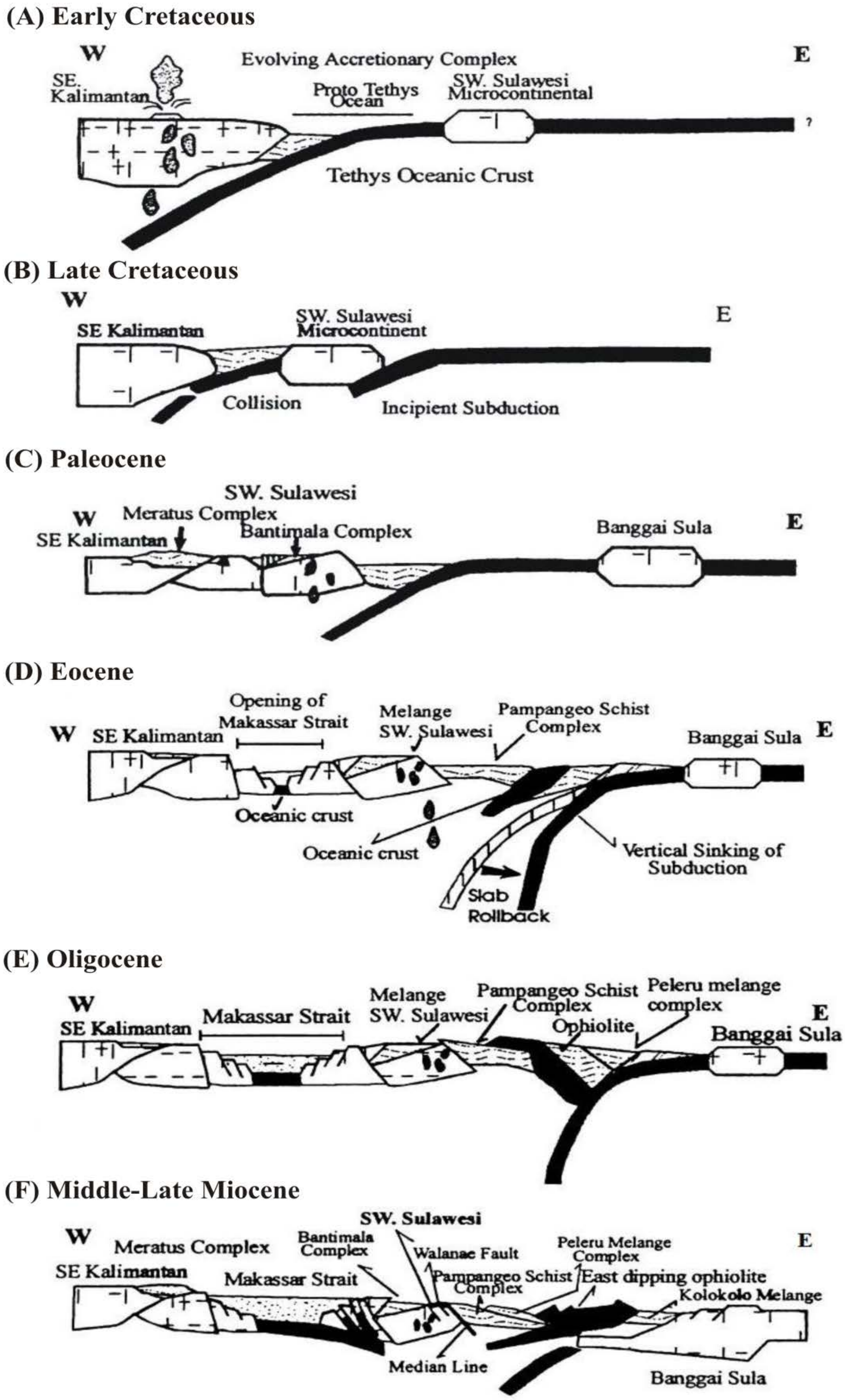

Figure 2.2 Interpretation of tectonic evolution of Sulawesi based on seismic reflection and gravity models, in addition to compilation geological information (based on Guntoro, 1999).

2.2 Geological Setting of South Arm of Sulawesi

2.2.1 Geomorphology

South arm Sulawesi can be divided into three striking geomorphic feature, they are the Western Divide Mountains Range to the west, the Bone Mountains Range to the east and the Walanae Depression, a low-lying split between these mountains representing graben-like structure (Fig. 1.1 and 2.3; van Leeuwen, 1981). These geomorphic features generally extend to NS to NW−SE.

Western Divide Mountains Range

The Western Divide Mountains consist of a chain of steep mountains, aligned roughly in a N–S direction (Fig. 2.3).The most conspicuous geomorphic feature in southern area is the cone of the extinct Lompobattang volcano 2.879 m high, which is the highest mountain in the South arm and was formed during the Late Quaternary. The elevation of middle to northern part of this mountain range is around 1000 to 1500 m, gradually decreasing northward. Drainage patterns in the southern area is generally radial described by young volcanic rocks of Lompobattang Volcano, to the south are generally a combination of dendritic which is describe similarity lithology and rectangular which is describe controlled by fracture. River flows directly into the Makassar Strait in the west and south, and to Tempe Lake via Walanae River in central depression of Walanae Depression prior to flow into the Gulf of Bone to the east. Western margin of this range is characterized by the karst terrains. Amid of karst terraces, pre-Cenozoic rocks is exposed, which characterized a topographically lower elevation terrain of quite difference features. To the west this range is bounded by the plain of Pangkajenne−Barru, the vast lowland area included Makassar−Maros. Eastern margin of the range shows different topography with steep slopes, where a lineament corresponding to WWF is distinctive (e.g. van Leeuwen, 1981; Sukamto, 1982; Sukamto and Supriatna, 1982; Barry and Grady, 1987; Guritno et al., 1996; van Leeuwen et al., 2010)

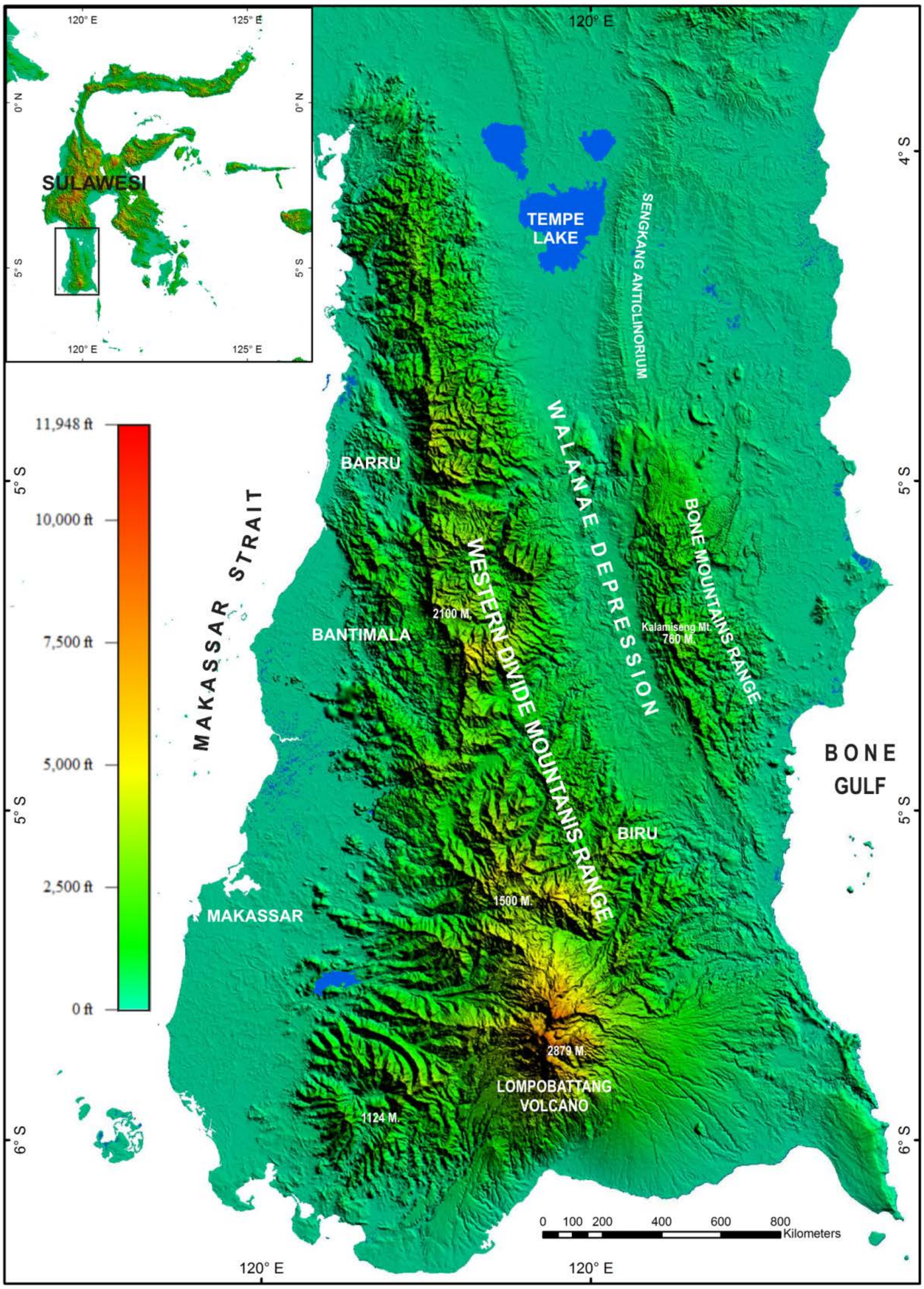

Figure 2.3 Geomorphic map of South Sulawesi showed three topographic expression differences include Western Divide Mountain Range, Walanae Depression and Bone Mountains Range

Bone Mountains

The Bone Mountains is generally narrower and lower in elevation than Western Divide Mountains (Fig. 2.3), with the highest summit of 760 m (Mt. Kalamiseng) and about 20 km wide from east to west in the southern part. The northern part of the mountains has a karst topography with conical hills where reef limestone of Taccipi Formation is exposed. To the east, elevation of mountains gradually descends to the level of the vast Bone plain. On the other hand, the western side of this mountain is characterized by a steep topography forming clear morphologic contrast with Walanae Depression across the lineament of EWF. Drainage patterns in this range are commonly described dendritic and rectangular.

Walanae Depression

The Walanae Depression is a N-S extending narrow basin between two mountain belts Along both eastern and western margin of the Depression, lineament of WWF and EWF lie along scarps bounding with the Western Divide Mountain Range and the Bone Mountains, respectively. The Eastern margin has distinct conversion line of slope angle and is accompanied by alluvial fan. While the lineament of WWF, which lies along scarp of Western Divide Mountains, does not extend to long and partly unclear. The Walanae Depression is narrow in the southern part, about 15 km in width, but gradually widened and is lower toward north, up to 35 km wide and down to 5-100 m in elevation (Fig. 2.3). Walanae River, the main stream in the depression flows at the western side northward into the Tempe Lake. Northeastern margin of the Tempe Lake is adjacent to a row of hills known as the Sengkang anticlinorium extending N–S direction. Drainage patterns in this range are commonly described trellis, particularly branch of Walanae main rivers in the east side.

2.2.2 Stratigraphy

There are distinct differences in geology between the western and eastern South Sulawesi, which are separated from each other by the WWF (Fig. 2.4 and 2.5; van Leeuwen, 1981; Sukamto, 1982; Wilson and Bosence, 1996; van Leeuwen et al., 2010).

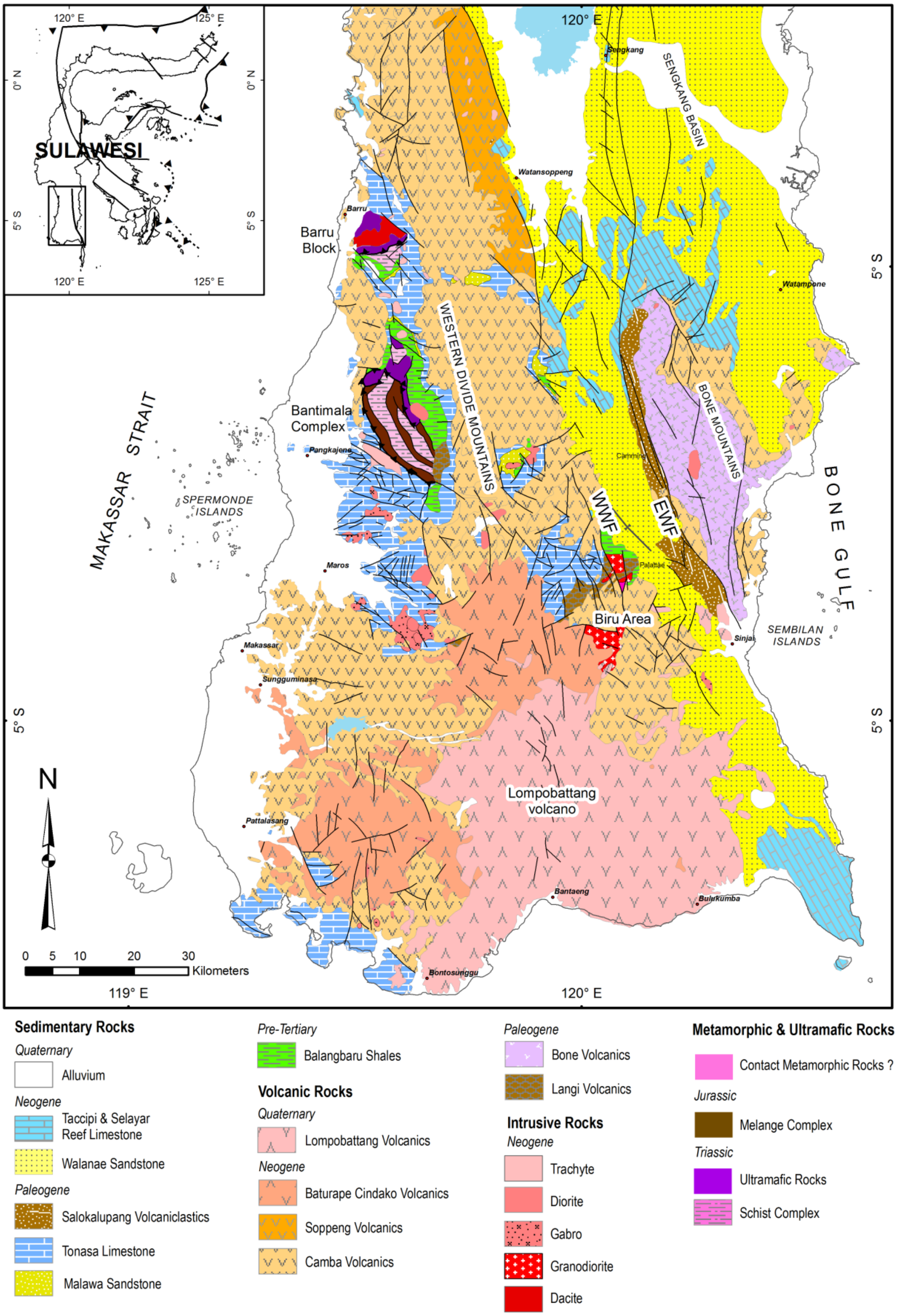

Figure 2.4 Geological Map of the South Sulawesi is showing location of West Walane Fault (WWF), East Walanae Fault (EWF) and Biru area (Modified after van Leeuwen, 1981; Sukamto, 1982; Sukamto and Supriatna, 1982; Wilson and Bosence, 1996).

Western Divide Mountain

The oldest rocks of Western Divide Mountains are found on the western side as the basement complex, the Bantimala and Barru tectonic complex (Fig. 2.4). The Bantimala Complex is composed by high pressure metamorphic rocks, mélange, radiolarian cherts, turbidity sediments, shallow sedimentary rocks and ultramafic rocks. The high pressure metamorphic rocks consist of glaucophane schist, albite-actinolite-chlorite schist, chlorite-mica schist, garnet glaucophane-quartz schist, garnet-chloritoid-glaucophane-quartz schist, serpentinite and eclogite (Miyazaki et al., 1996). Maulana (2009) distinguished three kinds of eclogite from eclogite facies assemblages, apatite-bearing eclogite, glaucophane eclogite and foliated epidote-quartz eclogite. The mélange occurs as a tectonic block, which contain sandstone, shale, siliceous shale, chert, basalt, schist, and felsic igneous rocks within a sheared matrix (Miyazaki et al., 1996).

The Middle Cretaceous (Late Albian−Early Cenomanian) chert unconformably overlies on the high-pressure metamorphic rocks (Wakita et al., 1996). These assemblages are unconformably overlain by shallow-marine clastic sedimentary units of the Early and Middle Jurassic Paremba sandstone (Sukamto and Westermann, 1993). The ultramafic rock is dominated by serpentinised peridotite which contains chromite lenses. These sequences have been interpreted to represent the subduction of a microcontinent underneath Sulawesi in Cretaceous age (Sukamto, 1982, Parkinson, 1998a; Wakita et al., 1996). K−Ar age dating of metamorphic rocks in Bantimala area from muscovite yield 111 Ma (Sukamto, 1982), mica from eclogite and pelitic schist yield ranging from 114 ± 6 – 132 ± 7 Ma (Wakita et al., 1994), eclogite rock yield 113 ± 3 Ma (Parkinson, 1998a).

Geological setting in the Barru area has not been well characterized, and the high-pressure assemblages of metamorphic rocks are not found. Structure features of the Barru and Bantimala Complexes are also quite different. Bantimala area has foliations commonly NNW−SSE occasionally NW−SE striking and steeply dipping to NE. Whereas WSW−ENE striking and steeply dipping to SE foliation are developed in Barru area. The result of K−Ar age yield 106 Ma from phengite for quartz-mica schist from Barru area (Wakita et al., 1994), suggesting that Bantimala and Barru complexes may have been formed as coeval tectonic event.

Early Cretaceous metamorphic rocks have been also found in Biru area, which is believed to be hornfels and has not been characterized (van Leeuwen, 1981; Sukanto and Supriatna, 1982). They are overlain with an unconformity by Upper Cretaceous marine sediments flysch of Marada Formation consisting of shales, silts and coarse to fine sandstones. Marada Formation equivalent with Balangbaru Formation in the Bantimala-Barru area, these are interpreted to have been formed in a fore arc basin (van Leeuwen, 1981; Sukamto, 1982; Hasan, 1991). The age of metamorphic rocks is not at present, but they may be correlative to the Marada Formation (Sukamto and Supriatna, 1982). The Biru metamorphic rocks and Marada formation are unconformably overlain by Langi Volcanics consisting of calc-alkaline volcanic rocks of Paleocene to Oligocene age, fission track-dating from lower part yielded ± 62 Ma (van Leeuwen, 1981) (49.8 ± 0.4 – 52,03 ± 0.5 Ma by Elburg et al., 2002). Similar rocks type also found in Bantimala area, namely, Bua or Alla volcanics (van Leeuwen, 1981; Sukamto 1982; Yuwono et al., 1988a).

Biru intrusive complex (BIC), Miocene plutonic rocks intrude in Biru area. It consists of syenite with 8.4 Ma of K/Ar age (Elburg et al., 2002) and granodiorite with 19 ± 3.4 Ma of fission track age (van Leeuwen, 1981). Basalt-andesite dykes also intrude associated with Sopo and Lemo volcanics of which ages are ~ 11– 10.3 Ma and ~ 7.6– 6.2 Ma, respectively (Elburg et al., 2002).

The eastside of the West Divide Mountain Range shows lowland topography represented by Walanae Depression (Fig. 2.3 and 2.4) It is thought that the Walanae fault system occurred at the end of the Middle Miocene, involving the development of Walanae Graben as a part of Sengkang Basin (Sukamto, 1982). The Depression is filled with Miocene to Quaternary Walanae Formation, thick sequence of sediments with intercalation of pyroclastics, and volcaniclastics, marls and limestones among silisiclastic rocks, initially in a marine environment but becoming a marginal marine towards the end of the Pliocene (van Leeuwen et al., 2010). Quaternary Marine fauna and terrestrial verterbrates fossil were found in this area (van den Bergh et al., 1995). The western part of the Depression is covered by alluvial fan deposit provided from Bone Mountains.

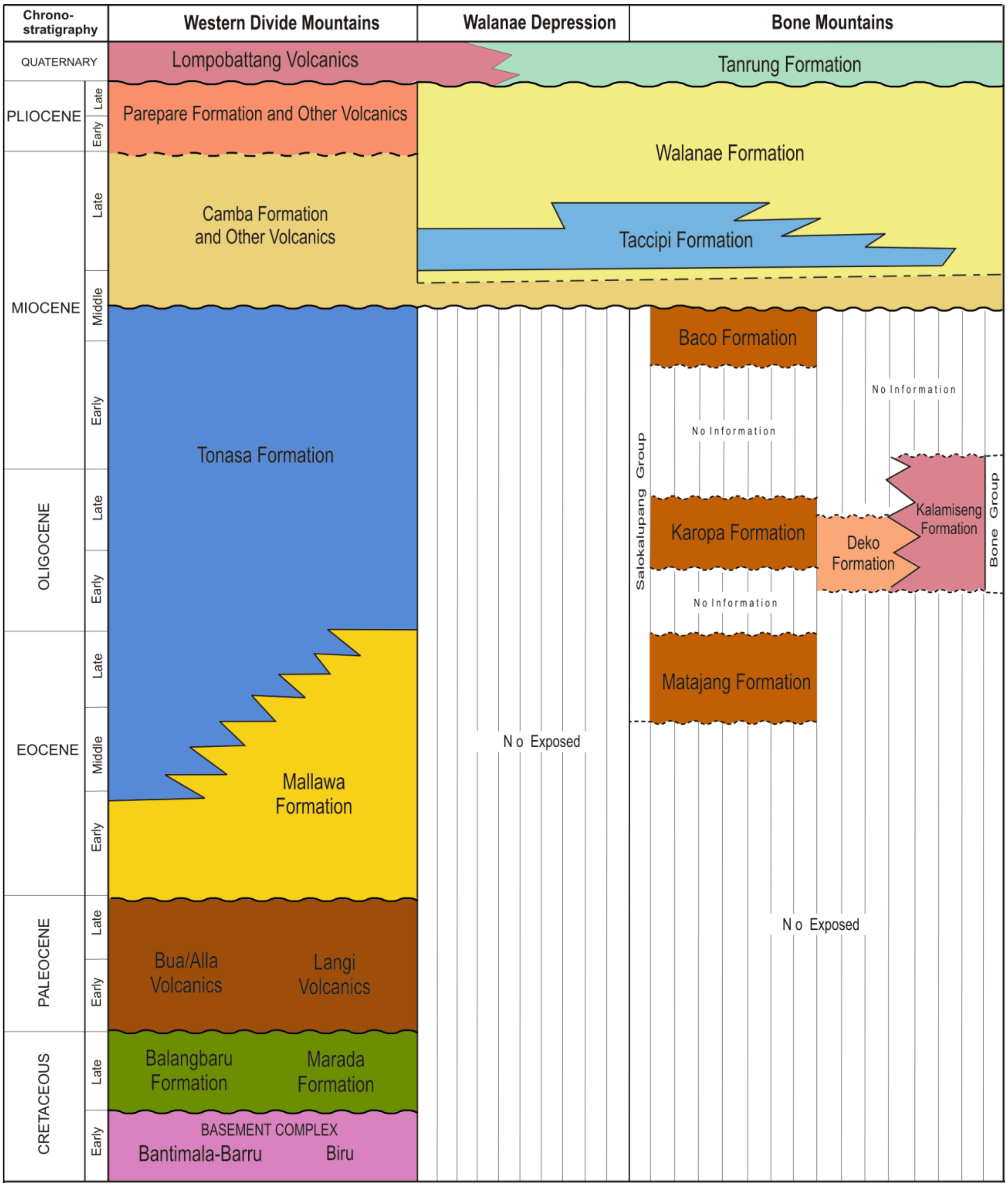

Figure 2.5 Stratigraphic chart from the west to the east of South Sulawesi. Modified after van Leeuwen, 1981; Sukamto, 1982; Sukamto and Supriatna, 1982; Wilson and Bosence, 1996; van Leeuwen et al., 2010.

Bone Mountains and Sengkang Basin

Four stratigraphic units of Cenozoic succession are recognized around Bone Mountain and Sengkang Basin (Fig. 2.4 and 2.5). A stratigraphic unit which lies on the west side of EWF trace is the Middle Eocene to Middle Miocene Salokalupang Group, the lowest unit in the area. The Salokalupang Group is comprised of three Formations (Matajang, Karopa and Baco Formations) and characterized by tuffaceous sandstones and mudstones intercalated by lavas and limestones deposited at a part of Sundaland continental margin (van Leeuwen et al., 2010). They are exposed along fault zone extending approximately 65 km with 2.5 to 3 km wide. The Oligocene to Lower Miocene Bone Group which occupies the Bone Mountains is adjacent to the Salokalupang Group at their western margin. The Bone Group is comprised of the Deko Formation and Kalamiseng Formation and is characterized by basalt-andesitic volcanic rocks with a series of interbed hemipelagic mudstones, which were probably formed by a subduction-related arc volcanism (van Leeuwen et al., 2010). The Bone Group is unconformably overlain by the Middle–Upper Miocene Camba Formation.

The Salokalupang Group is unconformably overlain by the Middle Miocene-Pliocene Walanae Formation at western margin and the Middle-Upper Miocene Taccipi Formation at the northern area of the Bone Mountains. The Walanae Formation interfingers with limestones of Taccipi Formation in the northern part of the Bone Mountains (BouDagher-Fadel, 2002). The Taccipi Formation is a typical reef knoll characterized by the presence of numerous bioclast components deposited in isolated shallow marine (Grainge and Davies, 1985; Mayall and Cox, 1988; Ascaria et al., 1997; BouDagher-Fadel, 2002). Massifs of bioclastic limestone of the Taccipi Formation represent karst landform on the north-western margin of the Bone Mountains, while the crystalline limestone of the Taccipi Formation is found in the deep underground in the Sengkang basin (Grainge and Davies, 1985; Mayall and Cox, 1988) and limitedly exposed only in the Sengkang anticline on the Pattirosompe hills.

2.2.3 Structural Geology of South Sulawesi

The tectonic evolution of Sulawesi have been influenced by large-scale strike–slip faults and fold and trust belts accommodating the successive collisions of the Western Sulawesi with the Banda Sea microplate and Banggai-Sula microplates and the consequent block rotations during the Late Cenozoic (Hamilton, 1979; Smith and Silver, 1991; Beaudouin et al., 2003; Hall, 1996; Bellier et al., 2006). There are a number of faults interpreted as strike–slip features, mostly with an sinistral motion, such as the Palu-Koro fault system (central Sulawesi), the Matano Fault (east arm), Lawanopo and Mendoke faults (southeast arm Sulawesi), the Walanae fault and Sadang fault (south arm Sulawesi). They often accompanied by fold and trust belts (Fig. 2.1). They are thought to have occurred as boundary sutures of tectonic provinces.

The southern arm Sulawesi is transected by two main faults, namely, the Sadang and Walanae faults. Sadang fault (Hamilton, 1979) or as referred the Masupu fault (Coffield et al., 1993; Guritno et al., 2006) is a N-S trending wrench fault located along the east side of the Mamasa granite of Central Highlands of Sulawesi (Hamilton, 1979; Coffield et al., 1993; Guritno et al., 2006). It have been interpreted to have a sinistral shear sense, but field interpretation and adjacent areas indicate the sense of movement is actually dextral (Coffield et al., 1993), possibly two phases of movement, the firtst phases with sinistral movement and the second phase with dextral movement. The fault system may extend southward to Walanae fault zone (Coffield et al., 1993; Guritno et al., 2006).

The Walanae fault system is one of the major structures developed in the southern part of south Sulawesi, which has been interpreted by many author as a major NW-SE strike–slip fault (Leeuwen, 1981; Sukamto, 1982; van Leeuwen et al., 2010). The Walanae fault system consists of two fault systems, West Walanae fault (WWF) and East Walanae fault (EWF).

WWF is running along eastern margin of the Western Divide Mountains Range. Commonly it is interpreted to uplift the West Divide Mountains Range where Cretacious basement rocks such as the Bantimala and Barru Metamorphic Complex are placed and older than the EWF (Sukamto, 1982; van Leeuwen et al., 2010).

EWF is running approximately N–S along the western margin of the Bone Mountains with a distinct topographic expression (Sukamto, 1982), and apparently continues to Masupu fault (Guritno et al., 1996). In the northern part, EWF cuts through the east flank of an anticlinal structure of the Neogene sediments (Leeuwen, 1981), where it divides the Sengkang Basin into two sub-basins (Grainge and Davies, 1985). EWF has been regarded as a sinistral strike–slip fault (Leeuwen, 1981; Sukamto, 1982;

Leeuwen et al., 2010). The EWF apparently continues southwards into a deep oceanic trough interpreted as a Neogene trench by Hamilton (1979).

A N-S trending narrow ridge in the middle part of Sengkang Basin corresponds to the geomorphic feature of Sengkang anticline. The fold involves Middle Miocene to Pliocene clastic sediments of Walanae Formation.

CHAPTER III. BIRU METAMORPHIC ROCKS

3.1 Occurrence of the Biru Metamorphic Rocks

Biru area is located about ±120 km southeast from Makassar, South Sulawesi. There is a small window of the Biru metamorphic rocks (BMR) exposed in a restricted area of 2 km square surrounded by the volcanic rock. The best outcrops can be found in the Bulubuluk River (Fig. 3.1) and the Bila River in Pammusureng area, a tributary of Biru River.

Along the Bila River, three different lithologies crop out. In the upper stream of the valley, epidote amphibolites which contain abundant epidote porphyroblasts with elongate shape and their long axis up to 2 cm in length occur. Garnet amphibolite occurs in the middle part of stream. In the downstream, near the contact with granodiorite, weakly folded mica schist is found. Metamorphic rocks in this location commonly have either schistosity, mylonitic or cataclastic foliations generally dipping toward SE. In some localities, lineation oriented to S−SE also develops (Fig. 1.b1).

Unlike in the Bila River, metamorphic rocks in the Bulubuluk River are generally amphibolites (Fig. 3.1. and 3.2). Distinct compositional banding developed in the rock defines schistosity, which dips 15–52° to SE.

3.2 Petrography and Mineral Chemistry

3.2.1 Petrography

On the basis of mineral assemblages are dominance of hornblende, most of metamorphic rocks can be classified into amphibolites. Inferred metamorphic facies are epidote-amphibolite and amphibolite facies (Table 3.1).

Three types of lithologies: epidote amphibolite (Fig. 3.3), garnet amphibolite (Fig. 3.4), and micas schist (Fig. 3.5) are exposed along the branch of Bila River. Amphibolite is characterized by mineral assembly of albite (30–35%) + hornblende (15-25%) + actinolite + epidote (10–15%) + chlorite (10% <) + quartz (10–15%). Large plagioclase and epidote crystals include hornblende, quartz and chlorite, which often show oriented inclusion array (Fig. 3.3). Chlorite also present filling or altering the rim of mafic minerals.

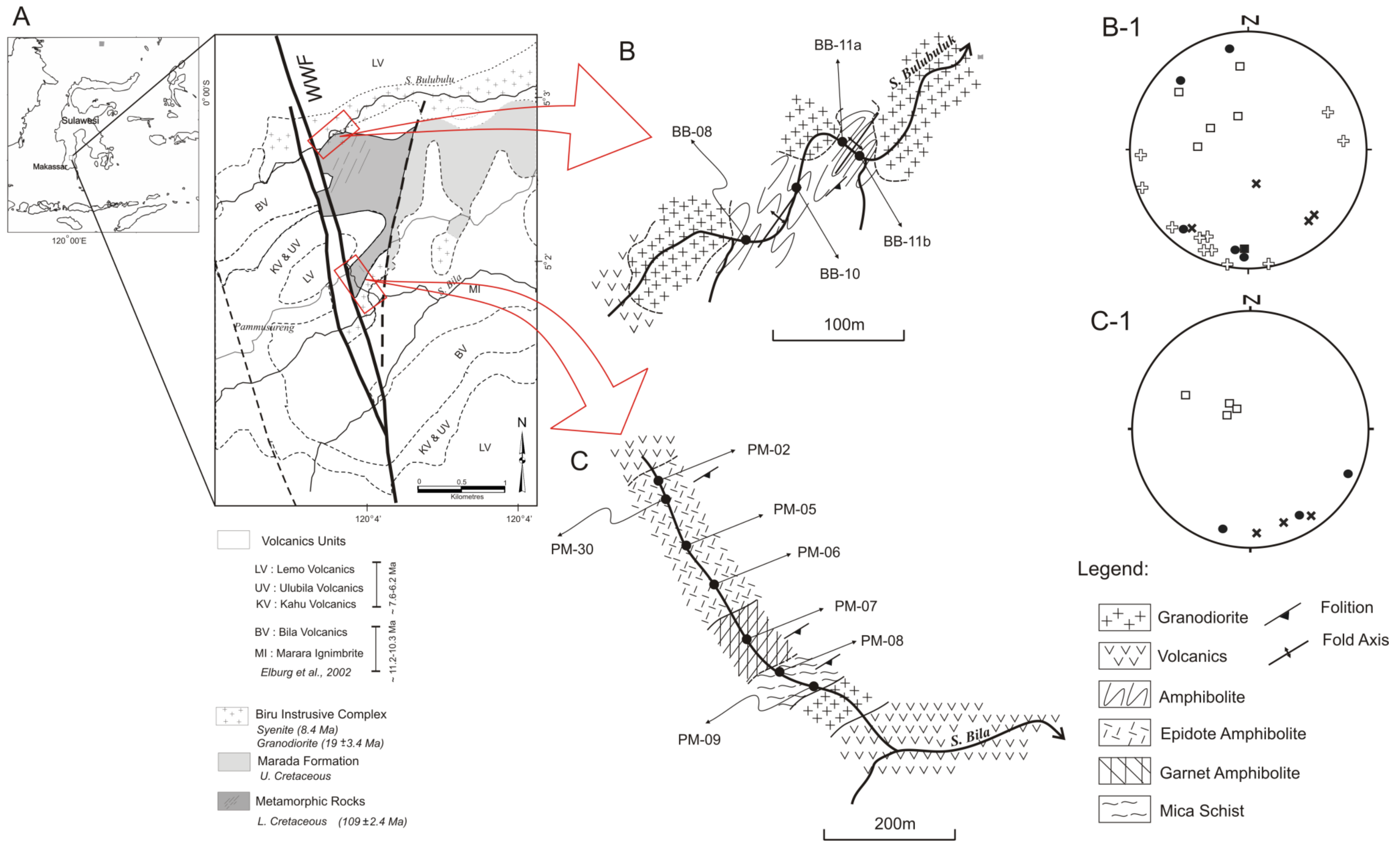

Figure 3.1 (a) Simplified of geological map of Biru area (modified after van Leeuwen, 1981; Elburg et al., 2002). (b) Section at the Bulubuluk River is showing sampling localities and (c) section at the Bila River. Lower hemisphere and equal-area stereographic projections of mesoscale structures in the Biru area. (b-1) Stereoplots data in the Bulubuluk River and (c-1) Bila River. Pole to foliations (open squares); stretching lineations (cross); fold axes (plus); pole to fold axial plan (filled squares); pole to dykes margin (filled circle).

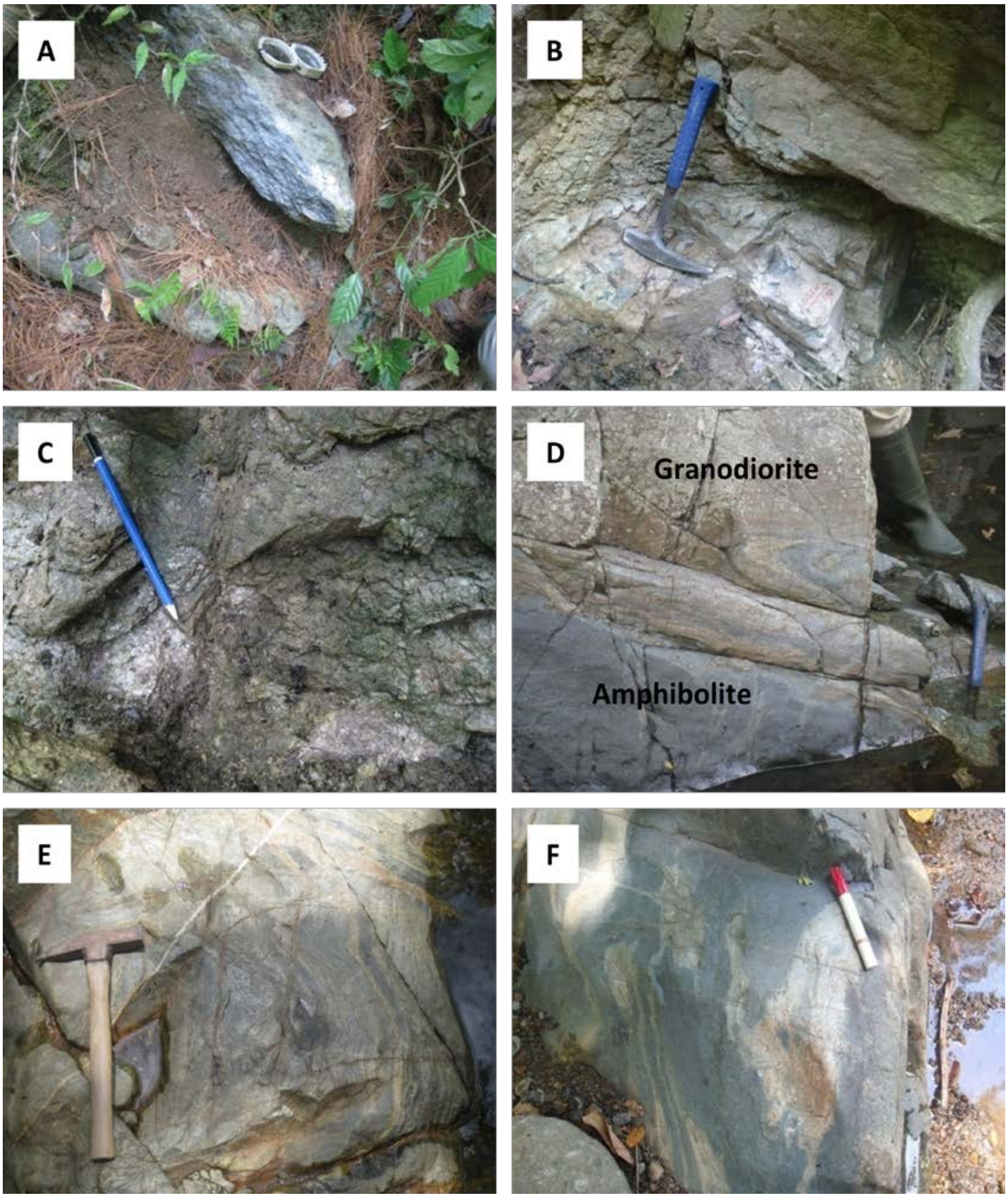

Figure 3.2 Representative metamorphic rocks outcrop in Biru area. Branch of Bila River: (a) Epidote amphibolite site PM-02; (b) garnet amphibolite site PM-07; (c) mica schist at site PM-08. Bulubuluk River: (d) Amphibolite contact with granodiorite at site BB-11a. (e) Amphibolite at site BB-11b; (f) amphibolite at site BB-10. These rocks are in contact with plutonic rocks, namely Biru intrusive complex (BIC) and covered by a six series of volcanics (Fig. 3.1a; Elburg et al., 2002).

Table 3.1 Mineral assemblages of the metamorphic rocks in the Biru Area

Sample No	Rock Name	Ep	Chl	Act	Hbl	Ms	Pr	Grt	Ab	Qtz	Rt	Hem	Py	Cal
	Epidote-Ampibolite Facies													
PM-02	Epidote Amphibolite	O	O	O	O				O	O	O	O	O	
PM-05	Epidote Amphibolite	O	O	O	O				O	O	O	O	O	
PM-06	Epidote Amphibolite	O	O	O	O			O	O	O	O	O	O	O
PM-30	Epidote Amphibolite	O	O	O	O				O	O	O	O	O	
PM-07	Garnet Amphibolite	O			O	O		O		O	O			O
PM-08	Mica Schist	O	O	O		O	O		O	O		O	O	
PM-09	Mica Schist		O			O			O	O		O	O	
	Amphibolite Facies													
BB-08	Amphibolite	O	O		O				O	O	O	O	O	
BB-10	Amphibolite	O	O	O	O				O	O		O	O	
BB-11	Amphibolite	O	O	O	O				O	O	O	O	O	O

Location: PM = branch of Bila River; BB = Bulubuluk River. Mineral abbreviations based on Kretz (1983); Ep = Epidote, Chl = Chlorite, Act = Actinolite, Hbl =Hornblende, Ms = Muscovite, Pr = Paragonite, Grt = Garnet, Ab = Albite, Qtz = Quartz, Rt = Rutile, Hem = Hematite, Py = Pyrite, Cal = Calcite.

The garnet amphibolite is characterized by the mineral assembly of hornblende + garnet + plagioclase + epidote + muscovite + chlorite + quartz. Garnet commonly occurs as porphyroblasts up to 4 mm in sizes and has euhedral–subhedral shape with abundant microfractures (Fig. 3.4). Epidote also was occurred as porphyroblast (Fig. 3.5). The mica schist is composed of actinolite, epidote, muscovite, chlorite and quartz. Preferred orientation of muscovite and actinolite defines schistosity. All samples in this facies contain small amounts of rutile, hematite and pyrite as secondary minerals.

Rocks exposed in Bulubuluk River are commonly amphibolites, which contain mainly plagioclase, hornblende, actinolite, chlorite and quartz (BB-10 and BB-11; Fig. 3.6). Schistosity is defined by the preferred orientation of hornblende and actinolite. Plagioclase porphyroblast show elongate shape and include hornblende, actinolite, chlorite and quartz inclusion showing weak linear alignment. Epidote minerals occur as minor component. As accessory minerals, rutile, hematite and pyrite occur.

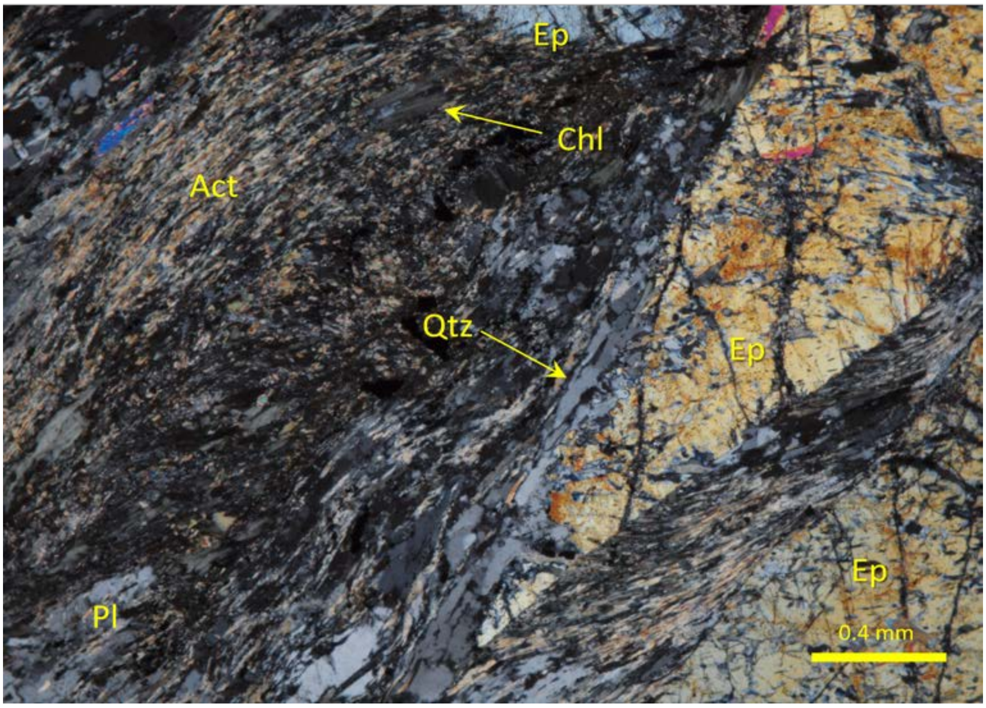

Figure 3.3 Photomicrograph epidote amphibolite (sample PM-02) with cross polar. Epidote is present as porphyroblast, quartz (Qtz), actinolite (Act) and plagioclase (Pl) define as the foliation.

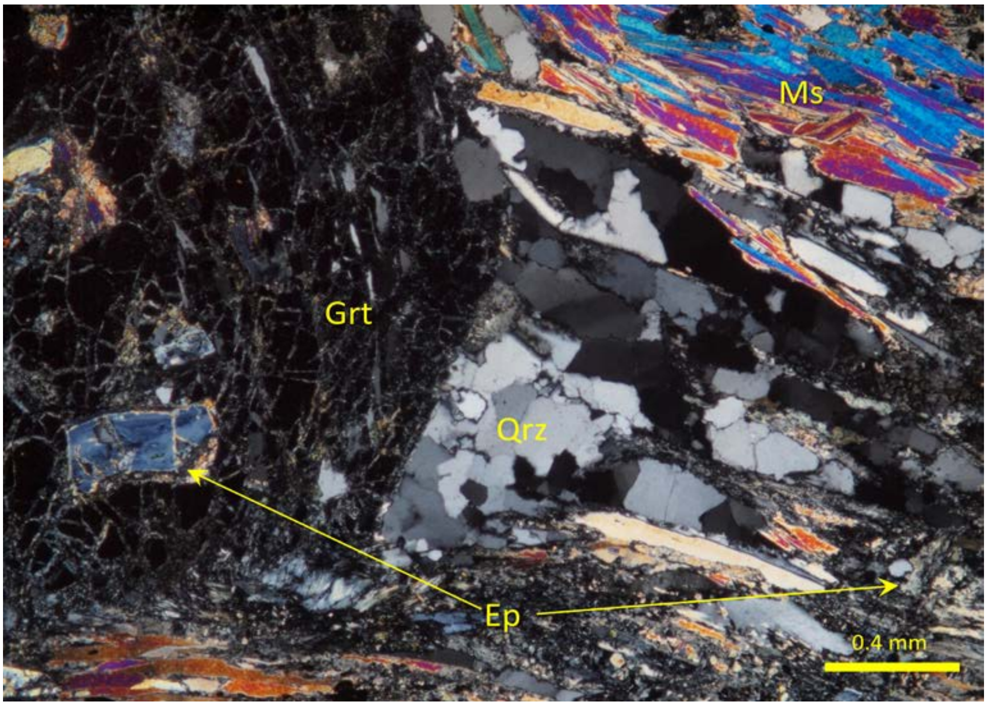

Figure 3.4 Photomicrograph garnet amphibolite (sample PM-07) with cross polar. Garnet is present as porphyroblast, quartz (Qtz), muscovite (Ms), epidote (Ep) define as the foliation and groundmass.

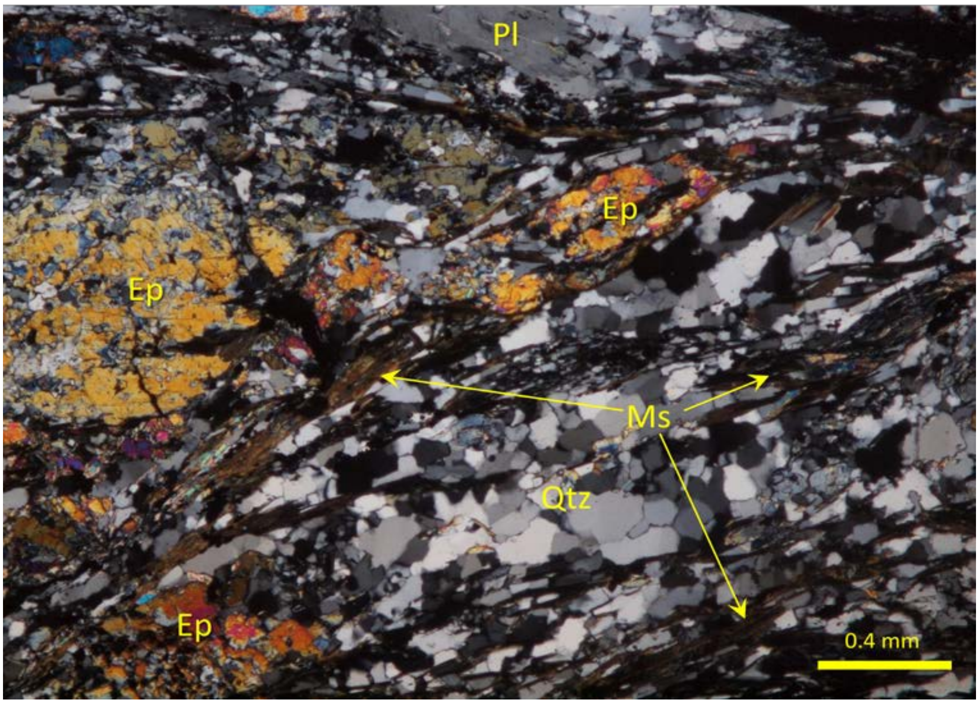

Figure 3.5 Photomicrograph mica schist (sample PM-08) with cross polar. Epidote is present as porphyroblast, plagioclase (Pl) and muscovite (Ms) define the foliation in a groundmass of quartz grains.

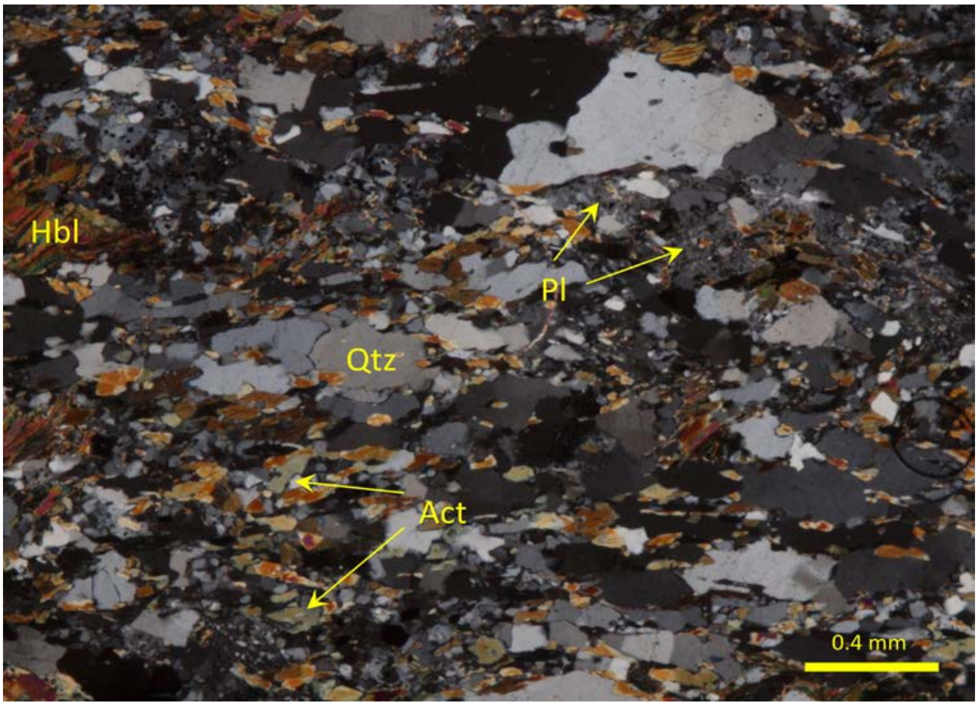

Figure 3.6 Photomicrograph amphibolite (sample BB-10) with cross polar. Quartz (Qtz), hornblende (Hbl) actinolite (Act) and plagioclase (Pl) were oriented define as foliation, these mineral assemblages are commonly in a amphibolite facies.

3.2.2 Mineral Chemistry

Chemical composition of the garnets in garnet amphibolite (PM07) and epidote amphibolite (PM-06) are dominated almandine component (X_{alm} = 57-68 % and X_{grs} = 20-30 %). Although chemical zoning are not so clear, U-shaped profile from Mg-rich (pyrope) rim to a core region low in Mg is identified, suggesting prograde growth zoning (Fig. 3.7). The relative proportions of iron and magnesium are indicative of temperature during garnet formation (Raheim & Green, 1974). Decrease of $Fe^{2+}/(Fe^{2+}+Mg)$ toward the rim indicates increasing temperature during garnet formation (Spear, 1993). Ca contents (grossular) increases from the core with a peak in the mantle zone and then decreases toward the rim, suggesting that garnets grew while the pressure was increasing in earlier stage, and then decreasing.

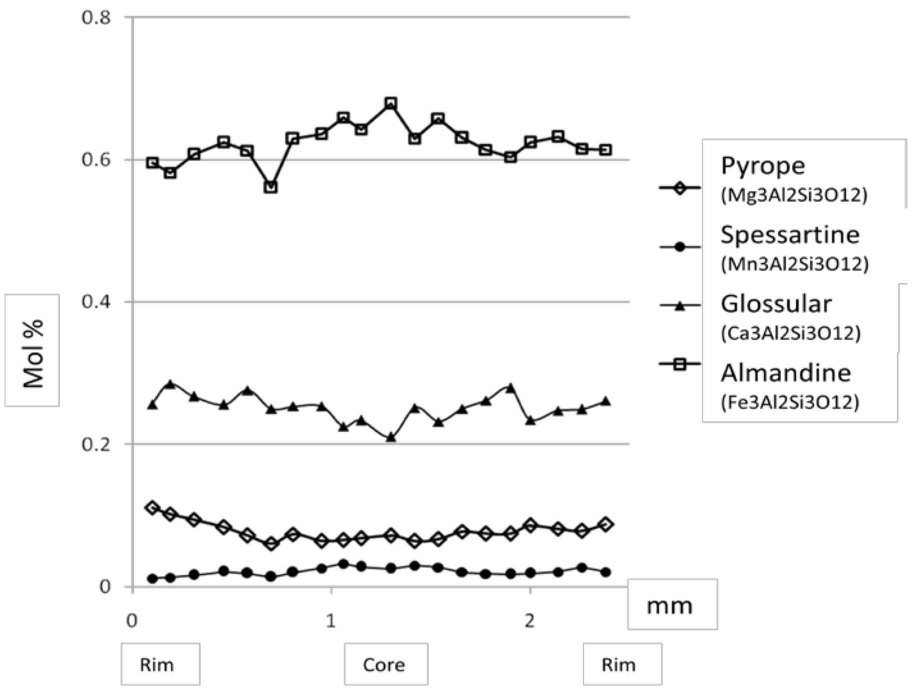

Figure 3.7 Chemical profiles of garnet of garnet amphibolite sample PM-07. Chemical data were listed in appendix 1.

As a function of $X_{Mg} = Mg/(Mg+Fe^{2+})$ versus Si content in formula (Fig. 3.8), all amphiboles are classified into Ca-amphibole, fallen in the actinolite, Mg-hornblende and Fe-hornblende field in the classification of Leake et al. (1997). Zoning is pronounced in actinolite from epidote-amphibolite and amphibolite facies (sample PM-02 and BB-11b), which show increasing both Mg and Fe contents towards the rim, whereas another sample (PM-07) from epidote-amphibolite facies is fallen in the Fe-hornblende field and does not show zoning.

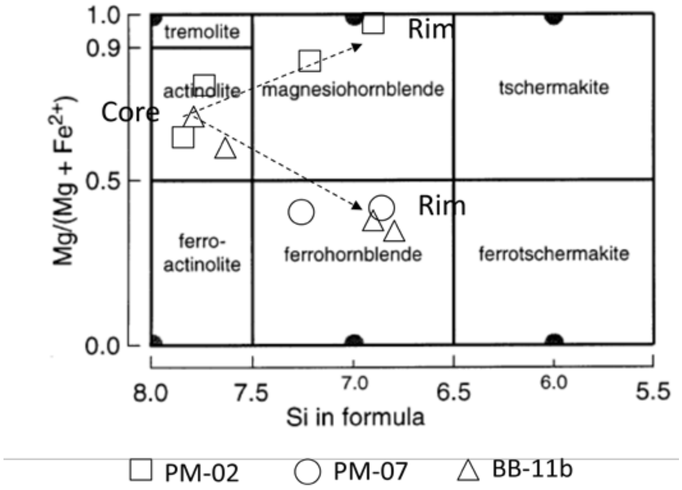

Figure 3.8 Classification of Ca-amphiboles according to Leake et al. (1997). The chemical zoning pattern (actinolite in cores, Mg-hornblende and Fe- hornblende in rims) indicates prograde metamorphic reactions.

Mica group minerals are muscovite and paragonite. Muscovite is present in sample PM-7 from garnet amphibolites facies, whereas paragonite occurred in the mica schist (sample PM-08 and PM-09). Paragonite characterized by high Na content and low or absent K contents, whereas muscovite shows low Na content and high K contents. Chlorites mostly present in all samples, representative chemistry data are listed in appendix 1 for epidote amphibolite (sample PM-02 and PM-02) and mica schist (PM-08).

Epidote is present in all the samples as elongated bipyramidal porphyloblast with the sizes ranging from 0.5 mm to 2 cm. Identification of epidote is confirmed by XRD analysis (Fig. 3.9) as well as optical microscopy and chemical analysis. Albite is present in all metamorphic rock samples. All analyses plagioclase show the Na/(Ca+Na+K)*100 values close to pure albite (>98% Ab).

Rutile is present in all metamorphic rocks as secondary mineral, representative chemical content is given in appendix 1. Hematite as secondary mineral occurs in parallel to foliation or in vein. Calcite was observed in the garnet amphibolite and amphibolites.

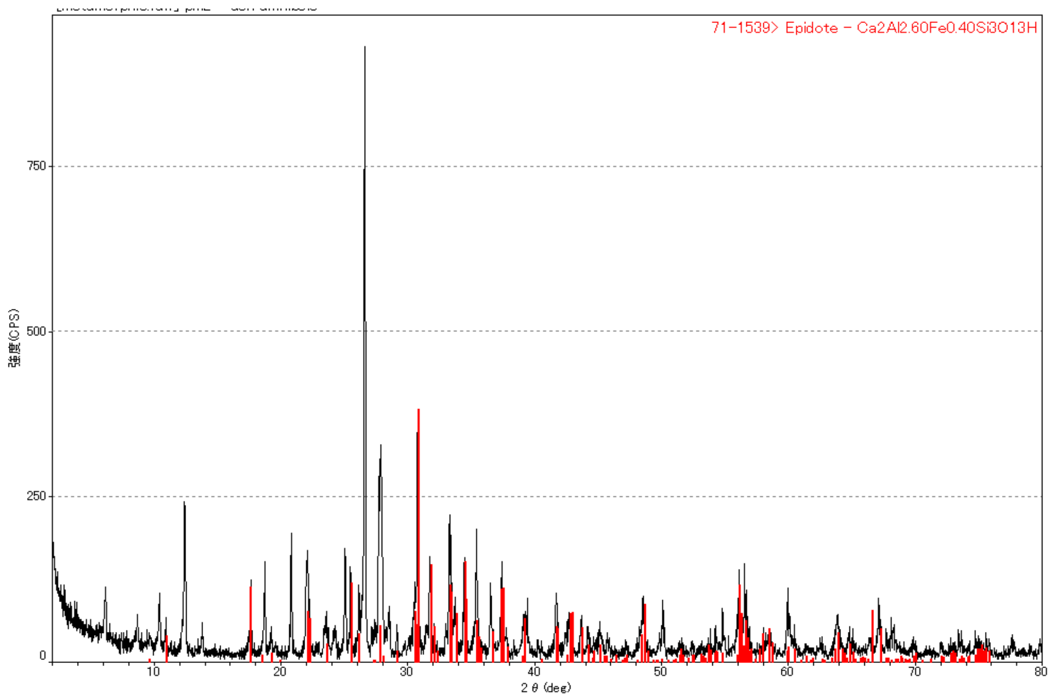

Figure 3.9 The XRD pattern of a representative epidote mineral is given overlapped peaks (red) of sample PM-02.

3.3 Thermobarometry

Most of mineral assemblages in the metamorphic rocks of the Biru area are characterized by that of amphibolite facies. Therefore using plagioclase-hornblende assemblages, it is possible to estimate the temperature of the biru metamorphic rock follow the thermometer calculation by Holland and Blundy (1994) and Blundy and Holland (1990). Pressure applied were from aluminium-in-hornblende geobarometer of Anderson and Smith (1995). Sample PM-2 from Bila River and BB-11 from Bulubuluk River were available of these assemblages as listed in EPMA data (Appendix 1). These mineral chemistries yields a temperature of 545,6±20°C and pressure of 29.8 – 30.6 kbar for PM-2, and temperature of 595,1±20°C and pressure of 45.3 – 43.6 kbar for BB-11. Results of P - T calculation from both locality indicated consistent metamorphic path estimation (Fig. 3.10) indicating that the metamorphic rocks in Biru area are medium-pressure and high-temperature type of metamorphism.

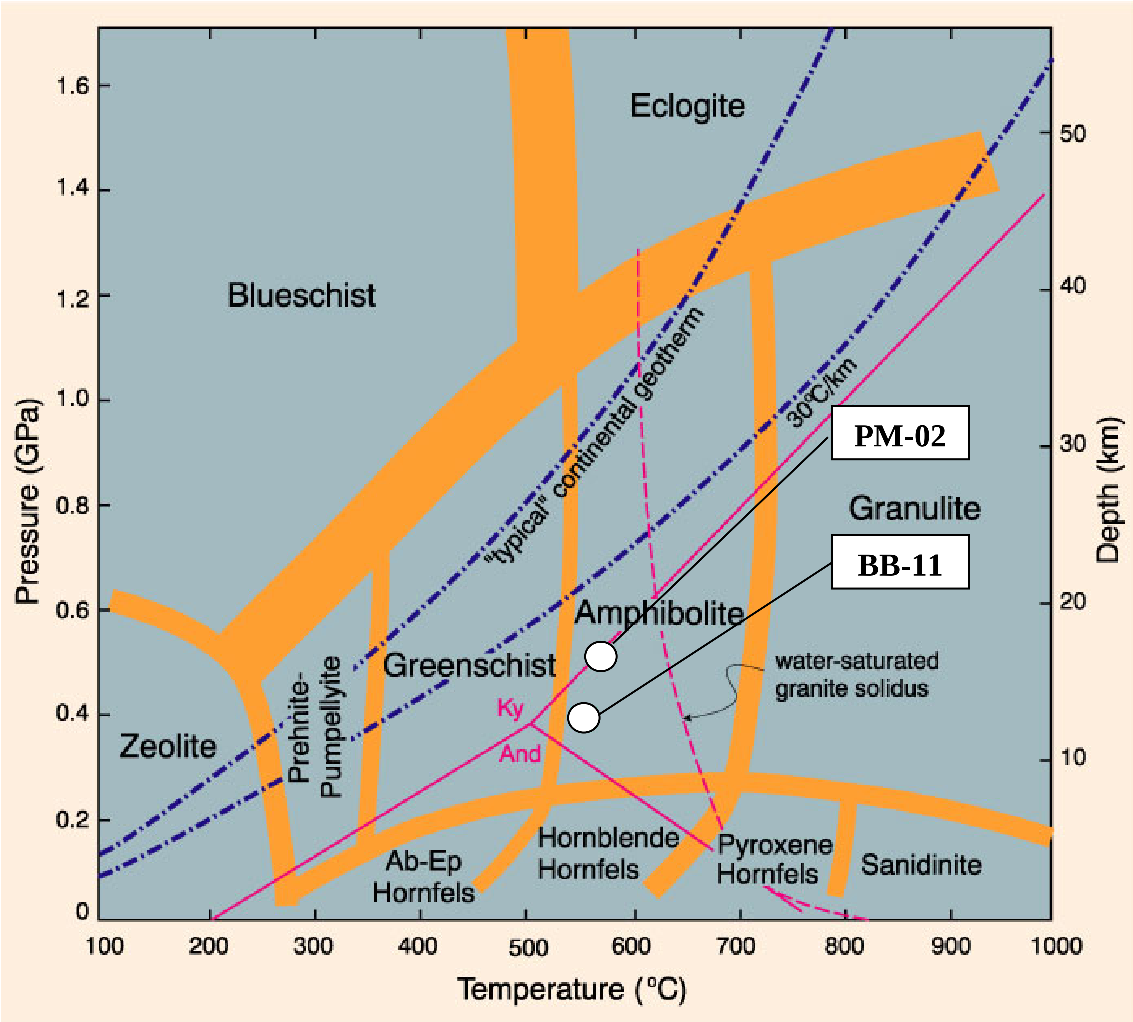

Figure 3.10 Inferred P - T diagram of ampibolite of Biru metamorphic rocks (facies diagram after Brown and Mussett , 1993)

3.4 Whole-Rocks Geochemistry

In order to understand protolith and tectonic condition associated with their genesis, whole-rock chemical compositions were determined. Major and trance elements for 11 samples were measured by XRF (Table 3.2).

Most of the tectonic discrimination diagrams, particularly those of Pearce and Cann (1973) as shown by diagrams (Fig. 3.11 and 3.12) suggest that the BMR formed in the tectonic settings: epidote amphibolite plotted in island-arc tholeiite (IAT), calc-alkali basalts and mid−oceanic ridge basalts (MORB). Whereas amphibolite mostly calc-alkali basalts as a protolith. Diagram by Meschede (1986): all epidote amphibolite samples field in calc-alkali basalts and within plat basalt and MORB as a protolith, amphibolite sample is not present in MORB.

Table 3.2 Major and trance elements from XRF data of metamorphic rocks in the Biru area

Location	Branch of Bila River							Bulubuluk River			
Rock Type	Epidote Amphibolite					Mica Schist		Amphibolite			
Sample	PM-02	PM-05	PM-06	PM-07	PM-30	PM-08	PM-09	BB-08	BB-10	BB-11a	BB-11b
SiO2	52.24	51.73	50.12	55.55	41.54	59.57	64.87	56.30	70.42	77.58	59.51
TiO2	1.02	1.26	0.83	0.70	1.19	1.67	0.68	0.74	0.59	0.22	0.65
Al2O3	18.09	17.87	19.11	18.94	18.29	17.79	18.26	15.12	14.61	5.23	17.00
FeO*	10.83	9.88	9.34	6.78	14.30	9.67	7.44	9.41	4.25	6.81	6.26
MnO	0.12	0.12	0.16	0.20	0.18	0.07	0.04	0.15	0.05	0.16	0.18
MgO	4.93	4.99	5.48	3.22	3.38	2.63	1.55	6.51	2.58	2.30	2.12
CaO	9.57	11.18	11.89	10.95	20.92	5.96	0.72	6.56	2.99	6.34	9.65
Na2O	2.72	2.61	2.80	2.72	0.12	0.75	2.40	5.34	3.93	0.86	2.88
K2O	0.70	0.35	0.39	1.62	0.35	1.69	3.13	0.36	1.16	0.27	1.25
P2O5	0.09	0.15	0.10	0.13	0.12	0.44	0.11	0.11	0.10	0.06	0.11
TOTAL	100.32	100.14	100.21	100.81	100.37	100.23	99.19	100.60	100.68	99.84	99.60
Ba	47.30	51.10	63.50	244.60	60.60	96.20	1588.70	80.60	158.90	24.00	157.80
Cu	25.69	123.33	136.86	19.05	9.13	30.02	87.78	80.59	33.90	221.31	14.60
Zn	68.51	69.68	78.83	73.78	63.73	68.65	135.43	73.16	21.73	34.33	58.52
Zr	53.80	74.50	55.60	82.50	84.10	92.60	117.70	77.50	101.70	75.60	73.80
Rb	11.62	7.40	7.60	32.15	4.30	19.87	53.14	7.25	22.43	4.80	29.62
Sr	293.30	321.80	326.40	303.80	548.90	265.70	74.10	221.00	232.40	157.80	288.80
Nb	3.48	5.35	3.42	3.39	3.14	5.86	5.06	3.06	5.77	5.02	3.91
Co	36.74	36.81	34.12	27.40	23.02	16.96	14.23	39.60	10.59	15.65	21.42
Cr	419.61	384.47	481.46	443.73	330.55	117.60	146.06	261.05	308.15	175.70	530.69
Ni	210.81	196.04	253.46	228.85	123.66	58.63	77.78	115.25	150.65	104.30	258.35
Y	18.30	20.70	16.30	19.50	21.80	28.70	28.30	17.50	25.40	27.20	18.80
V	278.60	307.40	269.10	255.90	259.80	353.30	208.50	279.30	53.20	36.50	249.70

* Fe total

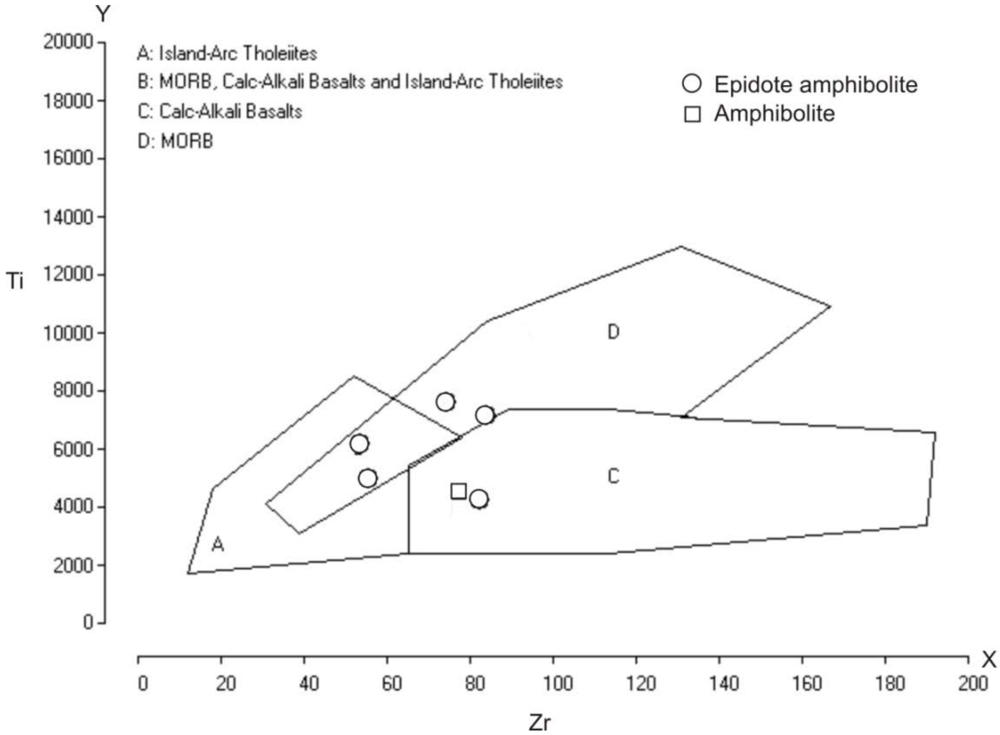

Figure 3.11 Discrimination diagram using Ti versus Zr (Pearce and Cann, 1973). The Biru amphibolites field on calc-alkali basalts (2 samples), MORB, calc-alkali basalts and island-arc tholeiites (2 samples) and MORB (2 samples).

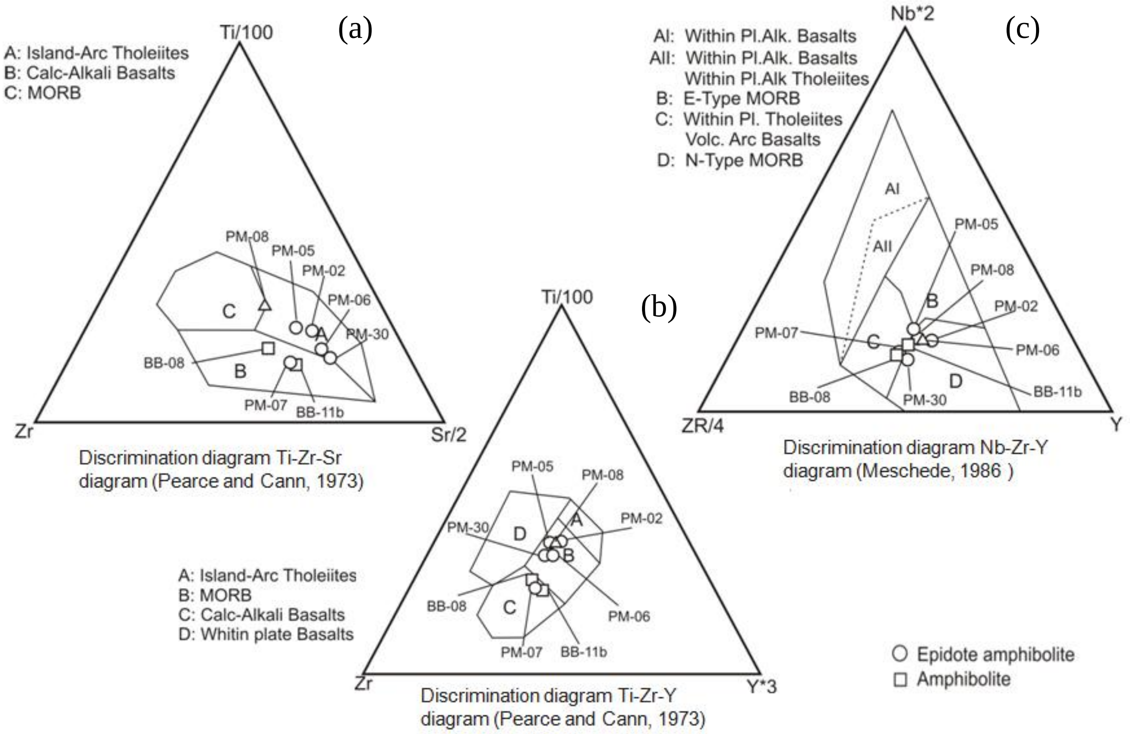

Figure 3.12 (a) Discrimination diagram using Ti-Zr-Sr diagram (Pearce and Cann, 1973) the samples as mostly island-arc tholeiites (4 samples), calc-alkali basalts (2 samples). (b) Discrimination using Ti-Zr-Y digram (Pearce and Cann, 1973) the samples as mostly MORB (4 samples), calc–alkali basalts (2 samples). (c) Samples plotted on Nb-Zr-Y by Meschede (1986) as mostly N–MORB (3 samples), within plate tholeiites volcanic, arc-basalts (2 samples) 1 samples in transition both of them.

3.5 Deformation Structures

Deformation structures pervasively are developed in the metamorphic rocks. One main schistosity (S1) defined by preferred orientation of major component of minerals is distinguished in the field. Epidote porphyroblast aligns with its long axis parallel to main schistosity (S1). Two groups of fold structure with different orientation and style is distinguished in the field (Bulubuluk River) (Fig. 3.2d, F1); tight to isoclinal fold with SSW trending axis and F2; gentle-open fold with ENE−WSW trending axis. Axial plane of F1 fold is parallel or subparallel to S1 schistosity. F2 folds are superimposed on preexisting F1 folds.

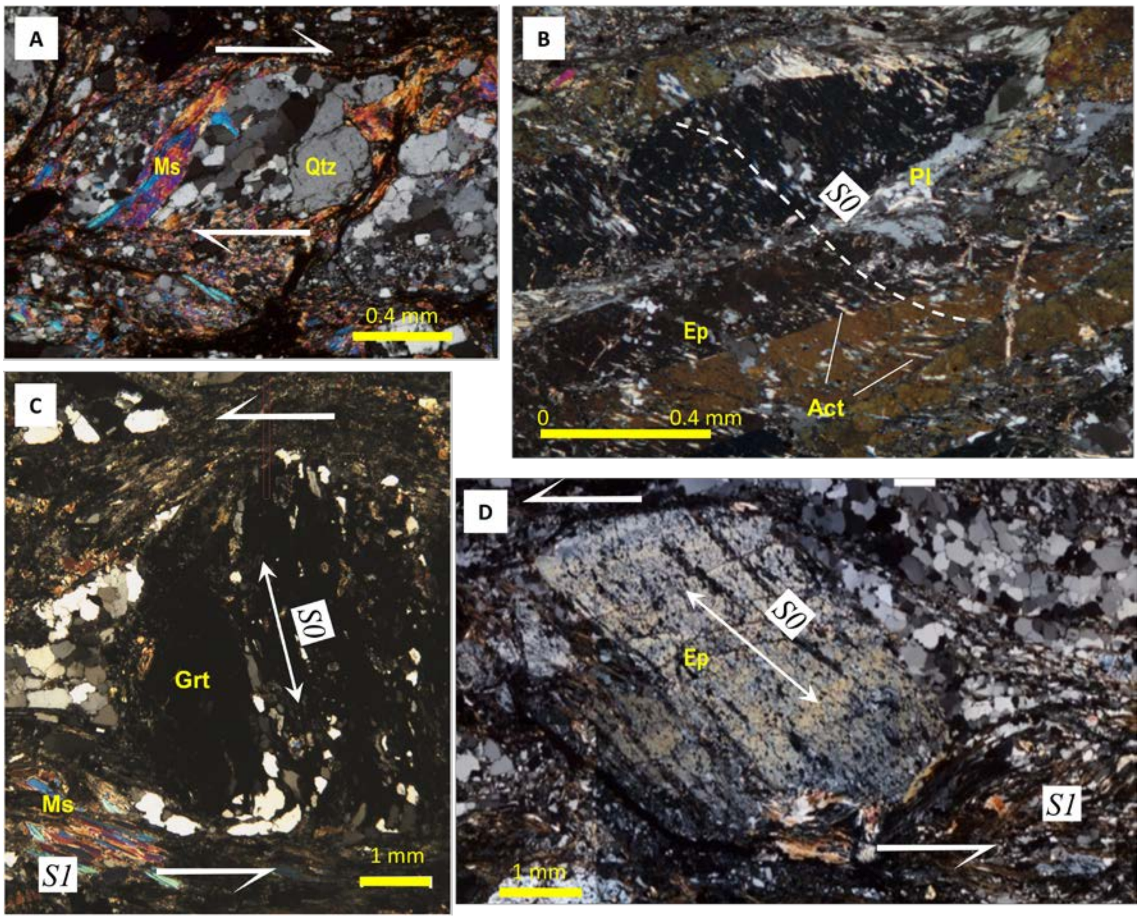

Figure 3.13 Deformation microstructures: (a) Cataclastic texture showing dextral shear (PM-09); (b) inclusion trail on epidote porphyroblast (PM-02); (c) S-shape inclusion trails of garnet porphyroblast are indicating sinistral sense of shear (PM-07); (d) epidote porphyroblast is rotate reflecting sinistral sense of shear (PM-08).

3.6 Deformation Microstructures

Schistosity is defined by banding and shape preferred orientation of major component of minerals. The chlorite and quartz inclusion in large epidote and albite porphyroblasts in sample PM-02, PM-05 show subhedral grain shape. They often align with its long axis parallel to main schistosity (S1), but partially oriented obliquely defining an older schistosity S0, as shown in Fig. 3.13b. Large grains in the rocks are fractured. Epidote porphyroblats is extended in brittle manner forming microboudin subparallel to S1. The spaces of the boudins are often filled by quartz pool (Fig. 3.15)

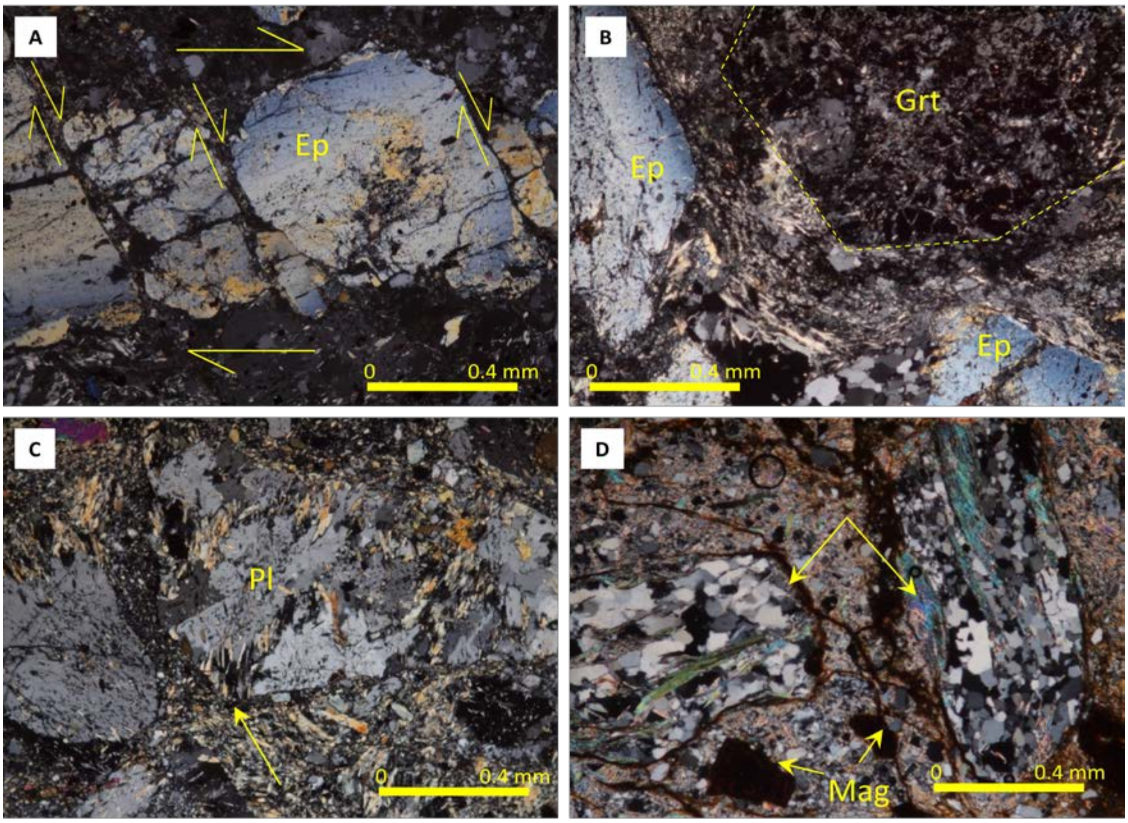

Figure 3.14 Cataclastic textures. (a) Microboudin developed in Epidote porphyroclast, domino−type fragmented porphyroclast of epidote (Ep) shows microfault normal to foliation indicated top to the right sense of shear (PM-05). (b) Garnet (Grt) grain collided with epidote minerals (PM-06). (c) Cataclasite fabric with angular fragments of plagioclase in a fine matrix. (d) Fragmented muscovite schist. Original rock fragments (arrow) are rotate, array of opaque minerals parallel to foliation plane (PM-09).

The schistosity S0 in porphyroblast of garnet amphibolite (Sample PM-07) is defined by shape preferred orientation of epidote, hornblende and muscovite and array of garnet (Fig. 3.13c). Epidote occasionally shows elongated shape and fractures filled by quartz. Asymmetric of domino-type boudin indicate dextral shear sense. Garnet porphyroblasts surrounded by the youngest schistosity defined by muscovite (S1). Garnet porphyroblast often exhibit strait or slightly curved inclusion trails which are discordant with external schistosity. Some porphyroblasts include S-shape inclusion trails, indicating rotation (Fig. 3.13c).

In the mica schist (sample PM-09), asymmetry of pressure shadows around quartz porphyroclasts and muscovite fishes indicate dextral sense of shear (Fig. 3.13a). Pyrite and hematite grains also present aligning parallel to schistosity but without pressure shadows surrounding. Therefore, they developed in hydrothermal process and possibly no more deformation after emplacement of plutonic rocks (Fig. 3.14d). Whereas mica schist of sample PM-08 (epidote-amphibolites facies) exhibits a sinistral sense of shear evidenced by asymmetry of pressure shadows around the epidote porphyroblasts (Fig. 3.13d).

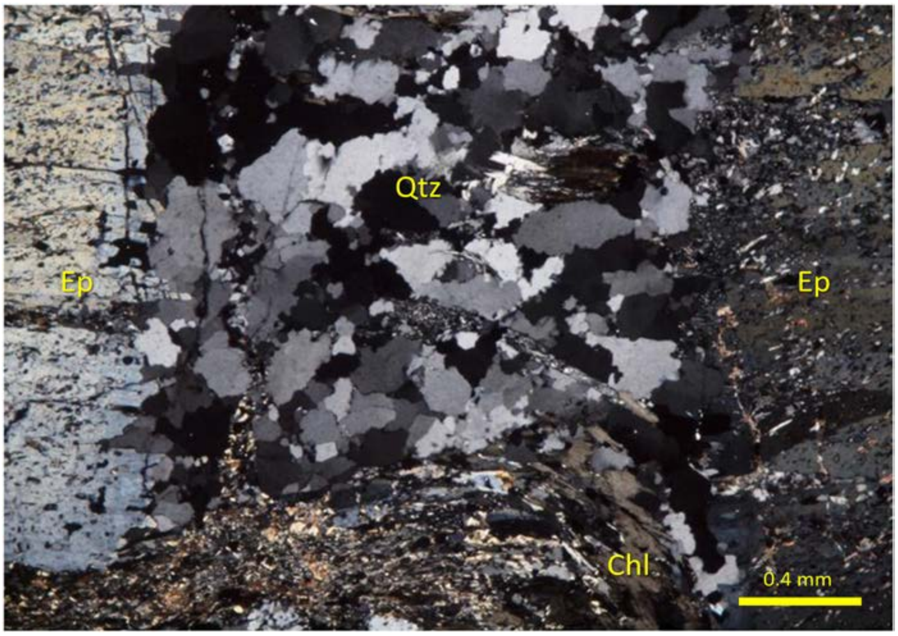

Figure 3.15 Epidote porphyroblats as a microboudin formed subparallel to S1. The spaces of the boudins (center) were filled by quartz pools (Qtz).

3.6.1 Texture of Quartz Aggregates

Mean grain sizes of quartz in metamorphic rocks (Fig. 3.17) range from 108 to 118μm for sample collected inside of the metamorphic body, 111μm for that 50m from boundary with granodiorite. In contrast, grain size of sample BB-11a close to the contact with granodiorite is 398μm in average.

Fig. 3.17 show that the aspect ratio of quartz grains slightly increases from samples (PM-02, PM-05, PM-07, PM-08) of Bila River (far from plutonic body intruded) to samples (BB-10 and BB-11a) of Bulubuluk River (close to plutonic body). All samples from Bila River have mean aspect ratio ranging from 1.3 to 1.6, whereas those of samples from Bulubuluk River are about 1.7.

Table 3.3 Texture of quartz grains

Sample No.	Grain Boundary and Size Distribution	Dynamic Recrystallization and Recovery
PM-2	Serieted , inequigranular	Very rare bulging (0.01-0.03 mm), very rare subgrains, low missorientation
PM-5	Equant to serieted, inequigranular	Very rare bulging (0.01-0.03 mm), very rare subgrains, low missorientation
PM-7	Serieted , inequigranular	Bulging is not present, very rare subgrains, low missorientation
PM-8	Polygonal, equigranular	Very rare bulging (0.02-0.05 mm), very rare of subgrains, low missorientation
BB-10	Elongated, inequigranular	Very rare bulging (0.02-0.03 mm), very rare subgrains, low missorietation
BB-11	Polygonal-elongated, inegranular	Very rare bulging (0.02-0.03 mm), very rare subgrains, low missorientation

Most of quartz grains show moderately seriate-interlobate boundary geometry caused by grain boundary bulging which is driven by local gradient of strain energy, although some quartz grains have polygonal shapes with straight grains boundaries (Table 3.3 and Fig. 3.16a). Dislocation substructures are not pervasively developed, although slight undulatory extinction associated with kink structure is observed as an array of elongated subgrains (Fig. 3.16b). Dynamically recrystallized grains formed by both bulging recrystallisation (BLG) and subgrain rotation (SGR) are hardly found in quartz aggregate in metamorphic rocks (Fig. 3.16b). Grain composing quartz pool filling the space of microboudin shows equant grain shape without evidence of deformation (Fig. 3.15). Grain boundary migration (GBM) minimizing grain boundary energy could be operated under high temperature and possibly both dynamic and static condition. Similar texture would be developed in both case, and therefore it can be hardly distinguished. However, mineral assembly and texture of Biru metamorphic rocks suggest epidote-amphibolite to amphibolite facies condition. Therefore, presently observed texture of quartz aggregates may have been developed under an effect of granodiorite intrusion.

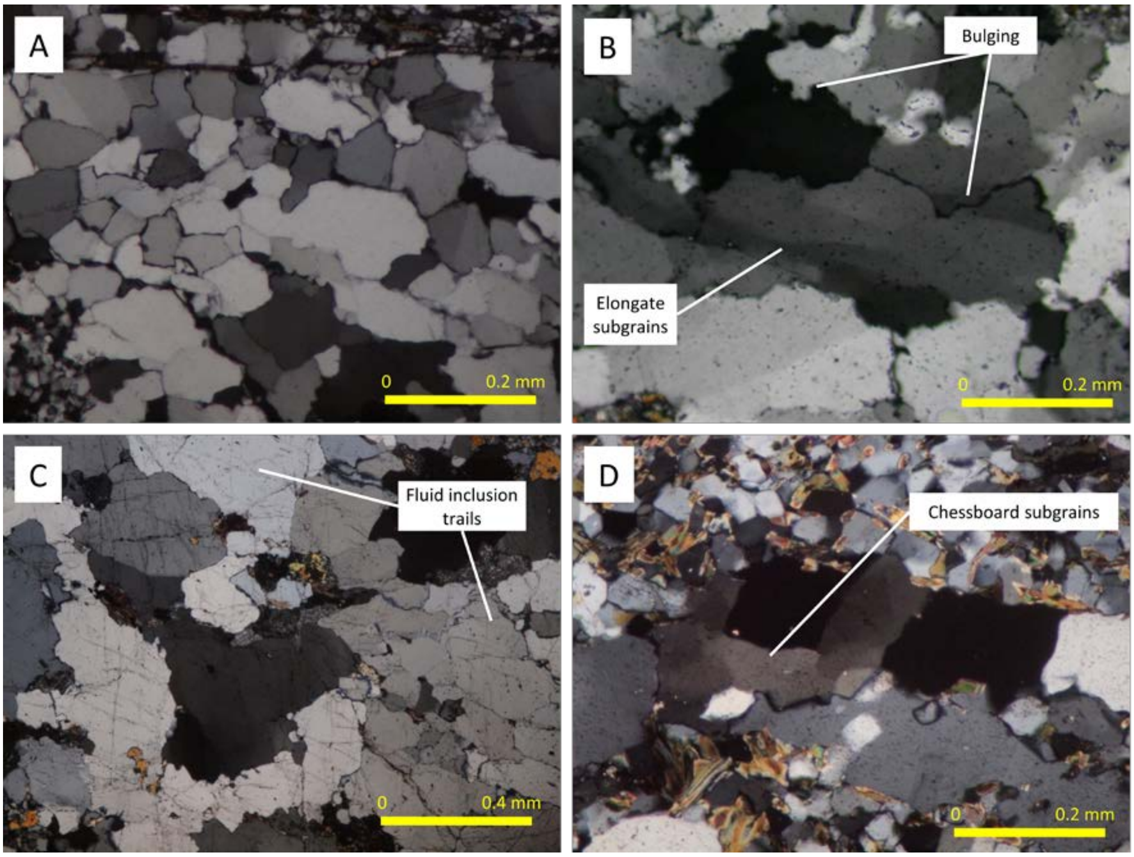

Figure 3.16 (a) Inequigranular-polygonal textures of quartz aggregate in sample PM-08. (b) Bulging grain boundary and elongate subgrains (PM-07). (c) Numerous fluid inclusion trails in core of quartz grains indicating fracturing and healing (BB-11a). (d) Relic of a chessboard subgrains in sample BB-10.

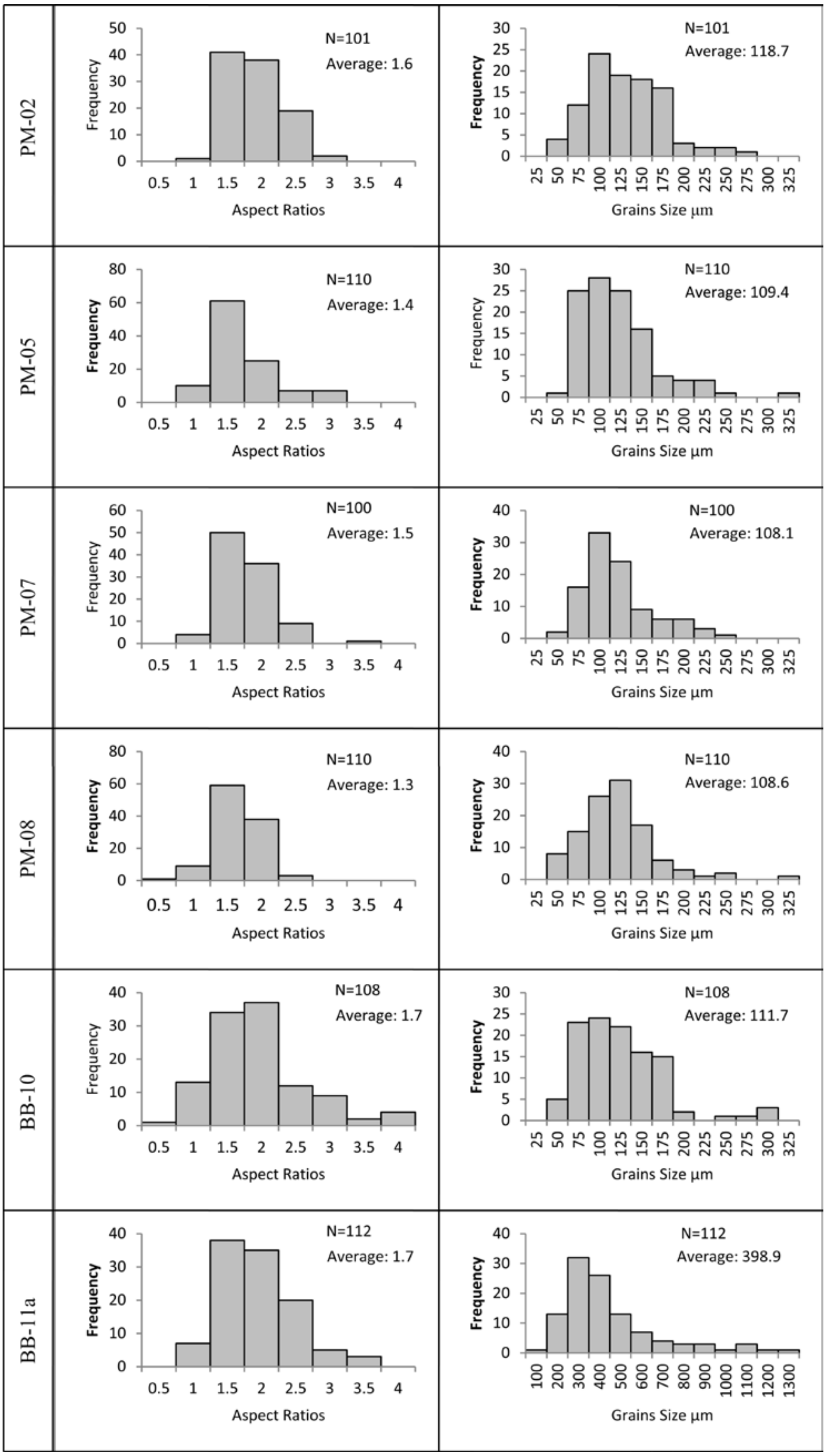

Figure 3.17 Graphs of distribution of aspect ratio (left column) and grains size (right column) calculated from log-axis and short-axis of quartz grains.

3.6.2 Crystallographic Preferred Orientation of Quartz

Crystallographic preferred orientation of quartz were measured using EBSD technique (Fig. 3.18) for four samples from Bila River (PM-2, PM-07 and PM-8) collected close to small granodiorite body and one from Bulubuluk River (BB-11) near from large granodiorite body.

C-axis LPO of PM-8 (Fig. 3.18c) forms small girdle around Z and a cross girdle diminished around Y, which dominant slip system is basal <a>. Asymmetric pattern suggests the non-coaxial character of quartz deformation. However, c-axis fabric patterns with maximum around Y are also obtained (PM-2; Fig. 3.18a), which suggests dominant operation of prism<a> slip system. The LPO patterns are not generally intense and some of them look to be controlled by orientations of a small numbers of host grains (Fig. 3.18b and Fig. 3.18c). They suggest that LPO patterns developed during plastic deformation were partially removed by annealing during later granodiorite intrusion.

3.7 K–Argon Dating

K–Ar dating of muscovite from garnet-amphibolite sample PM-07 from Bila River around Pammusureng village yielded 109 ± 2.4 Ma as listed in Table 3.4. It is chiefly consistent ages with another metamorphic complexes in the South Sulawesi, although slightly older than Barru complex (106 ± 6 Ma) and younger than the age of Bantimala complex (114 ± 6–132 ± 7 Ma) (Wakita et al., 1994).

Table 3.4 K–Ar ages whole-rock from metamorphic rock of PM-07 in Biru area

Sample No.	Measured Object (Mesh Size)	Potassium Content (wt.%)	Origin of Radioctive ^{40}Ar (10^{-8}cc STP/g)	K-Ar Age (Ma)	Origin of Non Radioctive ^{40}Ar (%)
PM-07	Muscovite (＃60-150)	7.914 ± 0.158	3465.9 ± 34.7	109.5 ± 2.4	5.6

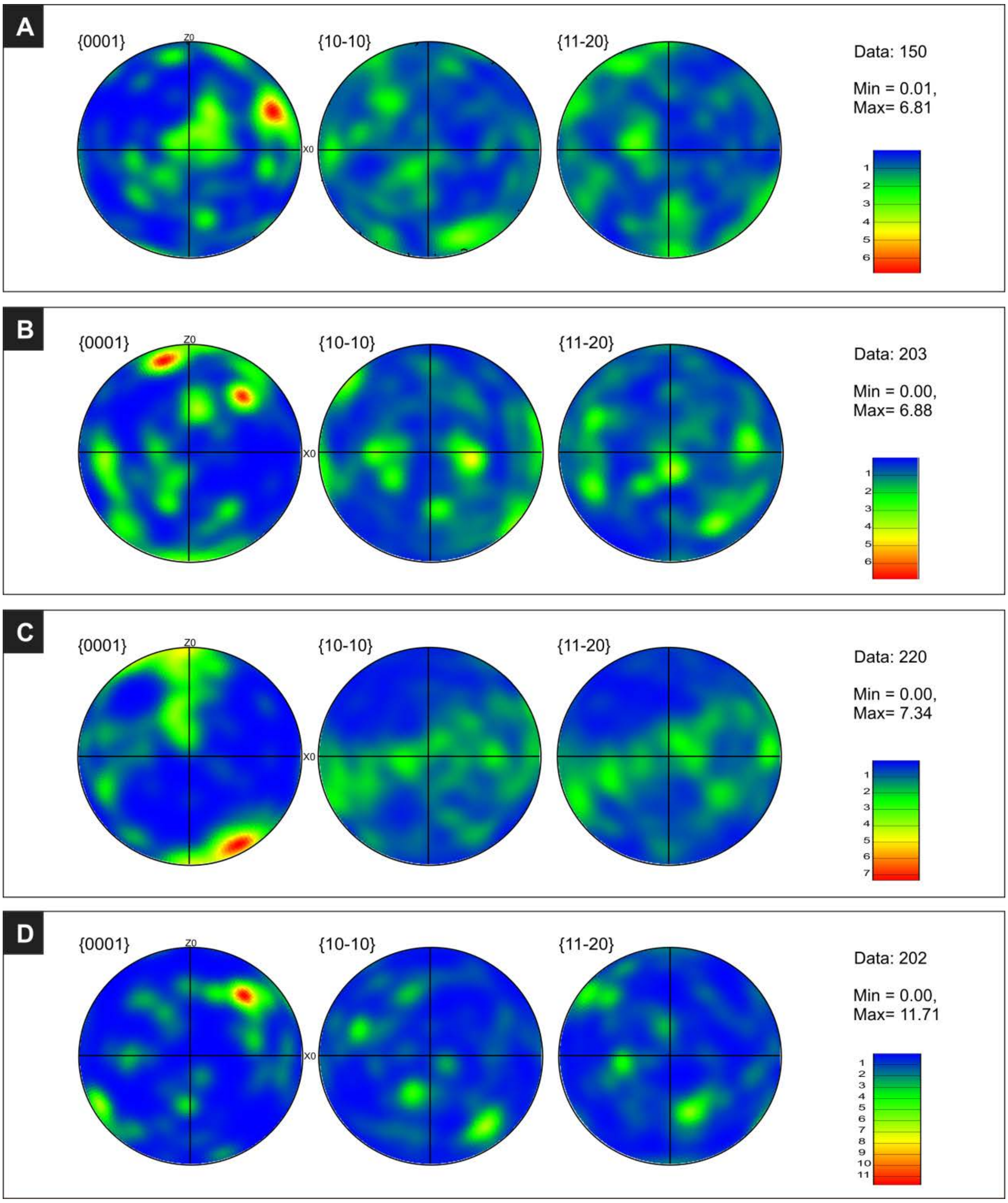

Figure 3.18 Stereoplots of quartz crystallographic orientation. Sample from branch of Bila River are (a) PM-2, (b) PM-07 and (c) PM-08 and sample from Bulubuluk River (d) BB-11a. ‘Min” and “Max” correspond to the minimum and maximum density correction. The poles of planes {0001} are the quartz [c] axes, whereas the poles to the sets of planes {11-20} or {10-10} correspond to the <a> axes.

3.8 Deformation and Metamorphic Sequence

The deformation and metamorphic sequences in the Biru area was summarized in Fig. 3.19. Mainly mafic volcanic rocks were metamorphosed in the epidote amphibolites and amphibolites facies in the first metamorphism (M1) during Early Cretaceous.

The metamorphism was simultaneous with deformation (D1). The oldest schistosity (S0) was defined by preferred orientation of quartz, amphiboles and plagioclases in core of garnet, epidote and plagioclase porphyroblasts. A main schistosity (S1) parallel to isoclinals fold axial plane (F1, F2) formed during the later stage of the first metamorphism (M1). The evidence of deformation (D1) in the quartz texture is commonly very limited, it seemingly caused by annealing and healing, although array of elongated subgrains and seriated boundaries as relict of deformation still recorded. *c*-axis LPO pattern of quartz from Bila River (PM-08) suggest the non-coaxial flow under the dominant operation of basal<a> slip system.

The second metamorphism (M2) is associated with the emplacement of granodiorite rocks during Middle Miocene (19 ± 3.4 Ma of fission track age by van Leeuwen, 1981). The emplacement of Biru granodiorite rocks was also facilitated by uplifting. The high quartz content of amphibolites close to granodiorite body indicated that the metamorphic rocks was affected by silisification at the contact in Bulubuluk River; BB-08, BB-10 and BB-11) and lower part of metamorphic in Bila River (PM-08; PM-09). This event removed texture of D1, particularly in quartz aggregates.

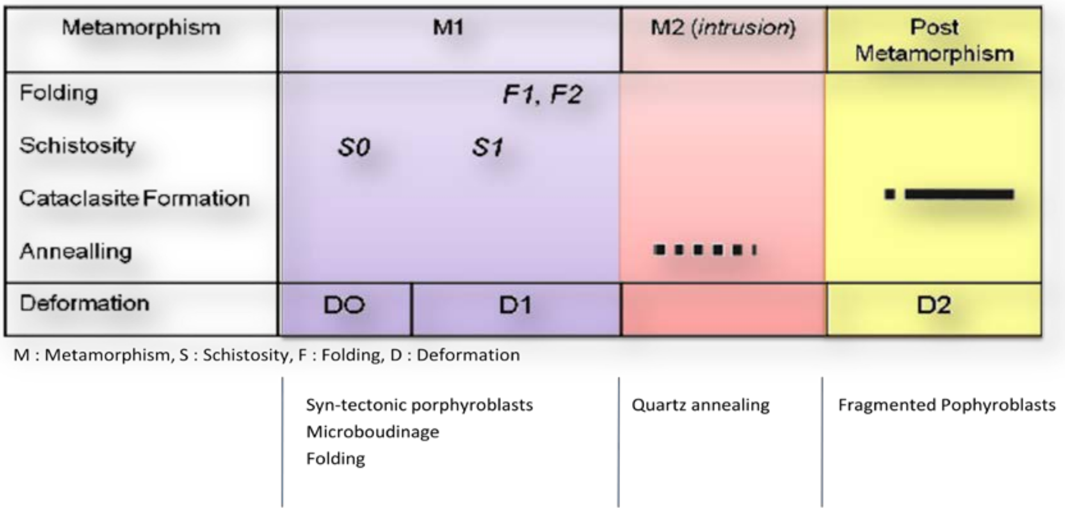

Figure 3.19 Summary of deformation and metamorphic sequences of Biru metamorphic rocks.

The second deformation (D2) is of post metamorphism and characteraized by pervasive cataclastic texture. The deformation may be related to uplift event and activity of WWF, which formed during regional extension in the Mid-Miocene (van Leeuwen et al., 2010).

3.8 Correlated with Basement Rocks in South Sulawesi

In this section, the Biru Metamorphic Complex will be compared with another basement Rocks in South Sulawesi. They are the Bantimala and Barru Complex, which are also exposed in the West Dividing Mountain Range.

Striking directions of Biru are generally WSW−ENE and ESE−WNW and vertical to steeply east dipping. Structure features in Barru mostly similar to that in Biru, and conformable with those of Biru metamorphic rocks, which is WSW−ENE striking and steeply dipping to SE, while Bantimala Complex is commonly NNW−SSE, occasionally NW-SE striking and roughly NE steep dipping.

Chemical data indicate that the protolithes of the basic metamorphic rocks in the Biru Complex are MORB, calc-alkali basalts and Island-arc tholeiites (IAT), which is similar to the tectonic environment of the Barru blocks. Ages of metamorphism for both complex also show similarities (Table 3.5), K-Ar dating of metamorphic rocks in Barru area yield 106 ± 6 Ma (Wakita et al., 1994), whereas that of mica in garnet-amphibolite from Bila River yielded 109 ± 2.4 Ma or lower Cretaceous series.

The metamorphic rocks in Bantimala Complex have quite different characteristics with Biru and Barru areas, with high grade of high pressure type metamorphism represented by eclogite and blueschist. The estimated P–T conditions from eclogites indicate that these metamorphic rocks were subducted to 65–85 km (Miyazaki et al., 1996). The ages of the highest grade rocks of the Bantimala metamorphic Complex are older than the Biru and Barru metamorphic rocks ranging from 114 ± 6 Ma to 132 ± 7 Ma (Wakita et al., 1994). However, some previous work proposed that the Pompangeo schist complex in central Sulawesi probably generated in same subduction system as well as Bantimala-Barru and other accretionary complex in western Sulawesi (e.g. Parkinson, 1998a).

Three metamorphic slices in South Sulawesi Bantimala, Barru and Biru areas are commonly spread extends to N−S directions. However the Bantimala Block shows a strong tectonic fabric striking, which is defined deep subduction zone. In the Barru area associated rocks relatively rare than Bantimala and protolith rocks are more felsic than in Bantimala (Table 3.5), indicated shallow tectonics environment, metamorphic in Barru relatively similar that in Biru area. Therefore, the Biru metamorphic rocks may also belong to a range of tectonic environment of the Bantimala-Barru Complexes.

Table 3.5 Summary of metamorphic rocks types, protolith and associated rocks of metamorphic rocks in South Sulawesi.

	Bantimala	Barru	Biru
Metamorphic Rocks Types	Eclogite Blueschist Greenschist	Amphibolite Greenschist Low grenschist	Amphibolite
Metamorphic Protolith	N-MORB OIB IAB	N-MORB OIB	N-MORB IAB IAT
P - T Condition	550-620 °C up to 2,8 GPa	500-520 °C 13 - 21 Kb	545-595 °C 2,76 -4,65 Kb
Associated Rocks			
Ultramafic Rocks	Present	Present	Not present
Melange	Present	Not present	Not present
Radiolarian Chert	Present	Present	Not present
Cretaceous Sedimentary Rocks	Present	Present	Present
Volcanics Paleogene	Present	Not present	Present

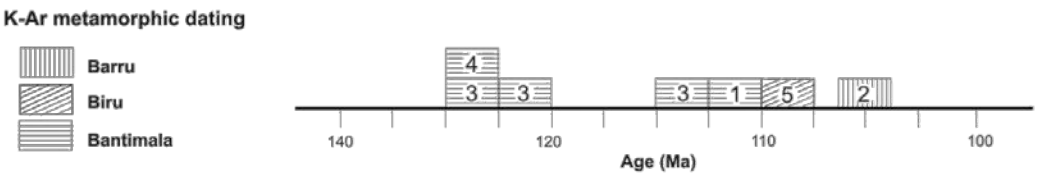

Metamorphic rocks types and protolith of Bantimala referred by Maulana (2009). Age dating references, 1: Sukamto (1982); 2: Wakita et al., 1994; 3: Wakita et al., 1996; 4: Parkinson et al., 1998; 5: present study.

Present position of these metamorphic rocks of two contrasting types of metamorphic are relatively parallel (Fig. 3.20), one representing very high temperature metamorphic blocks (Parkinson, 1998a; Miyazaki et al., 2004) of deep environment or the subduction zone (Bantimala) is crop out to the westward side and the other representing low-intermediate metamorphic grade of shallow crustal or volcanic arc (Barru and Biru) is crop out in the eastern side. They may constitute as pair metamorphic rocks in the same a plate tectonic and appear to be contemporaneous occurrence but they occur in the different metamorphic environment, however Bantimala complex slightly older than Barru and Biru blocks.

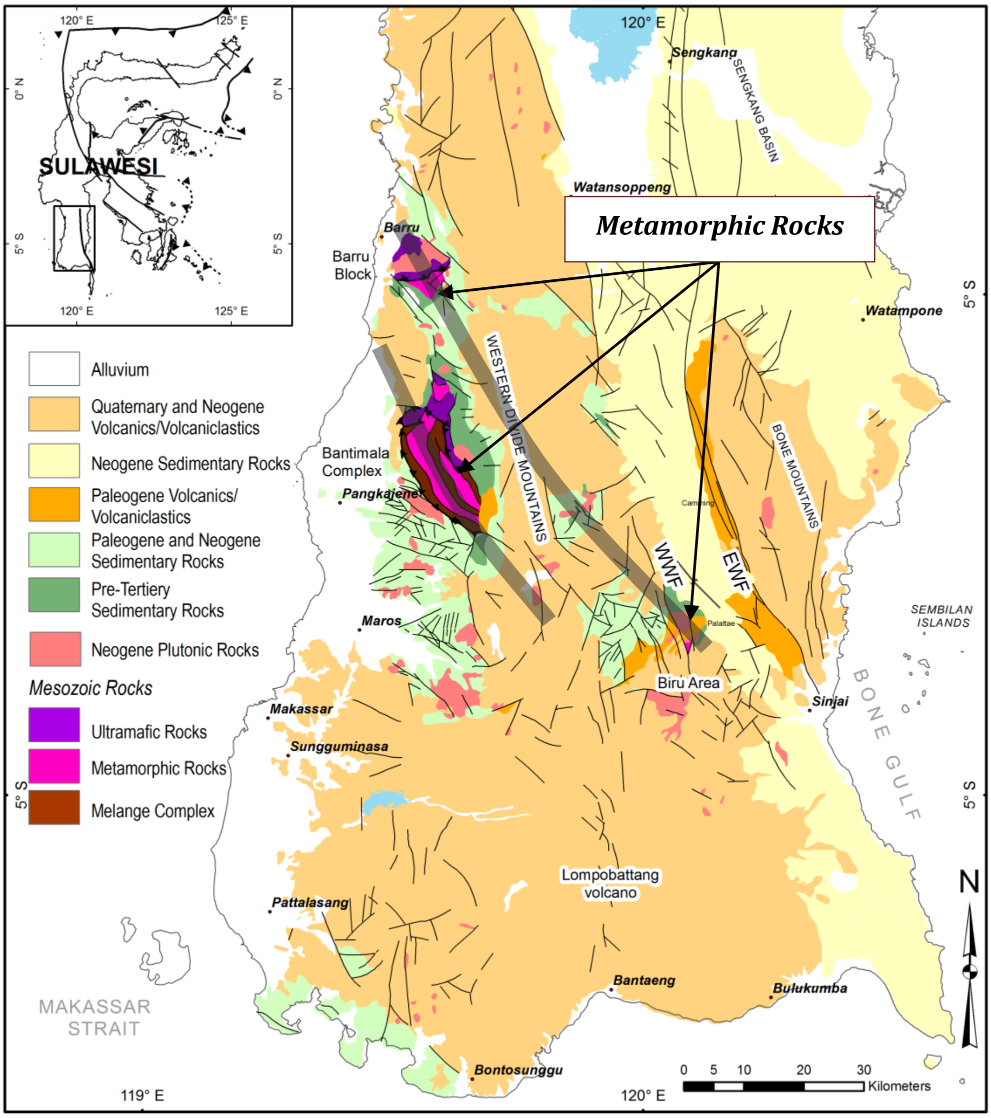

Figure 3.20 Geological map of the South Sulawesi area showing distribution adjacent three metamorphic blocks, Bantimala Complex at west side, Barru and Biru metamorphic at eastern side (denoted dark lines indicated resemblance of typical metamorphic rocks).

CHAPTER IV. WALANAE FAULT ZONE

4.1 West Walanae Fault Zone

Deformation and stress field associated with activity of the West Walanae fault zone were analyzed in the Biru area (Fig. 4.1), fault–slip data and dike segments data were listed in appendix 2 and 3 respectively.

4.1.1 Description of Deformation Structure

Deformations under brittle condition are well observed in Bulubuluk and Biru Rivers (Fig. 4.1). These structures are preserved widespread on Paleogene to Late Miocene volcanics and Miocene plutonic rocks. The meso–scale faults are mutually cross-cutting, but no specific generations of faulting can be defined. Fractures and joints are commonly filled by calcite and quartz. The width of fault is a few centimeter or lower. Numerous dissolution seams (Fig. 4.3b) with millimeter to centimeter in wide and containing sulfide minerals are found in this area. Andesite and basalt dike segments are present in various wide ranging from several centimeters to meter. Dike rocks also show numerous fractures and occasionally cross cut by faults (Fig. 4.2). A basaltic dyke in Biru river show structure of ductile deformation being dragged by a cross cutting fault (Fig .4.2), suggesting that faulting and intrusion of volcanic rocks were coeval.

In downstream of these rivers, the Cretaceous Marada formation consisting alternation of mudstones, siltstones and sandstones are widely exposed. They are well bedded and dip to low to moderately.

4.1.2 Minimum Principal Stress Orientation (σ_3) derived from Dike Segments

Dikes are planar tensile cracks filled with magma (Clemente et al., 2007), and dike walls are assumed to be perpendicular to the least compressive stress (Pollard, 1987; Clemente et al., 2007). Therefore, σ_3 paleostress orientation can be determined analyzing dikes.

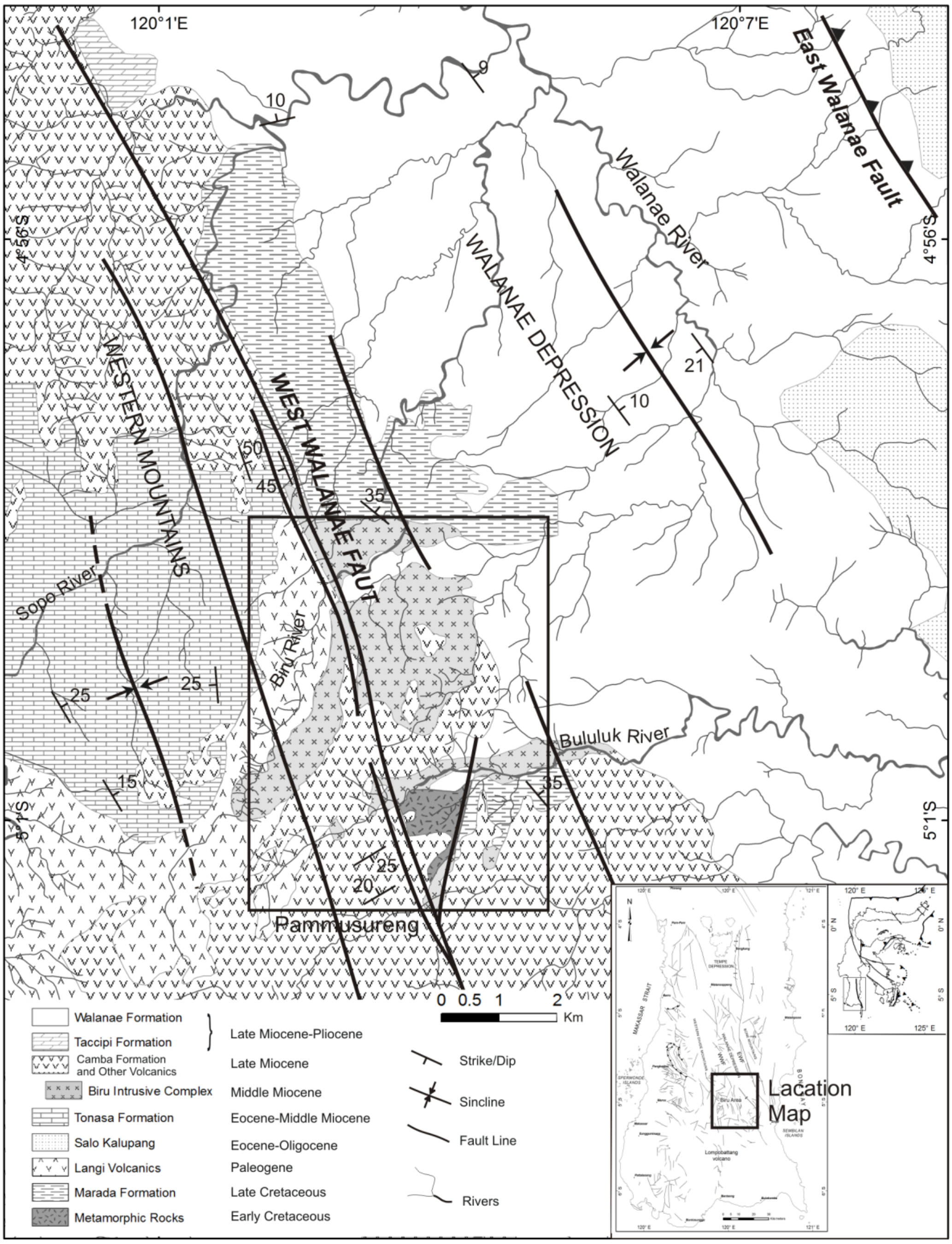

Figure 4.1 Geological Map around the West Walanae Fault Zone, paleostress field investigations of WWF were focused shown in box line (Modified after Leeuwen, 1981; Sukamto, 1982; Sukamto and Supriatna, 1982).

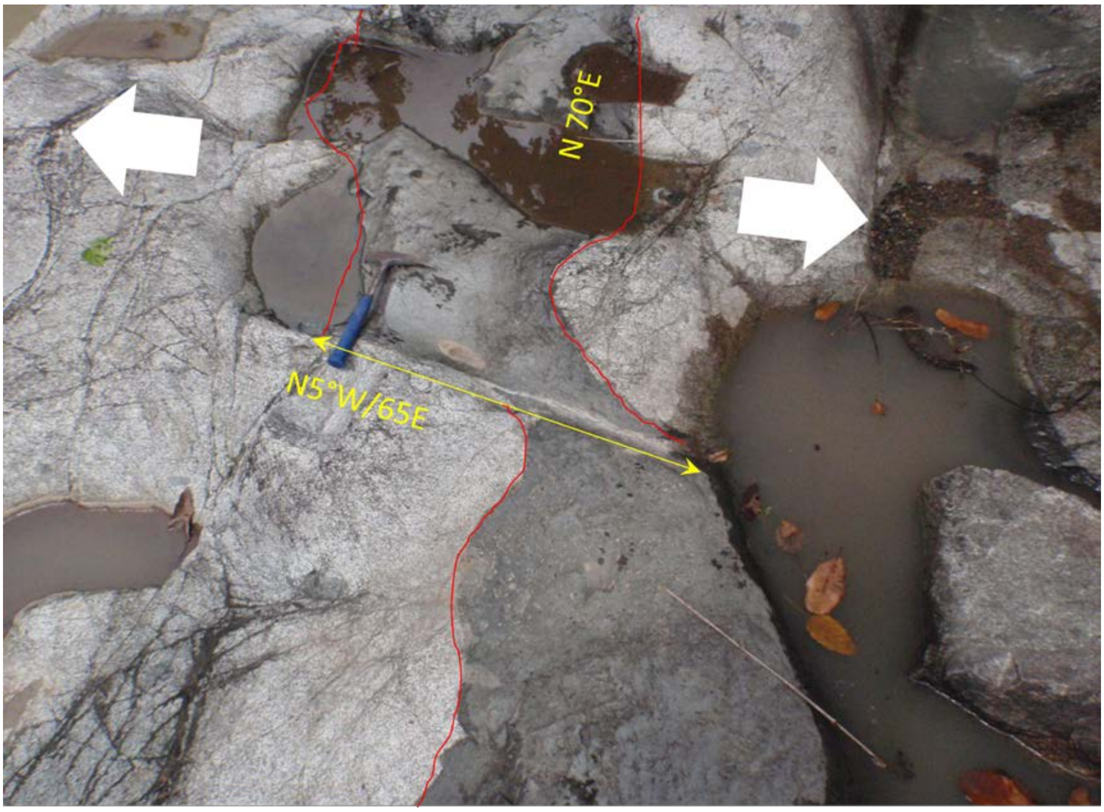

Figure 4.2 Basalt dike were cut granodiorite of Biru intrusive rocks. A left−stepping dike intrusion, well situated for stress determination. The corner were connected prior to dike intrusion, and extension direction (white arrow), which can be assumed to be close to the minimum principle stress.

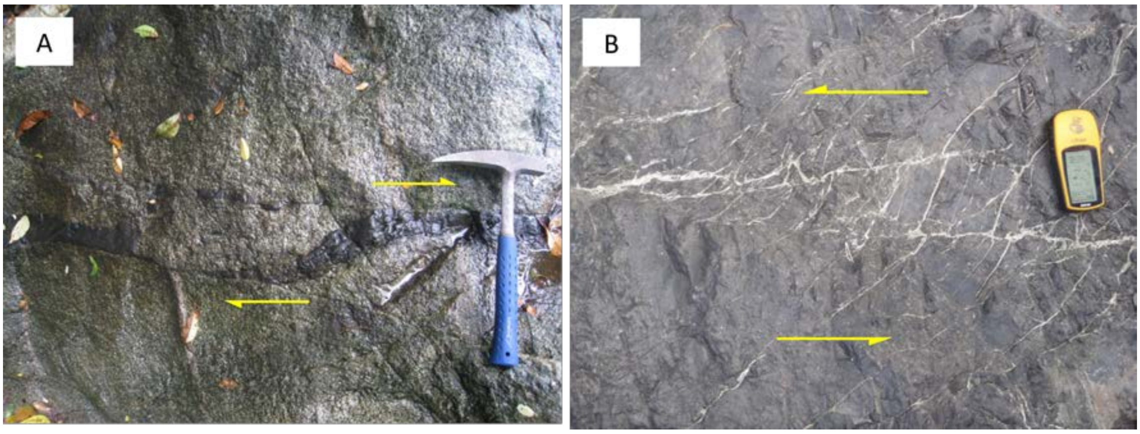

Figure 4.3 (a) A gouge at fracture showing sigmoidal tension gashes indicate dextral sense of shear. (b) A fibrous dissolution seams were filled calcite minerals shows sinistral sense of shear.

Langi Volcanics and Biru Granodiorite were cut by the Late Miocene to Pliocene dike intrusion. Poles to dike walls oriented into two main directions, predominantly NW–SE and subordinately SW–NE (Fig. 4.4). Inferred σ_3 is NW–SE and SW–NE. It is observed that some dike have both NE–SW and SSE–NNW trending poles of walls. Subordinate SSE–NNW dike wall may be a part of SW–NE trending dike, and therefore σ_3 could be inferred in the direction bisecting a larger angle between both dike walls, i.e. N–S.

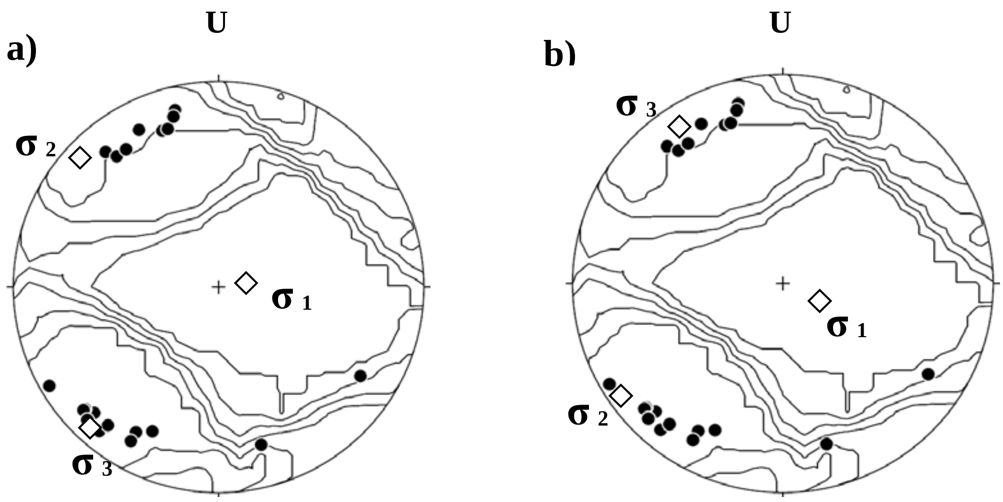

Figure 4.4 Poles to dike datasets orientation plotted in stereograms in equal-area and lower hemisphere projection (filled circle) with kamb contour from all of data. a) NW–SE σ_3 trending direction, b) SW–NE σ_3 trending direction.

4.1.3 Stress States Obtained from Fault–Slip data

σ_1 and σ_3 paired diagram of both Biru and Bulubuluk river show a few clusters relatively obvious but are differently oriented. Fault–slip data of the Biru river shows σ_1-axis trending around predominantly NNW–SSE and subordinately NNE–SSW and σ_3-axis plunging nearly vertical (Table 4.1; Fig. 4.5) with stress ratios of 0.5 and 0.9, respectively. On the other hand, σ_1 trending N-S and several clusters of σ_3 widely distributed along a plane striking E–W and vertical are obtained from fault–slip data of the Bulubuluk river. Their stress ratios range from 0.3 to 0.6.

Table 4.1 Result stress states analysis of West Walanae Fault

Sites	N	Stress Mode	SS	σ1		σ3		Φ	*n*	*r*	Rocks Unit
				Azimuth	Plunge	Azimuth	Plunge				
Biru River	29	Compressional	A	129	14	281	73	0.4	11	18	Vocanic Breccia (Langi Volcanics) Basalt,
		Compressional	B	153	35	33	34	0.6	8	21	Andesite (Dikes), Granodiorite, Granite (Biru Intrusive)
Bulubuluk River	23	Compressional	A	6	20	120	47	0.3	11	12	Granodiorite, Granite (Biru Intrusive)
		Compressional	B	335	24	123	61	0.6	11	12	Basalt (Dikes)

N: numbers of fault measured; SS: stress state; σ_1: maximum principal stress; σ_3: minimum principal stress; Φ = stress ratio, *n*: gives the numbers associated of fault–slip data (30° misfit); *r*: gives the number of data that cannot be related to a stress state (>30° misfit).

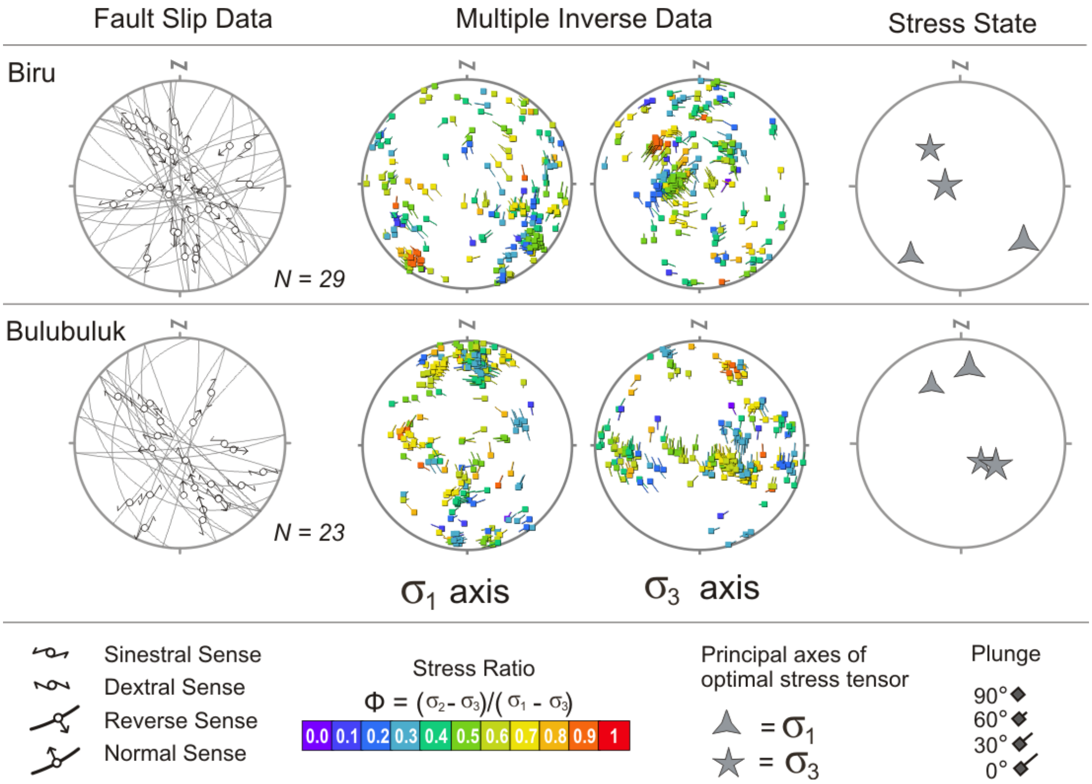

Figure 4.5 Paired diagrams of stereographic projection of fault slip data (left) calculate using multiple inverse method (middle), result of stress states analysis fault–slip data in Biru area (right).

4.2 East Walanae Fault Zone

4.2.1 Description of Deformation Structures

An intense deformation zone occupies the 2−3-km-wide area between the Bone Mountains and the Walanae Depression, where strata of the Salokalupang Group predominantly occur (Fig. 4.7). The trace of the EWF is postulated running along the western edge of this zone (Fig. 1.1 and 4.7). The outcrop of the main faults of the EWF has not been confirmed, but various deformation structures associated with faulting are observable along the trace of the EWF. A fault gauge zone containing a number of limestone breccias with worn surfaces (Fig. 4.8a) among a loose clayey matrix is exposed in the trace of the EWF over a 10-m-wide area at the central region in the E−W direction (Fig. 4.7a). At site b in Fig. 4.7, a volcano-clastic rock of the Salokalupang Group has a cataclastic texture with NNW−SSE striking foliation, which is nearly parallel to the trace of the EWF (Fig. 4.8b). Striations on the foliation in the cataclasite indicate a large component of dip−slipping, whereas a dextral shear sense is also inferred from the asymmetry of the pressure shadows surrounding some fragment of minerals (Fig. 4.8c) and the offset of a microfault. At a site on the west side and near the trace of the EWF in the central area (Fig. 4.7c), west-verging tight folds and related intense fractures are observable in the mudstone intercalated with beds of limestone of the Walanae Formation (Fig. 4.9a and c). The mudstones are highly sheared, showing a scaly fabric along which tight fold structures can be traced (Fig. 4.9b). The beds of limestone are crashed into breccia and mixed with the mudstones. A striation of scaly clay plunges at a high angle. Samples for radiocarbon dating were collected at the side of Fig. 4.9c.

The deformation zone is characterized by the development of various scales of tight folds (Fig. 4.8d) and numerous faults. Strata in this zone tend to dip eastward moderately to highly (Fig. 4.10a). The axes and axial planes of both the regional and mesoscale folds generally trend NE−SW and plunge at a low angle and dip eastward, respectively (Fig. 4.10b). Deformation associated with flexural slip folding tends to be localized particularly in the bed of mudstone and fine-grained tuff, which is sliced by numerous shear fractures subparallel or slightly obliquely (up to 30°) to a bedding plane (Fig. 4.8e). Striations on the plane of the shear fractures tend to be oriented nearly perpendicular to the fold axis but some are oblique to it (Fig. 4.10b). The mesoscale faults that are the subject of paleostress analysis have a few to several tens of centimeters of displacement and accompany a fault gauge of a few millimeters in wide. The striations of the mesoscale faults we observed are often unobvious, therefore only a single direction could be distinguished from each fault plane (Fig. 4.8f).

Carbonate rocks in the study area show a variety of deformation structure. Deformation of the carbonate rocks in the Salokalupang Formation, particularly in the vicinity of trace of the EWF, is very intense including numerous calcite veins and pressure-solution seams (Fig. 4.8g). Pressure-solution seams exhibiting an exaggerated wavy surface between which dark materials are included occur parallel or subparallel to the bedding plane. The veins are chiefly perpendicular or subperpendicular to the bedding plane and frequently cut through pressure-solution seams but occasionally dissected by them. Mechanical *e*-twins have developed pervasively in the calcite grains with thin (less than 5μm in thickness) and straight geometry (Table 4.3 and Fig. 4.8h). The calcite aggregates used for paleostress analysis consist of medium to coarse grains, mean diameter of each sample ranges from 60 to 800μm, and show random *c*-axis orientations (Fig. 4.11 and 4.12).

Overall, 70-76% of calcite grains have one and more twin sets, 17-23% have two or three twin sets, 0-5% have three twin sets, and 2-10% are untwinned grains in the limestone and calcareous rocks collected from the Salokalupang Group, Walanae Formation and crystalline limestone of the Taccipi Formation limitedly exposed at the Sengkang Anticline. By contrast, no twins are observed in the limestone samples of the Taccipi Formation exposed on the north-west margin of the Bone Mountains, which are lithologically bioclastic and without significant cementation and recrystallization.

In the Walanae Depression, although there seems to be no evidence of serious deformation, some gentle folds are developed (Fig. 4.7). Their NE−SW to NNE−SSW trends are sub-parallel to slightly oblique to the EWF.

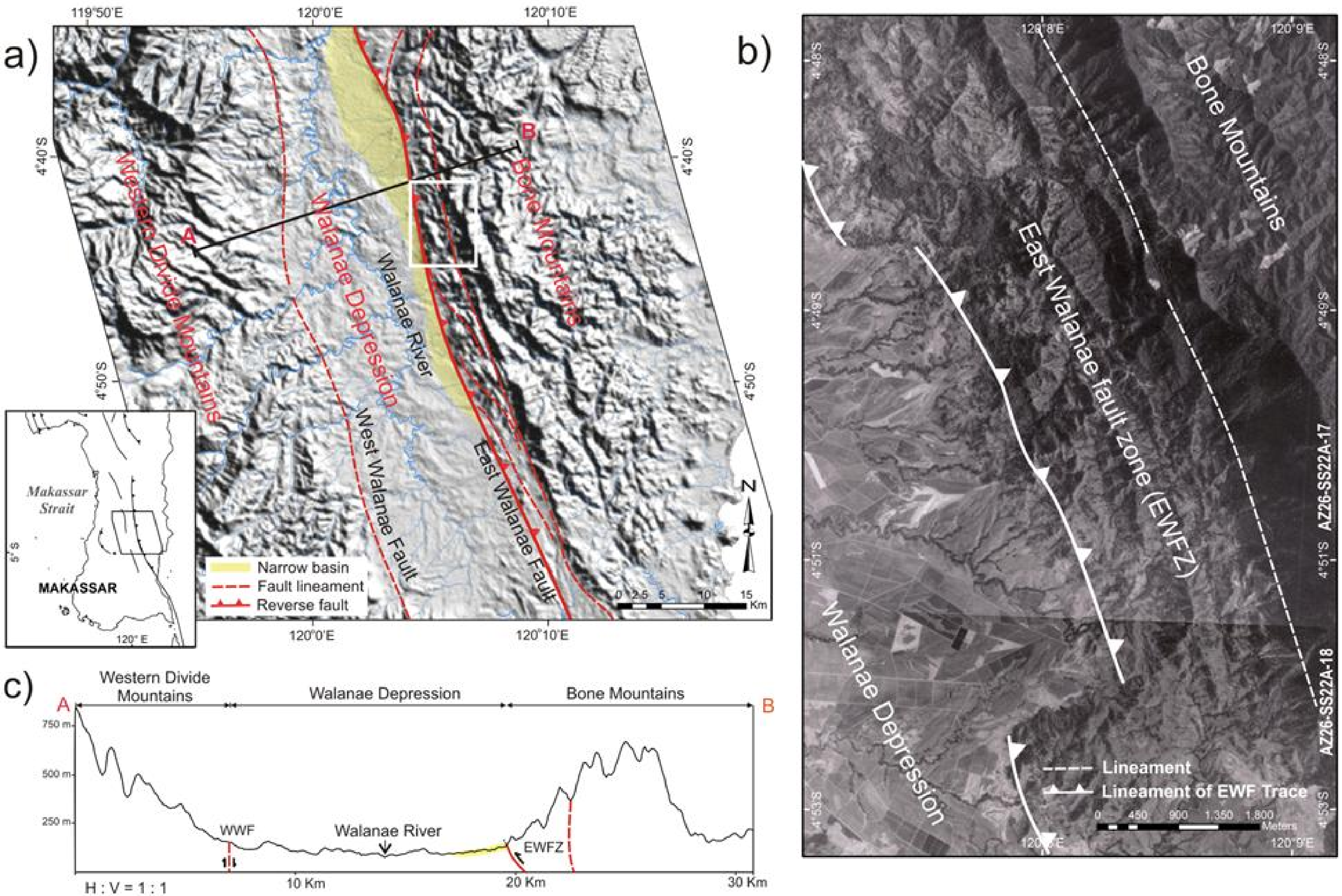

Figure 4.6 a)Topographic map around the East Walanae fault, b) aerial photograph showing a close up of landform features around the EWF (map location in white box at the Fig. 4.6a; sheets No: AZ26-SS22A-17 and AZ26-SS22A-18; BAKOSUTANAL, 1991) and c) profile across the WWF, Walanae Depression and East Walanae fault zone (EWFZ) along the section A-B. Trace of the EWF and related lineaments (red and white lines in the map and photograph, respectively), and narrow basin (colored in yellow in the map and profiles) are shown**.**

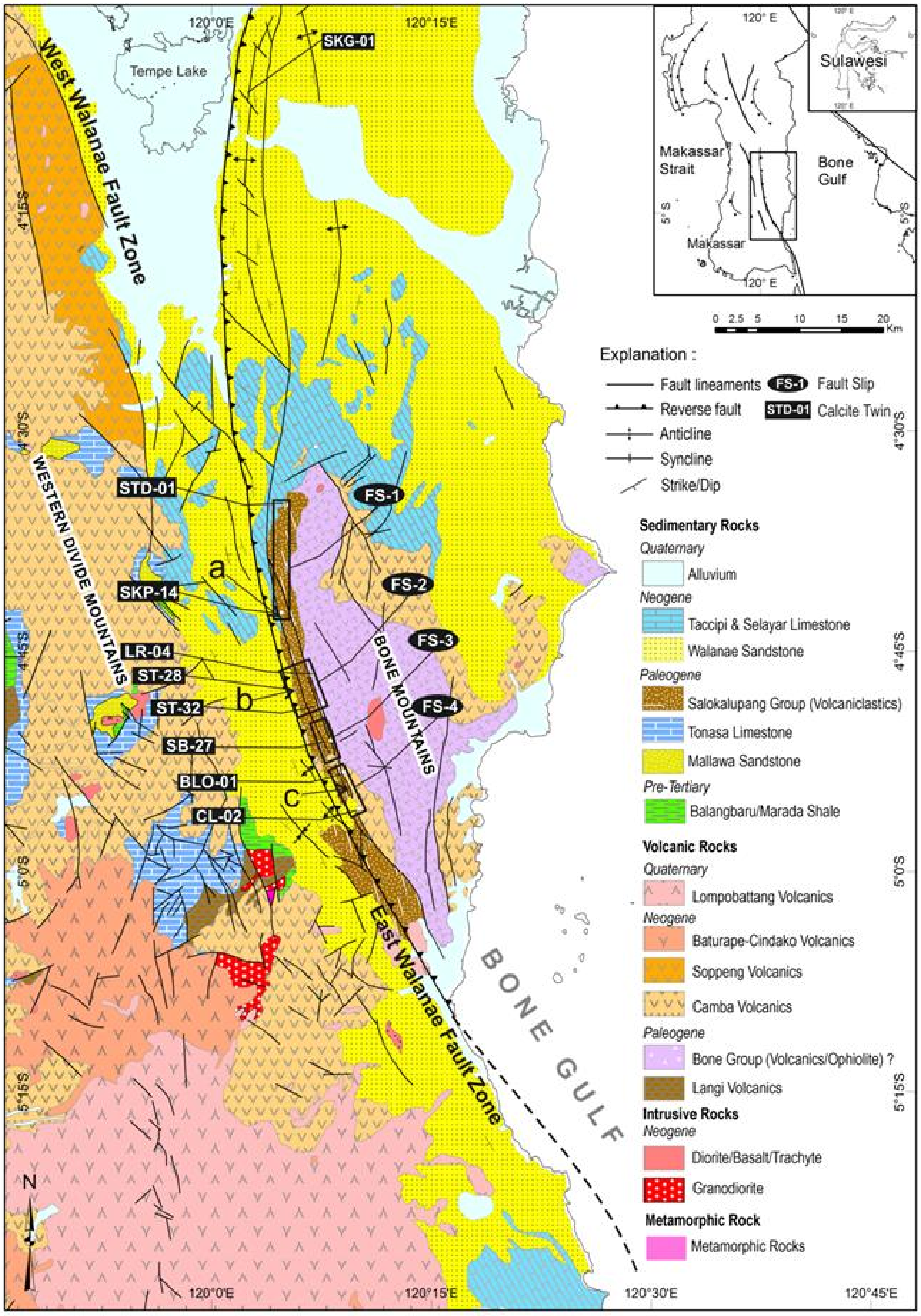

Figure 4.7 Geological map along the East Walanae fault zone (modified after Sukamto 1982; Sukamto & Supriatna, 1982). Sites of measurements of fault-slip data and sampling points for calcareous rocks are shown in the map.

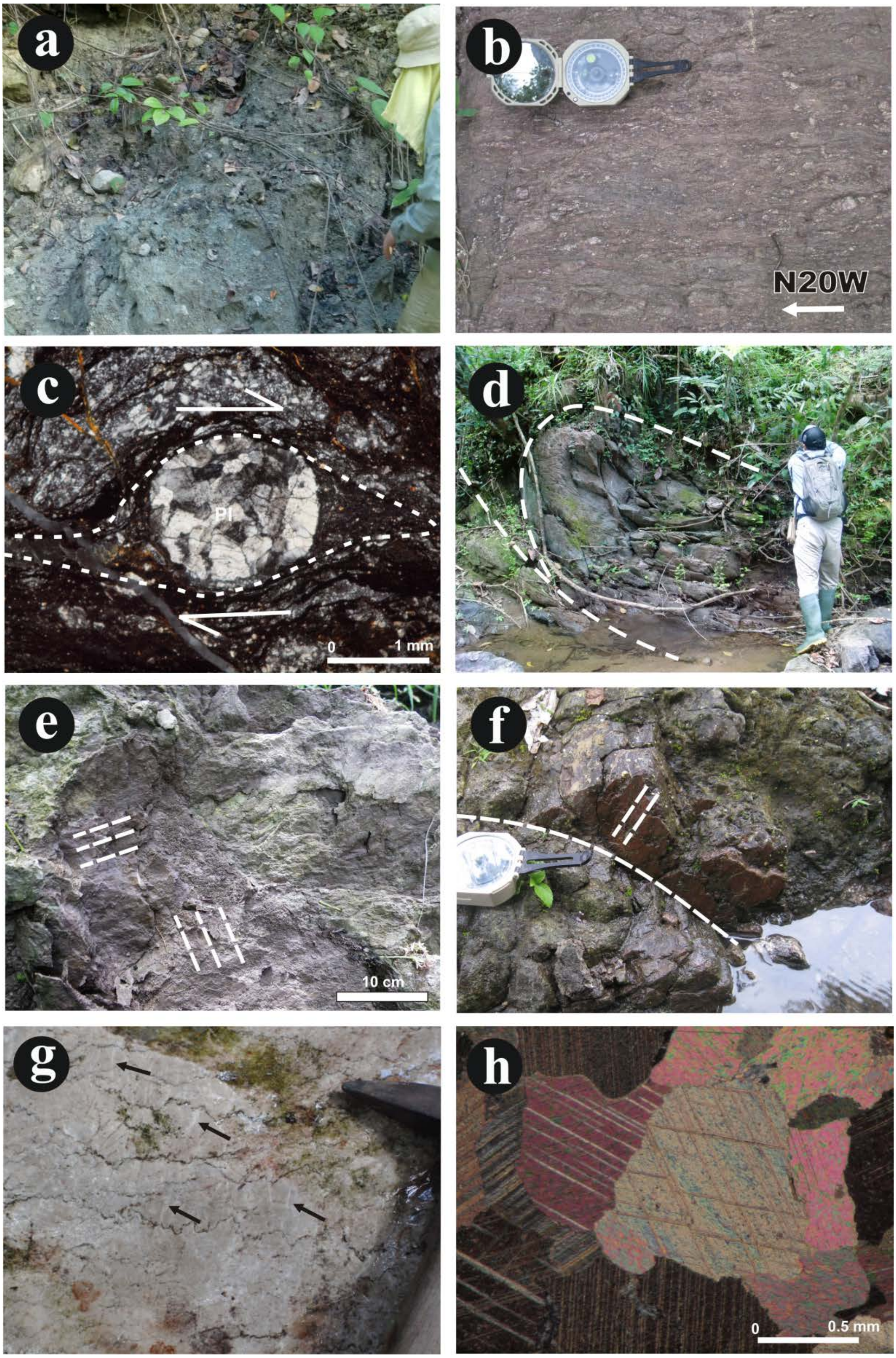
a
b
N20W
c
Pl
0
1 mm
d
e
10 cm
f
g
h
0
0.5 mm

Figure 4.8 Photographs of meso-and micro-scale deformation structures around EWF. (a) Fault gauge including limestone breccias in the fine grained matrix locality a in Fig. 4.7. The surface of breccias is worn. b) Cataclasite texture developed in a reddish mudstone showing a foliation and numerous porphyroclasts indicating an intense shearing around a fault near the EWF trace locality b in Fig. 4.7. (c) A rounded porphyroclast of a plagioclase aggregate (PL) in a cataclasite of Figure 6b, around which pressure shadow showing dextral sense of shear developed. (d) A hinge zone of a tight fold developed in the central area of intense deformation zone between the Bone Mountains and Walanae Depression. e) Planes of shear fracture in the reddish mudstone developed associated with flexural slip folding. Striations both steeply and gently plunging are found on the plane (dashed lines) around the EWF. f) A mesoscale fault of which the striation on the fault plane indicates dip-slip (dashed lines) at the central area of the deformation zone around the EWF. g) Pressure solution seams and calcite veins (arrow) developed in the limestone of the Salokalupang Group exposed in the southern part of the deformation zone. h) Calcite *e*-twins developed in the limestone of the Salokalupang Group (ST-32).

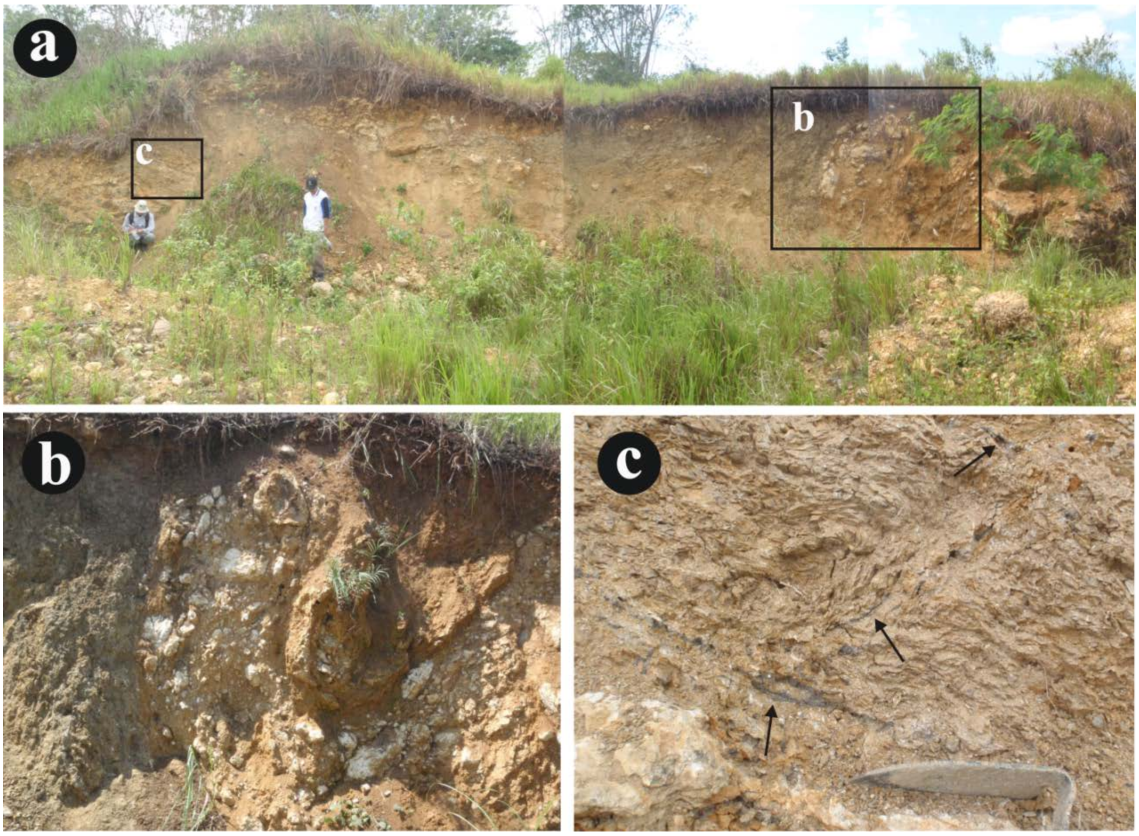

Figure 4.9 An outcrop of deformed strata of mudstone and limestone of the Walanae Formation in the vicinity of the EWF trace (locality c in Fig. 4.7). In the central part (rectangle b), a tight fold is developed. Sheared soils were sampled for radiocarbon dating at the east side of the outcrop (rectangle c). b) Close up of the tight fold in the central part of the outcrop, where beds of mudstones are intensely sheared and limestones are fragmented. c) The occurrence of sheared soils. Dark gray soils (arrows) are intercalated among the weathered mudstone intensely sliced.

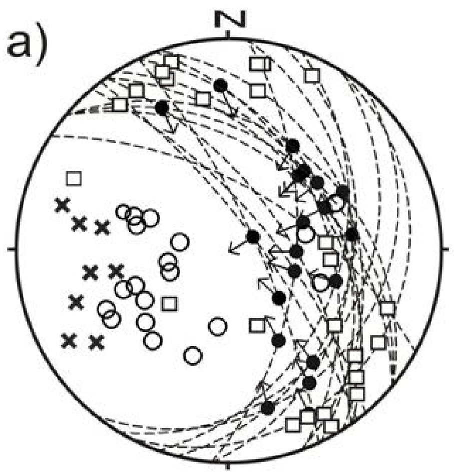

Figure 4.10 Stereographic plot (equal-area, lower hemisphere projection) showing the attitude of bedding (open circle), the orientations of mesoscale fold axes (open square), poles to axial planes (cross) and striations developed on the shear fractures occurring with the folds (filled circle). a) Northern area (represented by areas FS-1 and 2 in Fig. 4.7), b) Southern area (represented by areas FS-3 and 4 in Fig. 4.7).

4.2.2 Principle of the multiple inverse method (MIM) of fault-slip data

Paleostress tensors were determined by the multiple inverse method (Yamaji, 2000) using the MIM Software version 6.02 (Yamaji et al., 2010). The multiple inverse method first creates subsets from the dataset, the number of which equals the binomial coefficient: ${}_{N}C_{k} = N!/k!(N\text{-}k)!$, where N is the total number of fault-slip (or calcite twin) datasets and k is the number of elements comprising a subset (Fig 4.11). In this study, we used the value $k = 5$, which is recommended in the user's guide of MIM software package because solutions are stable at this value and larger (Yamaji et al., 2010). Then, an inversion scheme is applied to determine optimal stress tensors for each subset. Calculated stress orientations for all subsets are shown on paired diagrams consisting of a stereogram for the maximum principal stress (σ_1) and that for the minimum principal stress (σ_3) with values of stress ratio ($\Phi = (\sigma_2\text{-}\sigma_3)/(\sigma_1\text{-}\sigma_3)$). Stress tensors that are suitable for a large fault (or twin) population to be activated tend to form clusters on the paired diagrams, and as such, can be identified through inspection of the paired diagrams.

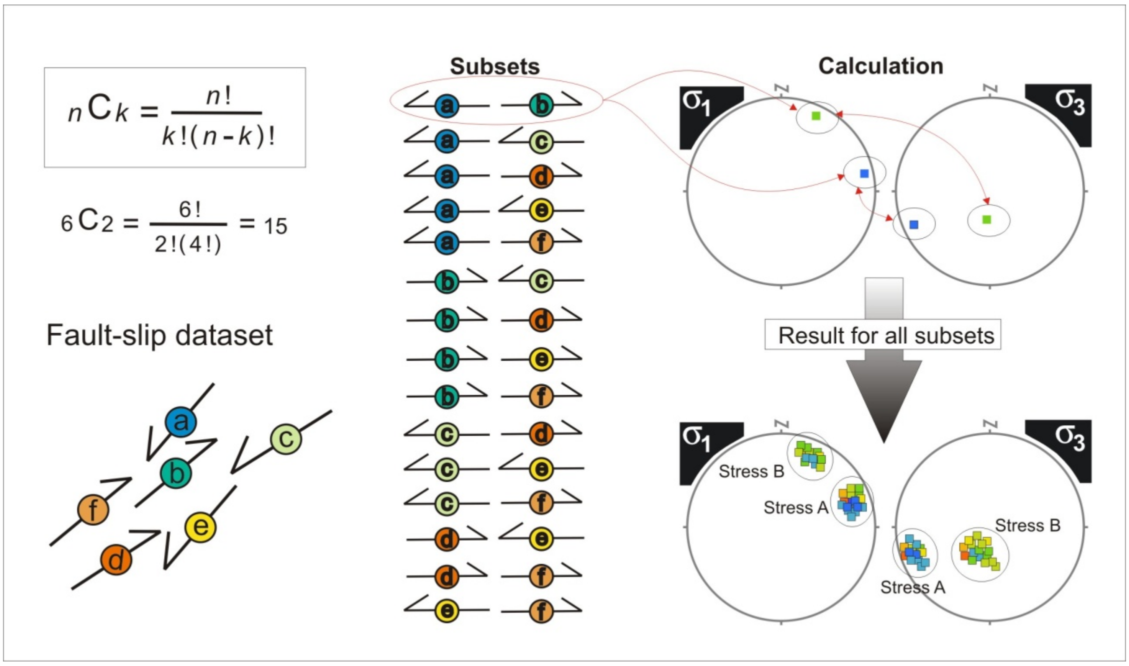

Figure 4.11 Schematic figure showing the procedure of the multiple inverse method (MIM). Detection of the stress states from a heterogeneous fault-slip dataset can be optimized through extracting subsets. The case of k = 2 is shown in this diagram. Homogeneous subsets are expected to concentrate their votes at the grid points corresponding to stresses A or B, while the meaningless solutions from heterogeneous subsets should be placed randomly.

4.2.3 Application of the multiple inverse method to calcite twin data

Calcite grains contain three equivalent *e*-planes on which twinning can occur (Fig. 4.12). The number of twin sets formed in a grain depends on the orientation of the principal stresses with respect to the glide directions on the *e*-planes and the resolved magnitude of differential stress for that *e*-plane set. Calcite twin data were measured from both veins and host rock (grains of fossil fragments or occupying former pore spaces). Data collected from a host rock might record total history of deformation, while a vein represents events during or after vein formation. Therefore, calcite twin data measured from veins and host rock were separately treated.

One to three poles of differently oriented twin lamellae and *c*-axis orientation were measured for each grain using a universal stage (U-Stage) optical microscope with up to 320 times of magnification. Measurement error of twin lamellae and *c*-axis orientations in calcite grains by U-stage is up to several degrees. About 60 to 90 calcite grains with medium to coarse grain size (60 to 800 μm) were measured from each of three mutually perpendicular thin sections for eleven samples. The dataset of calcite twin for our paleostress analysis consisted of the attitude of the *e*-plane, gliding direction and sense of shear of *e*-twinning. We prepared data files not only for twinned *e*-planes but also for the remaining untwinned *e*-planes in a grain with one or two twin sets. Untwinned *e*-plane in a twinned grain can be simply determined on the basis of crystallographic relationships with measured *e*-planes and *c*-axis (Fig. 4.12). On the other hand, grains without twin lamellae were not used for analysis because orientation of an untwinned *e*-plane cannot be directly determined by optical microscopy.

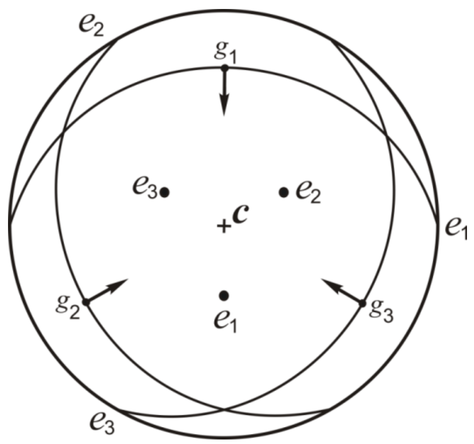

Figure 4.12 Stereographic projection (lower hemisphere, equal-area) showing the *c*-axis and three equivalent *e*-planes (e_1, e_2, e_3) and gliding directions of twinning (g_1, g_2, g_3) on respective *e*-planes in calcite crystal (modified after Evans and Groshong, 1994; Laurent et al., 2000). The arrow is parallel to the gliding direction; its head indicates that the upper part of the crystal moves upward, toward the *c*-axis, as a reverse fault.

We incorporated untwinned *e*-plane data for determining stress states with the multiple inverse method used for calcite twins (Fig. 4.13). In the first step of the analysis, significant clusters of stress states were identified from the paired diagrams of the twinned *e*-plane data as preliminary solutions for the stress states (stress A, B, and C in Fig. 4.13b). In the second step (Fig. 4.13c), the viability of the identified stress states was tested with untwinned *e*-plane data calculating misfit angle β, the angle on the untwinned *e*-plane between the calculated maximum shear stress direction for every identified stress state and the observed potential gliding direction. The stress states identified from twinned *e*-plane data should be compatible with the existence of untwinned *e*-planes. This compatibility can be evaluated by using misfit angle β. To judge whether or not the untwinned *e*-planes data were compatible the stress states identified in the first step, we tested if they have β values greater than a designated angle. We adopted β=30° as the angular threshold for this examination. This decision is consistent with previous paleostress analyses where the threshold of misfit angle ranges between β = 20° (e.g., Etchecopar et al., 1981; Sperner et al., 1993) and 30° (e.g., Nemcok and Lisle, 1995; Otsubo et al., 2009). If most untwinned *e*-plane data (95% or more in this study) are compatible, then the stress state is viable for both the twinned and untwinned *e*-planes, and is retained for comparison to the fault-slip analysis.

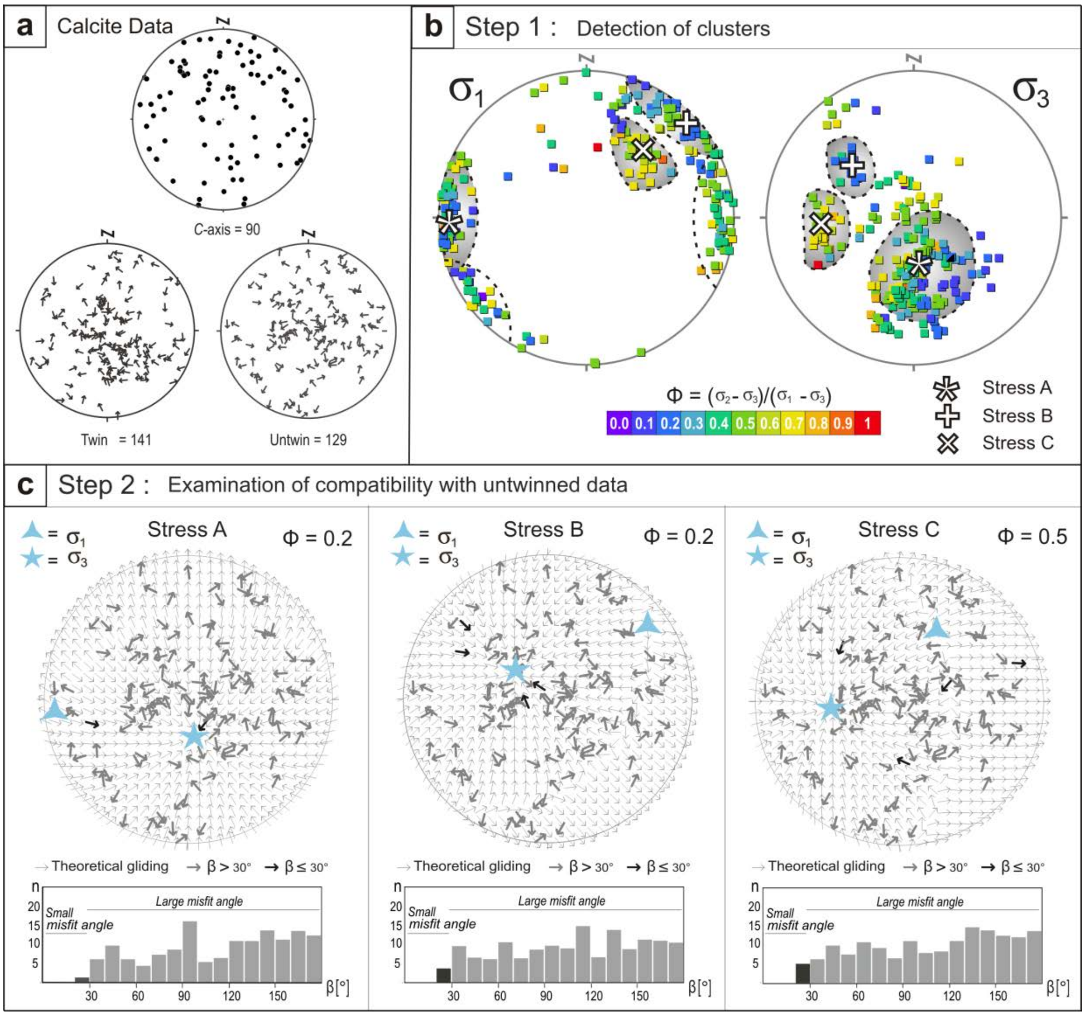

Figure 4.13 Simulation process to determine the stress states from calcite twin data using BLV-6 with the multiple inverse method (Yamaji, 2000). a) Calcite *c*-axis orientations (upper diagram), tangent-lineation diagram for twinned *e*-plane data (lower left diagram) and that for untwinned *e*-plane data (lower right diagram). b) Diagrams showing the procedure of the first step. A, B and C are significant cluster identified from a paired diagram. c) Diagrams showing the procedure of the second step. Candidates of stress state are plotted with untwinned plane data on the tangent-lineation diagrams, where thin gray arrows indicate the theoretical gliding directions for a given stress state, and thick arrows are those of untwinned plane data. The degree of misfit angle β can be distinguished by color; thick gray and black mean large misfit angles ($\beta \geq 30°$) and small misfit angles ($\beta < 30°$ in this case), respectively. Φ: stress ratios. n: number of datasets. The histogram shows the distribution of misfit angle of untwinned plane data with a given stress state.

The paired diagrams of the maximum principal stress (σ_1) and minimum principal stress (σ_3) calculated from calcite twin and fault−slip data are shown in Table 4.2, 4.3, 4.4 and Fig. 4.16, 4.17 and 4.18. Calcite twin data yielded a common distribution pattern (Fig. 4.16 and 4.17). σ_1 clusters are consistently approximately horizontal and converge into NE-SW to E-W directions for all the analyzed samples except STM-2 (collected from NE margin of the Bone Mountains), in which σ_1 tends to lie on the bedding plane with NNW to NE trending clusters. σ_3 clusters demonstrate a tendency to plunge nearly vertically（SKV-1, STV-3, and STV-4）or high to moderate angles toward the south (SKV-1, STV-2, LRV-2, SBV-5, BLV-6, and CLV-7). Most of the stress ratios Φ obtained from the calcite twin data show low values ranging from 0.1 to 0.6. The distribution of the stress orientations in the paired diagrams calculated from untwinned data show generally reversal patterns compared with those from twinned data.

Fault−slip data yielded similar stress tensor to the calcite twin data; σ_1 clusters are nearly horizontal and trend E−W to NE−SW and σ_3 clusters are vertical to steeply plunging with generally low Φ ranging from 0.1 to 0.8 (Table 4.4 and Fig. 18). Uniquely, the σ_3 cluster from the southern area (FS-4) is found to be plunging relatively low angle toward both NW and SE directions (Fig. 4.18).

4.2.5 Deformation condition estimated from occurrence and morphology of twin

It is well known that the morphology of calcite twin varies depending on temperature conditions. Ferrill et al. (2004) correlated mean calcite twin width with temperature of deformation such that thin twins (approximately 1μm) dominate below 170°C and thick twins (> approximately 2μm) dominate above 200°C. Calcite twin lamellae found in the study area have planer feature and the width of 1.8 to 4.5μm (Table 4.4 and 4.5). Considering the thin twin width which is measured by optical microscope tending to include only approximately 50% of the width of twinned material (Groshong, 1974), true twin widths of our samples are regarded as approximately 1 to 2μm. Therefore, it can be estimated that deformation temperatures was low, about 200°C or lower. It is much lower than those dislocation gliding being pervasively activated in calcite (higher than 250°C).

Table 4.2 Paleotress states determined from calcite twin data of East Walanae Fault, calcite twin data and paleostress states determined from veins.

Locality	Coordinates (Latitude/Longitude)	Lithology and units lithology	Number of twin datasets (T)	Number of untwin datasets (UT)	Stress states	σ_1	σ_3	Φ	Number of datasets compatible with the tensor (T)	Total number of datasets compatible with the tensors (TT)	Number of datasets incompatible with the tensor (UT)	Mean grain size (μm)	Mean width of lamella (μm)
SKV-1	4°42'28"S/120°04'40"E	Bioclastic Limestone of Salokalupang Group	164	106	A	21/6	257/78	0.3	64	145	103	399	1.2
					B	41/9	280/72	0.5	63		102		
					C	38/37	258/45	0.3	58		101		
					D	101/16	331/66	0.8	51		100		
LRV-2	4°46'36"S/120°06'51"E	Bioclastic Limestone of Salokalupang Group	132	138	A	61/0	151/37	0.3	58	83	134	189	0.7
					B	260/8	156/60	0.2	54				
STV-3	4°47'39"S/120°05'40"E	Bioclastic Limestone of Walanae Formation	121	149	A	27/10	207/79	0.3	50	102	143	185	0.6
					B	64/0	154/78	0.4	42		142		
					C	91/20	25/69	0.5	38		142		
STV-4	4°48'30"S/120°07'38"E	Bioclastic Limestone of Salokalupang Group	165	105	A	244/6	335/87	0.6	59	123	103	563	1.2
					B	35/24	268/54	0.6	55		101		
					C	20/7	122/55	0.6	48		100		
					D	90/30	27/56	0.6	48		100		
SBV-5	4°51'03"S/120°08'12"E	Calcareous Mudstone of Salokalupang Group	143	127	A	217/3	122/52	0.3	50	105	124	116	1.0
					B	54/4	150/49	0.3	43		122		
					C	0/20	119/56	0.3	40		121		
BLV-6	4°53'12"S/120°09'05"E	Bioclastic Limestone of Salokalupang Group	141	129	A	261/2	167/61	0.2	51	113	127	232	0.7
					B	51/8	311/46	0.2	46		125		
					C	32/40	265/34	0.5	38		124		
CLV-7	4°55'41"S/120°10'06"E	Reddish Bioclastic Limestone of Salokalupang Group	147	123	A	40/21	229/68	0.4	52	114	120	110	1.0
					B	90/29	240/56	0.3	44		118		
					C	240/8	214/75	0.5	46		117		
					D	98/72	210/71	0.5	42		116		

σ_1: Azimuth/plunge of maximum principal stress; σ_3: Azimuth/plunge of minimum principal stress; T: Twinned planes; TT: Total twinned planes compatible with the tensors; UT: Untwinned planes; A, B and C: stress states determined; Φ: Stress ratio.

Table 4.3 Paleotress states determined from calcite twin data of East Walanae Fault, calcite twin data and paleostress states determined from host rocks.

Locality	Coordinates (Latitude/Longitude)	Lithology and units lithology	Number of twin datasets (T)	Number of untwin datasets (UT)	Stress states	σ_1	σ_3	Φ	Number of datasets compatible with the tensor (T)	Total number of datasets compatible with the tensors (TT)	Number of datasets incompatible with the tensor (UT)	Mean grain size (μ m)	Mean width of lamella (μ m)
SKM-1	4°08'14"S/120°02'24"E	Crystalline Limestone of Taccipi Formation	105	165	A	46/8	160/71	0.4	44	90	160	821	1.5
					B	46/28	167/42	0.2	40		158		
					C	107/55	199/25	0.8	38		156		
STM-2	4°35'03"S/120°05'17"E	Coralline Limestone of Salokalupang Group	120	150	A	35/41	256/24	0.4	40	81	145	63	0.7
					B	350/2	259/25	0.3	37		143		
					C	330/35	92/36	0.8	34		142		
BLM-3	4°53'12"S/120°09'05"E	Bioclastic Limestone of Salokalupang Group	80	118	A	67/9	186/70	0.8	40	69	114	115	0.9
					B	307/10	59/64	0.2	34		112		
CLM-4	4°55'41"S/120°10'06"E	Reddish Bioclastic Limestone of Salokalupang Group	83	95	A	60/18	306/50	0.2	32	67	93	96	1.0
					B	58/53	206/31	0.7	30		92		
					C	158/20	284/57	0.3	28		91		

σ_1: Azimuth/plunge of maximum principal stress; σ_3: Azimuth/plunge of minimum principal stress; T: Twinned planes; TT: Total twinned planes compatible with the tensors; UT: Untwinned planes; A, B and C: stress states determined; Φ: Stress ratio.

Table 4.4 Paleotress states determined from fault−slip data of East Walanae Fault

Locality	Coordinates (Latitude/Longitude)	Lithology and units lithology	Number of twin datasets (T)	Number of untwin datasets (UT)	Stress states	σ_1	σ_3	Φ	Number of datasets compatible with the tensor (T)	Total number of datasets compatible with the tensors (TT)	Number of datasets incompatible with the tensor (UT)	Mean grain size (μ m)	Mean width of lamella (μ m)
SKM-1	4°08'14"S/120°02'24"E	Crystalline Limestone of Taccipi Formation	105	165	A	46/8	160/71	0.4	44	90	160	821	1.5
					B	46/28	167/42	0.2	40		158		
					C	107/55	199/25	0.8	38		156		
STM-2	4°35'03"S/120°05'17"E	Coralline Limestone of Salokalupang Group	120	150	A	35/41	256/24	0.4	40	81	145	63	0.7
					B	350/2	259/25	0.3	37		143		
					C	330/35	92/36	0.8	34		142		
BLM-3	4°53'12"S/120°09'05"E	Bioclastic Limestone of Salokalupang Group	80	118	A	67/9	186/70	0.8	40	69	114	115	0.9
					B	307/10	59/64	0.2	34		112		
CLM-4	4°55'41"S/120°10'06"E	Reddish Bioclastic Limestone of Salokalupang Group	83	95	A	60/18	306/50	0.2	32	67	93	96	1.0
					B	58/53	206/31	0.7	30		92		
					C	158/20	284/57	0.3	28		91		

σ_1: Azimuth/plunge of maximum principal stress; σ_3: Azimuth/plunge of minimum principal stress; A, B and C: Stress states determined; Φ: Stress ratio.

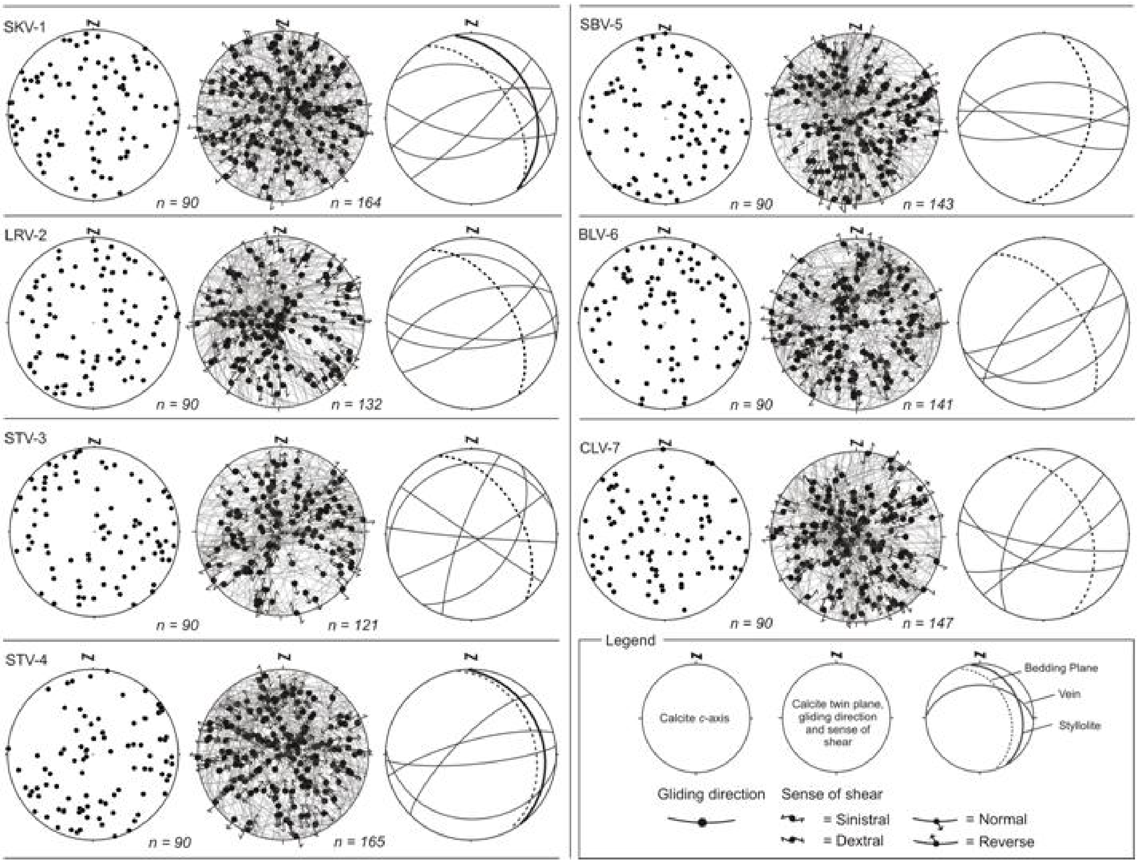

Figure 4.14 Left diagrams: *c*-axis orientations of sampled calcite aggregates from veins. Middle diagrams: Orientation of *e*-twin lamellae, gliding direction and shear sense of *e*-twins. *n*: number of *c*-axes and calcite twins. Right diagrams: Orientations of pressure solution seams, calcite veins and bedding plane attitude. All diagrams are equal-area, lower hemisphere projection.

Taccipi limestone samples collected at the Sengkang Anticline contain a number of twinned calcite grains. Inversely, no calcite *e*-twins were found in the limestone of the Taccipi Formation in the north-western margin of Bone Mountains. The texture, which shows no signs of compaction or cementation, also suggests that the limestone exposed at the marginal area of Bone Mountains has not experienced burial. The difference of texture suggests a contrast of tectonic environment between northern and southern parts that the Sengkang area had been deeply subsided, whereas the marginal area of the uplifting Bone Mountains has been at a shallow level or exposed since the Late Miocene.

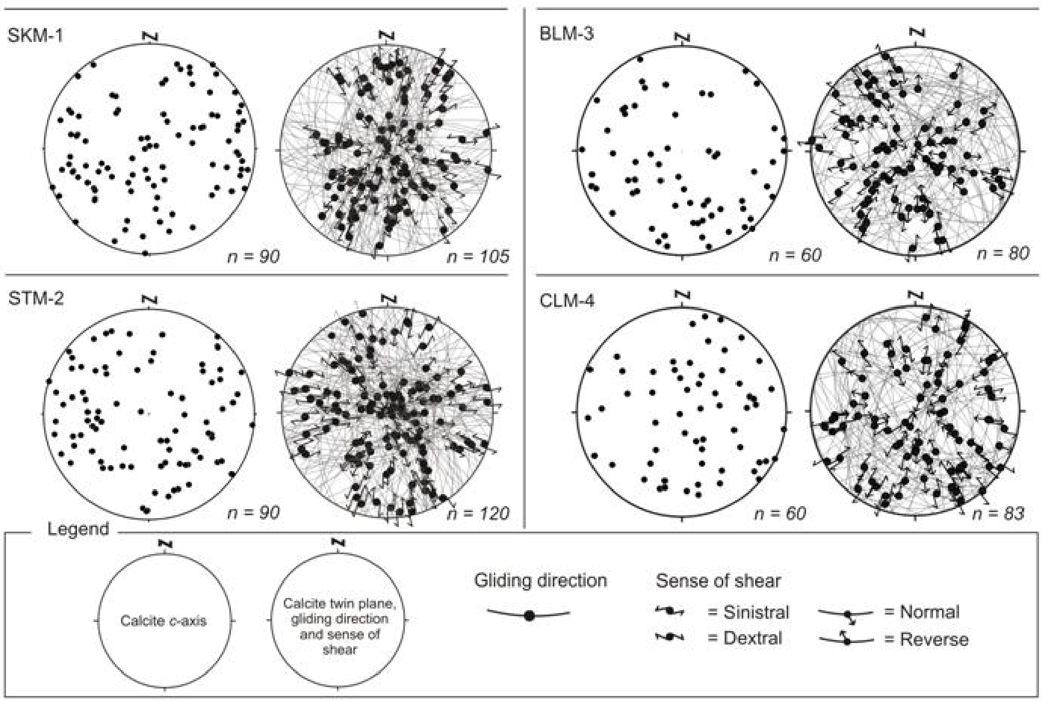

Figure 4.15 Left diagrams: *c*-axis orientations of sampled calcite aggregates from host rock. Right diagrams: Orientation of *e*-twin lamellae, gliding direction and shear sense of *e*-twins. *n*: number of *c*-axes and calcite twins. Both diagrams are equal-area, lower hemisphere projection.

4.2.6 Relationship between Inferred Stress States and Major Deformation Structures and Landforms

We applied the multiple inverse method to calcite twin data for determination of paleostress states, comparing distributions of stress clusters obtained from twinned data and those from untwinned data. Dominant stress states namely, NE−SW to E−W trending σ_1 and vertical to moderately plunging σ_3 with a low stress ratio, could activated the EWF as a reverse fault and account for the geological structures and landform features in the study area. Fold structures pervasively developed around the EWF could have been formed under these compressional stress regimes, resulting in significant shortening localized in the narrow zone between the Bone Mountains and the Walanae Depression. Concurrently, uplifting of the Bone Mountains and subsiding in the Walanae Depression have perhaps occurred, which may have promoted topographic contrast between the Bone Mountains and the Walanae Depression across EWF (Fig. 4.6).

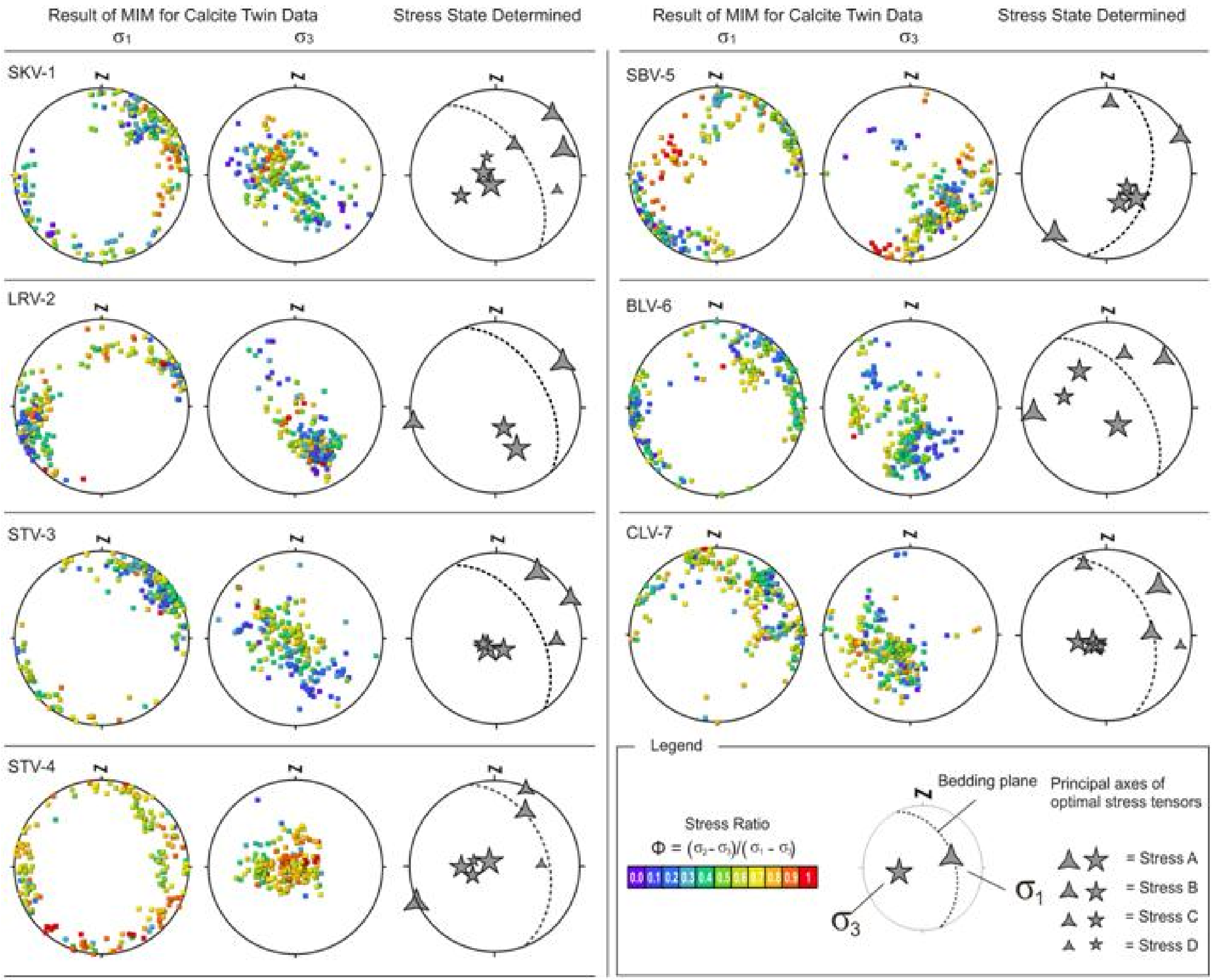

Figure 4.16 Left two diagrams: Paired diagrams obtained from calcite twin data of calcite veins. Right diagram: Stress states viable for both the twinned and untwinned *e*-planes. Stress orientations represented by larger symbols correspond to those of larger population of calcite twins with small misfit angles.

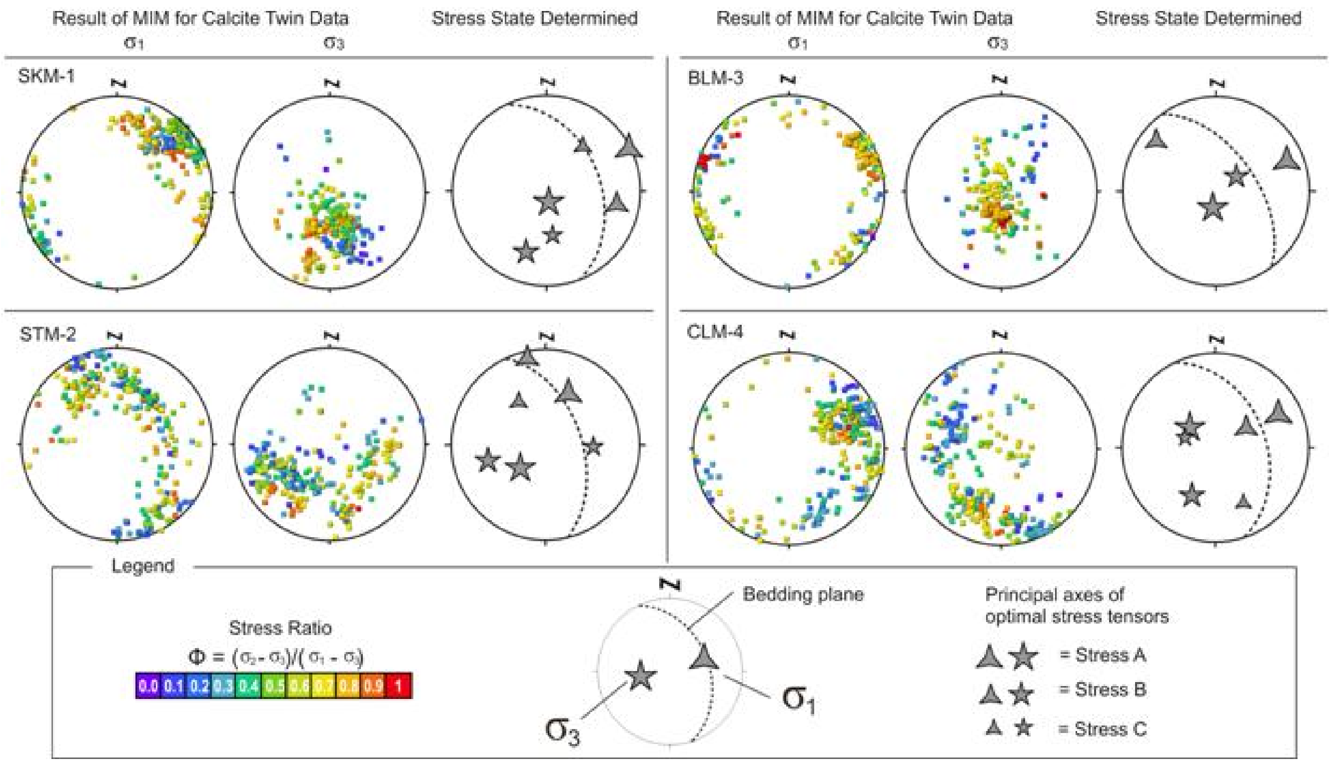

Figure 4.17 Left two diagrams: Paired diagrams obtained from calcite twin data of host rock samples. Right diagram: Stress states viable for both the twinned and untwinned *e*-planes. Stress orientations represented by larger symbols correspond to those of larger population of calcite twins with small misfit angles.

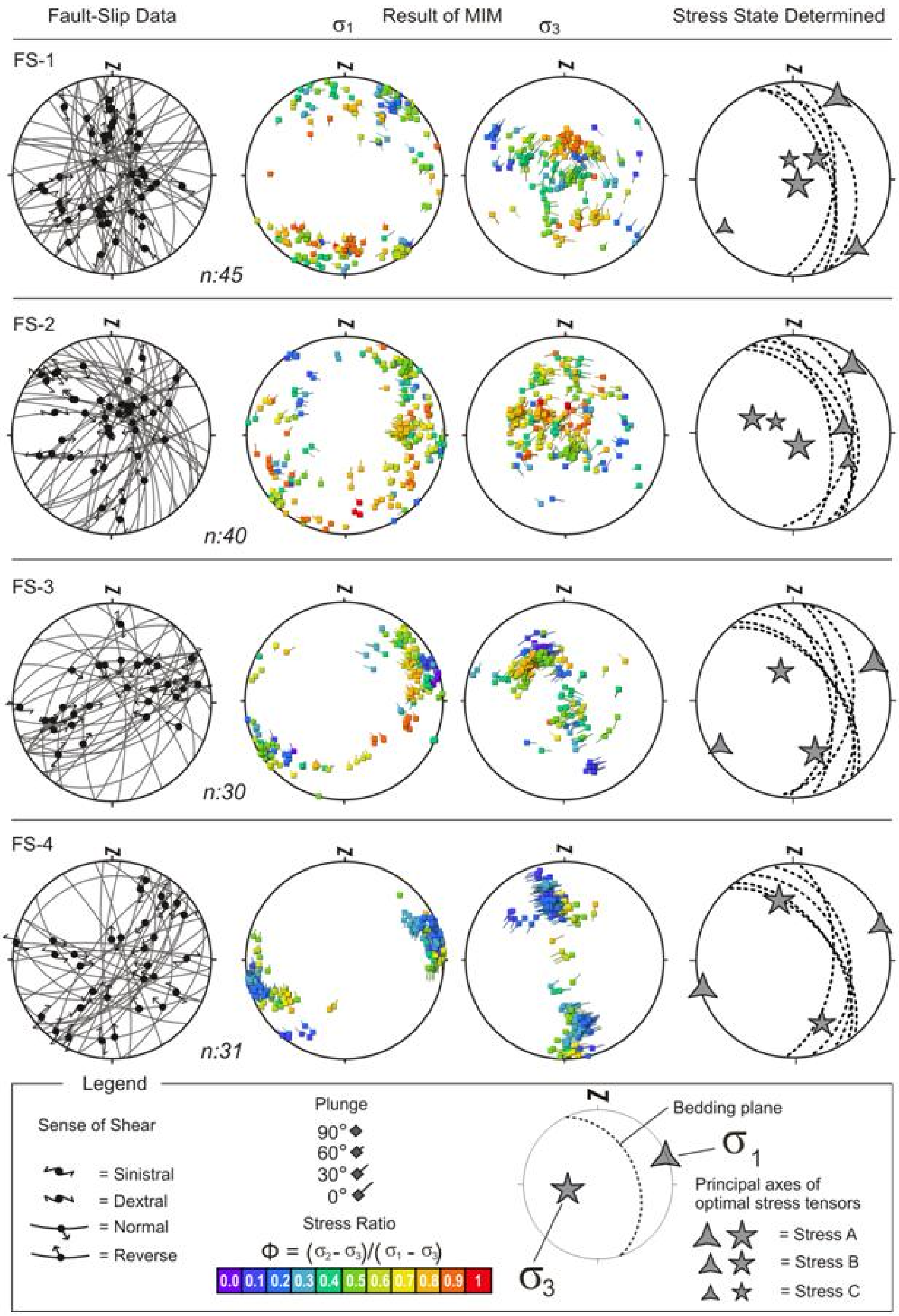

Figure 4.18 Paired stress diagrams and selected stress states obtained from fault-slip data. Stress orientations represented by larger symbols correspond to those of larger population of fault with low misfit angle. *n*: number of fault–slip data.

Obliquity of σ_1 (generally trending NE-SW) to the trace of the EWF (striking N-S in the northern part and NNW−SSE in the southern part) (Fig. 4.7) suggests a dextral component in the shear sense of the EWF. This is indicated from the NW-SE-trending folds and slightly oblique drainage pattern to the EWF trace developed in the deformation zone between the Bone Mountain and the Walanae Depression (Fig. 4.6 and 4.10) and the microstructure of cataclasite near the EWF trace (Fig. 4.8b). This tectonic condition with shortening and dextral component could be available under the stress configuration with the southward-plunging tendency of σ_3 inferred from calcite twin data.

Although the beddings of nine sampling sites are differently tilted by folding, most of the paired diagrams of calcite twin data consistently show stress states with nearly horizontal σ_1 and vertical-to-moderately plunging σ_3 throughout the areas (Fig. 4.16 and 4.17). Fault−slip data also yielded nearly horizontal and vertical σ_1 and σ_3 clusters, respectively (Fig. 4.15). Therefore, most of stress states obtained from both the calcite twin and fault−slip data predominantly record the latest and/or post folding stages. By contrast, a distinct stress distribution of STM-2 (Fig. 4.18), a dominant σ_1 cluster trending NE and lying on the bedding plane (approximately 45° dipping to NE) and a σ_3 cluster plunging SW could be interpreted as a record of layer-parallel compression at an early stage of deformation. Similarly, possible early stage stress clusters are found in some paired diagrams (SKM-1, SKV-1, BLV-6 and CLV-7 in Fig. 4.16), but are subordinate.

Previous stress inversions applied to the Zagros fold belt in Iran (e.g., Lacombe et al., 2006, 2007) and the Taiwan collision zone (e.g., Rocher et al., 1996; Lacombe et al., 1993, 1996) demonstrated that the timings of faulting and calcite twinning were dominantly both pre- and post-folding (e.g., Lacombe et al., 2009). In the deformation zone where tight folds are pervasively developed, it is reasonable to consider that the exerting duration of one stress state associated with fold development is much longer than that for activation of folding, which may promptly proceed at an early stage. A long duration of fold tightening after bedding tilting increases the possibility for strata to experience strong compression acting at a steep angle to the bedding plane, which may activate many faults and twins. This long-term compression from the NE−SW to E−W direction has also led to the contraction of the Walanae Depression growing large-scale gentle folds after the tightening of folds in the deformation zone near the EWF. This may have promoted differentiation of landforms in the Walanae Depression tending subsidence in the eastern part accompanied by deposition of alluvial fan deposit and upheaval in the western part. The tectonic setting for a long-term NE−SW to E−W compression around the EWF will be discussed in a later section.

4.2.7 Radiocarbon Dating $\delta^{13}C$ values

The samples used for radiocarbon dating were soils intercalated in the shear fractures formed in the weathered mudstone which is intensely sliced by flexural slip folding most likely associated with activity of the EWF (Fig. 4.9b). The soils include dark-brown organic matter. Samples ST-28A and ST-28B, which come from 50 cm and 30 cm beneath the surface, respectively, yielded ages of 3050 cal BP and 3990 cal BP, respectively (Table 4.4). These radiocarbon ages are consistent with the stratigraphic order. The $\delta^{13}C$ (PDB) values of the date soil samples are also shown in Table 4.5. Both samples show similar and significantly negative values, –18.4‰ for ST.28A and –19.6‰ for ST-28B, which are plausible for soils of grassland.

Table 4.5 Radiocarbon ages of sheared soil samples.

Sample number	Lab sample number [a]	Measured radiocarbon age	$\delta^{13}C$(‰)	Conventional radiocarbon age (BP) [b]	Calibrated age 2σ [c]
ST 28 A	Beta-286412	2940 ± 40	-18.4	3050 ± 40	Cal BC 1410-1210, Cal BP 3360-3160 (95% probably)
ST 28 B	Beta-286413	3900 ± 40	-19.6	3990 ± 40	Cal BC 2580-2460, Cal BP 3530-4410 (95% probably)

[a] Processing and measurement of samples were carry out at Beta Analytic Inc. Miami, Florida.
[b] Conventional ^{14}C ages were calculate according to Stuiver and Polach (1977)
[c] Calibration of radiocarbon age to calendar years were performed using “IntCal04” (calibration issue of radiocarbon, volume 46, 2004).

CHAPTER V. DISCUSSIONS

5.1 Formation of Accretionary complex

The tectonic history of Sulawesi have been began in the Late Jurassic–Early Cretaceous with the development of a continental arc in south-central Kalimantan associated with northeasterly subduction of Meso-Tethys (e.g. Hamilton, 1979; Parkinson et al., 1998; Guntoro, 1999; Hall, 1996; van Leeuwen et al., 2010). The accretionary complexes are represented by the Bantimala-Barru Complexes in the western Sulawesi and the Pompangeo Complex in the central Sulawesi. The Biru metamorphic rocks occupy the southern part of the backbone of the Western Divide Mountain Range with the Barru and Bantimala basement Complex. Based on petrographic, geochemical, structural and also chronological analyses conducted in his study, it can be considered that the Biru metamorphic rocks which has been believed as an undeformed hornfels is also a part of this metamorphic complex. The Biru Metamorphic Complex experienced some post-metamorphic events such as contact metamorphism and cataclasis associated with the plutonic intrusion and faulting of WWF, respectively.

5.2 Evolution of Walanae Fault System

The following section is a discussion of evolution of Walanae fault zone from Middle Miocene to Present. Previous studies on regional tectonics of South Sulawesi (van Leeuwen, 1981; Sukamto, 1982; Grainge and Davies, 1985) suggested that the Walanae fault occurred at the Middle Miocene as a normal fault under extensional tectonics and was then reactivated as a strike–slip fault with sinistral sense during Pliocene. However, there are few structural evidences for this sinistral faulting and the deformation explainable by the stress states inferred in this study involves strata of the Walanae Formation which have deposited from middle Miocene to Pliocene (van Leeuwen et al., 2010).

5.2.1 West Walanae Fault

The Walanae fault (termed WWF) may have begun to develop during the Middle Miocene (Fig. 5.1a). Widespread block-faulting took place in the Western Divide Mountains around 13–14 Ma (van Leeuwen et al., 2010). This event occurs at the end of activity of potassic volcanics of Camba Formation. The potassic magmatic activity may have been triggered by deep-seated faults tapping into mantle tectonic regime metasomatized by an earlier subduction event (van Leeuwen, 1981; Letellier et al., 1990). The potassic magmatism commenced throughout Western Sulawesi around the same time (Bergman et al., 1996; Polvé et al., 1997; Elburg et al., 2002), suggesting that during the Middle Miocene the entire region was affected by an extensional stress field (van Leeuwen et al., 2010).

The presence of cataclasite texture in the Biru metamorphic rocks are likely effect of uplifting. Some previous work also confirms that the Western Divide Mountain uplifted prior to the formation of Walanae Depression (termed Sengkang Basin in this study). A differential vertical movement in the order of 300–400 m is indicated at Biru area, which is evidenced that a basal Middle Miocene unit contains older limestone clasts (from Early Miocene to Late Eocene) in ascending sequence (van Leeuwen, 1981; van Leeuwen et al., 2010). Almost in the same time, the Biru granodiorite was intruded in the Biru area (Fission tract dating 19 ± 3.4 by van Leeuwen, 1981), the emergence of granitoid intrusion may be facilitated by WWF as a vertical channeling trough fault section.

The WWF was probably reactivated through this pathway (Fig. 5.1c), where dikes intrusion (e.g. Elburg et al., 2002) cuts the volcanics and plutonic rocks in Late Miocene to Pliocene. The N−S trending σ_3 is inferred from orientation of dike segments. However it is difficult to ascertain the sense of movement of the WWF, numerous displacements on the granodiorite rocks and orientation of dike segments suggesting dextral displacement. Most of the results of stress states analysis from fault population indicated compressional stress regime defined by σ_1-axis relatively horizontal and predominantly NNW−SSE and subordinately NNE−SSW, and highly plunging or nearly vertical σ_3-axis. Judging from dikes cut by faults, stress states inferred from fault−slip data is associated with later events. Probably the recent activity of WWF is an uplifting of West Mountain Range as a response to the consequent motion of Australian microcontinents toward to the west.

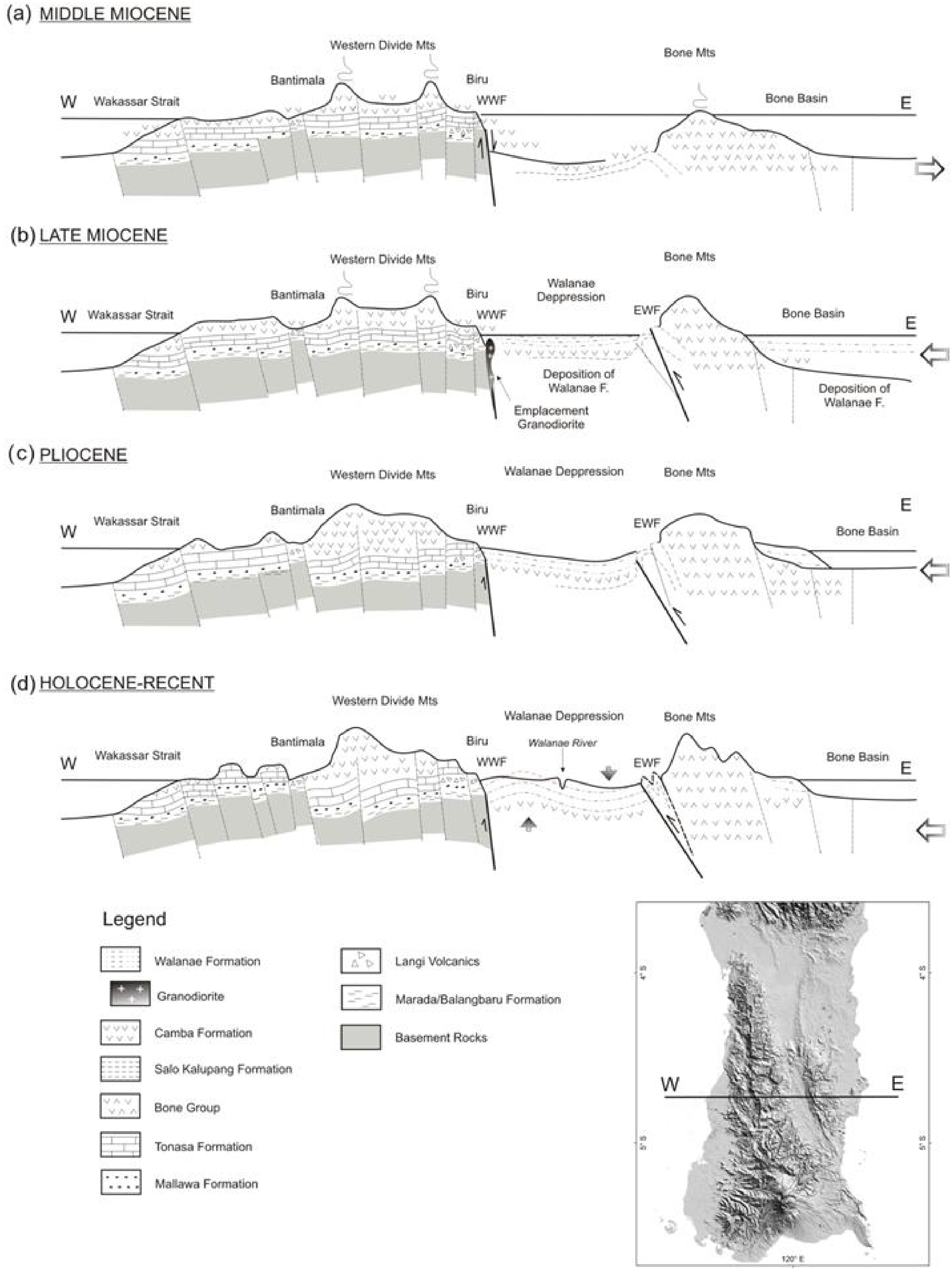

Figure 5.1 Schematic cross section E-W South Sulawesi illustrated evolution of Walanae Fault during Middle Miocene to Present. (a) Upliflting of Western Mountains range, formation of Walanae fault, initiation of Walanae depression. (b) Granodiorite emplacement around WWF, Deposition sediments of Walanae Formation. (c) Formation of east Walanae fault (EWF). (d) Uplifting of Walanae Depression, shortening of rocks of Walanae Formation, erosion in central depression.

5.2.2 East Walanae Fault

During the Pliocene a major tectonic event took place in South Sulawesi, which is widely attributed to the collision of the Banggai-Sula continental fragment with the east arm of Sulawesi. Consistent E−W to NE−SW compression stress states obtained from fault slip and calcite twin along western margin of Bone Mountains to Sengkang area. This caused significant shortening of crust with development of north-trending large scale folds in Walanae Depression and central part of Sengkang Basin (e.g. van Bemmelen, 1949), tight−fold and thrust in the Salokalupang Formation. When the EWF occurred as a south-north trending reverse fault, Bone Mountains moved up to west, and Sengkang Basin was divided into two sub−basin. Reverse faults cutting the strata of the Walanae Formation have been identified in a seismic profile crossing EWF for oil and gas exploration in the Sengkang area, which is considered to be responsible for the creation of a trough in the West Sengkang Basin (Grainge and Davies, 1985) or causing a separation of east and west Sengkang basin during the deposition of Walanae Formation. Therefore, E−W to NE−SW shortening associated with the activity of EWF probably began at the late stage of deposition of the Walanae Formation, namely late Miocene. The collision of the Banggai-Sula microcontinent with Sulawesi may have affected in long-range, generating stress states with strong E−W to NE−SW trending σ_1 through the south arm Sulawesi and activating EWF and folding and uplifting in the Bone Basin (Yulihanto, 2004). Westward motion of Banggai-Sula microcontinent possibly causing granitoid magmatism and rapid uplift in northern−central Sulawesi (Bergman et al., 1996; van Leeuwen and Muhardjo, 2005). Although some authors have suggested that it started somewhat earlier (e.g. Hamilton, 1979; Polvé et al., 1997).

Late Quaternary deformation around EWF is confirmed by radiocarbon ages of approximately 3000 and 4000 years of the sheared soils near the EWF trace, although no obvious tectonic landform has been found, and current seismicity around EWF seems relatively low compared to central and northern area in Sulawesi (e.g., Bellier et al., 2006; Socquet et al., 2006; Tanioka and Yudhicara, 2008). Beaudouin et al., (2003) proposed based on seismotectonic study that the present day deformation and stress field in south arm of the sulawesi are characterized by compression regime with ESE−WNW (N99°E)-trending σ_1. A report on the focal mechanisms for the period from 1976 to 2000 by Tanioka and Yudhicara (2008) showed dominance of reverse faults in South Sulawesi. Strain rate of 3 mm/yr or less below is suggested by GPS and earthquake slip vector for the area covering the Makassar block (Socquet et al., 2006) where the EWF is included. Therefore, it is acceptable that the stress states of E−W to NE−SW general compression have been consistent since late Miocene.

EWF is the subject of observation as a seismic source. As reported by Supartoyo and Surono (2008) in the catalog of destructive earthquakes in Indonesia, large earthquakes were recorded in South Sulawesi, Makassar in 1820 and Bulukumba in 1828, although their magnitudes are unknown. Elucidation of the history of the activity of EWF and associated stress states will be useful for assessment of future activity and extent of damaged area, hence crucially important for prevention of earthquake disaster.

CHAPTER VI. CONCLUSIONS

On the basis of metamorphic, structural and chronological similarities, the Biru Metamorphic Complex exposed in southern part of the West Divide Mountain Range was assessed as a main part of the basement of South Sulawesi with the Bantimala Metamorphic Complex and Barru Metamorphic Block. Multiple inverse paleotress analysis using both fault slip and calcite twin data with observations of deformation structures and geomorphology along the Walanae fault system were provided important information contributing for understanding the activity of Walanae fault and Neogene-Quaternary tectonics of South Sulawesi. Several points of conclusions can be drawn as following:

1. The Biru Metamorphic Complex comprises metamorphic rocks of epidote-amphibolite and amphibolites facies.
2. The Biru Metamorphic Complex shows a general trend of schistosities with NE−SW striking and south dipping schistosities. The schistosity (S0) defined by preferred orientation of mineral inclusions in core of garnet, epidote and plagioclase porphyroblasts and main schistosity (S1) parallel to isoclinals fold axial plane (F1, F2) were formed during the plastic deformation (D1) simultaneous with a regional metamorphism (M1).
3. The evidence of D1 deformation is commonly very limited in the quartz texture, it is seemingly caused by a contact metamorphism in association with the emplacement of the Biru granodiorite rocks (M2) in Middle Miocene, although array of elongated subgrains and seriated boundaries still be preserved as a relic of D1. *c*-axis LPO pattern of quartz suggests the non-coaxial flow under the dominant operation of basal<a> slip system.
4. In some area, metamorphic rocks show an overprint of cataclastic texture (D2). Annealing of plastic deformation structures and superimposed cataclastic deformation are probably resulted from the Middle Miocene uplifting of the West Divide Mountain Range associated with formation of Walanae fault System.
5. Major and trace elements characterize the plotolith of the Biru metamorphic rocks as mid-oceanic ridge basalts (MORB), calc-alkali basalts and island-arc tholeiites (IAT).

6. K−Ar dating for muscovite in a mica schist yielded an Early Cretaceous age (109±2.4 Ma), comparable to those of the Bantimala Metamorphic Complex and Barru Metamorphic Block.
7. Fault−slip data of the Biru area adjacent to the West Walanae fault zone shows σ_1-axis ranging from NNW−SSE to NNE−SSW and σ_3-axis nearly vertical.
8. Calcite twin data were available for the multiple inverse method and provided chiefly obvious and reliable stress tensors as well as fault−slip data. Both calcite twin and fault−slip data yielded consistent stress states throughout the whole study area: a predominance of NE−SW-to-E−W trending σ_1 and vertical to moderately-south-plunging σ_3 with generally low stress ratio. These stress states could activate the EWF as a reverse fault with a dextral shear component and account for constructional deformation structures and landform around the trace of the fault.
9. Most of the calcite twins and mesoscale faults were activated during the latest stage of folding or later. Calcite twin data from several localities also suggest activation during early stages of folding.
10. Based on the morphology and width of twin lamellae in the limestone and calcareous rock samples, the strata in the deformation zone along the EWF may have deformed around 200℃.
11. Inferred paleostress states around the EWF were most likely generated under the tectonic conditions influenced by the collision of Sulawesi with the Australian fragments (the Banggai-Sula) since the Late Miocene.
12. The Late Quaternary radiocarbon ages (3050 cal BP and 3990 cal BP) of sheared soils indicated that the deformation still active at present day in the EWF zone.

REFERENCES

Ahmad, W. (1975) Geology along the Matano fault zone, East Sulawesi, Indonesia. In: Wiryosujono, Sudrajat, A. (Eds.) Regional Conference on the Geology and Mineral Resources of Southeast Asia, Jakarta, 143–150.

Anderson, J.L. and Smith, D.R. (1995) The effects of temperature and O2 on the Al-in-hornblende barometer. American Mineralogist, 80, 549.559.

Ascaria, N.A., Harbury, N.A. and Wilson, M.E.J. (1997) Hydrocarbon potential and development of Miocene knoll-reefs, South Sulawesi. In: Howes, J.V.C., Noble, R.A. (eds), Proceedings of the Petroleum Systems of SE Asia and Australasia Conference, Indonesian Petroleum Association, Jakarta, May 1997, 569–584.

Beaudouin, T.H., Bellier, O. and Sebrier, M. (2003) Present-day stress and deformation field within the Sulawesi Island area (Indonesia): geodynamic implications. Bulletin de la Société géologique de France 174, 305– 317.

Bellier, O., Sebrier, M., Seward, D., Beaudouin, T., Villeneuve, M., and Putranto, E. (2006) Fission track and fault kinematics analyses for new insight into the Late Cenozoic tectonic regime changes in West-Central Sulawesi (Indonesia). Tectonophysics, 413, 201–220.

Berry, R.F. and Grady, A.E. (1987) Mesoscopic structures produced by Plio-Pleistocene wrench faulting in South Sulawesi, Indonesia. Journal of Structural Geology 9, 563–571.

Bergman, S.C., Coffield, D.Q., Talbot, J.P. and Garrard, R.J. (1996) Tertiary tectonic and magmatic evolution of western Sulawesi and the Makassar Strait, Indonesia. Evidence for a Miocene continent-continent collision. In: Hall, R., Blundell, D.J. (eds), Tectonic Evolution of SE Asia, Geological Society, London, Special Publications 106, 391–430.

Blundy, J.D. and Holland, T.J.B. (1990) Calcic amphibole equilibria and a new amphibole-plagioclase geothermometer. Contribution to Mineralogy and Petrology, 104, 208.224.

Boudagher-Fadel, M.K. (2002) The Stratigraphical relationship between planktonic and larger benthic foraminifera in Middle Miocene to Lower Pliocene carbonate facies of Sulawesi, Indonesia. Micropaleontology 48 (2), 153-176.

Brown, G.C. and Musset, A.E. (1993) The Inaccessible Earth: An Integrated View of its Structure and Composition, Chap-man & Hall London.

Clemente, C.S., Amoros, E.B., and Crespo, M.G. (2007) Dike intrusion under shear stress: Effects on magnetic and vesicle fabrics in dikes from rift zones of Tenerife (Canary Islands). Journal of Structural geology, 29, 1931-1942.

Coffield, D.Q., Bergman, S.C., Carrard, R.A., Guritno, N., Robinson N.M. and Talbot, J. (1993) Tectonic and stratigraphic evolution of the Kalosi PCS area and associated development of a Tertiary petroleum system, South Sulawesi, Indonesia. Proceedings Indonesian Petroleum Association, 22nd Annual Convention, V.1, 679–706.

Elburg, M., van Leeuwen, T.M., Foden, J. and Muhardjo. (2002) Origin of geochemical variability by arc-continent collision in the Biru area, Southern Sulawesi (Indonesia). Journal of Petrology 43, 581–606.

Etchecopar, A., Vasseur, G. and Daignieres, M. (1981) An inverse problem in microtectonics for the determination of stress tensors from fault striation analysis. Journal of Structural Geology 3, 51-65.

Evans, M.A. and Groshong Jr., R.H. (1994) Microcomputer techniques and applications: a computer program for the calcite strain-gauge technique. Journal of Structural Geology 16 (2), 277-281.

Ferrill, D.A, Morris P., Evans M.A., Burkhard M., Groshong R.H. and Onasch C.M. (2004) Calcite twin morphology: a low-temperature deformation geothermometer. Journal of Structural Geology 26, 1521-1529.

Grainge, A.M. and Davies, K.G. (1985) Reef exploration in the East Sengkang Basin, Sulawesi, Indonesia. Marine and Petroleum Geology 2, 142–155.

Groshong, R.H. Jr., 1974. Experimental test of least-squares strain calculations using twinned calcite, Geological Society of America Bulletin, 85, 1855-1864.

Guntoro, A. (1999) The formation of the Makassar Strait and the separation betweenSE Kalimantan and SW Sulawesi. Journal of Asian Earth Sciences 17, 79–98.

Guritno, N., Coffield, D.Q. and Cook, R.A. (1996) Structural development of Central South Sulawesi. Proceedings of the Indonesian Petroleum Association, 25th Annual Convention, 253–266.

Hall, R. and Wilson, M.E.J. (2000) Neogene sutures in eastern Indonesia. Journal of Asian Earth Sciences 18, 781–808.

Hall, R. (1996) Reconstructing Cenozoic SE Asia. In: Hall, R. & Blundell, D. J. (eds) Tectonic Evolution of SE Asia. Geological Society, London, Special Publications, 106, 153–184.

Hamilton, W. (1979) Tectonics of the Indonesian region. U.S. Geological Survey Professional Paper 1078, 1-345.

Hasan, K. (1991) The Upper Cretaceous Flysch succession of the Balangbaru Formation, Southwest Sulawesi. In: Proceeding Indonesia Petroleum Association 20th annual convention, 183-208.

Holland, T. J. B. and Blundy, J. D. (1994) Non-ideal interactions in calcic amphiboles and their bearing on amphibole-plagioclase thermometry. Contributions to Mineralogy and Petrology, 116, 433-447.

Itaya, T. and Takasugi, H. (1988) Muscovite K-Ar ages of the Sanbagawa schists, Japan and argon depletion during cooling and deformation. Contrib. Mineral. Petrol., v. 100, 281-290.

Itaya, T., Nagao, K., Inoue, K., Honjo, Y., Okada, I. and Ogata, A. (1991) Argon Isotope analysis by a newly developed mass spectrometric system for K-Ar dating. Mineralogical J., V. 15, 203-290.

Itaya, T. and Fujino, M. (1999) K-Ar age - chemistry – fabric relations of phengite from the Sanbagawa high-pressure schists, Japan. Island Arc, v. 8, 523-536.

Kadarusman, A., Miyashita, S., Maruyama, S., Ishikawa, A. and Parkinson, C.D. (2004) Petrology, geochemistry and paleogeographic reconstructions of the East Sulawesi Ophiolite, Indonesia. In: Dilek, Y., Harris, R. (Eds.), Special Issue on Continental Margins in the Pacific Rim. Tectonophysics 392, 55–83.

Katili, J.A. (1978) Past and present geotectonic position of Sulawesi, Indonesia. Tectonophysics, 45: 289-322.

Kimura, J.I. and Yamada, Y. (1996) Evaluation of major and trace element XRF analyses using a flux to sample ratio of two to one glass beads. Journal of Mineralogy, Petrology and Economic Geology, 91, 62–72.

Kretz, R. (1983) Symbols of rock-forming minerals. American Mineralogist, 68, 277–279.

Lacombe, O. and Laurent, P. (1996). Determination of deviatoric stress tensors based on inversion of calcite twin data from experimentally deformed monophase samples: preliminary results. Tectonophysics 255, 189-202.

Lacombe, O., Angelier, J., Laurent, P., Bergerat, F. and Tourneret, C. (1990) Joint analyses of calcite twins and fault–slips as a key for deciphering polyphase tectonics: Burgundy as a case study. Tectonophysics 182, 279-300.

Lacombe O., Angelier J. and Laurent, P. (1993) Calcite twins as markers of recent compressional event in an active orogene: the reefal limestones of southern Taiwan. Computes rendus de l'Académie des Sciences, Paris, t.316, II, 1805-1813.

Lacombe, O., Angelier, J., Rocher, M., Bergues, J., Chu, H.-T., Deffontaines B., and Hu, J-.C. (1996) Stress patterns associated with folding at the front of a collision belt: example from the Pliocene reef limestones of Yutengping (Taiwan). Bulletin de la Societe geologique de France 167, 361-374.

Lacombe, O., Mouthereau, F., Kargar, S. and Meyer, B. (2006) Late Cenozoic and modern stress fields in the western Fars (Iran): implications for the tectonic and kinematic evolution of Central Zagros. Tectonics 25, TC1003, doi:10.1029/2005TC001831.

Lacombe, O., Amrouch, K., Mouthereau, F. and Dissez, L. (2007) Calcite twinning constraints on late Neogene stress patterns and deformation mechanisms in the active Zagros collision belt. Geology 35, 263-266, doi:10.1130/G23173A.

Lacombe, O., Malandain, J., Vilasi, N., Amrouch, K. and Roure, F. (2009) From paleostresses to paleoburial in fold-thrust belts: preliminary results from calcite twin analysis in the outer Albanides. Tectonophysics, Geology of the Vertical Movements of the Lithosphere 475, 128-141.

Laurent, P., Kern, H. and Lacombe, O. (2000) Determination of deviatoric stress tensors based on inversion of calcite twin data from experimentally deformed monophase samples, part II, uniaxial and triaxial stress experiments. Tectonophysics 327, 131-148.

Leake, B. E., Woolley, A. R., Arps, C. E. S., Birhc, W. D., Gilbert, M. C., Grice, J. D., Hawthorne, F. C., Kato, A., Kisch, H. J., KRIVOVICHEV, V. G., Linthout, K., Mandarino, J. A., Nickel, E. H., Rock, N. M. S., Schumacher, J. C., Smith, D. C., Stephenson, N. C. N., Ungaretti, L., Whittaker, E. J. W. and Youzhi, G. (1997).

Nomenclature of amphiboles: Report of the subcommittee on amphiboles of the International Mineralogical Association Commission on new minerals and mineral names. Mineralogical Magazine, 61, 295-321.

Letellier, J., Yuwono, Y.S., Soeria-Atmadja, R. and Maury, R.C. (1990). Potassic volcanism in central Jawa and South Sulawesi, Indonesia. Journal Southeast Asian Earth Sciences 4, 171–187.

Nemcok, M. and Lisle, R.J. (1995) A stress inversion procedure for polyphase fault/slip data sets. Journal of Structural Geology 17 (10), 1445-1453.

Maulana, A. (2009) Petrology, Geochemistry and metamorphic evolution of the South Sulawesi basement complex, Indonesia, Master Thesis, The Australian National University. 212.

Maulana, A., Ellis, D, J. and Christy, A, C. (2010) Pre-tertiary tectonic evolution of the South Sulawesi basement rocks, Indonesia: Constraint from Petrology and Geochemistry Data. In: Paleoclimate in Asia During the Cretaceous, IGCP-507, extended abstracts, Geological Agency-Ministry of Energy and Mineral Resources Republic of Indonesia, 75-76.

Mayall, M. J. and Cox, M., (1988) Deposition and diagenesis of Miocene limestones, Senkang Basin, Sulawesi, Indonesia. Sedimentary Geology 59, 77-92.

Meschede, M. (1986) A method of discriminating between different types of mid-ocena ridge basalts and continental tholeiites with the Nb-Zr-Y diagram. Chemical Geology, 56, 207-218.

Miyazaki, K., Zulkarnain I., Sophaheluwakan, J. and Wakita, K. (1996) Pressure-temperature conditions and retrograde paths of eclogites, garnet-glaucophane rocks and schists from South Sulawesi, Indonesia. Journal of Metamorphic Geology 14, 75-80.

Nagao, K., Nishido H., Itaya T. and Ogata K. (1984) K–Ar age determination method. Bulletin of Hiruzen Research Institute, Okayama University of Science 9, 19–38.

Otsubo, M., Shigematsu, N., Kitagawa, Y. and Koizumi, N. (2009) Stress history in the forearc region of the Nankai trough subduction zone: paleostress analysis based on faults in core samples from the Kumano Ichiura and Kihoku Miyama sites, Kii Peninsula, SW Japan. Journal of the Geological Society of Japan 115, 457-469.

Parkinson, C.D., Miyazaki, K., Wakita, K., Barber, A.J. and Carswell, P.A. (1998) An overview and tectonic synthesis of the pre-tertiary very-high pressure metamorphic and associated rocks of Java, Sulawesi and Kalimantan, Indonesia. Island Arc 7, 184–200.

Parkinson, C. D. (1998a) An outline of the petrology, structure and age of the Pompangeo Schist Complex, Sulawesi, Indonesia. The Island Arc 7, 231-245.

Parkinson, C.D. (1998b) Emplacement of the east Sulawesi ophiolite: evidence from subophiolite metahomorphic rocks, Journal of Asian Earth Science 16, 13-28.

Pearce, J. A. and Cann, J. R. (1973) Tectonic setting of basic volcanic rocks determined using trace element analyses. Earth and Planetary Science Letters, 19, 290-300.

Pollard, D.D. (1987) Elementary fracture mechanics applied to the structural interpretation of dykes. In: Halls, H.C., Fahrig, W.F. (Eds.), Mafic Dyke Swarms. Geological Association of Canada Special Paper 34, 5-24.

Polvé, M., Maury, R.C., Bellon, H., Rangin, C., Priadi, B., Yuwono, S., Joron, J.L. and Soeria-Atmadja, R. (1997) Magmatic evolution of Sulawesi: constraints on the Cenozoic geodynamic history of the Sundaland active margin. Tectonophysics 272, 69–92.

Raheim, A. and Green, D. H. (1974) Experimental determination of the temperature and pressure dependence of the Fe-Mg partition coefficient for coexisting garnet and clinopyroxene. Contibutions to Mineralogy and Petrology, 48, 179-203.

Reimer, P.J., Baillie, M.G.L, Bard E., Bayliss, A., Beck J.W., Bertand, C.J., Blackwell, P.G., Buck, C., Burr, G.S., Cutler, K.B., Damon, P.E., Edwards, R.L., Fairbanks, R.G., Friedrich, M., Guilderson, T.P., Hogg, A.G., Hughen, K.A., Kromer, B., McCormac, G., Manning, S., Ramsey, C.B., Reimer, R.W., Remmele, S., Southon, J.R., Stuiver, M., Talamo, S., Taylor, F.W., van der Plicht, J. and Weyhenmeyer, C.E. (2004). IntCal04 terrestrial radiocarbon age calibration, 0-26 cal kyr BP. Radiocarbon 46, 1029-1058.

Rocher, M., Lacombe O., Angelier J. and Chen H.W. (1996) Mechanical twin sets in calcite as markers of recent collisional events in a fold-and-thrust belt: Evidence from the reefal limestones of southwestern Taiwan, Tectonics 15 (5), 984-996.

Sasajima, S., Nishimura, S., Hirooku, K., Otofuji, Y., van Leeuwen, T.M., and Hehuwat, F. (1980) Paleomagnetic studies combined with fission-track datings on the western arc of Sulawesi, East Indonesia. Tectonophysics 64, 163–172.

Simandjuntak, T. O. and Barber, A. J. (1996) Contrasting Tectonic Styles in the Neogene Orogenic Belts of Indonesia. In: Hall, R. & Blundell, D. J. (eds) Tectonic Evolution of SE Asia. Geological Society, London, Special Publications, 106, 185–201.

Smith, R. B. and Silver, E. A. (1991) Geology of a Miocene collision complex, Buton, eastern Indonesia. Geological Society of America Bulletin, 103, 660–678.

Spear, F. S. (1993) Metamorphic phase equilibria and pressure-temperature-time path. Mineralogical Society of America, Washington D.C.

Stuiver, M. and Polach, H.A. (1977) Discussion reporting of 14C data. Radiocarbon 19, 355–363.

Socquet, A., Simon, W., Vigny, C., McCaffrey, R., Subarya, C., Sarsito, D., Ambrosius, B. and Spakman, W. (2006) Microblock rotations and fault coupling in SE Asia triple junction (Sulawesi, Indonesia) from GPS and earthquake slip vector data. Journal of Geophysical Research 111, B08409, doi: 10.1029/2005JB003963.

Sperner, B., Ratschbacher, L. and Ott, R. (1993) Fault-striae analysis: a Turbo Pascal program package for graphical presentation and reduced stress tensor calculation. Computers and Geosciences 19, 1361-1388.

Sukamto, R. (1975) The structure of Sulawesi in the light of plate tectonics. Paper presented at the Regional Conference on the Geology and Mineral Resources of SE Asia, Jakarta, 1–25.

Sukamto, R. (1982) The geology of the Pangkajene and western part of Watampone, Sulawesi. Geological Research and Development Centre, Bandung. Quadrangles Series, scale 1:250,000.

Sukamto, R. and Supriatna, S. (1982) The geology of the Ujung Pandang, Benteng and Sinjai, Sulawesi. Geological Research and Development Centre, Bandung. Quadrangles Series, Scale 1 : 250.000.

Sukamto, R. and Westermann, G.E.G. (1993) Indonesia and Papua New Guinea. In Westermann, G.E.G. (ed.) The Jurassic of the circum-Pacific, Cambridge University Press. 181-93.

Supartoyo, and Surono. (2008) Catalogue of earthquake destructive in Indonesia 1969-2007. Centre of Volcanology and Geological Hazard Mitigation, Geology Agency, Ministry of Energy and Mineral Resources Indonesia, 1-159.

Tanioka, Y. and Yudhicara. (2008). Teleseismic body wave data analysis for the May 4, 2000, Sulawesi Earthquake. Jurnal Geoaplika 3 (2), 071-080.

Van Bemmelen, R.W. (1949) The Geology of Indonesia, vol. 1a. Government Printing Office, The Hague. 1- 732.

Van den Bergh, G.D., Lumbanbatu, U.M., de Boer, P.L. and Azis, F. (1995) Lithostratigraphy of the West Sengkang Basin. In: The Geology and Stratigraphy of the Vertebrate – Bearing Deposits in the Sengkang Basin. Special Publication 18, GRD Centre, Bandung.

Van Leeuwen, T.M. (1981) The geology of southwest Sulawesi with special reference to the Biru area. In: Barber, A., Wiryosujono, S. (eds.), The Geology and Tectonics of Eastern Indonesia, Geological Research and Development Centre, Special Publication 2, 277–304.

Van Leeuwen, T. M. and Muhardjo. (2005) Stratigraphy and tectonic setting of the Cretaceous and Paleogene volcanic–sedimentary successions in northwest Sulawesi, Indonesia implications for the Cenozoic evolution of Western and Northern Sulawesi. Journal of Asian Earth Sciences, 25, 481–511.

Van Leeuwen, T.M., Susanto, E.S., Maryanto, S., Hadiwisastra, S., Sudijono, and Muharjo. (2010) Tectonostratigraphic evolution of Cenozoic marginal basin and continental margin successions in the Bone Mountains, South Sulawesi, Indonesia. Journal of Asian Earth Sciences 38, 233-254.

Wakita, K., Munasri, Sopaheluwakan J., Zulkarnain I. and Miyazaki K. (1994) Early Cretaceous time-lag between the age of radiolarian chert and its metamorphic basement in Bantimala area, South Sulawesi, Indonesia. The Island Arc 3, 90-102.

Wakita, K., Sopaheluwakan, J., Miyazaki, K., Zulkarnaen, I. and Munasri. (1996) Tectonic evolution of the Bantimala Complex South Sulawesi, Indonesia. In: Hall, R., Blundell, D.J. (Eds.), Tectonic Evolution of SE Asia. Geological Society of London Special Publication 106, 353–364.

Watkinson, I.M. (2011) Ductile in the metamorphic rocks of central Sulawesi. In: Hall, R., Cottam, M.A., Wilson, M.E.J. (eds), The SE Asian Gateway: History and

Tectonics of the Australia–Asia Collision, Geological Society of London, Special Publications 355,157-176.

Wilson, M. E. J. and Bosence D. W. J. (1996). The tertiary evolution of South Sulawesi: a record in redeposited carbonates of the Tonasa Limestone Formation. In Tectonic Evolution of Southeast Asia (ed. R. Hall and D. Blundell); London, Geological Society Special Publication 106, 365–389.

Wilson, M.E.J. and Moss, S.J. (1999) Cenozoic paleogeographic evolution of Sulawesi and Borneo. Palaeogeography, Palaeoclimatology and Palaeoecology 145, 303–337.

Wilson, M.E.J., Bosence, D.W.J. and Limbong, A. (2000) Tertiary syntectonic carbonate platform development in Indonesia. Sedimentology 47, 395–419.

Yamaji, A. (2000) The multiple inverse method: a new technique to separate stresses from heterogeneous fault–slip data. Journal of Structural Geology 22, 441–452.

Yamaji, A., Sato, K. and Otsubo, M. (2010) Multiple Inverse Method main processor, Version 6.02. Division of Earth and Planetary Sciences, Kyoto University, Kyoto.

Yulihanto, B. (2004) Hydrocarbon play analysis of the Bone Basin, South Sulawesi. Proceedings IPA-AAPG of Deepwater and Frontier Exploration in Asia and Australasia Symposium, December 2004, 1- 16.

Yuwono, Y.S., Maury, R., Soeria-Atmadja, R. and Bellon, H. (1988a) Tertiary and Quaternary geodynamic evolution of South Sulawesi constraints from the study of volcanic units. Geology Indonesia Jakarta 13, 32–48.

Yuwono, Y.S., Priyomarsono, S., Maury, R.C., Rampnoux, J.P., Soeria-Atmaja, R., Bellon, H. and Chotin, P. (1988b) Petrology of the Cretaceous magmatic rocks from Meratus Range, Southeast Kalimantan. Journal of Southeast Asian Earth Sciences 2, 15–22.

ACKNOWLEDGMENTS

First, foremost I thank my supervisor Dr. Osamu Nishikawa for his acceptance, advice, time, support, guidance us a living in Japan. He has provided great teaching of structural geology in the field observation, laboratory and reporting, it made me much confidence." Thank you so much for everything".

I am also extremely grateful to my advisor Prof. Takashi Uchida for acceptance, facility, invaluable suggestion and support over the past three years." Thank you so much for everything".

I would like to thank Professor Emeritus Isao Takashima who gave me a chance to study in Akita University.

I would like to thank Prof. Daizo Ishiyama for acceptance, opportunity and the laboratory facility.

I would wish to thank Prof Atzusi Yamaji (Kyoto University) for his constructive advice and his encouragement using MIM program for calcite twin.

I would wish to thank to Dr. Takeyuki Ogata and Dr. Azuza Kondou for their guidance and assistance of EPMA and XRF analyses.

I would like to thank Dr. Jun Moto and Dr. Fukuda (Tohoku University) for their kind assistance and facility of EBSD analyses at Tohoku University.

I would like to thank Dr. Adi Maulana (Hasanuddin University) for their kind assistance to calculate thermobarometry.

I wish to expresses thanks to my laboratory colleagues of graduate and undergraduate students for their understanding during my studies.

I would like to thank Japan International Cooperation Agency (JICA) for providing the funds during my studies under Hasanuddin University (UNHAS) - Japan Bank International for Cooperation (JIB) Loan No. IP−541.

Finally, I would like to thank my parents, my wife and my son: My study is a product of all your prayer and support. Saying thank you does not seem like enough for you.

APPENDIX 1

Electron Probe Micro-Analyzer (EPMA) data

Sample			PM-02						Sample	PM-05			
Mineral	Hbl	Act	Hbl	Act	Chl	Ab	Ep	Hem	Mineral	Chl	Ab	Ep	Rt
	Core	Rim	Core	Rim									
SiO2	48.17	53.18	50.51	55.20	28.95	69.71	39.06	0.29	SiO2	27.06	69.26	39.20	0.02
TiO2	0.13	0.07	0.03	0.06	0.06	0.00	0.08	0.02	TiO2	0.02	0.01	0.12	98.89
Al2O3	8.81	2.09	7.34	8.31	19.75	20.02	25.96	0.10	Al2O3	18.59	19.57	27.68	0.02
FeO	11.11	16.47	10.28	6.89	12.18	0.03	8.70	90.23	FeO	14.84	0.03	6.97	0.45
MnO	0.27	0.66	0.30	0.20	0.18	0.00	0.06	0.00	MnO	0.24	0.00	0.04	0.01
MgO	15.98	13.12	16.26	14.52	24.80	0.00	0.08	0.05	MgO	21.69	0.00	0.08	0.00
CaO	10.88	12.42	12.25	11.50	0.00	0.18	23.15	0.03	CaO	0.09	0.23	23.76	0.17
Na2O	0.75	0.24	0.73	1.80	0.02	11.71	0.00	0.03	Na2O	0.01	11.60	0.00	0.01
K2O	0.20	0.12	0.14	0.16	0.05	0.10	0.00	0.02	K2O	0.01	0.07	0.02	0.01
Cr2O3	0.09	0.05	0.02	0.02	0.01	0.00	0.00	0.01	Cr2O3	0.00	0.00	0.00	0.00
NiO	0.03	0.01	0.04	0.03	0.00	0.00	0.00	0.01	NiO	0.01	0.00	0.00	0.05
Total	**96.41**	**98.42**	**97.89**	**98.69**	**85.99**	**101.75**	**97.09**	**90.78**	**Total**	**82.54**	**100.77**	**97.87**	**99.62**

Continued

Sample	PM-7												
Mineral	Hbl	Hbl	Ms	Ep	Cal	Hem	Grt						
	Core	Rim					Ln 1	Ln 2	Ln 3	Ln 4	Ln 5	Ln 6	Ln 7
SiO2	57.99	51.92	49.06	39.41	0.00	2.168	39.07	39.25	39.30	39.15	39.28	42.41	39.48
TiO2	0.02	0.00	0.34	0.15	0.02	0.765	0.15	0.12	0.13	0.11	0.10	0.11	0.10
Al2O3	26.60	28.35	29.67	28.65	0.01	0.74	21.38	21.56	21.73	21.60	21.54	22.93	21.51
FeO	0.83	3.60	0.02	5.78	0.02	84.938	28.33	26.99	28.36	28.89	28.88	22.20	30.01
MnO	0.01	0.00	0.00	0.05	0.04	0.059	0.54	0.60	0.74	0.97	0.86	0.66	0.92
MgO	0.37	1.60	3.17	0.08	0.01	0.369	2.90	2.67	2.48	2.18	1.88	1.65	1.93
CaO	8.36	9.96	0.02	23.62	53.13	0.941	9.49	10.33	9.73	9.30	10.03	9.44	9.23
Na2O	6.55	4.58	2.43	0.01	0.02	0.015	0.03	0.01	0.03	0.02	0.03	1.09	0.03
K2O	0.15	0.33	0.00	0.01	0.00	0.021	0.00	0.01	0.00	0.00	0.01	0.26	0.00
Cr2O3	0.01	0.01	0.02	0.00	0.01	0.024	0.05	0.00	0.05	0.03	0.00	0.01	0.00
NiO	0.00	0.00	0.28	0.00	0.00	0.006	0.01	0.00	0.00	0.03	0.02	0.04	0.00
Total	**100.89**	**100.36**	**101.53**	**97.76**	**53.26**	**90.046**	**101.94**	**101.54**	**102.55**	**102.28**	**102.63**	**100.78**	**103.21**

Continued

PM-7												
Grt												
Ln 8	Ln 9	Ln 10	Ln 11	Ln 12	Ln 13	Ln 14	Ln 15	Ln 16	Ln 17	Ln 18	Ln 19	Ln 20
39.38	39.32	39.03	38.68	35.62	39.09	39.03	39.48	39.29	39.25	39.29	40.39	39.47
0.11	0.13	0.13	0.09	0.08	0.13	0.12	0.13	0.12	0.10	0.10	0.10	0.12
21.54	21.69	21.14	21.41	19.91	21.59	21.33	21.30	21.39	21.04	21.54	22.41	21.88
29.75	30.09	30.31	31.47	30.41	30.85	29.51	29.51	28.78	30.03	29.47	28.19	28.23
1.18	1.49	1.26	1.16	1.53	1.26	0.93	0.85	0.81	0.85	0.95	1.29	0.97
1.68	1.70	1.76	1.85	3.57	1.73	2.01	1.94	1.94	2.23	2.13	2.10	2.29
9.22	8.18	8.40	7.56	5.70	8.43	9.00	9.59	10.18	8.72	9.01	9.27	9.53
0.02	0.04	0.02	0.02	0.03	0.01	0.04	0.04	0.03	0.01	0.02	0.32	0.01
0.01	0.00	0.00	0.00	0.10	0.00	0.00	0.00	0.00	0.00	0.00	0.00	0.00
0.04	0.00	0.00	0.03	0.00	0.01	0.00	0.00	0.00	0.00	0.02	0.00	0.04
0.00	0.00	0.00	0.01	0.04	0.03	0.00	0.02	0.02	0.00	0.04	0.00	0.00
102.92	**102.63**	**102.04**	**102.27**	**96.98**	**103.12**	**101.96**	**102.85**	**102.54**	**102.24**	**102.57**	**104.07**	**102.53**

Continued

Sample	PM-08				Sample	BB-11				
Mineral	Pr	Chl	Ab	Ep	Mineral	Act	Hbl	Act	Hbl	Ep
						Core	Rim	C	R	
SiO2	48.41	25.85	69.58	38.80	SiO2	55.16	43.30	52.70	42.41	38.53
TiO2	0.08	0.08	0.02	0.18	TiO2	0.01	0.22	0.10	0.14	0.06
Al2O3	39.74	23.26	19.72	25.16	Al2O3	2.59	8.39	2.71	8.50	24.43
FeO	0.66	24.41	0.13	11.57	FeO	12.22	24.56	16.53	26.48	10.24
MnO	0.04	0.12	0.02	0.18	MnO	0.86	0.53	0.55	0.54	0.63
MgO	0.13	14.61	0.00	0.07	MgO	14.52	6.45	12.84	5.54	0.03
CaO	0.13	0.04	0.09	22.59	CaO	12.07	11.21	11.95	11.65	23.34
Na2O	7.10	0.04	11.96	0.01	Na2O	0.27	0.87	0.35	0.97	0.02
K2O	0.56	0.28	0.07	0.00	K2O	0.11	0.99	0.12	1.19	0.00
Cr2O3	0.00	0.02	0.00	0.07	Cr2O3	0.00	0.00	0.04	0.00	0.00
NiO	0.04	0.01	0.00	0.02	NiO	0.03	0.03	0.00	0.00	0.00
Total	**96.90**	**88.70**	**101.59**	**98.64**	**Total**	**97.84**	**96.54**	**97.88**	**97.41**	**100.71**

APPENDIX 2

Fault-Slip Data of East Walanae Fault

Location	No.	Fault Plane		Striae		Azimuth	Sense of
		Strike (°)	Dip (°)	Strike (°)	Plunge (°)	striae (°)	Shear
FS - 1	1	N 20 E	78 W	N 30 E	52 N	210/52	Reverse
	2	N 50 E	78 W	N 70 E	24 W	250/24	Reverse
	3	N 75 E	72 N	N 80 E	36 W	260/36	Reverse
	4	N 70 E	71 N	N 72 E	22 W	252/22	Sinistral
	5	N 72 E	65 N	N 47 E	42 N	227/42	Reverse
	6	N 60 E	75 S	N 80 E	47 E	260/47	Reverse
	7	N 12 W	60 E	N 10 E	42 N	190/42	Sinistral
	8	N 2 W	71 W	N 27 W	42 W	153/42	Dextral
	9	N 70 W	88 E	N 65 W	50 E	65/50	Sinistral
	10	N 89 W	74 N	N 60 E	69 N	240/69	Reverse
	11	N 72 W	72 E	80 E	57 E	80/57	Reverse
	12	N 2 W	64 W	N 7 W	50 N	80/58	Reverse
	13	N 35 E	80 E	N 40 E	51 N	7/50	Dextral
	14	N 10 W	85 E	N 5 E	45 E	5/45	Dextral
	15	N 11 E	78 E	N 25 E	15 N	212/12	Sinistral
	16	N 35 E	79 E	N 32 E	12 N	212/12	Reverse
	17	N 10 W	74 E	N 35 W	18 N	35/18	Sinistral
	18	N 45 E	72 N	N 45 E	30 N	225/30	Reverse
	19	N 35 E	72 W	N 20 E	30 N	200/30	Sinistral
	20	N 60 W	55 E	210 W	54 N	210/54	Reverse
	21	N 35 W	35 E	15 E	66 E	15/66	Reverse
	22	N 18 E	35 W	2 E	21 S	2/21	Dextral
	23	N 70 E	81 E	88 W	55 E	88/55	Reverse
	24	N 85 W	50 S	160 W	30 S	160/30	Dextral
	25	N 55 E	52 S	50 E	70 S	50/70	Dextral
	26	N 10 W	68 E	N 12 W	16 S	12/16	Dextral
	27	N 10 E	72 W	20 E	26 S	20/26	Reverse
	28	N 35 W	72 E	30 W	18 N	30/18	Reverse
	29	N 57 W	70 E	58 W	24 N	58/24	Sinistral
	30	N 68 W	80 N	110 W	43 W	110/43	Sinistral
	31	N 20 W	62 W	40 W	50 N	163/47	Dextral
	32	N 70 W	60 S	85 E	10 E	85/10	Reverse
	33	N 10 E	41 W	35 E	N 60 S	35/60	Sinistral
	34	N 52 E	81 S	72 E	N 70 S	72/70	Dextral
	35	N 30 W	65 W	N 30 W	17 N	30/27	Sinistral
	36	N 60 E	15 S	N 70 E	78 S	70/78	Sinistral
	37	N 30 W	65 W	N 45 W	20 S	135/20	Sinistral
	38	N 28 W	75 E	N 25 W	26 E	25/26	Sinistral
	39	N 20 W	54 W	N 10 W	27 S	170/27	Reverse
	40	N 5 E	82 W	N 5 W	47 S	175/47	Sinistral
	41	N 5 W	82 E	N 5 W	22 N	5/22	Reverse
	42	N 4 E	70 E	N 20 W	41 E	20/41	Sinistral
	43	N 40 W	85 S	N 35 W	35 S	145/35	Reverse
	44	N 9 E	65 E	N 40 E	50 E	40/50	Reverse
	45	N 20 E	65 W	N 40 E	48 S	40/48	Reverse

Location	No.	Fault Plane		Striae		Azimuth	Sense of
		Strike (°)	Dip (°)	Strike (°)	Plunge (°)	striae (°)	Shear
FS - 2	1	N 55 W	35 E	N 40 W	5 N	310/5	Dextral
	2	N 70 W	80 E	N 65 W	25 S	115/25	Dextral
	3	N 45 W	80 W	N 50 W	40 N	310/40	Reverse
	4	N 55 W	80 E	N 50 W	25 S	130/25	Dextral
	5	N 20 W	65 E	N 10 W	40 W	170/40	Reverse
	6	N 10 W	79 E	N 10 W	45 W	170/45	Sinistral
	7	N 2 W	65 E	N 18 W	8 W	172/8	Dextral
	8	N 70 W	75 E	N 60 W	54 N	300/54	Riverse
	9	N 55 W	35 E	N 58 W	35 N	300/35	Dextral
	10	N 35 W	40 E	N 85 W	32 S	95/32	Sinistral
	11	N 15 E	80 W	N 25 E	46 W	205/46	Reverse
	12	N 25 E	45 E	N 2 E	12 W	182/12	Dextral
	13	N 25 E	35 E	N 8 W	25 W	172/25	Sinistral
	14	N 45 E	25 E	N 60 W	75 S	120/75	Reverse
	15	N 15 E	55 E	N 20 E	12 E	20/12	Sinistral
	16	N 70 W	60 E	N 5 W	60 E	355/60	Sinistral
	17	N 18 E	65 E	N 40 W	70 E	320/70	Sinistral
	18	N 10 W	82 E	N 32 W	70 E	328/70	Sinistral
	19	N 50 W	25 N	N 62 E	27 S	62/27	Sinistral
	20	N 40 E	55N	N 35 W	10 E	325/10	Sinistral
	21	N 50 W	52 E	N 70 W	28 N	290/28	Dextral
	22	N 2 E	64 E	N 30 W	60 E	330/60	Sinistral
	23	N 55 W	35 E	N 60 W	60 N	300/60	Sinistral
	24	N 62 W	38 N	N 55 W	16 N	305/16	Sinistral
	25	N 60 W	25 E	N 38 W	48 E	322/48	Dextral
	26	N 55 W	80 E	N 50 W	60 W	130/60	Dextral
	27	N 65 W	62 E	N 42 W	10 E	318/10	Sinistral
	28	N 10 W	80 E	N 60 W	67 N	240/67	Sinestral
	29	N 70 W	60 E	N 85 W	48 N	275/48	Sinestral
	30	N 10 W	52 E	N 70 W	50 N	290/50	Dextral
	31	N 65 W	62 E	N 60 W	44 N	290/44	Riverse
	32	N 30 W	65 E	N 60 E	64 S	60/64	Dextral
	33	N 40 E	82 W	N 60W	69 S	120/69	Dextral
	34	N 15 E	68 W	N 55 W	60 N	305/60	Dextral
	35	N 50 E	85 W	N 50 E	90 S	130/90	Dextral
	36	N 42 W	67 E	N 49 W	79 E	311/79	Sinestral
	37	N 10 W	75 E	N 50 E	60 S	50/60	Sinistral
	38	N 10 W	88 W	N 50 W	61 N	310/61	Sinestral
	39	N 45 E	68 E	N 80 E	54 N	280/54	Sinistral
	40	N 14 E	89 W	N 50 W	90 W	130/90	Dextral

Location	No.	Fault Plane		Striae		Azimuth	Sense of
		Strike (°)	Dip (°)	Strike (°)	Plunge (°)	striae (°)	Shear
FS - 3	1	N 60 E	55 E	N 10 W	59 E	350/59	Reverse
	2	N 60 E	79 W	N 70 E	23 W	250/23	Sinistral
	3	N 35 E	81 E	N 30 E	33 E	30/33	Sinistral
	4	N 10 W	40 E	N 20 W	38 E	340/38	Dextral
	5	N 40 E	72 W	N 10 W	65 W	170/65	Reverse
	6	N 85 E	45 W	N 55 E	65 W	235/65	Reverse
	7	N 35 E	20 E	N 40 E	85 E	40/85	Dextral
	8	N 30 W	80 E	N 20 E	30 E	20/30	Dextral
	9	N 50 W	60 E	N 75 W	63 E	285/63	Reverse
	10	N 80 E	68 E	N 70 E	43 E	250/43	Sinistral
	11	N 70 E	60 E	N 55 E	37 E	55/37	Sinistral
	12	N 65 E	82 W	N 65 E	47 W	245/47	Dextral
	13	N 45 E	60 E	N 75 E	59 E	75/59	Dextral
	14	N 60 E	55 E	N 65 E	70 E	65/70	Reverse
	15	N 70 E	40 E	N 70 E	6 E	70/16	Sinistral
	16	N 10 E	62 E	N 40 E	37 E	40/37	Dextral
	17	N 70 E	88 S	N 70 E	43 S	72/43	Sinistral
	18	N 55 W	30 E	N 50 E	25 E	50/25	Reverse
	19	N 60 E	65 N	N 50 E	34 N	230/34	Sinistral
	20	N 60 E	45 E	N 50 W	40 E	50/40	Reverse
	21	N 10 E	60 W	N 25 E	36 W	215/36	Dextral
	22	N 85 E	62 N	N 80 E	8 N	260/8	Sinistral
	23	N 85 W	32 N	N 70 W	10 N	70/10	Reverse
	24	N 30 E	45 W	N 30 E	30 W	210/30	Dextral
	25	N 60 E	62 W	N 30 E	50 W	210/50	Dextral
	26	N 67 W	68 N	N 36 W	50 N	36/50	Sinistral
	27	N 45 E	50 E	N 25 E	52 E	25/52	Dextral
	28	N 3 W	75 E	N 5 W	45 E	5/45	Dextral
	29	N 40 E	32 W	N 80 E	10 W	260/10	Dextral
	30	N 60 E	80 E	N 60 E	5 E	60/5	Dextral

Location	No.	Fault Plane		Striae		Azimuth	Sense of
		Strike (°)	Dip (°)	Strike (°)	Plunge (°)	striae (°)	Shear
FS - 4	1	N 89 E	52 W	N 5 E	55 W	185/55	Sinistral
	2	N 5 E	80 W	N 10 E	10 W	190/10	Dextral
	3	N 50 E	80 W	N 10 E	10 W	190/10	Reverse
	4	N 35 E	45 E	N 40 E	17 W	220/17	Dextral
	5	N 75 E	50 E	N 70 E	30 E	70/30	Reverse
	6	N 75 E	10 N	N 25 E	26 E	25/26	Sinistral
	7	N 50 E	45 E	N 30 E	45 W	110/45	Reverse
	8	N 20 E	82 E	N 25 E	15 E	25/15	Dextral
	9	N 35 E	65 W	N 20 W	15 W	195/15	Dextral
	10	N 35 E	60 E	N 10 E	30 E	10/30	Reverse
	11	N 45 E	70 E	N 40 E	32 W	220/32	Sinistral
	12	N 70 E	68 E	N 85 W	52 E	95/52	Reverse
	13	N 50 E	48 E	N 10 E	30 E	30/30	Sinistral
	14	N 30 W	78 E	N 38 E	40 E	38/40	Sinistral
	15	N 5 W	79 W	N 10 W	47 W	190/47	Dextral
	16	N 30 E	75 E	N 25 E	40 E	25/40	Reverse
	17	N 35 E	75 E	N 25 E	15 E	25/15	Dextral
	18	N 42 E	52 E	N 40 E	15 E	40/15	Dextral
	19	N 80 W	82 E	N 85 W	2 E	275/2	Sinistral
	20	N 85 W	72 E	N 60 E	47 E	60/47	Sinistral
	21	N 30 E	89 W	N 50 E	47 W	230/47	Sinistral
	22	N 89 E	79 W	N 60 E	32 W	240/32	Sinistral
	23	N 50 W	52 E	N 70 W	28 E	290/28	Sinistral
	24	N 75 W	40 W	N 30 W	14 W	160/14	Reverse
	25	N 65 W	75 W	N 60 E	26 W	240/26	Reverse
	26	N 20 E	50 E	N 50 E	50 E	50/50	Dextral
	27	N 10 W	75 E	N 10 W	68 E	350/68	Reverse
	28	N 65 E	80 W	N 55 E	56 W	235/56	Dextral
	29	N 5 W	28 E	N 40 W	35 W	140/35	Sinistral
	30	N 85 W	69 W	N 70 W	27 W	110/27	Sinistral
	31	N 65 W	85 S	N 60 W	18 S	120/18	Sinistral

Fault-Slip Data of West Walanae Fault

Location	No.	Fault Plane		Striae		Azimuth	Sense of
		Strike (°)	Dip (°)	Strike (°)	Plunge (°)	striae (°)	Shear
Bulubuluk River	1	N 5 E	24 N	N 10 E	55 W	170/55	Sinistral
	2	N 25 E	80 W	N 15 E	32 W	175/32	Sinistral
	3	N 45 W	80 W	N 50 W	40 E	130/40	Dextral
	4	N 30 W	60 W	N 0 W	35W	180/35	Sisnitral
	5	N 75 W	70 W	N 80 W	10 W	110/10	Dextral
	6	N 45 W	70 W	N 50 W	30 W	130/30	Dextral
	7	N 61 W	52 W	N 50 E	59 W	130/59	Dextral
	8	N 50 W	80 W	N 50 W	17 N	310/17	Dextral
	9	N 50 W	85 E	N 40 W	38 E	320/38	Dextral
	10	N 50 W	85 E	N 40 W	58 E	320/58	Sinistral
	11	N 75 W	88 E	N 70 W	64 N	290/64	Dextral
	12	N 25 E	80 E	N 35 E	30 E	35/30	Dextral
	13	N 85 E	75 E	N 60 E	40 E	60/40	Sinistral
	14	N 85 E	85 S	N 81 E	45 S	81/45	Sinistral
	15	N 20 W	89 W	N 10 W	71 W	170/71	Dextral
	16	N 20 W	60 W	N 80 E	58 W	260/58	Dextral
	17	N 50 W	60 W	N 40 W	53 W	140/53	Dextral
	18	N 70 E	55 W	N 65 W	26 W	115/26	Dextral
	19	N 45 W	80 E	N 50 W	40 E	310/40	Dextral
	20	N 50 W	60 W	N 40 W	28 W	310/40	Sinistral
	21	N 30 W	50 W	N 20 W	19 W	160/19	Sinistral
	22	N 40 E	87 W	N 22 E	17 W	202/17	Sinistral
	23	N 10 E	80 E	N 20 E	65 E	20/65	Sinistral

Location	No.	Fault Plane		Striae		Azimuth	Sense of
		Strike (°)	Dip (°)	Strike (°)	Plunge (°)	striae (°)	Shear
Biru River	1	N 55 E	75 E	N 40 E	20 E	40/20	Dextral
	2	N 30 E	85 E	N 2 W	64 E	358/64	Sinistral
	3	N 20 W	80 W	N 25 W	28 W	155/28	Sinistral
	4	N 20 W	70 W	N 20 W	22 W	160/22	Sinistral
	5	N 55 W	70 E	N 50 W	51 E	110/10	Dextral
	6	N 40 W	85 E	N 85 W	17 E	310/51	Dextral
	7	N 5 W	89 E	N 10 W	27 E	350/27	Dextral
	8	N 70 E	80 N	N 65 E	25 N	245/25	Dextral
	9	N 10 W	75 E	N 25 E	45 E	25/45	Sinistral
	10	N 2 W	80 W	N 10 E	42 W	190/42	Dextral
	11	N 80 E	70 S	N 70 E	28 S	70/28	Sinistral
	12	N 60 W	70 S	N 86 W	30 S	94/30	Sinistral
	13	N 75 E	78 S	N 70 W	55 S	120/55	Sinistral
	14	N 50 W	65 E	N 20 W	56 E	340/56	Sinistral
	15	N 50 W	80 E	N 40 W	44 E	320/44	Sinistral
	16	N 50 E	70 W	N 45 E	67 W	225/67	Dextral
	17	N 40 W	75 W	N 10 W	50 W	170/50	Sinistral
	18	N 50 W	60 E	N 70 W	29 E	290/29	Sinistral
	19	N 30 W	75 E	N 20 W	38 E	340/38	Sinistral
	20	N 30 W	75 W	N 52 E	80 W	227/80	Sinistral
	21	N 5 W	82 W	N 10 W	43 W	170/43	Sinistral
	22	N 73 E	56 S	N 70 W	60 S	120/60	Sinistral
	23	N 20 E	75 W	N 20 E	7 W	200/17	Dextral
	24	N 40 E	30 W	N 5 E	20 W	175/20	Dextral
	25	N 85 E	75 S	N 61 W	47 S	129/47	Sinistral
	26	N 20 E	35 E	N 50 E	28 E	50/28	Dextral
	27	N 60 E	65 N	N 85 W	30 N	275/30	Sinistral
	28	N 75 W	80 W	N 85 W	41 W	115/41	Riverse
	29	N 40 W	58 E	N 70 W	37 E	290/37	Dextral

APPENDIX 3:

Dike Segments Data

Location	Site	Latitude (°S)	Longitude (°N)	Plan Direction		wide (m)	Lithology
				Strike	Dip		
Biru River	1	-5.00222	120.04653	N 50 E	75 E	1	Basalt
	2	-5.00317	120.04675	N 52 E	70 E	4	Basalt
	3	-5.00675	120.04756	N 72 E	70 E	2.2	Basalt
	4	-5.00675	120.04756	N 70 W	70 E	1	Basalt
	5	-5.00675	120.04756	N 76 E	78 E	2.3	Basalt
	6	-5.00675	120.04756	N 45 W	75 E	1	Granodiorite
	7	-4.99294	120.05081	N 72 E	70 E	3	Dolerite
	8	-4.99256	120.05072	N 75 W	70 E	2.5	Basalt
	9	-4.99231	120.05081	N 70 W	77 E	1.5	Granodiorite
	10	-4.99231	120.05081	N 82 W	78 E	1	Basalt
	11	-4.99197	120.05081	N 25 E	66 W	3.5	Basalt
	12	-4.99028	120.05097	N 63 E	75 E	1	Andesite
	13	-4.98753	120.05253	N 32 W	68 W	2	Basalt
	14	-4.98697	120.05356	N 45 E	80 W	0.5	Basalt
	15	-4.98636	120.05592	N 20W	85 E	1.5	Granodiorite
	16	-4.98636	120.05592	N 50 W	80 E	3.3	Andesite
	17	-4.98572	120.05883	N 75 E	75E	1	Basalt
Bulubuluk River	1	-5.03431	120.06736	N 79 E	75 E	0.5	Basalt
	2			N 56 E	70 E	0.4	Basalt
	3			N 45 W	80 E	1	Basalt
	4			N 60 W	75 E	0.5	Basalt
	5			N 51 W	75 E	1	Basalt

APPENDIX 4

Calcite Twin from Host Rocks

Location : STM-1
Rock Type : Crystalline Limestone

Grains No.	C - Axis			Calcite Twins						U-Stage Recalculate				Thin Section Rotation				Twin plane (e1)					Twin plane (e2)					Twin plane (e3)					Thin Section
	Strike (IV)	Dip (NS)	R/L Dip Direct.	Ttwin plane (e1)		Ttwin plane (e2)		Ttwin plane (e3)		C-axis		Twin Plane		C-axis		Twin Plane		Twin Plane		Slip Direction		Shear Sense	Twin-untwin Plane		Slip Direction		Shear Sense	Twin-untwin Plane		Slip Direction		Shear Sense	
				IV	NS	IV	NS	IV	NS	Az	Plg	Az	Plg	Az	Plg	Az	Plg	Az	Plg	Az	Plg		Az	Plg	Az	Plg		Az	Plg	Az	Plg		
1	148	11	R	178	4R					302	11	272	4	4.2	21.8	338.4	4.5	N68E	86S	71	35	R	N60W	85S	295	35	S	N87W	38S	183	38	N	XZ
2	87	37	R	119	30R					3	37	331	30	72.7	58.9	28.8	48.4	N62W	42S	148	24	R	N3W	55W	301	51	S	N43E	13W	227	1	N	
3	274	25	L	297	37L					176	25	333	37	244.4	3.1	28.2	55.5	N62W	35S	255	26	S	N83W	43N	78	18	D	N37E	85W	218	5	N	
4	104	6	L	133	9L					166	6	137	9	53.6	15.3	25.2	7.2	N66W	82S	117	18	R	N18W	84E	347	50	N	N28W	48W	213	44	N	
5	88	19	R	114	28R					2	19	336	28	70.5	41	35.9	47.5	N56W	43S	303	2	D	N6W	66W	326	48	S	N3E	53W	341	31	S	
	88	19	R			73	3R			2	19	17	3	70.5	41	86.7	24																
6	308	8	L	333	9L					142	8	297	9	29.9	9.4	0	18.2	N90E	71S	266	13	D	N56W	70N	8	68	N	N35W	63S	160	27	N	
7	324	18	L	0	19L					306	18	270	19	5.6	29.7	330.7	17.6	N62E	72S	70	26	D	N64W	87S	195	56	S	N68W	30S	231	27	N	
8	98	7	L	124	11L					172	7	146	11	59.8	14.8	34.4	7.3	N56W	82S	126	16	D	N14W	84E	352	50	N	N22W	51W	216	47	N	
9	243	43	L	216	15L					27	43	54	15	111.6	61.2	129.2	26.9	N38E	64W	337	61	R	N58W	19N	85	11	S	N38W	45W	179	31	R	
10	13	14	L	156	20L					257	14	114	20	320.8	8.2	187.4	10	N84W	79N	281	18	R	N39E	34E	148	32	N	N12E	66W	357	51	N	
11	108	3	R	132	9R					342	3	318	9	48.3	23.8	21.2	24.8	N68W	76S	117	23	D	N33W	89W	326	70	S	N22W	47W	188	30	N	
12	148	13	R	168	11R					302	13	282	11	3.5	23.7	345	14.6	N75E	75S	83	31	D	N70W	79	279	43	S	N86W	47S	244	30	N	
13	204	8	L	202	42L					66	8	68	42	138.4	16.2	157.3	46.5	N65E	44N	290	33	S	N14E	79W	197	12	D	N68E	77S	86	52	N	
14	263	3	L	208	21L					7	3	62	21	75.7	24.8	139.7	29.8	N50E	61N	44	11	S	N83W	45S	101	3	S	N14W	55E	83	54	S	
15	278	29	R	250	11R					172	29	200	11	240.9	7.2	87.9	9.7	N7W	80W	182	31	R	N18W	52E	59	52	N	N58W	81W	300	28	D	
16	292	31	L	320	10L					338	31	310	10	37.4	50.9	12.7	23.5	N78W	66S	137	54	R	N16W	56W	318	37	S	N72E	12S	229	7	N	
17	192	38	R	198	4R					258	38	252	4	311.6	30.6	139.8	2.9	N50E	88N	240	76	R	N78E	41S	93	15	S	N6E	57E	8	7	D	
18	273	48	R	263	50R					177	48	187	50	245.8	26.1	253.1	28.2	N18W	62E	352	18	S	N52W	50N	114	17	D	N28W	89S	335	81	R	
19	272	23	R	304	20R					178	23	146	20	246.2	1	216.3	1.5	N50W	88S	302	3	D	N8W	64W	205	49	N	NN3E	73W	191	28	N	
20	240	2	L	220	1R					30	2	230	1	100.4	20.9	119.8	13	N30W	76W	24	25	S	N1E	45W	302	41	N	N6W	85W	179	48	D	
21	238	42	L	235	2L					32	42	35	2	117.7	58.9	105.5	19.8	N15E	70W	256	69	R	N867W	42N	61	26	S	N60W	25W	152	14	N	
22	148	28	L	175	2L					122	28	95	2	197.2	15.1	343.4	0	N74E	89S	254	27	D	N45W	81W	142	36	D	N64W	39N	10	38	N	
23	98	38	L	132	16L					172	38	138	16	241.4	16.2	28	0.7	N72W	89S	298	28	R	N1W	82W	186	40	D	N21W	39E	55	38	N	
24	98	34	L	90	50L					172	34	180	50	241.2	12.2	248	28	N22E	62E	25	54	R	N46W	80N	316	13	D	N18W	87S	163	51	D	
25	68	0	L	46	6L					202	0	224	6	91.5	20.3	112.5	9.9	N22E	81W	18	30	S											

Continued

26	5	46	L	15	1L			265	46	255	1	312.8	40.1	143.7	4.7	N55E	86N	251	78	R	
27	289	45	R	314	32R			161	45	136	32	233.5	23.9	210.4	15.2	N60W	74N	306	23	D	
28	208	0	R	187	34L			242	0	83	34	131.8	10.1	166	33.8	N75E	56N	272	25	S	
29	143	47	R	156	50R			307	47	294	50	349	56.3	333.7	53.9	N65E	37S	88	17	D	
30	302	47	L	348	28L			328	47	282	28	13.9	63.5	337.7	30.2	N68E	59S	115	52	R	
31	10	48	R	340	30R			80	48	110	30	172.5	47.1	187.6	20.7	N82W	70N	57	61	R	
32	73	45	L	43	30L			197	45	227	43	261.1	23.8	288.8	14	N19E	75E	193	22	S	
33	68	50	L	44	36L			202	50	226	44	264	29.1	286.1	19.5	N17E	N71E	185	27	S	
	136	45	L			192	19L	134	45	78	19	212.8	28.2	154.3	22						
34	68	28	L	43	48L			202	28	227	48	267.5	7.3	282.9	31.1	N14E	59E	52	47	S	
35	103	0	L	123	14L			167	0	147	14	54	21.4	36	4.6	N50W	85S	130	46	R	
38	354	10	L	357	20L			276	10	273	20	339.8	11.6	168.5	17.4	N19W	49W	227	46	D	YZ
39	184	15	R	189	34R			266	15	261	34	328.6	12.4	164.2	34.5	N46W	35W	258	34	D	
40	157	0	R	167	18R			293	0	283	18	359.5	8.4	176.7	11.9	N8W	51W	298	46	D	
41	161	11	L	184	43L			109	11	86	43	179.6	3.3	315.5	37.9	N25W	69E	130	49	R	
42	188	32	R	163	28R			262	32	287	28	317.8	26.6	184.2	19.8	N2E	41W	341	19	S	
	188	32	R			209	6R	262	32	241	6	317.8	26.6	132.9	16.1						
43	11	5	R	38	1R			79	5	52	1	149.6	8.8	121.8	12.4	N63W	74S	120	5	D	
44	132	5	L	108	17L			318	5	162	17	22.5	21	46	37.7	N46E	80E	60	59	R	
45	6	43	R	32	22R			84	43	58	22	172.2	41.4	300.9	9.4	N52W	87N	310	36	D	
46	156	23	L	190	44L			114	23	80	44	188.4	12.8	310	36.6	N30W	67E	138	29	D	
	156	23	L			148	27L	114	23	122	27	188.4	12.8	357.5	36.7						
47	94	18	L	114	6R			176	18	336	6	64.2	4	43.3	14.1	N48E	75W	14	67	R	
	94	18	L			78	9R	176	18	12	9	64.2	4	80.2	12.5						
48	104	9	L	84	4L			166	9	186	4	53.8	12.4	74.6	25.9	N73E	85S	72	1	S	
49	104	2	L	134	8R			166	2	316	8	53.2	19.3	24	7.9	28E	68W	14	32	D	
50	314	10	L	248	50L			316	10	22	50	18.9	25.2	264	29.1	N72W	51N	110	11	S	
51	164	26	L	148	9R			106	26	302	9	182.5	18.3	11	2.9	N13E	63W	224	45	R	
	164	26	L			193	30L	106	26	77	30	182.5	18.3	314.5	23						
52	88	14	L	102	38L			182	14	168	38	70	8	49.3	59.3	N42E	60E	85	49	R	
53	227	20	L	221	24L			43	20	49	24	119.6	35.1	292.3	8.8	N59W	83N	303	18	D	
54	47	14	R	55	32L			43	14	215	32	117.4	29.4	115.5	48.8	N88E	47S	224	39	N	

N5W	43W	278	42	N	N18W	85W	165	37	D
N69W	59S	282	4	S	N14W	53E	0	19	D
N28W	84E	155	46	S	N25W	42E	35	39	N
N4E	71W	0	11	D	N51W	61S	116	59	N
N22W	41S	219	35	R	N89E	13S	145	7	N
N30W	54W	287	45	S	N22E	12N	21	12	N
N56W	22N	326	8	N	N43E	50W	239	19	D
N20W	40E	97	36	D	N26W	87E	338	52	D
N65E	68N	252	19	D	N38W	67W	185	15	N
N30W	82E	138	56	D	N12E	72w	215	52	N
N12W	77W	342	25	S	N45W	44W	251	43	N

N87W	56S	116	30	S
N76W	48S	121	19	S
N70W	75S	115	18	N
N34W	82W	148	8	N
N55W	65W	168	56	R
N70E	72S	106	62	N
N85E	65S	264	2	D
N80E	21N	357	22	N
N8E	83E	11	21	S
N83E	86N	265	36	R
N64W	70S	293	15	D
N16W	87E	348	42	N
N79W	38S	191	38	N
N34W	82E	145	11	D
N4E	65W	199	33	N
N86E	52N	77	11	S
N5E	75W	194	32	D

N40E	73E	218	5	D
N8E	71E	188	2	N
N74E	70S	238	34	N
N58E	34N	11	27	N
N68E	37S	135	35	N
N78E	60N	287	41	N
N60W	85S	319	75	N
N42W	86W	142	46	N
N73E	71N	68	8	N
N24W	67E	65	68	N
N22W	77E	23	74	N
N28W	42W	219	41	N
N44W	57S	142	9	N
N65E	63N	61	10	N
N47W	74W	312	13	D
N1E	40W	345	13	D

Continued

																										N54E	74N	236	15	S	
55	35	8	L	56	24L			235	8	214	24	122.5	4.8	110.9	41.4	N88W	56S	264	10	D	N13E	75E	182	41	N	N7E	78W	5	12	D	
56	43	1	R	57	20L			47	1	213	20	117.4	15.8	108.3	37.8	N89W	44S	226	35	R	N8E	86E	186	49	N	N55E	80N	52	15	N	
57	130	43	R	164	26R			320	43	286	26	7.4	57.4	182.5	18.3	N2W	43W	185	4	D	N34W	31W	312	9	N	N44E	27E	56	6	D	
58	123	27	R	104	21R			327	27	346	21	25.2	44.5	54.9	0.4	N64E	66N	38	45	R	N44W	21W	185	17	N	N84E	55S	102	27	D	
59	251	1	L	324	28L			19	1	306	28	88.5	21.7	200.6	13.9	N24E	46	7	17	S	N28W	53W	317	20	D	N4E	42w	260	40	N	
60	130	0	L	143	30L			140	0	127	30	25.9	16.7	1.1	41.2	N10E	79E	177	50	R	N74W	81N	88	64	N	N46W	88N	316	52	N	
61	158	0	L	183	9L			112	0	87	9	166.6	20.3	148.5	0.6	N58E	89S	238	49	S	N76W	78N	101	18	S	N47E	45S	61	7	N	XY
62	3	43	L	43	18L			267	43	227	18	18.2	16.9	341.6	45.8	N72E	45S	227	22	D	N12E	65E	51	57	S	N37E	74E	80	4	N	
63	327	10	R	350	14R			123	10	100	14	160.8	34.2	148.4	14.3	N57E	N75N	263	60	R	N64E	62N	91	19	S	N50E	34N	6	25	N	
64	272	22	R	238	19R			358	22	392	19	245.3	46	287.8	38.4	N18E	52E	179	23	S	N14W	43E	103	37	S	N40W	73N	358	64	N	
65	293	35	L	257	21L			337	35	13	21	226.5	29	265.3	45.2	N8W	45E	5	11	S	N83W	53N	97	2	D	N38W	85W	167	80	N	
66	289	25	R	268	47R			161	25	182	47	144.5	72.3	64.8	64.9	26W	26W	206	22	R	N58E	47N	330	47	N	N35W	24E	97	19	D	
67	53	7	L	24	37L			217	7	246	37	320.9	51.3	8.9	31.8	N82W	52S	251	37	R	N32W	11E	334	1	N	N26E	71E	60	60	D	
68	333	16	L	354	33L			297	16	276	33	184.1	17.5	10.8	7.1	N80W	82S	130	75	R	N34W	67N	137	1	S	N67E	66N	64	10	D	
	333	16	L			296	40L	297	16	334	40	184.1	17.5	226.5	23.4																
69	316	19	L	32	53R			314	19	58	53	196.9	29.1	98.7	0.2	N8W	89E	188	29	R	N18W	32W	201	21	D	N2W	49W	202	34	D	
70	40	4	L	14	50R			230	4	76	50	325.1	38.4	107.1	8.2	N17E	81W	6	54	S	N70W	81S	283	59	S	N64W	12N	332	7	N	
71	193	19	L	220	38R			77	19	230	38	315.5	4.3	10.3	44.4	N80W	45S	118	18	S	N73W	85N	20	85	R	N1W	48W	330	30	N	
	193	19	L			157	34R	77	19	293	34	315.5	4.3	198	5.2																
72	55	33	R	42	26R			35	33	48	26	280.3	25.7	294.6	23.2	N26E	67E	203	7	D	N8E	52E	137	44	N	N4E	75E	23	56	R	
73	348	12	R	42	43L			102	12	228	43	151.1	15.5	17.6	45.2	N74W	45S	142	29	R	N36W	27N	324	0	N	N66E	86S	168	16	D	
74	147	0	L	204	31R			123	0	246	31	171.7	30.3	1.9	31.1	N89W	58S	164	58	R	N20W	45E	151	11	S	N8E	58W	199	17	D	
75	272	7	R	223	47L			178	7	47	47	240.4	74.9	278.3	9	N9E	80E	149	76	R	N45W	32S	230	33	R	N74E	72N	297	66	N	
	272	7	R			252	50R	178	7	198	50	240.4	74.9	45.6	58.6																
76	251	40	L	205	45L			19	40	65	45	264	25.5	287.9	0.7	N18E	89E	199	49	R	N8E	32E	70	30	N	N38W	78E	327	28	D	
77	9	9	R	44	27L			81	9	226	27	326.2	4.9	354.4	48.1	N85E	41S	128	32	R	N7E	87W	6	7	S	N54E	54N	300	37	D	
78	264	30	L	240	29L			6	30	30	29	254.6	37.7	278.8	31.4	N9E	58E	176	22	S	N28W	33E	94	29	N	N28W	69E	358	52	N	
79	267	17	L	238	22L			3	17	32	22	252.6	50.9	285.4	36.1	N16E	53E	169	32	S	N38W	14E	84	14	N	N38W	60E	356	45	D	
80	80	19	L	58	24R			190	19	32	24	322	80.2	284	34.5	N14E	56E	87	55	R	N15E	56E	90	55	R	N60W	51E	228	50	N	
81	55	5	L	28	28L			215	5	242	28	316.5	52.1	357.8	34.1	N88E	56S	238	27	R	N12W	10E	149	3	N	N22E	67E	55	53	D	
82	97	34	R	64	25R			353	34	26	25	241	33.6	277.7	36.7	N8E	54E	184	6	S	N40W	58E	326	12	D	N35W	83E	353	76	R	
	97	34	R			109	35R	353	34	341	35	241	33.6	230	30.2																

Continued

83	264	43	L	196	50R		6	43	254	50	252.8	24.8	24.2	26.8	N66W	63S	272	27	R	N48E	83W	231	28	D	N58E	13N	257	5	N	
84	115	5	R	103	35L		335	5	167	35	202.9	53.6	106.4	72.7	N16E	17W	224	9	R	N89W	74N	309	65	R	N10W	55E	140	35	S	
84	38	38	R	14	34R		52	38	76	34	287.5	12.7	121.6	1.3	N32E	89W	214	45	R	N23E	59E	87	57	N	N3W	84E	2	18	D	
86	112	11	L	205	50L		158	11	65	50	182	66.3	103.7	2	N14E	88W	199	67	R	N48W	78S	168	71	R	N70E	61S	177	60	R	
87	299	21	R	243	45L		151	21	27	45	154.7	63	267.8	18.6	N12W	72E	137	57	R	N70W	38S	174	34	N	N40E	83N	249	76	R	
88	299	12	R	289	38L		151	12	341	38	173.1	60.6	231.2	27.4	N38W	62E	106	49	R	N64W	23S	184	22	N	N50E	74N	264	64	N	
89	268	23	R	278	34L		182	23	352	34	6.8	87.9	240	33.5	N30W	57E	55	58	R	N70E	74N	354	75	N	N78W	43S	190	42	R	
90	350	22	L	2	37R		280	22	88	37	182.1	0.5	122.5	11.5	N34E	78W	32	7	D	N60W	35S	172	30	N	N2E	50W	341	21	D	

Location : STM-2
Rock Type : Coral Limestone

Grains No.	C - Axis			Calcite Twins						U-Stage Recalculate				Thin Section Rotation				Twin plane (e1)					Twin plane (e2)					Twin plane (e3)					Thin Section
	Strike (IV)	Dip (NS)	R/L Dip Direct.	Ttwin plane (e1)		Ttwin plane (e2)		Ttwin plane (e3)		C-axis		Twin Plane		C-axis		Twin Plane		Twin Plane		Slip Direction		Shear Sense	Twin-untwin Plane		Slip Direction		Shear Sense	Twin-untwin Plane		Slip Direction		Shear Sense	
				IV	NS	IV	NS	IV	NS	Az	Plg	Az	Plg	Az	Plg	Az	Plg	Az	Plg	Az	Plg		Az	Plg	Az	Plg		Az	Plg	Az	Plg		
1	72	22	L	86	9L					198	22	184	9	155.3	67.1	115.8	59.7	N28E	31W	321	30	N	N86E	46N	21	45	N	N58W	9	311	3	N	XZ
2	62	0	R	38	5R					28	0	52	5	148.2	43.3	168	24.9	N78E	65N	49	48	R	N58W	39N	111	9	S	N30W	57W	229	28	D	
	62	0	R			43	38L			28	0	227	38	148.2	43.3	211.7	53.6																
3	72	28	R	37	38R					18	28	53	38	125	20.9	327	1.1	N56E	88S	58	43	R	N12E	56W	357	22	D	N5E	80W	190	24	D	
	72	28	R			96	18R			18	28	354	18	125	20.9	101.2	32.8																
4	318	0	L	338	18L					312	0	112	18	47.5	31.3	17	28.1	N72W	61S	115	16	R	N8W	49W	179	5	S	N14W	43W	183	17	S	
	318	0	L			288	7L			312	0	342	7	47.5	31.3	84	41																
5	18	4	R	44	8R					72	4	46	8	183.3	11.3	160.7	26.6	N72E	63N	56	30	D	N88E	74S	214	71	N	N62W	71N	304	15	S	
6	322	32	L	298	30L					308	32	332	30	65.9	4.2	83	16.3	N8W	74W	182	29	S	N44W	79W	313	18	D	N22W	74E	36	72	N	
7	255	5	L	284	9R					15	5	166	9	129	43.9	81.6	57.5	N10W	32W	347	3	D	N32E	79W	261	76	D	N85E	46N	74	12	S	
8	230	16	L	202	22L					40	16	68	22	150.4	23.5	167.4	2	N77E	87N	75	51	R	N76E	86N	72	51	R	N74E	41N	310	39	N	
9	224	11	L	205	23L					46	11	65	23	158.7	24.2	164.7	3.2	N75E	87N	64	73	R	N86W	49W	297	25	S	N45E	62W	43	5	D	
10	117	26	R	128	9R					333	26	322	9	82.2	20.3	63.1	30.4	N26W	60W	319	24	D	N10W	89S	177	84	N	N12E	63W	200	15	S	
11	155	15	R	117	34R					295	15	333	34	45.6	8.9	85.3	12.8	N8W	78W	176	2	S	N74W	54S	263	31	D	N58W	62N	75	54	N	
12	126	7	L	116	3R					324	7	334	3	63.8	33.2	72.1	41.6	N18W	49W	198	34	N	N38W	56S	321	2	D	N22W	66W	298	57	S	
13	313	0	R	294	10R					137	0	156	10	52	34.6	65.1	53.9	N26W	37W	209	31	N	N63W	61S	127	18	D	N25W	73W	310	56	S	
14	290	16	R	263	9R					160	16	187	9	65.1	61.1	121.7	59.4	N32E	31W	6	16	S	N88W	24S	110	7	D	N30W	57W	225	56	R	
15	54	11	L	54	13L					216	11	216	13	166.6	47.5	168.7	48.9	N70E	41N	290	26	D	N36E	42N	228	12	D	N80E	16N	347	18	R	
16	130	14	R	97	8R					320	14	353	8	64.4	25.2	98.6	42.6	N8E	47W	202	16	S	N64W	58S	296	2	D	N20W	82E	19	77	N	
17	36	9	R	28	4R					54	9	62	4	166.6	20.6	176.4	18.7	N87W	72N	80	17	R	N68E	45N	8	42	N	N72E	76N	264	39	S	
18	278	12	R	284	22L					172	12	346	22	91.1	62.1	93.3	27.6	N4W	62W	278	63	R	N80E	29N	44	8	S	N72W	32S	141	19	N	
19	334	15	L	355	28L					296	15	275	28	46.3	9.6	223.2	13.6	N46W	76N	81	74	R	N23W	72W	163	16	S	N62W	68S	285	30	D	
20	264	15	R	283	16R					186	15	167	16	122	65.4	78.1	64.3	N12W	26W	187	10	D	N36E	44W	317	43	R	N77W	20N	79	9	S	
21	238	10	R	222	15L					212	10	48	15	161.2	49.3	157.7	19.9	N68E	70N	327	71	R	N64W	39N	106	9	S	N26E	31W	24	2	D	
22	214	0	L	228	15L					56	0	42	15	175	25.8	152.7	23.3	N64E	67N	246	8	D	N75E	85E	111	73	R	N70W	47W	318	33	N	
	214	0	L			184	13L			56	0	86	13	175	25.8	5.4	5.1																
23	42	9	R	25	22R					48	9	65	22	161.8	24.6	165.4	4	N75E	85N	48	81	R	N72W	52N	292	17	S	N50E	59N	44	10	D	
24	110	18	R	132	9R					340	18	318	9	85.9	30	59.4	28.2	N32W	62W	154	11	D	N8E	81W	349	67	S	N16E	38W	238	28	S	
25	137	14	R	158	17R					313	14	292	17	58.4	21.2	45	5.5	N45W	85W	142	52	R	N7W	77W	349	20	S	N46W	45W	264	38	D	
26	163	17	R	176	10R					287	17	274	10	41.7	1.9	208.2	3.2	N62W	86N	116	20	R											

Continued

																					N26W	74W	345	36	N						
																										N42W	63W	192	58	N	
27	268	15	L	250	18L			2	15	20	18	110.4	36	130.1	30	N40E	59W	28	19	R											
																					N60W	29W	306	25	N						
																										N6E	68W	209	45	D	
28	23	34	L	50	27L			247	34	220	27	214.8	37.1	190.4	54.7	N80W	35N	72	20	D											
																					N645W	75N	331	67	N						
																										N22W	54E	153	9	S	
29	304	29	L	283	17L			326	29	347	17	77.6	15	93.2	32.7	N4E	58W	212	38	S											
	304	29	L			332	40L	326	29	298	40	77.6	15	245	7.1						N26W	83E	145	59	R						
																										N5W	85E	8	67	N	
30	74	18	L	132	28R			196	18	318	28	146	64.8	70.8	12.4	N20W	78W	183	62	R											
	74	18	L			183	20R	196	18	267	20	146	64.8	212	14.7						N58W	75N	94	62	R						
																										N34E	61E	142	59	N	
31	220	31	R	203	24R			230	31	247	24	19.3	56.6	48.8	65.4	N42W	25W	157	10	N											YZ
	220	31	R			254	28R	230	31	196	28	19.3	56.6	4	29						N86W	60E	151	56	R						
																										N65W	59S	227	58	R	
32	283	18	R	292	7R			167	18	158	7	356	1.6	178.4	12.3	N88E	77N	309	32	N											
	283	18	R			248	17R	167	18	202	17	356	1.6	17.9	27.5						N74W	63S	135	43	N						
																										N3E	84W	251	19	D	
33	190	21	R	188	22R			260	21	262	22	79.6	70.1	83.9	71.6	N8W	19W	201	10	R											
																					N35W	44W	218	50	N						
																										N12E	44W	298	44	N	
34	138	18	L	123	18L			132	18	147	18	150.9	20.8	162.6	12	N73E	78N	64	37	R											
	138	18	L			176	20L	132	18	94	20	150.9	20.8	112.4	30.9						N22E	59W	19	5	D						
																										N64E	43N	327	44	N	
35	176	0	R	164	18R			274	0	286	18	114.3	50.8	146	64.8	N65E	25N	259	10	S											
	176	0	R			198	9R	274	0	252	9	114.3	50.8	74.9	55.9						N16W	34W	170	4	D						
																										N34E	62W	336	59	R	
36	97	26	L	56	15R			173	26	34	15	353.3	11	52	14.9	N38W	75W	321	10	S											
																					N29E	43E	193	14	N						
																										N58E	47N	6	42	N	
37	176	0	L	198	27L			94	0	72	27	114.3	50.8	90.7	21.9	N1W	68W	214	55	R											
	176	0	L			148	22L	94	0	122	22	114.3	50.8	140	22						N50E	68N	16	55	R						
																										N32W	13W	311	3	N	
38	155	22	R	179	19R			295	22	271	19	166.7	62.7	110.8	70	N23E	19W	209	3	D											
																					N71E	51N	325	50	R						
																										N50W	30N	103	13	S	
39	63	20	R	38	30R			27	20	52	30	50.6	6.7	74.9	12.4	N16W	78W	165	8	S											
	63	20	R			72	11L	27	20	198	11	50.6	6.7	20.6	20.9						N70W	69S	282	19	D						
																										N45W	72N	90	66	N	
40	352	37	L	28	36L			278	37	242	36	182.6	83.4	17	67.7	N76W	22S	188	23	R											
	352	37	L			333	22L	278	37	297	22	182.6	83.4	169.5	61.4						N71E	28N	344	30	R						
																										N53E	31N	309	32	N	
41	320	12	L	342	21L			310	12	288	21	171.8	45.5	153.8	66.3	N65E	24N	11	21	N											
																					N75E	63N	281	49	S						
																										N65W	54N	92	28	D	
42	277	15	R	262	40L			173	15	8	40	2	4.1	234.8	18.8	N35W	72E	331	17	D											
																					N3E	30E	185	29	N						
																										N5W	62E	30	22	S	
43	104	0	L	132	5L			166	0	138	5	189.1	10.8	164.7	27.6	N75E	62N	57	30	D											
																					N88W	72S	211	69	N						
																										N54W	77W	312	16	S	
44	97	7	R	68	9R			353	7	22	9	199.1	9.8	39.2	10.9	N52W	80S	138	43	R											
																					N63W	55N	1	53	N						
																										N10W	87W	276	78	D	
45	142	0	L	152	14L			128	0	118	14	159.1	37.8	140	30.9	N50E	59N	243	20	D											
	142	0	L			106	8R	128	0	344	8	159.1	37.8	194.2	17.4						N75W	72N	91	38	R						
																										N84E	65N	57	44	R	
46	17	16	L	36	18L			253	16	234	18	70.3	62.6	41.6	52.4	N48W	39W	168	28	R											
	17	16	L			342	9R	253	16	108	9	70.3	62.6	131.2	39.1						N42E	51N	1	38	R						
																										N8W	10W	241	8	N	
47	25	0	L	18	30L			245	0	252	30	71.5	44.8	44	72.7	N46W	18W	267	13	D											
	25	0	L			64	22L	245	0	206	22	71.5	44.8	15.6	33.5						N75W	56S	124	26	D						
																										N18E	59W	358	31	S	
48	153	18	L	121	18R			117	18	329	18	137.2	27.6	193.3	35.1	N76W	54N	100	6	S											
																					N9W	46W	350	2	D						
																										N43E	70S	153	70	N	
49	218	40	L	336	32R			52	40	114	32	79.8	3.7	129	15.6	N38E	74W	220	7	S											
																					N54W	55S	291	24	D						
																										N24W	44E	92	42	N	
50	302	14	R	290	15L			148	14	340	15	166.1	14.3	197.6	24.8	N72W	65N	294	12	S											
																					N47E	59E	34	22	D						
																										N74E	72S	186	72	N	
52	161	11	R	173	12L			289	11	97	12	144.3	57.3	116.8	38.6	N28E	52W	247	39	R											
																					N85E	49N	50	36	R						
																										N40E	8W	26	3	N	
53	275	27	R	272	13L			175	27	358	13	353.6	13	207	9.6	N63W	80N	302	33	R											
	275	27	R			310	22R	175	27	140	22	353.6	13	154.8	13.2						N65E	77N	49	49	R						
																										N68E	48S	200	40	N	
54	45	0	L	40	19R			225	0	50	19	50.2	33.3	67.4	21	N24W	69W	321	37	R											
	45	0	L			68	9L	225	0	202	9	50.2	33.3	24.9	22.7						N76W	67S	126	28	R						
																										N3E	67E	136	32	D	
55	101	0	R	147	10R			349	0	303	10	191	8.5	162.3	48.7	N72E	41N	31	31	N											

Continued

	101	0	R			194	14L	349	0	76	14	191	8.5	91.3	35.4						N2E	55W	188	10	D						
																										N88W	32W	148	6	S	
56	8	18	R	2	23L			82	18	268	23	99	32.6	101.3	73.9	N13E	17W	278	17	R											
																					N27W	83W	160	61	D						
																										N42E	82N	37	43	S	
57	76	21	L	61	15L			194	21	209	15	9.5	23.7	24.3	31.8	N66W	58S	131	27	S											
																					N72E	60S	246	8	S						
																										N78W	89N	4	85	N	
58	168	5	R	183	15L			282	5	87	15	128.8	54.3	104.4	35.9	N14E	55W	233	42	R											
																					N71E	50N	37	34	R						
																										N25E	10W	317	11	N	
59	146	20	L	128	15L			124	20	142	15	142.8	23	160.9	17.4	N71E	73N	64	23	S											
																					N48E	50N	342	48	N						
																										N38E	79W	229	44	D	
60	158	12	L	136	25R			112	12	314	25	134.6	35	190.6	50.6	N70W	40N	100	2	S											
																					N9W	50W	180	11	D						
																										N52E	82S	98	82	N	
61	332	5	L	358	2R			298	5	92	2	151.9	47.6	111	49	N22E	41W	210	7	S											
																					N20W	70N	1	69	N						
																										N78W	30N	292	5	S	
62	119	0	R	128	12R			331	0	322	12	252.5	33.4	248.5	18.9	N21W	72E	32	68	R											XY
	119	0	R			88	4R	331	0	2	4	252.5	33.4	290.4	35						N20E	54E	196	6	S						
																										32W	46N	125	23	D	
63	135	19	R	143	35R			315	19	307	35	245.3	9.7	66.7	7.8	N22W	82W	252	83	R											
																					N10W	72E	2	35	S						
																										N38W	74E	134	15	D	
64	102	4	R	134	9R			168	4	316	9	271.8	41.9	241.5	19	N28W	71E	139	36	R											
	102	4	R			86	22R	168	4	4	22	271.8	41.9	291.9	16.9						N22E	74E	177	54	R						
																										N32E	70E	192	43	D	
65	8	18	R	356	18R			82	18	94	18	180.5	9	189.4	16.4	N83W	73N	290	36	S											
																					N27E	79E	77	23	D						
																										N88W	89S	95	75	N	
66	293	12	R	308	13L			157	12	322	13	254.1	46.7	248.9	18	N22W	71E	46	71	R											
																					N27E	42E	197	7	S						
																										N58W	32N	117	3	D	
67	8	17	R	6	34R			82	17	84	34	181.1	8.2	171	22.3	N82E	67N	54	48	S											
																					N77E	67N	53	50	N						
																										N74W	80N	288	8	S	
68	94	0	R	108	18R			356	0	342	18	282.9	38.9	269.9	19.2	N1W	71E	29	54	R											
																					N40E	56E	209	16	S						
																										N8W	31E	128	24	D	
69	37	24	L	20	20R			233	24	70	20	4.8	41.5	170.2	3.6	N80E	87N	73	75	R											
																					N27W	56W	316	23	S						
																										N22E	29E	31	5	D	
70	57	26	L	74	4R			213	26	16	4	345.7	54.6	307.2	33.3	N36E	56E	72	42	R											
	57	26	L			34	20L	213	26	236	20	345.7	54.6	4.1	36.6						N88W	54S	226	45	R						
																										N78W	10S	158	8	N	
71	53	19	R	97	30R			37	19	353	30	323.7	12.8	281.9	8.8	N12E	81S	13	8	R											
																					N75E	67N	287	49	N						
																										N83E	44S	119	31	N	
72	248	4	R	275	9R			202	4	175	9	317	39.5	280.6	47.8	N88W	43N	320	35	R											
	248	4	R			232	12R	202	4	218	12	317	39.5	340.1	40.3						N70E	48S	243	8	S						
																										N84E	42S	86	2	S	
73	318	13	R	343	32R			132	13	107	32	224.8	35.8	188.2	34.6	N82W	55N	286	12	D											
																					N35W	83N	126	73	S						
																										N10W	35E	9	13	N	
74	108	5	L	89	8L			162	5	181	8	263.7	41.6	289.5	47	N20E	43E	26	6	S											
																					N32W	41E	137	8	D						
																										N8W	69E	76	70	S	
75	324	28	R	343	9R			126	28	107	9	206.6	43.7	205.6	17.7	N64W	73N	22	73	R											
	324	28	R			297	12R	126	28	153	12	206.6	43.7	248.9	45.2						N21W	45E	152	8	S						
																										N31W	55E	132	23	S	
76	280	12	R	298	20R			170	12	152	20	272.6	50.2	242.2	52	N28W	37E	335	3	D											
																					N8E	59E	114	59	N						
																										N32E	30E	46	9	S	
77	287	16	R	270	24R			163	16	180	24	260.5	52.4	288	63	N18E	27E	145	21	R											
	287	16	R			316	15R	163	16	134	15	260.5	52.4	225.3	38.6						N45W	52N	343	31	R						
																										N5W	55E	111	52	N	
78	285	12	R	262	12R			165	12	188	12	265.2	49.1	300.3	50.5	N30E	40E	200	9	S											
	285	12	R			312	12R	165	12	138	12	265.2	49.1	231.6	38.2						N38W	52N	345	27	R						
																										N10W	64E	57	64	N	
79	202	14	R	218	8R			248	14	232	8	9.8	24.6	351.7	29.5	N82E	61S	255	13	D											
																					N68W	81S	230	79	N						
																										N78W	56S	133	26	R	
80	310	8	R	280	9R			140	8	170	9	236.3	35.8	273.4	47.2	N4E	42E	11	8	S											
	310	8	R			328	9L	140	8	302	9	236.3	35.8	229.1	12						N42W	78E	358	71	R						
																										N36W	82E	24	82	R	
81	218	0	R	191	10R			232	0	259	10	346.7	22.8	15.8	14.7	N75W	74S	278	24	R											
	218	0	R			238	18R	232	0	212	18	346.7	22.8	337.4	48.4						N67E	42S	136	38	N						
																										N58E	89N	60	56	N	
82	320	12	L	344	32L			310	12	286	32	237.6	13.5	50.3	15.4	N40E	74W	283	67	R											
																					N4W	72E	360	6	S						
																										N55W	56N	101	31	D	
83	254	14	L	228	7R			16	14	222	7	305	23.5	341.2	34	N82E	55S	76	8	S											

Continued

																						N2E	53E	171	13	D					
																											N32E	80W	318	80	N
84	301	7	R	283	11R			329	7	167	11	253.3	26.1	268.5	48.6	N2W	42E	41	32	N										
	301	7	R			312	1L	329	7	318	1	253.3	26.1	239.3	27						N32W	62E	148	3	D					
																										N8E	80E	179	37	S
85	327	34	R	345	32R			123	34	105	32	197.9	45.9	186.8	33.4	N83W	57N	315	44	R										
	327	34	R			8	18R	123	34	82	18	197.9	45.9	180.5	9						N88E	80N	298	71	R					
																										N82W	30N	45	25	N
86	226	14	L	243	11R			44	14	207	11	332.1	14.6	326.5	44.3	N68E	45S	159	47	N										
	226	14	L			203	15L	44	14	67	15	332.1	14.6	350.8	2.1						N82E	88S	260	37	R					
																										N89W	89S	270	26	S
87	253	2	L	232	14R			17	2	218	14	308.9	35.1	341.5	42	N74E	47S	74	4	S										
																					N9E	44E	178	10	D					
																										N37E	80E	105	80	R
88	143	13	L	128	8R			127	13	322	8	220	32.9	246.7	22.5	N22W	68E	145	28	R										
																					N48E	32E	54	30	N					
																										N68W	78N	305	49	D
89	234	6	R	238	8L			216	6	32	8	334.3	36	323.3	24.9	N54E	65S	87	53	R										
																					N84E	58S	248	23	S					
																										N58E	40S	180	35	N
90	43	12	R	47	9L			47	12	223	9	335.8	15	343.5	35.2	N75E	55S	129	49	N										
																					N40E	81S	42	16	D					
																										N8E	89E	263	13	S
91	123	24	R	134	23R			327	24	316	23	257.7	9.6	247.9	6.5	N22W	83E	339	15	R										
																					N5W	88E	176	44	D					
																										N12W	54E	76	54	N

Location : BLM-3
Rock Type : Bioclastic Limestone

Grains No.	C - Axis			Calcite Twins						U-Stage Recalculate				Thin Section Rotation				Twin plane (e1)					Twin plane (e2)					Twin plane (e3)					Thin Section
	Strike (IV)	Dip (NS)	R/L Dip Direct.	Ttwin plane (e1)		Ttwin plane (e2)		Ttwin plane (e3)		C-axis		Twin Plane		C-axis		Twin Plane		Twin Plane		Slip Direction		Shear Sense	Twin-untwin Plane		Slip Direction		Shear Sense	Twin-untwin Plane		Slip Direction		Shear Sense	
				IV	NS	IV	NS	IV	NS	Az	Plg	Az	Plg	Az	Plg	Az	Plg	Az	Plg	Az	Plg		Az	Plg	Az	Plg		Az	Plg	Az	Plg		
1	190	17	L	158	8L					80	17	112	8	38.5	2.8	70.1	10.6	N20W	78W	163	16	S											XZ
																							N3W	81E	7	48	D						
																												N4E	66W	196	25	N	
2	70	19	L	85	1L					200	19	185	1	330	24.6	322	2.6	N52E	87S	59	72	R											
						32	9L			200	19	238	9	330	24.6	12.5	25.7						N86W	63S	279	8	S						
																												N38E	46E	190	25	N	
3	149	30	L	152	22L					121	30	118	22	255	12.5	254	4.1	N16W	86E	16	83	R											
																							N12W	68W	18	16	S						
																												N38W	62E	126	26	D	
4	107	22	R	123	1L					343	22	147	1	130	26.4	106	9.8	N16E	80W	203	36	D											
																							N65E	77N	55	37	S						
																												N38E	37W	13	19	N	
5	43	34	R	4	48R					47	34	86	48	191	18.6	225	28	N45W	62N	320	9	S											
						67	22R			47	34	23	22	191	18.6	167	13.2						N76E	76N	261	18	D						
																												N84W	83S	243	79	N	
6	38	28	R	3	14L					52	28	267	14	194	11.7	44.5	34	N45W	55W	171	41	R											
																							N60W	55N	339	43	N						
																												N77E	79N	257	9	S	
7	258	38	L	279	16L					12	38	351	16	163	31.5	135	18.1	N45E	72W	236	32	D											
																							N85W	74N	81	44	R						
																												N80E	31N	334	31	N	
8	275	34	L	253	20L					355	34	17	20	147	33.4	161	13.1	N71E	76N	49	57	R											
						294	23L			355	34	336	23	147	33.4	123	29.7						N33E	58W	221	12	D						
																												N75E	33N	307	28	N	
9	298	4	L	270	24L					332	4	0	24	113	13	147	22.5	N57E	66N	241	10	D											
						322	32L			332	4	308	32	113	13	97.5	46.6						N8E	42W	309	39	N						
																												N1W	62W	344	28	D	
10	314	20	R	334	24R					136	20	116	24	271	5.6	252	5.8	N18W	84E	343	3	D											
																							N14E	71W	220	53	S						
																												N16E	61E	52	46	S	
11	332	8	R	348	1R					118	8	102	1	76.1	9.7	60.6	18.6	N28W	71W	321	29	D											
																							N17W	72E	100	70	N						
																												N10E	71W	197	19	S	
12	73	38	R	101	12R					17	38	349	12	168	30	132	15	N38E	75W	231	30	D											
																							N75W	70N	94	27	S						
																												N70E	34N	57	9	N	
13	157	27	L	168	2L					113	27	102	2	249	8.4	60.6	17.5	N29W	72W	288	64	R											
						128	7L			113	27	142	7	249	8.4	99.7	5.4						N10E	85W	193	24	R						
																												N8E	78E	7	8	S	
14	68	25	L	76	16L					202	25	194	16	330	30.9	326	19.8	N56E	69S	99	61	R											
						32	47L			22	25	238	47	167	16.3	357	62.3						N86E	27S	167	29	R						
																												N88W	57S	269	3	S	
15	72	2	R	93	2R					18	2	357	2	336	4.2	136	2.9	N36W	87W	45	17	R											
																							N48E	65S	208	36	N						
																												N74E	60S	131	36	N	
16	52	24	L	74	25L					218	24	196	25	346	35.1	324	28.9	N55E	60S	66	22	D											
						6	43R			218	24	196	43	346	35.1	314	45.2						N46E	44S	214	10	N						
																												N87W	77S	253	37	R	
17	313	0	L	293	18L					317	0	337	18	96.8	13.5	123	24.6	N34E	64W	222	20	S											
																							N18W	64W	331	21	D						
																												N7E	77E	121	76	N	
18	247	14	L	222	6R					23	14	228	6	164	5.6	2.8	20.5	N88W	69S	117	48	R											
						283	4R			23	14	167	4	164	5.6	124	0.7						N34E	89W	214	6	D						
																												N88E	61N	306	49	N	
19	263	15	L	238	40L					7	15	32	40	150	11.7	181	27.7	N89W	62N	283	21	S											
																							N34E	66W	26	19	D						
																												N55E	51N	336	51	N	
20	223	24	L	232	17R					47	24	218	17	189	8.8	349	28.4	N78E	62S	222	48	R											
						184	30L			47	24	266	30	189	8.8	42.6	49.9						N48W	40W	178	32	R						
																												N84E	59N	50	44	N	
21	58	0	L	40	14L					212	0	230	14	228	12	212	29	N58W	60N	96	38	N											YZ
						90	4R			212	0	230	4	228	12	223	29.9						N46W	59N	73	57	N						
																												N54W	77W	282	65	N	
22	140	20	R	120	4L					310	20	150	4	94.7	62	41.8	49.8	N48W	40W	168	26	R											
																							N21E	53W	316	50	R						
																												N75E	15N	66	2	S	
23	28	32	R	28	24R					62	32	62	24	268	34.5	259	37.7	N12W	53E	164	7	D											
						358	7L			62	0	272	7	228	42	206	70.7						N64W	19N	60	17	N						
																												N1E	81E	128	39	R	
24	72	35	R	114	43R					18	35	336	43	83	1.7	100	30.6	N10E	58W	231	48	N											
																							N34W	87E	145	8	R						
																												N9E	69E	36	50	S	
25	32	1	R	14	31R					58	1	76	31	229	38	275	45.2	N6E	44E	182	4	S											
																							N75W	41N	95	8	D						
																												N42W	89E	36	80	R	

Continued

26	291	16	R	308	17R					159	16	142	17	27.2	39.1	18	54.2	N73W	44S	256	27	D	N2W	73E	125	55	R	N34W	63W	310	30	S	
27	167	9	L	172	12R					103	9	278	12	280	78.6	183	73.1	N88W	16N	329	15	R	N80W	24S	219	22	R	N4E	37E	96	27	R	
28	143	20	R	123	22R					307	20	327	22	99.3	64	81.9	47.8	N8W	42W	229	38	R	N43W	51W	159	25	D	N30E	47W	16	14	S	
29	74	42	R	37	19L					16	42	233	19	90.1	3	206	31	N38E	59E	59	33	R	N58W	58N	76	50	R	N26E	82E	28	25	D	
						68	14R			16	0	233	14	48	4	212	31.9																
30	28	10	R	18	10L					62	10	252	10	241	41.3	212	50.9	N58W	38N	109	10	D	N787W	59N	301	27	D	N31W	85E	131	76	R	
						34	30R			62	0	236	30	228	42	193	30.5																
								64	11R	62	0	26	11	228	42	239	5.9																
31	115	21	L	88	9L					155	21	182	9	19.5	41.3	38.6	17.8	N52W	71S	282	56	S	N36W	69W	256	69	R	N8W	69E	3	27	S	
32	46	25	L	40	3L					224	25	230	3	201	21.6	225	30	N45W	59N	324	15	S	N68W	85S	147	81	S	N84E	67N	265	4	D	
33	23	7	R	14	6L					67	7	256	6	238	46.6	217	55.6	N54W	34N	106	16	D	N42W	67N	15	63	R	N8E	44E	175	13	S	
34	58	18	R	48	4R					32	18	42	4	246	11.4	232	22	N38W	67E	125	36	S	N38W	65W	207	64	R	N2E	69E	7	13	S	
						94	5R			32	0	356	5	228	12	53.5	23.9																
35	324	24	R	334	6R					126	24	116	6	350	61.4	2.5	81.5	N87W	7S	166	8	N	N73E	56S	143	55	N	N46W	33S	286	19	S	
36	186	34	R	180	4R					264	34	270	4	171	48.2	216	69.6	N54W	20N	328	7	R	N45E	49N	243	20	S	N84W	66N	55	58	R	
37	144	14	R	134	14R					306	14	316	14	90	68.9	77.5	60.7	N12W	28W	224	25	R	N47E	35W	0	28	R	N80E	13S	118	9	D	
38	188	6	R	173	1R					262	6	277	1	215	61.4	224	77	N46W	13N	26	23	N	N89W	43N	309	32	D	N25W	48E	109	39	S	
39	74	0	R	98	1R					16	0	352	1	48	4	49.1	28	N42W	62W	223	63	N	N66W	81N	110	24	S	N18W	79E	349	34	D	
40	194	17	L	183	4R					76	17	267	4	257	52.4	218	66.7	N52W	23N	112	7	S	N24W	63E	33	59	R	N28E	42E	118	89	N	
41	124	2	L	146	18L					146	2	124	18	307	32.5	320	57.8	N50E	32E	111	29	R	N9E	66E	20	25	D	N56E	78S	218	53	R	XY
42	72	11	R	58	2R					18	11	32	2	133	20.5	148	30.6	N57W	59N	254	27	S	N15E	62W	11	9	D	N48E	85E	81	79	N	
43	43	5	R	28	11R					47	5	62	11	152	45.6	152	61.6	N62E	28N	331	29	N	N34E	61W	240	36	D	N88E	61N	60	42	S	
44	23	0	L	1	11L					247	0	269	11	177	59.9	226	59	N45W	31N	116	11	S	N28E	23W	220	5	N	N84E	55N	342	54	R	
45	352	23	L	358	28L					278	23	272	28	239	46.3	230	42	N40W	47E	341	22	S	N5W	60E	149	39	S	N28W	17E	57	18	N	
46	308	17	L	283	20L					322	17	347	20	286	27	295	4.7	N26E	86E	194	70	R	N38E	43E	69	25	S	N14W	62E	348	5	D	
						341	31L			322	0	289	31	303	35.3	248	35.8	N22W	54E	348	13	D	N22E	29E	136	27	N	N66E	40S	79	13	S	
47	54	3	L	30	13L					216	3	240	13	155	32.3	184	45.7	N85W	43N	292	16	S	N34E	53W	32	1	D	N78E	83N	35	76	R	
48	346	0		316	17R					284	0	134	17	264	65.8	321	48.3	N51E	42S	187	32	N	N85E	11N	286	4	S	N25W	48E	39	46	R	
						4	16R			284	0	86	16	264	65.8	184	84.5	N85W	5N	276	0	R	N34W	46E	25	42	R	N24E	46E	150	38	R	
49	28	14	L	18	3L					242	14	252	3	187	46.2	189	61	N81W	29N	2	29	N	N70E	59N	274	36	D	N60W	62N	89	46	S	
50	356	0	L	337	6L					274	0	293	6	240	69.6	271	55.5	N2E	34E	131	28	R	N28W	46E	64	46	S	N48E	23S	187	17	N	
						23	8R			274	0	67	8	240	69.6	163	64.7	N74E	26N	294	19	R											

Continued

51	124	0	R	123	8R					326	0	327	8	305	31.7	297	27.3	N26E	63E	43	28	D										
																							N58E	73S	224	39	S					
																												N38E	31E	120	31	N
52	68	37	R	93	18R					22	37	357	18	106	29.1	120	3.4	N30E	86W	25	64	R										
																							N35E	39W	254	27	S					
																												N14W	63W	172	13	D
53	127	9	L	138	6L					143	9	132	6	314	37.7	305	46.9	N34E	43E	173	32	N										
																							N35E	76E	66	66	D					
																												N87E	57S	245	18	S
54	193	4	L	208	8L					77	4	62	8	188	69.6	158	60.4	N68E	30N	293	22	D										
																							N50W	41E	71	37	S					
																												N68E	7S	180	8	N
55	48	15	L	26	1L					222	15	244	1	171	31.3	175	57	N85E	32N	347	32	N										
																							N64E	72N	246	31	D					
																												N29E	75N	92	39	S
56	90	0	L	71	1L					0	0	199	1	138	0	146	17.5	N55E	71N	269	60	S										
																							N22E	84E	200	13	N					
																												N66E	69S	87	46	D
57	83	6	L	114	6L					7	6	156	6	135	8.6	316	24.6	N46E	65S	131	65	R										
						74	2L			7	0	196	2	140	6.6	146	14.3	N56E	76N	250	46	S										
																							N22E	83W	23	1	D					
																												N64E	73S	91	58	R
58	102	14	R	127	8R					348	14	323	8	301	6.1	295	30.8	N26E	59E	135	58	N										
																							N12E	78W	2	40	S					
																												N56E	87W	237	21	D
59	43	4	R	64	4R					47	4	26	4	153	45.2	143	25.8	N54E	63W	185	58	R										
																							N80W	49N	87	14	S					
																												N4E	27E	7	11	N
						21	4R			47	0	69	4	158	43.4	173	64	N84E	26N	320	24	N										
																							N35E	57W	235	27	D					
																												N85E	67N	53	51	R
60	94	21	R	127	10R					356	21	323	10	117	3.5	293	29.8	N24E	59E	124	59	R										
																							N25E	66E	131	66	N					
																												N53E	75W	237	17	S

Location : CLM-4
Rock Type : Bioclastic Limestone

Grains No.	C - Axis			Calcite Twins						U-Stage Recalculate				Thin Section Rotation				Twin plane (e1)					Twin plane (e2)					Twin plane (e3)					Thin Section
	Strike (IV)	Dip (NS)	R/L Dip Direct.	Ttwin plane (e1)		Ttwin plane (e2)		Ttwin plane (e3)		C-axis		Twin Plane		C-axis		Twin Plane		Twin Plane		Slip Direction		Shear Sense	Twin-untwin Plane		Slip Direction		Shear Sense	Twin-untwin Plane		Slip Direction		Shear Sense	
				IV	NS	IV	NS	IV	NS	Az	Plg	Az	Plg	Az	Plg	Az	Plg	Az	Plg	Az	Plg		Az	Plg	Az	Plg		Az	Plg	Az	Plg		
1	78	16	L	86	1R					192	16	4	1	14.2	72.2	47.3	58.8	N75W	17S	260	8	S	N65W	8N	15	9	N	N68E	39S	125	35	R	XZ
2	76	0	R	54	12R					14	0	36	12	28.5	57.2	10	35.5	N70W	53S	150	46	R	N48W	29S	154	13	N	N24W	44W	307	26	S	
						83	2L			14	0	187	2	28.5	57.2	40.3	61.2																
3	67	14	L	74	3L					203	14	196	3	357	63.4	22.6	59	N67W	31S	267	15	S	N16E	11E	21	2	N	N68E	50S	130	47	R	
4	141	30	L	126	14L					129	30	144	14	158	46.2	127	53.2	N37E	37W	32	6	N	N68E	70S	327	70	R	N72W	38N	108	1	S	
5	151	16	L	141	17L					119	16	129	17	145	32.8	141	41.9	N52E	48W	348	45	N	N34E	76W	231	47	S	N85E	64N	73	22	S	
6	124	0	L	14	24L					146	0	256	24	109	45.9	310	23.3	N41E	67E	96	63	R	N55E	27N	254	9	S	N18W	45W	173	12	D	
7	162	17	L	154	6R					108	17	296	6	152	23.7	126	18.9	N35E	70W	222	18	D	N78E	87N	75	57	R	N78E	42N	308	36	N	
8	108	36	L	124	8R					162	36	326	8	172	73.8	101	39.9	N12E	50W	250	45	R	N26E	41N	33	39	R	N30E	13E	148	12	N	
9	97	21	R	120	2L					353	21	150	2	63.4	38.5	106	50.1	N15E	50W	199	3	S	N64W	45S	117	1	D	N26W	78W	262	77	S	
10	47	23	L	64	4R					223	23	26	4	325	51.1	14.3	47.8	N77W	41S	266	16	D	N14E	26E	184	5	N	N48E	66E	109	63	D	
11	38	25	R	65	9R					52	25	25	9	7.1	15.8	19.4	44.2	N72W	45S	167	41	N	N62E	65S	237	9	D	N65W	86W	298	48	R	
						24	7L			52	25	246	7	7.1	15.8	331	24.3																
12	162	32	L	134	4L					108	32	136	4	167	29.5	122	41	N32E	48W	30	2	D	N74E	33N	350	33	N	N74W	49N	296	10	S	
13	93	0	L	112	13L					177	0	158	13	61	59.9	110	63.5	N20E	25W	7	7	S	N86W	28S	115	11	D	B28W	56W	238	57	R	
14	172	30	L	143	7L					98	30	127	7	169	20.7	131	35.3	N42E	55W	33	13	D	N78E	42N	350	43	N	N74E	58N	297	17	S	
15	96	16	L	114	16L					174	16	156	16	77.9	75	118	63.9	N27E	26W	337	21	S	N5E	12E	84	12	N	N45W	38W	207	37	R	
16	58	36	L	73	10L					212	36	197	10	304	62.6	13.2	64.5	N78W	25S	256	12	S	N56E	59S	173	56	R	N37E	54E	131	55	R	
						27	15L			212	36	243	15	304	62.6	325	30.6																
17	138	0	L	128	12L					132	0	142	12	121	35.4	126	50.4	N36E	39W	286	39	N	N4E	64W	195	26	D	N53E	74W	35	46	S	
18	168	28	R	187	5R					282	28	263	5	295	4.3	324	8.6	N55E	82S	54	6	S	N7E	66E	165	42	N	N15E	68W	339	58	S	
19	63	0	R	84	9R					27	0	6	9	9.5	50.5	45.7	50.6	N44W	39W	304	10	S	N42E	34S	56	10	D	N56E	25S	227	5	D	
						50	32L			27	0	220	32	9.5	50.5	311	55.8																
20	128	28	L	114	4L					142	28	156	4	151	56.9	101	55.5	N11E	34W	211	13	D	N67E	59N	349	59	R	N64W	24N	109	4	S	
21	66	18	R	50	9R					24	18	40	9	76.9	34	64.5	19.8	N26W	70W	179	49	N	N16E	64W	6	22	S	N27W	31W	332	1	D	YZ
22	100	36	L	98	2L					170	36	172	2	350	49.5	49.7	67.9	N40W	22W	140	0	S	N31E	43S	58	17	D	N88W	65S	218	58	R	
23	359	35	L	12	9L					271	35	258	9	196	24.9	226	17.7	N34W	71E	130	17	S	N27E	40N	41	35	N	N89W	86N	274	55	R	
24	63	21	R	68	18L					27	21	202	18	79.6	30.6	32.6	35.9	N58W	53S	127	7	S	N19W	33W	271	32	N	N18E	44W	214	14	S	
25	223	20	L	213	4R					47	20	237	4	75.5	12.3	51	3	N38W	86W	142	20	D	N6E	83e	12	44	D	N8W	53W	236	51	N	

Continued

26	272	12	L	242	4L			358	12	28	4	79.4	59.7	59.7	31.9	N30W	57W	205	52	R											
																					N34E	40W	360	25	S						
																										N75W	13S	283	1	N	
27	252	24	L	262	12L			18	24	8	12	85.9	37.7	74.1	50.4	N16W	39W	302	30	D											
																					N18W	75W	196	63	R						
																										N27E	55W	19	14	S	
28	240	18	R	243	3L			210	18	27	3	34.5	28.4	58.6	32.9	N32W	57W	154	8	S											
																					N83W	48S	261	18	D						
																										N61W	87S	131	77	R	
29	243	25	L	232	5R			27	25	218	5	84.1	29.6	49.6	21.9	N40W	68W	149	22	D											
																					N8E	82W	355	57	S						
																										N11E	37W	241	31	N	
30	304	25	L	280	5L			326	25	350	5	154	64.7	69.4	69.4	N21W	20W	191	11	D											
						330	14R	326	25	120	14	154	64.7	262	57.1						N8W	33E	120	27	D						
																										N56E	50N	310	49	R	
31	334	12	L	318	1R			296	12	132	1	214	54.2	238	72	N32W	17E	14	13	N											
						3	7R	296	12	87	7	214	54.2	243	26.8						N27W	63E	116	50	S						
																										N85E	47N	293	26	D	
32	276	10	R	262	3R			174	10	188	3	31.7	64.1	50.2	51.9	N40W	38W	265	33	S											
																					N34W	5W	23	3	N						
																										N84E	41S	125	31	S	
33	35	32	L	283	10L			235	32	347	10	22.9	4.2	86	70.3	N5W	20W	199	9	N											
						343	18L	235	32	287	18	22.9	4.2	210	44						N60E	46N	16	45	R						
																										N45W	70W	149	30	N	
34	321	5	R	337	7R			129	5	113	7	249	68.4	247	52.4	N22W	38E	59	38	R											
						298	4R	129	5	152	4	249	68.4	351	85.5						N83E	4S	240	3	R						
																										N7E	25E	193	15	N	
35	302	0	R	317	12R			148	0	133	12	235	88	271	69.3	N3E	20E	97	21	R											
						270	1R	148	0	133	1	235	88	239	73						N32W	16E	61	17	R						
																										N61W	25S	212	26	N	
36	284	30	R	254	14R			166	30	196	14	351	56.4	35.9	42.4	N54W	48S	277	29	S											
																					N36E	14E	191	6	N						
																										N62E	57S	111	50	D	
37	298	27	L	268	2L			332	27	362	2	141	63	58.7	58	N31W	32W	188	22	R											
						317	1L	332	27	313	1	141	63	232	73						N38W	16E	113	9	D						
																										N67W	25N	88	10	S	
38	331	35	R	308	20R			119	35	142	20	289	44.6	304	68.5	N34E	21	97	19	S											
						0	18R	119	35	90	18	289	44.6	256	28.4						N14E	61E	9	36	D						
																										N40E	64E	190	46	R	
39	254	8	R	256	4L			196	8	14	4	44	43.5	60.7	45.9	N28W	41W	164	13	S											
						228	14R	196	8	222	14	44	43.5	40.3	17.4						N50W	73W	199	71	R						
																										N82W	31S	263	11	D	
40	243	30	R	254	17R			207	30	196	17	20.5	28.1	31.9	41.6	N58W	48W	164	37	N											
						216	22R	207	30	234	22	20.5	28.1	32.9	5.5						N58E	85S	292	65	E						
																										N56W	84S	293	63	S	
41	123	18	L	143	12R			147	18	307	12	305	31.8	272	12.2	N4E	77E	11	38	R											XY
						88	6L	147	18	182	6	305	31.8	330	4.2						N60E	86S	236	54	R						
																										N38E	32E	121	33	N	
42	351	22	L	23	18L			279	22	247	18	243	7.7	213	9.8	N56W	80N	123	1	D											
						337	7L	279	22	293	7	243	7.7	260	20.6						N10W	68W	7	37	S						
																										N10W	61E	20	44	N	
43	292	10	R	295	7L			158	10	335	7	311	19.6	300	6	N30E	83E	39	52	D											
						324	17R	158	10	126	17	311	19.6	282	39.8						N14E	50E	172	23	D						
																										N29E	46E	154	41	N	
44	21	38	L	16	16L			249	38	254	16	38.4	9.5	219	12.9	N50W	76E	21	76	R											
						342	16L	249	38	288	16	38.4	9.5	253	12.6						N16W	77E	350	29	R						
																										N77W	70S	276	17	D	
45	326	0	R	349	9R			124	0	101	9	273	24.5	249	38.3	N21W	52E	142	21	D											
						301	8R	124	0	149	8	273	24.5	301	22.1						N32E	67E	206	11	S						
																										N32E	59E	36	5	S	
46	108	19	R	132	8R			342	19	318	8	120	7.8	284	12.2	N14E	77E	180	47	R											
																					N19W	87E	56	8	S						
																										N20E	57W	328	53	D	
47	148	14	R	143	1R			302	14	307	1	267	11.6	276	22.6	N6E	66E	29	47	S											
																					N30W	76E	330	0	D						
																										N9E	78W	207	53	R	
48	37	4	R	68	6R			53	4	22	6	193	27.3	161	16.1	N72E	74N	257	20	D											
						17	9R	53	4	73	9	193	27.3	214	37.4						N56W	52N	318	18	S						
																										N68W	39N	356	36	N	
49	34	9	R	14	17L			56	9	256	17	194	33	221	12.2	N48W	78N	120	43	S											
																					N70W	31N	9	32	N						
																										N35W	71N	272	32	D	
50	283	22	L	247	11R			347	22	203	11	123	12.7	170	1.5	N80E	88N	80	17	S											
						210	9L	347	22	60	9	123	12.7	198	34.3						N73W	55N	107	12	S						
																										N17E	82E	186	50	N	
51	311	22	L	277	7L			319	22	353	7	99.4	1.2	136	2.6	N36E	88W	226	4	D											
						314	4R	319	22	136	4	99.4	1.2	287	24						N18E	65E	65	59	R						
																										N24E	66W	237	51	N	
52	18	14	R	5	8R			72	14	85	8	211	42.1	229	37.9	N42W	51N	123	20	S											
						54	28R	72	14	36	28	211	42.1	162	41.8						N72E	48N	264	13	D						
																										N82W	24N	51	19	N	
53	23	0	L	8	16L			247	0	262	16	209	27.4	227	13.7	N44W	75E	126	37	S											
																					N88W	39N	55	31	N						
																										N86W	75N	284	33	D	

Continued

54	2	12	L	352	11L					268	12	278	11	233	18	243	18.7	N26W	71E	152	2	S											
																							N58W	53N	94	32	D						
																												N22W	49N	23	40	N	
55	51	8	R	68	3R					39	8	22	3	176	25.6	163	13.4	N64E	77N	266	45	D											
																							N67W	73N	104	35	S						
																												N74E	38N	14	34	N	
56	48	28	L	18	4L					222	28	252	4	13.7	6.4	215	24.5	N55W	65N	334	47	R											
						38	7R			222	28	52	7	13.7	6.4	190	29.8						N70W	60N	25	60	R						
																												N64W	62S	156	47	N	
57	101	9	R	113	5R					349	9	337	5	131	2.4	303	6.8	N34E	85E	207	48	R											
																							N66E	82S	68	23	D						
																												N32E	62W	345	55	N	
58	278	18	L	253	8R					352	18	197	8	129	11.6	164	1.4	N74E	89N	74	18	S											
																							N31E	52W	349	29	N						
																												N22E	82E	193	46	R	
59	295	14	L	306	8L					335	14	324	8	117	0.3	289	9.8	N18E	81E	191	42	R											
																							N4E	79W	358	17	D						
																												N38E	66E	80	57	R	
60	358	42	L	11	7L					272	42	259	7	56.5	12	223	22.4	N47E	67E	91	59	R											
																							N8W	75W	173	2	S						
																												N47W	54W	266	46	D	

Calcite Twin from Veins

Location : SKV-1

Rock Type : Bioclastic Limestone

Grains No.	C - Axis			Calcite Twins						U-Stage Recalculate				Thin Section Rotation				Twin plane (e1)					Twin plane (e2)					Twin plane (e3)					Thin Section
	Strike (IV)	Dip (NS)	R/L Dip Direct.	Ttwin plane (e1)		Ttwin plane (e2)		Ttwin plane (e3)		C-axis		Twin Plane		C-axis		Twin Plane		Twin Plane		Slip Direction		Shear Sense	Twin-untwin Plane		Slip Direction		Shear Sense	Twin-untwin Plane		Slip Direction		Shear Sense	
				IV	NS	IV	NS	IV	NS	Az	Plg	Az	Plg	Az	Plg	Az	Plg	Az	Plg	Az	Plg		Az	Plg	Az	Plg		Az	Plg	Az	Plg		
1	273	14	L	294	9L					357	14	336	9	52.7	51.9	81.1	42.8	N9W	57W	327	15	S											XZ
	273	14	L			272	43L			357	14	358	43	52.7	51.9	57.1	80.9						N33W	10W	230	10	N						
	273	14	L					243	14L	357	14	207	14	52.7	51.9	20	19.9											N70W	70S	140	55	R	
2	141	8	R	132	3L					309	8	138	3	110.3	29.6	95.3	24.5	N6E	66W	196	20	R											
	141	8	R			171	27R			309	8	279	27	110.3	29.6	148.9	26.3						N58E	63N	52	15	S						
																												N15W	37W	322	18	N	
3	327	25	L	304	22L					303	25	326	22	128.4	39.6	102.2	50.2	N12E	39W	355	14	D											
																							N68E	46N	248	0	S						
																												N34E	72W	283	72	R	
4	108	0	L	135	10L					162	0	135	10	70.4	35.8	94.8	17	N6E	73W	349	42	R											
	108	0	L			88	10L			162	0	182	10	70.4	35.8	45.8	28						N47W	62W	147	21	D						
																												N18W	26W	247	26	N	
5	37	12	L	59	11R					233	12	31	11	355.2	11.5	5.2	42	N85W	47S	159	45	N											
	37	12	L			17	11R			233	12	73	11	355.2	11.5	324.6	19.1						N56E	79S	231	12	D						
																												N62E	79E	52	43	N	
6	111	18	R	104	22R					339	18	346	22	81.8	52.2	73.1	58.1	N18W	31W	302	23	D											
	111	18	R			154	9R			339	18	296	9	81.8	52.2	122.5	23						N32E	66W	7	47	R						
																												N15W	44W	229	42	R	
7	213	30	L	224	21L					57	30	46	21	323	43.1	341.3	43	N73E	47S	244	8	S											
																							N39E	37E	187	22	N						
																												N48E	59E	98	51	D	
8	103	19	R	95	12L					347	19	175	12	70.1	55.5	53.4	25.8	N38W	65W	194	59	R											
	103	19	R			58	8L			347	19	212	8	70.1	55.5	12.9	24						N78W	65S	131	47	R						
																												N27E	46W	359	27	S	
9	263	14	L	270	8L					7	14	360	8	37.1	51.6	48	46	N42W	43W	289	26	S											
																							N54W	30S	222	50	N						
																												N64W	43S	144	25	D	
10	315	28	R	284	30R					135	28	166	30	86.7	0.8	60.2	7.1	N30W	82W	326	14	D											
																							N4E	64E	59	60	N						
																												N16E	70W	211	36	S	
11	240	27	L	268	18L					30	27	2	18	354.4	56.4	44.6	56	N46W	34W	142	6	S											
	240	27	L			218	9L			30	27	52	9	354.4	56.4	344.2	29.9						N75E	61	135	58	R						
																												N50W	38S	289	16	S	
12	278	16	L	287	4R					352	16	163	4	60.9	53.4	68.2	32.1	N22W	58W	271	56	R											
	278	16	L			36	38L			352	16	234	38	60.9	53.4	187.4	11.5						N82W	79N	79	59	R						
																												N8E	24W	204	7	N	
13	84	14	L	104	11L					186	14	166	11	41.7	23.8	63.3	25.9	N27W	65W	153	2	S											
	84	14	L			62	8R			186	14	28	8	41.7	23.8	10.4	40.4						N80W	49S	265	17	D						
																												N66W	52S	267	32	D	
14	334	38	L	298	38L					296	38	332	38	146.6	44.2	113.4	66	N24E	24W	353	12	N											
	334	38	L			351	32L			296	38	279	32	146.6	44.2	152.8	29.9						N64E	61N	8	56	R						
																												N56W	69W	260	57	D	
15	246	9	R	250	10R					204	9	200	10	21.6	25.6	26	25.6	N64W	64S	1211	13	S											
	246	9	R			283	35			204	9	167	35	21.6	25.6	63.7	33.9						N26W	56W	155	3	S						
																												N72E	47S	241	12	D	
16	323	18	L	332	12L					307	18	298	12	119.1	36.5	122.9	26.5	N34E	63W	336	60	R											
	323	18	L			294	50L			307	18	336	50	119.1	36.5	139.8	74.9						N50E	15W	291	19	R						
																												N9W	73W	184	36	D	
17	56	14	R	38	11L					34	14	232	11	359.9	43.3	355.5	12.8	N86E	77S	148	77	R											
	56	14	R			84	9R			34	14	6	9	359.9	43.3	39.3	46.7						N50W	44W	301	8	S						
																												N54E	35S	223	5	N	
18	128	27	R	123	3L					322	27	147	3	111.5	52.2	86.1	28.3	N8W	62	213	49	R											
	128	27	R			91	30R			322	27	359	30	111.5	52.2	50.3	68						N40W	22W	143	2	D						
																												N57E	55N	29	35	S	
19	143	34	L	143	32L					127	34	127	32	269.9	7.7	270.9	5.9	N1E	85E	175	55	R											
																							N3E	80E	9	36	S						
																												N4W	83E	176	16	D	
20	48	13	R	50	20L					42	13	220	20	351.6	38.5	10.1	10	N80W	80S	262	61	R											
	48	13	R			30	19R			42	13	60	19	351.6	38.5	329.8	33.2						N60E	57S	73	20	D						
																												N88W	35S	149	31	N	
21	148	14	R	134	14L					302	14	136	14	120.8	30.5	92	13.9	N3E	76W	191	35	R											
																							N86E	80N	49	43	S						
																												N62W	28W	298	28	N	
22	38	25	L	57	15L					232	25	213	15	2.4	0.6	14.6	17.1	N76E	73S	127	52	R											
	38	25	L			8	30L			232	25	262	30	2.4	0.6	163.1	18.6						N76E	71N	58	46	R						
																												N73E	70E	57	39	N	
23	16	14	L	357	7R					254	14	93	7	159.1	1.5	311.3	3.7	N42E	87S	220	31	R											
	16	14	L			24	22L			254	14	246	22	159.1	1.5	170	3.6						N80E	85N	260	5	S						
																												N64E	80N	53	46	N	
24	87	0	R	68	8R					3	0	22	8	44.2	37.9	17.9	42.5	N74W	47S	284	4	D											
	87	0	R			92	7R			3	0	358	7	44.2	37.9	50.8	45						N40W	46W	188	37	R						
	87	0	R					114	14R	3	0	336	14	44.2	37.9	83.7	47.4											N8W	43W	178	5	S	
25	46	18	L	27	18L					224	18	243	18	5.9	10.2	350	1.3	N80E	89S	81	36	R											
																							N70W	89W	290	36	S						
																												N86W	62S	84	63	N	
26	335	20	R	15	38R					115	20	75	38	286.4	1.4	302	37.7	N32E	53	84	45	R											
	335	20	R			322	17R			115	20	128	17	286.4	1.4	97.5	7.6						N8E	83W	0	45	R						
																												N22W	84W	337	10	N	
26	338	11	R	327	23R					112	11	123	23	113.9	4.4	98.6	0.1	N8E	89E	188	16	D											
	338	11	R			12	7R			112	11	78	7	113.9	4.4	323.1	12.9						N54E	78S	69	27	R						
																												N3E	86E	56	3	S	
27	223	22	L	194	27L					47	22	256	27	339.5	43.2	165.4	13	N75E	77N	327	76	R											
	223	22	L			243	32L			47	22	27	32	339.5	43.2	353	62						N73E	27S	140	24	R						
																												N54E	61S	84	45	D	
28	37	15	R	8	28R					53	15	82	28	339.1	34.1	305.7	26.5	N38E	63E	28	23	D											
	37	15	R			38	12L			53	15	232	12	339.1	34.1	356	11.9						N88E	78S	247	59	R						
																												N3E	81W	265	4	N	
29	50	12	L	45	6L					220	12	225	6	6.8	17.3	359.4	20.5	N89E	69S	261	21	D											
	50	12	L			27	45R			220	12	63	45	6.8	17.3	301.8	49						N32E	41E	205	6	D						
	50	12	L					88	28R	220	12	2	28	6.8	17.3	43.6	66											N46W	23W	176	17	R	

Continued

30	143	8	R	134	6R					307	8	316	6	8	22.2	358.4	20.1	N88E	70S	94	17	D											YZ
	143	8	R			178	39R			307	8	272	39	8	22.2	226.4	1						N43W	89S	317	33	R						
																												N76W	75S	267	47	S	
31	55	11	L	34	27R					215	11	56	27	103.1	11.4	106.8	54.3	N16E	35W	281	37	R											
	55	11	L			82	12L			215	11	188	12	103.1	11.4	304.4	4.6						N34E	85S	37	35	R						
																												N12W	85E	55	11	S	
32	18	35	R	3	18R					72	35	87	18	92.1	68.7	53.1	55.9	N38W	34W	188	27	D											
	18	35	R			35	31R			72	35	55	31	92.1	68.7	112.3	56.9						N23E	34W	330	29	R						
																												N85W	4N	79	2	N	
33	48	37	L	58	22L					222	37	212	22	264.9	8.4	99.8	0.4	N8E	89E	189	35	R											
																							N6W	66E	82	66	N						
																												N18W	89W	341	40	S	
34	93	38	L	108	18L					177	38	162	18	294.3	30.7	320.6	25.2	N52E	66S	227	9	S											
	93	38	L			141	43L			177	38	129	43	294.3	30.7	321.4	62.5						N52E	27E	98	21	S						
																												N7E	38E	140	28	N	
35	320	47	L	326	29L					310	47	304	29	201.1	14.8	18.6	3.7	N72W	87S	265	82	R											
	320	47	L			273	47L			310	47	357	47	201.1	14.8	173	33.7						N83E	56N	66	25	D						
	320	47	L					12	50L	310	47	258	50	201.1	14.8	235.9	12.5											N35W	76N	144	8	S	
36	278	0	R	248	14R					172	0	202	14	324.3	4.9	112.2	1.9	N21E	8S	22	9	R											
	278	0	R			284	25L			172	0	346	25	324.3	4.9	164.3	11.4						N74E	77N	262	37	R						
	278	0	R					298	28R	172	0	152	28	324.3	4.9	320.7	38.7											N52E	51S	148	52	R	
37	14	43	L	28	9L					256	43	242	9	238.2	5.8	78.6	24.4	N12W	65W	195	44	R											
	14	43	L			55	35L			256	43	215	35	238.2	5.8	270.9	9.4						N2E	81E	1	4	S						
																												N55W	60E	97	4	N	
38	54	34	L	30	30L					216	34	240	30	270.6	8	73.7	3.9	N18W	87W	341	35	R											
	54	34	L			74	14L			216	34	196	14	270.6	8	296.9	1.5						N27E	88E	208	16	S						
																												N8W	56E	113	53	N	
39	297	0	L	286	34L					333	0	344	34	339.9	16.2	171.4	17.5	N3E	72E	4	10	D											
	297	0	L			328	2R			333	0	122	2	339.9	16.2	8.6	33.3						N83W	57S	114	24	S						
																												N38E	65E	215	7	D	
40	146	7	L	168	22L					124	7	102	22	4	37.1	26.3	58.6	N64W	32S	158	24	R											
																							N65E	58S	75	18	D						
																												N73W	75S	261	62	R	
41	136	43	L	116	26L					134	43	154	26	317.3	59.4	320.9	36	N62E	53S	151	53	R											
	136	43	L			168	26L			134	43	102	26	317.3	59.4	24.1	62.5						N65W	27S	271	11	S						
																												N2W	31E	16	10	D	
42	243	30	L	270	16R					27	30	180	16	137.8	39.5	308	12.5	N38E	78E	164	72	R											
	243	30	L			228	27L			27	30	42	27	137.8	39.5	121.9	46.4						N22E	43W	16	14	D						
																												N64E	47N	255	12	S	
43	118	40	L	102	10L					152	40	168	10	308.6	46.7	321.2	15.2	N52E	74S	185	70	R											
	118	40	L			146	16L			152	40	124	16	308.6	46.7	358.4	45						N88E	44S	254	15	S						
																												N87E	26S	92	3	S	
44	144	37	R	142	4L					306	37	128	4	199.9	4.4	1.2	32.6	N86W	57S	230	47	R											
	144	37	R			175	40R			306	37	275	40	199.9	4.4	224.2	2.1						N47W	69N	326	39	S						
																												N82W	65N	58	55	N	
45	124	34	L	124	18L					146	34	146	18	319.7	46.5	334.2	34.8	N65S	56S	207	42	R											
	124	34	L			98	28R			146	34	352	28	319.7	46.5	161.8	17.1						N73E	72N	298	67	R						
	124	34	L					154	30R	146	34	296	30	319.7	46.5	25.6	4.9											N65W	85S	289	46	R	
46	32	32	L	18	4R					238	32	72	4	74.7	1.5	71.6	39.7	N19W	50W	259	51	R											
	32	32	L			58	36L			238	32	212	36	74.7	1.5	272.4	11.5						N3E	78E	9	32	R						
																												N48W	71N	123	25	N	
47	58	43	L	90	50L					212	43	180	50	268.5	17.4	281.7	37.1	N12E	53W	55	42	R											
																							N265W	76E	337	7	D						
																												N64E	84N	343	34	D	
48	94	32	R	114	18R					356	32	336	18	161.8	22.4	167.7	0.3	N88E	89N	78	73	R											
	94	32	R			58	28R			356	32	32	28	161.8	22.4	131.9	41.2						N42E	48W	22	22	D						
																												N74W	63N	288	4	S	
49	328	38	L	348	13L					302	38	282	13	203.3	4.3	35.2	24.2	N56W	66S	164	56	R											
	328	38	L			299	24L			302	38	331	24	203.3	4.3	174.9	2.7						N86E	87N	265	8	D						
																												N35W	73N	330	16	S	
50	304	21	L	324	14L					326	21	306	14	357.2	2.3	11.4	17	N79W	72S	116	42	N											
	304	21	L			283	30L			326	21	347	30	357.2	2.3	166.6	15.9						N78E	74N	51	59	R						
																												N68E	86S	246	14	D	
51	353	9	L	358	16R					277	9	92	16	40.1	28.7	44.8	53.9	N47W	37S	213	37	R											
	353	9	L			24	34L			277	9	246	34	40.1	28.7	67.7	1.4						N24W	89W	335	61	R						
																												N30W	78W	319	40	S	
52	11	4	R	36	4R					79	4	54	4	62.6	41.1	92.7	33.5	N3E	56W	346	22	S											
	11	4	R			9	21R			79	4	81	21	62.6	41.1	64.2	58.2						N28W	31W	252	31	R						
																												N47W	26W	262	22	D	
53	358	1	R	328	18R					272	1	122	18	45.5	37	359.5	47.7	N89E	43S	263	9	D											
	358	1	R			8	8L			272	1	262	8	45.5	37	57.1	29.6						N34W	60W	307	32	S						
																												N47W	87S	219	88	N	
54	313	13	L	324	2L					317	13	306	2	0.9	13.4	6.3	28.1	N85W	61S	145	55	R											
	313	13	L			283	25R			317	13	167	25	0.9	13.4	311.6	27.3						N42E	62S	218	7	D						
																												N85W	55N	352	54	N	
55	258	10	R	274	4R					192	10	176	4	302.5	0.6	318.7	5.6	N68E	85S	238	7	S											
	258	10	R			228	24R			192	10	222	24	302.5	0.6	90.8	3.2						N1W	86W	359	9	R						
																												N22E	78E	193	35	N	
56	243	15	R	258	18L					207	15	12	18	107.6	3.8	140.1	21.4	N50E	68N	241	23	S											
	243	15	R			228	2R			207	15	222	2	107.6	3.8	101.5	22.6						N12E	68W	323	64	R						
																												N17W	71W	339	19	D	
57	148	38	R	158	9R					302	38	292	9	203.3	4.3	23.6	26.1	N68W	64S	204	65	R											
																							N15E	72W	327	21	S						
																												N28E	72E	78	26	D	
58	48	29	R	70	25R					42	29	20	25	124	47.9	139	31.6	N50E	58N	11	47	R											
	48	29	R			9	38R			42	29	81	38	124	47.9	75.7	74.7						N15W	17W	324	7	D						
																												N72W	24S	284	20	S	
59	23	10	L	6	9L					247	10	264	9	73.1	24.9	54.8	28.8	N36W	62W	319	11	D											
	23	10	L			53	6R			247	10	37	6	73.1	24.9	110.8	26.8						N21E	64W	20	3	S						
																												N7W	80W	340	53	S	
60	100	6	R	74	14R					350	6	16	14	209.6	56.7	262.9	62.1	N8W	26E	164	5	S											XY
	100	6	R			118	3L			350	6	152	3	209.6	56.7	189.2	41.5						N83W	48N	320	26	R						
																												N60E	31N	263	7	D	
61	280	14	L	254	16L					350	14	16	16	205	64.4	265	63.9	N7W	27E	148	12	S											
	280	14	L			31	1L			350	14	239	1	205	64.4	296.9	23.3						N26E	67E	170	55	N						
																												N50E	22N	253	9	D	
62	39	20	L	68	14L					231	20	202	14	277.1	14.8	254	34.1	N15W	57E	138	33	R											
	39	20	L			35	50L			231	20	235	50	277.1	14.8	80.4	10.4						N10W	80W	336	52	R						
																												N4W	75W	320	67	N	
63	168	11	L	148	12R					102	11	302	12	154	2.5	148.6	32.4	N58N	57N	345	57	R											
	168	11	L			194	3R			102	11	256	3	154	2.5	306.9	9.1						N38E	81S	213	23	R						

Continued

																										N39E	74E	208	33	N
64	91	4	L	123	4R			179	4	327	4	226.5	48	178.3	44.6	N89E	45N	285	17	D										
	91	4	L			74	9R	179	4	16	9	226.5	48	258.6	57.6						N11E	32E	35	26	R					
																										N41W	28E	37	27	N
65	328	21	R	283	9R			122	21	167	9	174.6	9.7	210.8	41.5	N60W	49N	326	26	N										
	328	21	R			322	34R	122	21	128	34	174.6	9.7	187.1	3.3						N83W	87N	96	25	S					
																										N76W	56S	153	49	N
66	322	6	R	297	14R			128	6	153	14	168.4	24.7	196.6	32.2	N73W	57N	292	9	S										
																					N52E	52N	38	18	D					
																										N75E	87S	237	82	N
67	230	43	R	264	53R			220	43	186	53	256	1.2	51.6	1.1	N38W	89W	321	11	S										
																					N2E	70W	206	50	N					
																										N5E	67E	30	54	N
68	280	15	L	286	15L			350	15	344	15	204.3	65.4	192.1	63	N8E	26N	308	14	D										
																					N50W	29N	71	23	S					
																										N60W	20N	68	16	N
69	77	3	R	137	25R			13	3	313	25	249.9	53	142.1	48.4	N53E	42W	274	31	R										
																					N15W	81W	221	81	N					
																										N82E	47S	224	33	N
70	80	16	L	110	9L			190	16	160	9	239.8	35.2	202.1	39.4	N68W	50N	295	4	D										
	80	16	L			63	7L	190	16	207	7	239.8	35.2	263.1	38.5						N80W	51E	173	2	S					
																										N5E	39E	17	11	S
71	176	20	R	194	47R			274	20	256	47	124.3	15.2	92.3	18.7	N3E	51E	140	39	R										
	176	20	R			143	23R	274	20	307	23	124.3	15.2	140.6	42.6						N52E	48N	275	23	S					
																										N45E	75E	82	66	N
72	332	0	L	304	18L			298	0	326	18	156.1	21.7	162.5	54.2	N83E	35N	330	35	N										
	332	0	L			354	34L	298	0	276	34	156.1	21.7	112.8	24.4						N24E	65W	206	5	D					
																										N35E	83W	219	31	D
73	162	29	R	156	20R			288	29	294	20	123.5	30.8	135.7	30.8	N45E	60W	44	3	S										
																					N37W	50E	346	37	N					
																										N38E	68W	239	52	D
74	172	14	L	140	11L			98	14	130	11	333.9	2.4	173.6	22.3	N86E	68N	284	43	R										
	172	14	L			189	2L	98	14	81	2	333.9	2.4	314	8.3						N44E	82S	222	14	D					
																										N68E	71N	298	66	N
75	224	7	R	264	43L			226	7	6	43	281.9	27.9	7.5	83.2	N84E	6S	99	1	R										
																					N45W	85W	313	33	S					
																										N58E	74W	252	40	D
76	350	22	L	347	20R			280	22	103	20	125.9	20.9	341.6	2.5	N74E	88S	74	31	D										
	350	22	L			303	50R	280	22	147	50	125.9	20.9	27.5	2.7						N64W	87S	118	20	D					
																										N32E	27W	310	27	N
77	77	4	L	113	34R			193	4	337	34	247	46.3	143.1	71	N54E	19N	262	9	R										
	77	4	L			50	50L	193	4	220	50	247	46.3	72.5	4.8						N28W	85W	294	84	R					
																										N67E	39E	215	16	N
78	292	22	L	258	34L			338	22	12	34	172	65.2	299.2	79.5	N29E	10E	158	9	R										
																					N35E	45W	258	35	D					
																										N70W	53N	54	49	R
79	298	14	R	288	8R			152	14	162	8	195.6	31.7	204.1	41	N65W	48N	330	34	R										
	298	14	R			32	8R	152	14	58	8	195.6	31.7	303.7	29.9						N35E	60E	194	31	S					
																										N87W	59N	273	2	D
80	256	24	L	278	27L			14	24	352	27	272.5	71.6	194.2	77.1	N85W	12N	310	8	N										
																					N8W	39E	66	39	N					
																										N58E	26S	197	17	N
81	293	35	L	298	11L			337	35	332	11	140.2	71.3	177.7	53.2	N89E	37N	35	32	R										
																					N56E	6S	142	6	N					
																										N15E	39W	249	34	D
82	70	40	R	58	3R			20	40	32	3	331.6	74.4	275.8	44.4	N8E	46E	65	42	R										
	70	40	R			104	43R	20	40	346	43	331.6	74.4	108.4	78.3						N18E	12W	318	18	N					
																										N80W	51S	214	48	R
83	9	7	R	345	40R			81	7	105	40	318	11.4	358.3	13.9	N87E	77S	267	4	S										
	9	7	R			18	2R	81	7	72	2	318	11.4	308.3	15.4						N38E	75E	212	21	D					
																										N19E	51E	171	29	N
84	68	14	L	82	8R			202	14	8	8	254	34.1	243.6	59.1	N25W	30E	85	30	R										
																					N38W	75E	340	47	D					
																										N11E	67E	179	28	S
85	46	26	L	53	18R			224	26	37	18	268	13.9	296.6	52.1	N28E	39E	71	29	S										
																					N47W	83W	317	25	D					
																										N24E	66W	236	51	N
86	302	3	R	272	7R			148	3	178	7	184.8	39.4	225.2	45	N45W	45N	133	2	S										
	302	3	R			318	47R	148	3	132	47	184.8	39.4	17.4	5.2						N74W	84S	123	77	R					
																										N54E	38N	48	5	S
87	189	32	R	154	30R			261	32	296	30	107.2	12.8	126.4	37.4	N25E	53W	253	37	R										
																					N15W	79W	167	6	D					
																										N34E	75E	59	60	N
88	211	8	R	226	11L			239	8	44	11	291.5	18.4	295.4	42.4	N26E	48E	105	47	R										
	211	8	R			181	4L	239	8	89	4	291.5	18.4	320.5	3.2						N52E	86S	228	30	S					
																										N1E	84N	3	28	D
89	155	14	R	182	38R			295	14	268	38	142	28.2	105.5	20.9	N15E	70W	205	24	D										
90	155	14	R			128	18R	295	14	322	18	142	28.2	158.4	51.3						N68E	38N	296	30	S					
																										N32E	40W	257	26	N
91	150	5	R	154	4R			300	5	296	4	153.4	26.5	151.4	22.8	N62E	67N	276	55	R										
																					N68E	62N	256	12	S					
																										N50E	60N	27	44	N

Location : LRV-2
Rock Type : Bioclastic Limestone

Grains No.	C - Axis: Strike (IV)	C - Axis: Dip (NS)	C - Axis: R/L Dip Direct.	Calcite Twins: Ttwin plane (e1) IV	Ttwin plane (e1) NS	Ttwin plane (e2) IV	Ttwin plane (e2) NS	Ttwin plane (e3) IV	Ttwin plane (e3) NS	U-Stage Recalculate: C-axis Az	C-axis Plg	Twin Plane Az	Twin Plane Plg	Thin Section Rotation: C-axis Az	C-axis Plg	Twin Plane Az	Twin Plane Plg	Twin plane (e1): Twin Plane Az	Twin Plane Plg	Slip Direction Az	Slip Direction Plg	Shear Sense	Thin Section
1	296	35	R	315	12R					154	35	135	12	34.9	68.9	59.1	43	N32W	47W	268	44	R	XZ
	297	35	R			268	10R			333	35	182	10	107.4	14.7	134.5	63.9						
2	156	34	L	162	18L					114	34	108	18	21.5	36.9	35.1	24.8	N50W	66S	281	41	S	
3	198	0	L	191	22L					72	0	79	22	209.2	14.5	15.9	4.4	N85W	86S	278	54	R	
4	238	3	R	268	9R					212	3	182	3	179.2	45.7	134.3	62.9	N44E	27W	32	27	D	
	238	3	R			250	18L			212	3	20	18	179.2	45.7	152.8	32.7						
5	150	16	R	158	1L					300	16	112	1	71.2	13.1	52.5	18.3	N38W	71W	318	14	D	
6	312	40	R	338	23R					138	40	112	23	20.1	57	32.4	30.6	N68W	59S	237	58	R	
7	204	0	R	183	29R					246	0	267	23	205.3	19.2	242.7	18.7	N36E	71N	140	9	S	
8	89	23	R	97	24L					1	23	173	24	131.1	31	101.5	76.5	N13E	13N	315	13	R	
	89	23	R			58	14R			1	23	32	14	131.1	31	167.1	31.6						
9	35	28	L	140	2L					235	28	130	2	226.5	43.3	64.6	32.7	N27E	58W	223	56	R	
10	75	0	R	57	18R					15	0	33	18	154.5	51.4	165.8	27.6	N76E	63N	20	58	R	
	75	0	R			100	8R			15	0	350	8	154.5	51.4	115.9	45						
11	327	34	L	338	4L					303	34	292	4	85.9	2.1	56.6	15.1	N35W	74W	321	18	D	
12	183	14	R	191	1R					267	14	259	1	229.7	10.5	214.3	9.5	N65W	80N	306	12	D	
13	103	20	R	127	15R					347	20	323	15	115.5	32.7	88.8	28.2	N2W	61W	186	18	D	
14	308	9	R	334	35R					142	9	116	35	68.6	46.2	21	38.8	N68W	52S	129	23	D	
15	314	35	R	340	26R					136	35	110	26	28.3	54.5	28.4	30.4	N64w	60S	203	60	R	
16	181	21	R	157	10R					269	21	293	10	236.7	12.9	62	12.1	N27W	77W	192	71	R	
17	128	20	L	141	14L					142	20	129	14	55.4	53.2	52.2	39.5	N38W	69W	219	61	R	
18	78	42	R	44	40R					12	42	46	40	139.1	11.2	163.5	3.1	N73E	86N	73	19	S	
19	297	20	L	314	2L					333	20	316	2	101	28.5	73	34.1	N18W	55W	340	8	D	
	297	20	L			264	11R			333	20	6	11	101	28.5	138	42.7						
20	256	9	L	234	26L					14	9	36	26	149.1	43.1	164.1	19.3	N73E	70N	39	59	R	
	256	9	L			283	16L			14	9	347	16	149.1	43.1	114.4	36.6						
21	226	0	L	206	22L					44	0	64	22	188.7	35.6	187	6.3	N83W	83N	333	63	R	
22	14	32	L	358	16L					256	32	272	16	240.6	28.5	234.2	7.8	N36W	82N	250	72	R	
23	114	0	R	134	27R					336	0	316	27	92.9	47.7	90.3	14.6	N1W	76W	250	77	R	
	114	0	R			87	23R			336	0	3	23	92.9	47.7	133.2	30.9						
24	100	28	L	110	21L					170	28	160	21	80.5	78.4	75.2	67	N15W	22W	244	44	R	
	100	28	L			68	43R			170	28	22	43	80.5	78.4	146.1	8.5						
25	240	38	R	218	20R					210	38	232	20	233.9	66.1	215.2	42	N54W	48N	8	45	R	
	240	38	R			278	10L			210	38	352	10	233.9	66.1	119.1	43.4						
26	296	18	R	318	30R					154	18	132	30	71.1	60.8	34.4	49.7	N56W	41W	158	46	D	
27	294	0	L	280	40L					336	0	350	40	92.9	47.7	122.1	13.5	N32W	77W	11	58	R	
	294	0	L			323	2L			336	0	307	2	92.9	47.7	65.6	27.8						
28	0	19	L	17	18L					270	19	253	18	235.6	11	225.5	24	N44W	57N	107	47	D	
29	74	30	R	52	24R					16	30	38	24	144.9	22.3	166.8	20	N88E	70N	73	11	S	
30	120	13	L	102	10R					150	13	348	10	191	15.2	221.2	15.5	N48W	75N	131	3	S	
	120	13	L			146	9R			150	13	304	9	191	15.2	187.2	49						
31	338	10	L	8	16L					292	10	262	16	173	57.2	108.4	68.7	N18W	21W	210	5	R	

Twin plane (e2): Twin-untwin Plane Az	Twin-untwin Plane Plg	Slip Direction Az	Slip Direction Plg	Shear Sense
N44E	26W	276	23	D
N64W	36S	186	33	N
N37W	77E	140	11	S
N64E	56N	268	35	D
N15W	83E	12	76	N
N12W	19W	346	2	N
N88E	44N	56	27	D
N76E	59N	72	10	R
N71E	47S	214	32	N
N25E	44W	225	18	D
N3W	60E	78	60	N
N32W	86W	153	57	N
N38E	79W	19	61	R
N7W	78W	319	31	S
N18W	30W	355	4	N
N15W	30S	335	7	S
N12W	34W	172	2	N
N41E	52W	336	50	N
N38W	46N	138	11	S
N24E	53W	219	19	D
N46W	48N	315	3	S
N5W	60E	356	1	D
N43E	60W	21	24	S
N56W	81W	20	70	R
N28W	46W	263	42	R
N3E	51W	307	46	S
N26W	62W	186	45	R
N42W	87W	314	68	N
N43E	52W	356	44	N
N83W	41N	347	40	R

Twin plane (e3): Twin-untwin Plane Az	Twin-untwin Plane Plg	Slip Direction Az	Slip Direction Plg	Shear Sense
N76E	39S	122	30	D
N84W	59S	109	23	D
N73W	54N	60	46	N
N50W	46N	118	14	S
N5W	65W	194	33	S
N60E	39S	87	20	D
N80W	75S	252	61	N
N7E	86E	182	42	S
N65E	88N	246	44	S
N74W	21N	306	8	S
N22E	70W	212	26	S
N32W	66E	1	51	N
N45E	37W	268	23	S
N34E	23W	221	3	N
N75E	31S	83	4	D
N58W	72N	118	10	D
N58W	30S	284	10	D
N31E	83E	203	44	S
N14E	85W	328	83	N
N89W	25N	304	15	S
N64E	42N	56	9	D
N48W	46N	104	27	D
N54E	38N	41	10	S
N76E	23N	14	22	N
N14E	37E	153	26	N
N27E	10W	232	4	N
N75E	9N	262	2	N
N18W	78E	343	5	S
N45E	84W	232	61	S
N85E	75S	240	57	N

Continued

	338	10	L			328	18R			292	10	122	18	173	57.2	164.8	28.1					
32	312	14	R	304	16L					138	14	326	16	181.3	22.6	213.4	36.6	N57W	54N	315	17	N
	312	14	R			338	18R			138	14	112	18	181.3	22.6	154.9	32.2					
33	296	0	R	273	8R					154	0	177	8	204	20.8	31.8	2.3	N65E	58N	63	3	D
	296	0	R			314	17R			154	0	136	17	204	20.8	177.7	21.4					
34	234	20	L	262	32L					36	20	8	32	78.3	14.2	250.7	12.5	N19W	77E	125	69	R
35	175	0	L	154	14R					95	0	296	14	138.5	53.7	183.3	58	N87W	31N	87	3	S
	175	0	L			204	34L			95	0	66	34	138.5	53.7	109.4	16.5					
36	184	18	R	194	9R					266	18	256	9	117.9	71.6	101.3	60.1	N11E	30W	250	26	R
37	102	6	L	76	17R					168	6	14	17	208.1	6.1	61.9	0.9	N29W	89W	151	10	D
38	132	24	R	158	20L					318	24	112	20	217.4	47.2	154	30.2	N63E	59N	266	33	D
	132	24	R			102	34R			318	24	348	34	217.4	47.2	243.4	27.9					
39	335	7	L	354	9L					295	7	276	9	174.3	53.1	142.9	62.5	N54E	28N	42	7	D
	335	7	L			312	24L			295	7	318	24	174.3	53.1	217.4	47.2	N52W	42N	106	18	S
40	68	23	L	74	6L					202	23	196	6	32.4	30.6	44.6	16.4	N47W	74S	295	48	S
	68	23	L			36	43L			202	23	234	43	32.4	30.6	14.6	61.6					
41	129	27	R	164	35R					321	27	286	35	223.2	46.1	220.5	76.9	N50W	14E	45	15	R
42	223	18	L	244	14L					47	18	26	14	85.5	22.4	67.1	11.7	N22W	79W	164	33	D
	223	18	L			219	27R			47	18	231	27	85.5	22.4	44	55.8					
43	190	7	L	168	40L					80	7	102	40	115.6	46	139.4	13.2	N48E	77W	24	62	R
	190	7	L			204	4R			80	7	66	4	115.6	46	95.6	44.1					
44	353	9	R	333	47R					97	9	117	47	139.7	44.5	148	3.5	N58E	87N	46	81	R
	353	9	R			15	20R			97	9	75	20	139.7	44.5	113.3	32.2					
45	278	27	R	280	24R					172	27	170	24	13.5	9.6	14.9	6.4	N15E	83S	266	70	R
46	278	0	L	255	18L					352	0	15	18	215.3	6.5	63.2	1	N27W	89W	152	16	D
	278	0	L			276	24L			352	0	354	24	215.3	6.5	236.7	18.4					
48	217	17	L	205	10R					53	17	245	10	90	26.5	82.7	55.5	N8W	35W	281	34	D
	217	17	L			244	27L			53	17	26	27	90	26.5	76.7	2.8					
	217	17	L					192	30L	53	17	78	30	90	26.5	118.7	23					
49	289	7	R	264	18L					161	7	6	18	202.9	11	238.1	5.8	N32E	84E	146	11	S
	289	7	R			304	2L			161	7	326	2	202.9	11	200.1	28.2					
50	348	9	R	10	8L					102	9	260	8	146.5	43.6	109.5	60.6	N20E	29W	2	10	D
51	278	0	R	252	14R					172	0	198	14	215.3	6.5	38.8	22.6	N54W	67W	199	68	R
52	254	0	L	250	22R					16	0	200	22	49.6	12.9	32.4	28.5	N56W	62S	279	36	D
	254	0	L			220	18L			16	0	50	18	49.6	12.9	88	24.1					
	254	0	L					283	24L	16	0	347	24	49.6	12.9	233.2	24					
53	316	9	R	333	17L					134	9	297	17	181.6	28.9	188.8	59.5	N81W	31N	356	31	R
	316	9	R			297	18R			134	9	153	18	181.6	28.9	189.3	9.7					
54	203	8	R	200	21R					247	8	250	21	87.5	55	75.2	67	N15W	23W	289	19	R
55	150	21	R	140	35L					300	21	310	35	198.2	59.9	230.2	57.6	N40W	33N	121	12	S
	150	21	R			186	24R			300	21	264	24	198.2	59.9	105	76.9					
56	263	18	R	234	30R					187	18	216	30	29.1	16	31.5	44.9	N58W	46S	204	46	R
57	268	20	R	259	10R					182	20	191	10	24.7	13.2	38.2	14.7	N53W	75S	129	7	S
58	317	0	R	304	20R					133	0	146	20	187.8	36.3	183.1	13	N86W	77N	323	74	R
	317	0	R			350	13R			133	0	100	13	187.8	36.3	142.7	40.1					
59	338	27	R	337	5L					112	27	293	5	151.4	23.7	169.7	52.5	N80E	37N	309	30	N
60	324	14	L	354	25R					306	14	96	25	195.1	51	136.2	28.7	N35E	61W	239	37	D
	324	14	L			314	9L			306	14	316	9	195.1	51	198.7	40.3					
61	348	14	L	353	12R					282	14	97	12	57.8	4.4	218.5	13.8	N52E	77N	119	39	R
62	63	0	R	74	16R					27	0	16	16	342.2	31.6	326.2	18.7	N56E	72S	74	44	D
	63	0	R			34	4R			27	0	56	4	342.2	31.6	9.2	15.8					
63	322	24	L	334	15L					308	24	296	15	84	0	249.7	2.3	N20W	87S	159	14	R
64	256	14	R	243	24L					194	14	27	24	330.8	48.5	334.8	8.6	N65E	82S	171	81	R
	256	14	R			287	8R			194	14	163	8	330.8	48.5	287.1	42					
65	287	13	L	317	10L					343	13	313	10	292.2	21.5	261.9	14.7	N8W	76E	357	17	D
	287	13	L			295	4L			343	13	335	4	292.2	21.5	281.4	28.4					
66	267	15	L	270	20L					3	15	360	20	313.1	21	310	16	N40E	74E	62	54	D

N75E	61N	323	61	R
N64E	57N	54	20	D
N88E	69N	269	3	D
N12W	59W	209	26	S
N19E	73W	228	59	R
N60E	24N	25	16	S
N75W	53N	52	46	N
N27W	63E	123	45	R
N80E	54N	336	54	R
N78W	29S	227	25	N
N75W	63N	312	42	R
N56W	34S	288	18	D
N4E	45W	196	12	D
N24E	58W	223	28	R
N75W	77S	114	36	S
N24W	71E	335	23	S
N14W	87W	170	63	R
N70W	61N	41	59	R
N47E	72W	276	67	R
N31W	68E	341	26	N
N4W	65W	182	10	S
N71W	81N	76	69	R
N15W	46W	219	41	N
N15E	14W	218	6	R
N86W	86S	97	32	D
N74W	66S	261	43	D
N54E	49N	238	6	D
N27E	75W	212	19	D
N73W	49N	40	49	R
N7W	87E	355	19	N
N82W	75S	268	35	S
N11E	70E	33	47	N
N18E	48E	36	21	D
N11E	61E	171	31	D
N70E	76E	245	20	D

N45W	38N	108	20	S	YZ
N58E	57N	54	8	D	
N46W	54N	337	30	N	
N40W	69W	317	9	D	
N3W	30W	187	2	D	
N3W	8W	323	5	N	
N84W	71N	257	45	S	
N34W	88W	152	72	N	
N65W	35N	110	4	S	
N50W	43S	189	39	N	
N18W	62E	138	40	S	
N13E	79W	6	34	S	
N88E	15N	277	4	S	
N32W	85N	30	80	N	
N76E	74S	253	14	D	
N45E	71N	95	22	D	
N28E	66W	23	13	S	
N85E	48N	49	39	N	
N85W	49N	84	13	S	
N82W	73N	93	21	D	
N37W	65W	35	65	R	
N63E	77N	249	22	D	
N15E	38W	358	15	S	
N76E	27N	74	2	D	
N38W	88N	323	38	N	
N72W	89S	110	66	R	
N53W	51N	310	4	S	
N71E	86S	85	58	D	
N58W	32N	323	13	N	
N38W	60W	258	57	N	XY
N70E	31S	163	31	N	
N6E	66W	229	58	N	
N72E	66S	201	61	R	
N50E	68S	228	7	S	
N29E	45E	160	38	N	

Continued

67	37	18	R	22	7R			53	18	68	7	359.7	5	18	6.9	N72W	84S	109	8	S	N72E	64S	228	42	N	N80E	69N	38	61	N
68	121	15	L	96	37L			149	15	174	37	266.1	44.1	293.9	72.5	N24E	18E	70	14	R	N18E	21E	195	2	N	N15E	66E	165	50	S
69	92	0	L	74	20L			178	0	196	20	307.5	36	336.1	53.9	N687E	37S	91	19	S	N7E	55E	12	8	D	N47E	79S	194	7	N
70	278	14	L	258	17L			352	14	12	17	301.6	21.7	322.1	18.3	N52E	71S	227	15	S	N2E	89E	1	35	D	N30E	42E	125	43	N
	278	14	L			315	27L	352	14	315	27	301.6	21.7	270.9	0.2															
71	40	7	R	13	10L			50	7	257	10	2.3	16	35.4	15.7	N65W	74S	303	9	S	N73E	52S	219	36	N	N82E	81N	62	66	N
72	332	8	R	339	9R			118	8	111	9	238.6	22.7	231.9	19.5	N38W	70E	328	18	D	N25W	71E	147	37	S	N31W	59E	42	58	R
73	303	0	L	327	13L			327	0	303	13	271.2	29.5	254.5	7.5	N14W	83E	355	57	R	N29E	67E	201	18	S	N30E	37E	116	29	R
74	302	14	L	308	28L			328	14	322	28	277.5	16.7	277.1	1.7	N8E	85E	8	85	R	N44E	49E	65	23	S	N19E	69W	247	63	N
	302	14	L			267	6R	328	14	183	6	277.5	16.7	314	41.9															
75	248	18	L	234	4L			22	18	36	4	331.7	15.6	350.2	24.7	N80E	66S	91	22	S	N44E	65S	211	27	D	N62E	86N	311	87	N
76	223	14	R	204	18R			227	14	246	18	11	35.8	31.4	28.5	N59W	61S	287	25	S	N70W	79.S	262	69	N	N50W	35W	155	18	S
77	243	25	L	214	17L			27	25	56	17	334.5	7.6	2.7	4.5	N89W	86S	272	8	R	N51E	58S	191	46	N	N48E	74N	27	53	N
78	290	20	R	272	14R			160	20	178	14	278	52.7	307	50	N37E	40S	202	11	S	N4W	72E	48	68	R	N51W	23N	309	5	N
	290	20	R			312	8L	160	20	318	8	278	52.7	265.6	18.7															
79	217	20	R	205	20R			233	20	245	20	21.1	37.5	32	30.7	N58W	60S	280	35	S	N67W	40S	196	40	N	N83W	58S	116	26	D
80	254	5	L	288	40L			16	5	342	20	328.4	29.5	116.2	5.3	N26E	84W	20	50	R	N80E	87S	256	54	R	N83E	26S	131	23	N
	254	5	L			225	25L	16	5	45	25	328.4	29.5	349.9	2															
81	288	15	L	248	11L			342	15	22	11	291.6	19.3	333.4	22.4	N64E	63S	241	4	S	N12W	46E	147	21	D	N12E	73W	328	67	N
82	288	10	L	282	37L			342	10	348	37	290.5	24.2	120.4	1.6	N30E	88W	215	72	R	N68E	61S	243	5	S	N46E	47S	73	26	S
	288	10	L			247	4L	342	10	23	247	290.5	24.2	336.4	28.9															
83	193	8	R	184	11R			257	8	266	11	34.2	14.1	43.3	11.2	N48W	79W	310	17	S	N58W	65S	237	64	N	N64W	82S	124	44	D
84	215	4	R	208	22R			235	4	62	22	12.7	23.1	185	2.7	N85W	88N	88	73	R	N48W	63S	313	63	S	N80E	49S	232	27	D
85	283	9	R	298	16R			167	9	152	16	292.1	43.8	269.3	46.2	N2W	44E	174	4	D	N27E	61E	136	59	R	N44E	37E	63	15	S
86	225	3	R	203	15R			225	3	247	15	2.6	27.2	30.2	25.5	N60W	65S	295	2	S	N72E	42S	213	30	D	N80E	86S	88	64	N
87	313	9	R	332	14L			137	9	298	14	256.2	33.4	250.8	4.1	N18W	85E	11	82	R	N22E	39E	39	16	S	N46W	55E	317	14	D
88	48	20	L	82	21L			222	20	188	21	9.9	43.4	323.6	56.4	N54E	34S	229	3	D	N40W	45S	310	8	S	N58W	73S	273	56	N
	48	20	L			25	41L	222	20	245	41	9.9	43.4	50.6	45.9															
89	70	22	L	80	12L			200	22	190	12	343.2	54.6	324.5	47.3	N56E	43S	86	26	D	N78E	82S	192	81	R	N89W	44S	228	33	N
	70	22	L			230	20L	200	22	40	20	343.2	54.6	347.6	8.4															
90	110	14	L	126	14L			160	14	144	14	280.9	47	260.8	41.1	N8W	49E	12	24	D	N45E	30S	58	9	S	N26E	53E	164	41	N
	110	14	L			88	23L	160	14	182	23	280.9	47	313.6	59															
91	94	17	R	108	10R			356	17	342	10	306	18.9	290.5	24.2	N21E	66E	194	17	D	N9E	62E	182	13	D	N38E	86E	173	85	N

Location : STV-3
Rock Type : Bioclastic Limestone

Grains No.	C - Axis: Strike (IV)	C - Axis: Dip (NS)	C - Axis: R/L Dip Direct.	Calcite Twins: Ttwin plane (e1) IV	Ttwin plane (e1) NS	Ttwin plane (e2) IV	Ttwin plane (e2) NS	Ttwin plane (e3) IV	Ttwin plane (e3) NS	U-Stage Recalculate: C-axis Az	C-axis Plg	Twin Plane Az	Twin Plane Plg	Thin Section Rotation: C-axis Az	C-axis Plg	Twin Plane Az	Twin Plane Plg	Twin plane (e1): Twin Plane Az	Twin Plane Plg	Slip Direction Az	Slip Direction Plg	Shear Sense	Thin Section
1	342	9	L	14	18L					288	9	256	18	326.1	19.7	167.7	0.2	N78E	89E	250	40	S	XZ
2	288	47	L	334	38L					342	47	296	38	10	74	126.9	26.8	N36E	64N	337	60	R	
	288	47	L			284	16L			342	47	346	16	10	74	12.8	22.3						
3	348	50	R	8	31R					102	50	82	31	102.5	21.5	333	78.6	N64E	11S	106	9	R	
	348	50	R			310	40R			102	50	140	40	102.5	21.5	299.6	10.9						
4	327	49	L	350	17L					303	49	280	17	4.3	48.2	43.4	32.8	N48W	58S	288	33	S	
5	154	30	R	173	17R					296	30	277	17	341.6	37.4	307.8	9.4	N38E	81E	47	47	D	
	154	30	R			120	28R			296	30	330	28R	341.6	37.4	81.7	9.2						
6	258	4	L	237	7L					12	4	33	7	219.2	54.3	21.8	20.7	N68W	69E	227	68	R	
7	225	16	R	248	5R					225	16	202	5	193.1	21.5	47.6	21.2	N44W	69S	160	46	R	
8	232	21	L	257	4L					38	21	13	4	166.5	53.2	96.9	12.6	N6E	77W	201	50	R	
9	187	40	R	193	21R					263	40	257	21	6.6	18.7	137.2	4.8	N46E	85N	45	26	S	
10	218	22	R	223	10R					232	22	227	10	191.5	12.7	199.7	14.9	N7W	75N	295	20	S	
11	183	0	L	203	20L					87	0	67	20	151.8	2.4	271.9	16	N4E	74W	179	12	S	
12	158	34	L	187	38L					112	34	83	38	110.6	5.7	216.2	9.2	N54W	80N	125	8	R	
	158	34	L			138	1L			112	34	132	1	110.6	5.7	203.8	0.2						
13	242	44	R	212	32R					208	44	238	32	220.2	4.2	10.6	57.8	N80E	33S	229	27	R	
14	203	34	L	228	36L					67	34	42	36	132.5	36.8	167.5	16.9	N78E	73N	65	36	S	
15	228	40	R	254	40R					222	40	196	40	209.1	3	326	8.3	N48E	82S	225	5	S	
	228	40	R			186	22R			222	40	264	22	209.1	3	104.7	33.5						
16	171	7	R	191	38R					279	7	259	38	330	11.4	146.2	1.7	N56E	89N	53	70	S	
17	260	17	R	229	2R					190	17	221	2	228.4	34.2	111.3	27.1	N21E	62W	224	36	D	
	260	17	R			194	1R			190	17	256	1	228.4	34.2	22.3	14.4						
18	164	26	R	132	8R					286	26	318	8	342.6	27.7	12	38.9	N88W	51S	112	13	S	
	164	26	R			184	24R			286	26	266	24	342.6	27.7	308.1	0.9						
19	161	0	R	183	1R					289	0	267	1	318	14.9	90.5	18.1	N1E	72W	351	29	S	
20	164	13	L	186	14L					106	13	84	14	309.9	4.2	341.2	15	N70E	74S	75	14	S	
	164	13	L			138	13L			106	13	132	13	309.9	4.2	351.2	20.7						
21	153	24	L	138	18L					117	24	132	18	294.7	4.4	43.8	42	N80W	47W	303	11	S	
	153	24	L			184	12L			117	24	86	12	294.7	4.4	315.4	8.9						
22	182	0	L	244	1L					88	0	26	1	151.2	1.6	131.8	2.5	N42E	88N	42	4	D	
23	334	9	R	358	17R					116	9	92	17	306.3	14.2	350.3	20	N81E	70S	80	2	S	
24	306	0	R	278	14R					144	0	172	14	289.7	39.6	26.9	42.8	N62W	47S	271	25	S	
	306	0	R			320	4R			144	0	130	4	289.7	39.6	145.6	29.1						
25	274	12	R	252	12R					176	12	198	12	245.1	39.9	292.3	5.8	N22E	85E	197	45	S	
27	319	0	R	298	1R					131	0	152	1	301.8	31.1	33.4	29.7	N56W	60S	289	26	S	
	319	0	R			338	4R			131	0	112	4	301.8	31.1	113.5	30.7						
28	256	42	L	243	15L					14	42	27	15	125.1	78.6	158	22	N68E	68N	358	67	R	
30	248	18	L	224	22L					22	18	46	22	190	62.3	138.6	5	N48W	85N	243	66	R	
31	208	12	L	196	10L					62	12	74	10	157.8	29.3	149.9	12.8	N60E	78N	269	66	D	
32	174	0	L	198	5L					96	0	72	5	326.3	4.7	108.4	35.3	N18E	55W	352	33	S	

Twin plane (e2): Twin-untwin Plane Az	Twin-untwin Plane Plg	Slip Direction Az	Slip Direction Plg	Shear Sense
N64E	44S	133	43	N
N78W	68S	193	96	R
N30E	80E	46	59	D
N75E	17S	193	16	N
N8W	81W	344	37	S
N41W	72W	199	49	S
N34W	23E	1	14	N
N68W	81S	133	67	R
N45W	72E	330	38	D
N85W	72N	80	40	D
N62W	56S	130	21	D
N66W	89N	114	5	S
N21E	77W	16	1	S
N30E	84W	319	18	N
N14E	57W	200	8	D
N32E	18W	318	24	N
N48W	75N	331	53	R
N38E	89E	39	41	D
N82W	75N	285	26	D
N82S	75S	84	14	S
N47E	82E	47	9	S
N70E	73S	97	57	N
N3E	50E	160	20	D
N58E	60N	278	30	S
N27W	23E	68	23	N
N24E	60W	309	59	R
N8E	46E	121	46	R
N24W	83E	143	64	S
N89E	61N	87	7	S
N72W	85N	289	10	D

Twin plane (e3): Twin-untwin Plane Az	Twin-untwin Plane Plg	Slip Direction Az	Slip Direction Plg	Shear Sense
N29E	82W	33	26	D
N12W	65E	46	62	D
N38E	40W	256	28	N
N70E	70S	99	53	D
N72W	78S	279	42	S
N5E	51W	232	41	D
N50E	86W	231	23	S
N40E	36E	158	34	N
N58W	20S	180	18	N
79W	85N	299	74	R
N81E	79N	327	25	N
N65W	44N	102	15	D
N46E	46N	57	13	S
N14E	78W	207	46	D
N12W	49W	190	24	D
N28W	68E	164	29	D
N18E	72E	187	27	S
N45E	53E	216	11	D
N40E	18E	140	19	D
N14E	67E	179	27	D
N12E	69E	171	41	N
N64E	70N	316	69	N
N15E	64E	328	60	N
N65W	58N	312	28	D
N22E	87E	295	47	R
N33E	58E	45	19	D
N43E	77E	201	59	D
N48E	84N	242	66	D
N56E	47N	20	30	N
N18W	4E	147	2	N

Continued

33	204	18	L	178	15L			66	18	92	15	260.2	26.5	264.5	51.4	N5W	38E	131	29	R	N34W	74E	335	27	D	N11E	81E	139	24	S	YZ
34	297	19	L	315	5L			333	19	315	5	99.2	59	95.8	81.4	N8E	9W	283	9	N	N18W	45W	204	33	D	N35E	44W	355	33	S	
35	58	40	R	32	19R			32	40	58	19	100.1	4.6	260.1	18.8	N10W	72E	153	40	R	N39E	88E	39	14	N	N2W	59W	311	51	N	
36	74	25	L	46	24R			196	25	44	24	33.3	19.8	264.1	5.5	N7W	87E	356	25	R	N87W	17S	219	15	N	N83E	71N	67	38	N	
37	101	10	R	123	4R			349	10	327	4	75	48	72.1	70.6	N18W	21W	257	19	N	N37W	55W	173	37	D	N52W	56W	340	37	S	
38	55	5	R	37	12R			35	5	53	12	65	3	252.4	14.6	N18W	75E	9	60	R	N14W	73W	186	49	N	N43W	83W	316	18	D	
39	131	0	R	108	4R			319	0	342	4	60	79	67.1	55.8	N24W	34W	255	36	R						N78E	19N	12	18	N	
	131	0	R			134	20L	319	0	136	20	60	79	350.8	68.5						N82E	22S	136	19	R						
40	98	14	R	74	48R			352	14	16	48	79.8	44.3	110.2	14.5	N20E	75W	359	35	R	N35E	8W	252	5	N	N52W	67W	151	41	D	
41	116	11	L	152	8R			154	11	298	8	36.1	61.9	201.2	77.2	N68W	12N	30	14	R	N83E	58S	125	46	R	N16W	61W	304	51	S	
42	77	40	L	81	4L			193	40	189	4	17.2	18.9	55.4	29	N36W	60W	151	11	S						N82E	55S	240	16	D	
	77	40	L			108	47L	193	40	162	47	17.2	18.9	357.5	34.4						N88E	56S	254	31	D						
43	56	0	L	80	25L			214	0	190	25	60	4	32.2	25.2	N58W	64S	287	29	D						N58W	64W	216	64	N	
	56	0	L			33	15L	214	0	57	15	60	4	255.8	18.4						N14W	72E	6	48	R						
44	73	16	L	81	4L			197	16	189	4	42.9	20.1	55.4	29	N35W	40W	204	27	N						N65W	65S	291	19	D	
	73	16	L			107	43L	197	16	163	43	42.9	20.1	1.6	36.8						N88W	53S	263	10	D						
45	237	13	L	213	1L			33	13	57	1	73.1	4.9	241.1	19	N28W	70E	123	54	R						N8E	84W	188	2	N	
	237	13	L			260	13L	33	13	10	13	73.1	4.9	74.6	27.3						N17W	63W	250	62	N						
46	260	38	L	288	43R			10	38	162	43	101.5	21.7	1	37.3	N89W	53S	107	19	D						N58E	49N	248	11	S	
	260	38	L			263	6R	10	38	187	6	101.5	21.7	53	30.8						N36W	60S	144	1	D						
47	310	8	L	298	4R			320	8	152	4	94.1	75.7	50.2	65.7	N40W	25W	187	21	D						N28E	29W	319	28	R	
	310	8	L			328	6L	320	8	302	6	94.1	75.7	194.7	81.5						N75W	9N	63	6	D						
48	314	0	L	316	10L			316	0	314	10	60	82	119.2	78.3	N30E	11W	342	9	R						N62E	7S	104	6	N	
	314	0	L			286	4R	316	0	164	4	60	82	53.2	53.8						N38W	37W	230	38	R						
49	256	44	L	228	14L			14	44	42	14	106.5	17	254	3.9	N16W	86E	162	33	R	N48E	85E	52	35	D	N28E	34W	345	20	N	
50	283	30	L	304	13L			347	30	326	13	102.6	42.3	96.7	67.9	N6E	23W	288	23	N	N9W	66W	195	44	D	N39E	62W	19	34	S	
51	78	0	L	94	8L			192	0	176	8	60	26	49.3	41.5	N40W	48W	275	40	D						N40W	79W	158	41	D	
	78	0	L			50	14L	192	0	220	14	60	26	226	2						N45W	88N	134	67	R						
52	83	24	R	88	9R			7	24	2	9	87.4	28.1	71.1	35.5	N18W	54W	234	22	D						N6W	78W	250	78	R	
	83	24	R			38	12L	7	24	52	12	87.4	28.1	252.4	13.7						N28W	77E	18	66	R						
53	238	24	L	198	28L			32	24	252	28	84.1	5.5	207.3	29.6	N64W	60N	106	20	S	N56E	70N	61	16	D	N20W	20W	267	71	N	
54	83	35	R	80	2R			7	35	10	2	99.2	24.9	62.3	28	N26W	62W	153	4	D	N18E	82E	45	74	N	N41E	46W	240	19	S	
55	93	26	R	129	17L			357	26	141	17	92.9	36.1	6.3	68.7	N85W	21S	108	4	D	N24W	77E	132	60	S	N4W	71E	49	31	S	
56	30	14	R	270	6L			60	14	0	6	255.1	21.3	67.6	37.8	N23W	53W	261	52	R	N52E	61S	228	6	S	N80W	48N	279	1	D	
57	158	16	R	133	14R			292	16	317	14	193.8	67.5	117.9	73.4	N28E	17W	233	8	D						N85W	46N	348	47	D	
	158	16	R			176	34R	292	16	274	34	193.8	67.5	189.6	43.4						N80W	46N	360	47	R						
58	203	17	R	188	13L			247	17	82	13	220.7	27.7	257.8	42.6	N12W	47E	357	11	S	N87W	53N	90	4	S	N47W	83W	182	82	N	
59	284	14	L	307	1L			346	14	323	1	82.1	49.9	63.9	75	N26W	15W	273	15	D	N32W	61W	181	49	D	N24E	56W	357	34	S	
60	160	20	R	178	11L			290	20	92	1	190.4	63.3	258.3	52.6	N12W	38E	131	25	S	N6E	25W	225	16	D	N89E	63N	67	39	R	
61	58	0	R	35	11R			32	0	55	1	60	6	251.4	16.7	N18E	74W	7	57	R	N16W	64W	195	47	N	N57W	83W	305	2	D	
62	89	10	R	93	17R			1	10	357	17	242.1	62	232	68.8	N37W	N23E	95	17	R	N40W	21E	89	16	D	N35E	35E	20	30	R	XY
63	123	15	L	153	9L			327	15	117	9	179.3	52.9	174.4	14.9	N85W	75N	331	74	R	N28W	40E	130	37	S	N18E	32W	217	10	N	
64	154	24	L	183	16L			116	24	87	16	184.6	3.7	341	12.1	N72E	78S	243	33	S						N60W	79S	124	25	N	
	154	24	L			130	5L	116	24	140	5	184.6	3.7	190.1	33.2						N80E	56N	351	56	N						
65	277	18	R	242	36R			173	18	208	36	232	33.6	262.8	11.6	N88W	78S	261	46	S	N36W	21E	51	22	N	N70W	78N	301	41	D	
66	148	14	L	150	28R			122	14	300	28	181.6	14.8	142.7	39.6	N52E	50N	36	20	D	N84E	62S	203	58	N						

Continued

																										N44W	69E	317	5	S
67	88	0	R	104	12R			2	0	346	12	243.2	52	210.6	61.2	N60W	29N	110	5	D										
	88	0	R			62	9R	2	0	28	9	243.2	52	288.3	51.6						N18E	28W	198	1	S					
																										N6E	36E	184	2	S
68	83	17	R	109	34R			7	17	341	34	258.2	68.1	158.8	74.1	N70E	16N	288	10	R										
																					N28W	50E	43	49	R					
																										N48E	35S	184	26	S
69	98	12	L	120	6R			172	12	330	6	229.8	39.4	192	48	N78E	41N	98	4	D										
	98	12	L			78	4R	172	12	12	4	229.8	39.4	260.8	54.3						N9E	35E	8	13	S					
																										N3W	41E	359	2	N
70	273	46	L	318	50L			177	46	312	50	237.9	6	114.6	54.2	N24E	36W	231	18	D										
																					N64W	31E	68	24	N					
																										N75W	54S	262	28	N
71	48	13	R	82	40R			42	13	8	40	307.6	45.2	350.3	83.5	N79E	7S	122	5	N										
																					N3E	68E	19	42	D					
																										N70E	75S	231	52	R
72	217	7	L	204	10R			53	7	246	10	311.1	33.1	306.9	12	N38E	78E	90	75	R										
																					N67E	52S	70	4	D					
																										N18E	45E	181	17	S
73	234	8	L	217	3R			36	8	233	3	296.6	45.8	302.7	26.2	N34E	64E	148	61	N										
	234	8	L			260	8L	36	8	10	8	296.6	45.8	259.3	58.7						N12E	32E	159	6	D					
																										N52E	33S	72	14	S
74	268	18	L	308	40L			2	18	322	40	245.5	69.9	134	60.6	N44E	30N	280	26	R										
																					N37W	62E	41	61	R					
																										N56E	42S	186	35	S
75	43	43	L	37	20R			227	43	53	20	92.3	1.5	324	41	N54E	46S	73	20	D										
	43	43	L			94	37R	227	43	356	37	92.3	1.5	166.3	86.7						N78E	4N	272	1	N					
																										N34E	31W	261	25	N
76	103	38	L	118	14L			167	38	152	14	229.5	13.1	207.6	31.7	N62W	59N	96	31	D										
																					N47W	77W	261	68	N					
																										N13W	71E	349	9	S
77	86	46	R	123	40R			364	46	327	40	40.9	81.5	135.1	64.4	N45E	25N	336	25	R										
																					N19E	24E	86	23	D					
																										N57W	38S	210	37	R
78	230	9	R	193	35R			220	9	257	35	287.1	30	114.7	12	N25E	77W	269	76	R										
																					N78E	40S	73	6	S					
																										N34W	56E	332	8	D
79	158	43	L	188	33L			112	43	82	33	16.2	11.8	353.3	25.3	N74W	65S	249	70	D										
	158	43	L			138	22L	112	43	132	22	16.2	11.8	194.5	15						N75W	74N	25	75	R					
																										N76W	75N	41	74	N
80	276	0	L	297	17L			354	0	333	17	230.3	51.6	184.1	58.4	N75W	32N	279	3	D										
	276	0	L			254	17L	354	0	16	17	230.3	51.6	278.2	64.7						N8E	25E	12	2	S					
																										N5E	35E	178	6	S
81	305	30	R	302	15R			145	30	148	15	209.1	14.5	204.1	29.1	N65W	60N	51	59	N										
	305	30	R			258	40R	145	30	192	40	209.1	14.5	249.3	11.2						N21W	79E	157	10	S					
																										N88W	43N	55	30	D
82	300	0	L	275	4L			330	0	355	4	196.8	43	231.1	55.7	N38W	34S	331	7	S										
	300	0	L			324	5L	330	0	306	5	196.8	43	169.9	31						N80E	58N	182	33	D					
																										N83E	44N	255	3	D
83	170	10	L	198	22L			100	10	72	22	164	1.6	337.7	27.2	N68W	63S	185	60	R										
																					N78W	79N	284	16	S					
																										N54E	70N	40	33	D
84	256	43	R	238	22R			194	43	212	22	250.3	8	272.2	22.9	N4E	68E	14	29	S										
																					N46W	76E	132	12	D					
																										N18W	72W	230	72	N
85	114	50	L	160	33L			156	50	110	33	44.8	0.5	7.5	6.3	N84W	84S	277	6	D										
																					N32W	54E	21	47	N					
																										N16W	65E	359	31	N
86	294	0	L	304	6L			336	0	326	6	204.1	46	187.4	45.6	N74W	45N	284	7	D										
																					N58W	54N	73	46	S					
																										N54W	34N	63	30	N
87	136	10	L	156	16L			134	10	114	16	188.2	25.6	177.5	8	N87E	82N	281	60	R										
																					N60W	66N	117	7	S					
																										N85E	48N	269	6	N
88	62	24	L	46	29L			208	24	224	29	267.7	22.7	278.3	11.4	N8W	79W	173	52	R										
																					N3E	54E	60	48	N					
																										N16W	71E	349	15	D
89	32	4	R	50	4R			58	4	40	4	312.3	27.4	297.1	40.2	N64W	49N	312	27	S										
																					N36E	80E	66	71	D					
																										N64E	62S	242	3	S
90	69	7	L	53	6L			201	7	217	6	268.1	40.9	286.3	34.2	N76W	55N	80	23	D										
																					N8W	34E	104	32	N					
																										N15W	60E	19	46	D
91	80	18	R	118	47R			10	18	332	47	266.4	68.2	117.3	67.6	N26E	22W	278	22	S										
																					N35W	61E	20	58	D					
																										N54E	51S	184	44	R
92	80	18	R			60	8R	10	18	30	8	266.4	68.2	289.8	49.6	N20E	41E	141	31	R										
																					N68W	7S	250	5	N					
																										N45W	35N	1	28	D

Location : STV-4
Rock Type : Calcareous Mudstone

Grains No.	C - Axis Strike (IV)	C - Axis Dip (NS)	C - Axis R/L Dip Direct.	Calcite Twins Ttwin plane (e1) IV	Calcite Twins Ttwin plane (e1) NS	Calcite Twins Ttwin plane (e2) IV	Calcite Twins Ttwin plane (e2) NS	Calcite Twins Ttwin plane (e3) IV	Calcite Twins Ttwin plane (e3) NS	U-Stage Recalculate C-axis Az	U-Stage Recalculate C-axis Plg	U-Stage Recalculate Twin Plane Az	U-Stage Recalculate Twin Plane Plg	Thin Section Rotation C-axis Az	Thin Section Rotation C-axis Plg	Thin Section Rotation Twin Plane Az	Thin Section Rotation Twin Plane Plg	Twin plane (e1) Twin Plane Az	Twin plane (e1) Twin Plane Plg	Twin plane (e1) Slip Direction Az	Twin plane (e1) Slip Direction Plg	Twin plane (e1) Shear Sense	Twin plane (e2) Twin-untwin Plane Az	Twin plane (e2) Twin-untwin Plane Plg	Twin plane (e2) Slip Direction Az	Twin plane (e2) Slip Direction Plg	Twin plane (e2) Shear Sense	Twin plane (e3) Twin-untwin Plane Az	Twin plane (e3) Twin-untwin Plane Plg	Twin plane (e3) Slip Direction Az	Twin plane (e3) Slip Direction Plg	Twin plane (e3) Shear Sense	Thin Section
1	137	24	L	143	8R					133	24	307	8	76.8	12.4	49.3	33.1	N40W	56W	298	29	D											XZ
	137	24	L			108	14L			133	24	162	14	76.8	12.4	98.9	33.4						N8E	56E	213	33	S						
	137	24	L					154	40L	133	24	116	40	76.8	12.4	255.8	9											N15E	81E	101	80	R	
2	294	12	R	307	10L					156	12	323	10	91.5	33.4	62.2	45.6	N28W	45W	319	14	D											
	294	12	R			313	50R			156	12	137	50	91.5	33.4	273.7	7.6						N4E	82E	70	82	R						
	294	12	R					261	9R	336	12	189	9	76.2	54.9	131.7	40.3											N1E	49E	77	49	R	
3	83	44	R	65	22R					7	44	205	22	249.6	83.5	145.3	23.8	N55E	67W	306	66	R											
	83	44	R			116	39R			7	44	334	39	249.6	83.5	24.4	70						N65W	20S	227	18	R						
																												N3E	33E	97	34	N	
4	164	17	R	178	4R					286	17	272	4	26.7	22.9	28.2	4.1	N62W	85S	254	84	R											
	164	17	R			203	53R			286	17	247	53	26.7	22.9	335.9	19.5						N65E	61S	67	3	D						
																												N88E	59S	263	8	D	
5	299	0	R	274	0R					151	0	176	0	79.2	42.1	113.8	49.8	N22E	41W	205	2	S											
	299	0	R			307	23R			151	0	143	23	79.2	42.1	84.3	18.2						N7E	71E	288	71	R						
																												N45W	39W	312	4	D	
6	314	23	R	310	21R					136	23	140	21	78.6	14.9	201.1	43.6	N70W	46N	86	24	N											
																							N64E	85S	65	16	R						
																												N75E	20S	83	3	S	
7	57	0	R	72	23R					33	0	18	23	165.3	40	167.2	67.2	N78E	23N	345	25	N											
	57	0	R			33	12L			33	0	237	12	165.3	40	178.6	15.9						N88E	75N	51	65	N						
																												N80W	66N	77	41	R	
8	216	0	L	235	12L					54	0	35	12	185	26.8	177.7	48.3	N87E	42N	22	40	N											
	216	0	L			183	4L			54	0	87	4	185	26.8	211.1	4.9						N58E	86N	116	44	N						
	216	0	L					214	33R	54	0	56	33	185	26.8	219.4	45.2											N52W	44N	325	17	S	
9	194	30	R	204	17R					256	30	246	17	358.3	9.3	181.5	6.3	N88W	81N	308	80	R											
	194	30	R			158	34R			256	30	292	34	358.3	9.3	13.5	36.7						N76W	53S	147	44	N						
																												N18E	60W	14	3	N	
10	173	29	L	204	22L					97	29	66	22	236.9	13.3	213	32	N58W	58N	103	29	D											
	173	29	L			154	41L			97	29	116	41	236.9	13.3	256.5	9.7						N14W	81E	163	16	S						
	173	29	L					168	1L	97	29	102	1	236.9	13.3	38.5	8.5											N56W	82S	297	42	R	
11	89	47	R	118	29R					1	47	332	29	294.6	83	47	64.6	N43W	25S	242	26	R											
	89	47	R			69	14R			1	47	21	14	294.6	83	161.3	58.1						N28W	63E	47	63	R						
																												N27E	36E	117	37	R	
12	68	50	R	70	21L					22	50	200	21	250.3	71.7	140.9	26.2	N50E	64N	311	64	R											
	68	50	R			94	1R			22	50	356	1	250.3	71.7	113.7	50.8						N24E	40S	272	59	R						
																												N60E	37S	187	31	N	
13	54	12	L	63	40L					216	12	207	40	160.7	28.2	140.5	6.3	N50E	83N	237	50	D											
	54	12	L			0	42L			216	12	270	42	160.7	28.2	355.4	25.5						N85E	66S	142	61	R						
																												N58E	33N	359	31	R	
14	114	36	R	143	11R					336	36	307	11	34.4	70.8	46.6	35.1	N54W	54S	238	55	R											
	114	36	R			94	40R			336	36	356	40	34.4	70.8	28.1	86.9						N58W	3S	217	4	N						
																												N51E	35S	101	28	N	
15	198	9	R	204	47R					252	9	246	47	191.4	7.7	340.1	14.9	N70E	76S	241	31	R											
	198	9	R			168	7R			252	9	282	7	191.4	7.7	32.3	13.7						N56W	77S	134	42	R						
																												N64E	88S	253	19	S	
16	278	2	R	334	28L					172	2	296	28	108.2	47.4	22.1	36.8	N68W	53S	137	31	D											
	278	2	R			18	50L			172	2	252	50	108.2	47.4	340.5	19.8						N70E	71S	97	52	R						
																												N52W	83N	120	51	S	
17	297	7	L	284	14R					333	7	166	14	76.6	49.1	103.5	34.4	N14E	55W	341	98	S											
	297	7	L			324	5L			333	7	306	5	76.6	49.1	51	30.3						N38W	60S	174	45	N						
																												N28W	14W	261	15	N	
18	26	45	L	5	16L					244	45	265	16	340.6	12.5	14.5	6.5	N77W	84S	183	15	S											
	26	45	L			60	24L			244	45	210	24	340.6	12.5	149.1	20.2						N70E	69N	20	61	R						
																												N54E	88S	131	52	N	
19	208	38	L	235	39L					62	38	35	39	228.6	42.8	219.4	63.1	N52W	26S	60	25	N											
	208	38	L			172	34L			62	38	98	34	228.6	42.8	241.5	15.8						N28E	75E	114	66	N						
																												N15W	57E	145	28	S	
20	132	18	L	146	8R					138	18	304	8	77.4	20.1	46.9	30.9	N45W	69S	311	11	D											
																							N10W	81E	57	80	N						
																												N52E	55S	210	17	S	
21	3	37	R	28	28R					87	37	62	28	238.5	24.7	216.8	38.3	N54W	51N	107	24	D											
	3	37	R			354	4R			87	37	96	4	238.5	24.7	36.9	2						N54W	88S	304	52	R						
	3	37	R					326	43R	87	37	124	43	238.5	24.7	262.3	7.2											N8W	83E	166	42	S	
22	205	50	L	242	35L					65	50	28	35	245.2	44.5	206.3	67.3	N64W	22N	90	10	D											
	205	50	L			180	33L			65	50	90	33	245.2	44.5	236.4	20.5						N34W	70E	25	66	R						
																												N27W	53W	177	22	S	
23	272	46	R	278	17R					178	46	172	17	118.6	4	110.9	32.6	N20W	58W	321	55	N											
	272	46	R			227	44R			178	46	223	44	118.6	4	329.4	2.5						N58E	80W	59	13	R						
																												N57E	88S	58	17	N	
24	227	51	R	248	19R					223	51	202	19	325.7	8.5	143.6	27.5	N54E	62N	336	63	R											
	227	51	R			214	52R			223	51	236	52	325.7	8.5	331.7	14.1						N32E	76S	78	49	S						
	227	51	R					201	8R	223	51	249	8	325.7	8.5	190.1	10.5											N80W	80N	284	21	D	
25	144	0	R	122	20R					306	0	328	20	55	26.8	56.6	56.1	N34W	33W	235	34	R											
	144	0	R			98	1R			306	0	352	1	55	26.8	107.4	50.3						N17E	40E	206	7	S						
																												N10W	81W	343	40	S	
26	68	0	R	74	10R					22	0	16	10	152.2	45.3	149.7	56.8	N60E	33N	343	34	N											
	68	0	R			35	9R			22	0	55	9	152.2	45.3	193.2	32.3						N76W	57N	84	28	S						
																												N42E	75N	248	60	D	
27	74	0	R	86	15R					16	0	4	15	144	47.4	129.1	64.7	N40E	25N	344	22	N											
	74	0	R			52	4R			16	0	38	4	144	47.4	173.7	40.3						N46W	49N	65	20	S						
																												N87E	52N	167	24	S	
28	104	18	L	118	5L					166	18	152	5	104.5	30.5	83.5	38.1	N8W	51W	344	12	D											
																							N14E	80W	289	80	R						
																												N38E	51W	228	32	S	
29	102	26	R	84	8R					348	26	6	8	80.7	72.8	131.1	57.6	N42E	32N	352	272	R											
	102	26	R			123	47R			348	26	327	47	80.7	72.8	2.6	65.3						N88W	24S	138	19	R						
																												N42W	45W	205	43	R	
30	339	17	R	6	3R					111	17	84	3	56.4	4.3	208.4	6.5	N62W	84N	116	18	R											
	339	17	R			327	4R			111	17	123	4	56.4	4.3	55.7	21.8						N34W	69W	246	69	N						
																												N18W	86E	345	41	D	

Continued

31	304	24	R	327	8R					146	24	303	8	208.7	40.7	160	33.2	N70W	55N	264	20	D											YZ
	304	24	R			283	4R			146	24	167	4	208.7	40.7	204.6	12.5						N65W	78N	343	75	R	N62E	36E	69	11	D	
32	97	0	R	120	15R					353	0	330	15	205.5	5.4	178.7	11.8	N88E	79N	86	8	D											
	97	0	R			78	20R			353	0	12	20	205.5	5.4	21.6	21.7						N69W	69S	231	66	R	N43W	66N	336	37	N	
33	12	12	L	355	10L					258	12	275	10	105.3	36.8	126.4	39.8	N35E	50N	219	3	S											
																							N10W	N35W	319	21	N	N47E	53W	44	6	S	
34	293	15	R	304	2R					157	15	146	2	207.1	27.1	188.1	26.8	N82W	63N	279	3	D											
	293	15	R			263	9R			157	15	187	9	207.1	27.1	221.4	0.5						N49W	89N	130	65	R	N65W	N84E	268	13	D	
35	127	11	L	138	5R					143	11	312	5	193.4	35.1	170.8	30.8	N80E	59N	272	21	D											
																							N64W	70W	89	52	S	N60W	31N	352	26	N	
36	314	38	L	324	8L					316	38	306	8	154.5	1.3	163.2	31.6	N74E	59N	314	15	N											
																							N36E	82S	212	18	S	N88E	70S	102	35	D	
37	352	24	L	354	43L					278	24	276	43	128.1	25.6	124.4	6.9	N34E	84E	240	76	R											
																							N76E	60N	129	4	S	N20E	52W	359	25	D	
38	292	8	L	294	9R					338	8	156	9	189.4	11.3	201.2	24.1	N68W	65N	316	43	S											
	292	8	L			308	42L			338	8	322	42	189.4	11.3	336	4.6						N65E	86S	244	25	S						
	292	8	L					259	27L	338	8	371	27	189.4	11.3	14.8	25											N77W	64S	172	63	R	
39	208	31	R	204	34R					242	31	246	34	95.5	14.4	99.8	12.7	N8E	77W	2	30	S											
	208	31	R			263	36R			242	31	187	36	95.5	14.4	242.6	17.6						N28W	73E	139	38	R	N12W	34W	287	37	N	
40	146	5	L	173	3L					124	5	97	3	170.2	43.5	131.5	52.5	N42E	38N	38	3	D											
	146	5	L			132	8R			124	5	318	8	170.2	43.5	174.1	24.7						N85E	65N	19	64	R	N44E	44N	227	25	D	
41	128	8	L	136	8R					142	8	314	8	189.9	33.8	170.7	27.1	N70E	61N	273	24	D											
																							N65W	32N	355	30	N	N70W	73N	78	63	S	
42	274	11	R	282	4L					176	11	348	4	216	10	199.1	6.6	N72W	83N	290	16	D											
	274	11	R			242	19R			176	11	208	19	216	10	62.7	7.6						N25W	83W	156	30	R	N48W	64N	4	57	N	
43	261	5	R	234	27R					189	5	216	27	39.7	3.6	73.5	6.3	N18W	83W	163	3	S											
																							N65W	74S	258	37	D	N65W	61N	73	53	S	
44	234	1	R	254	24R					216	1	196	24	55.8	26.1	238.4	3.9	N32W	87E	355	83	R											
	234	1	R			207	3R			216	1	243	3	55.8	26.1	83.4	40.4						N8W	50W	187	16	S	N32W	87N	349	49	N	
45	244	14	R	249	15L					206	14	21	15	57.8	9.8	31.6	25.6	N58W	64N	288	26	D											
	244	14	R			202	8L			206	14	68	8	57.8	9.8	82.6	52.5						N8W	37W	221	31	R	N6W	70W	180	15	S	
46	248	18	R	278	26R					202	18	172	26	57.8	4.3	226	22.2	N45W	67E	98	56	R											
																							N44W	68N	98	58	N	N52W	64S	278	45	D	
47	19	40	L	27	20L					251	40	243	20	105.4	8.1	92	25	N4W	64E	347	30	S											
																							N8E	79S	169	60	N	N37E	79W	217	2	S	
48	84	15	L	113	30L					186	15	157	30	225.3	5.1	221.7	35.5	N50W	55N	55	54	R											
	84	15	L			68	11L			186	15	202	11	225.3	5.1	52.8	9.2						N38W	80W	155	55	R	N18W	82W	166	27	D	
49	196	32	R	164	13L					254	32	106	13	105.9	16.5	152	59.5	N62E	30N	271	16	S											
																							N40W	80W	143	13	N	N47E	61S	80	44	D	
50	78	34	L	68	13L					192	34	202	13	243.6	13.2	54.3	7.7	N37W	83E	312	61	R											
	78	34	L			113	28L			192	34	157	28	243.6	13.2	219.6	34.5						N50W	55N	107	30	D	N3E	71W	202	44	N	
51	292	14	L	311	6R					158	14	139	6	207	25.7	185.7	34.5	N75W	56N	84	15	D											
	292	14	L			266	24R			158	14	184	24	207	25.7	231.2	12.3						N38W	78N	134	32	S	N42W	56N	327	15	S	
52	309	14	L	333	8L					321	14	297	8	172.6	18.2	153.7	35.9	N64W	55N	38	31	D											
	309	14	L			286	3L			321	14	344	3	172.6	18.2	197.3	10.2						N74W	79N	102	25	S	N75E	84S	238	70	N	
53	293	42	L	311	17L					337	42	319	17	344.3	12	168.9	17	N68E	72N	320	17	R											
																							N80W	61S	114	26	S	N46E	69S	220	10	D	
54	106	5	R	87	7L					344	5	183	7	195.8	8.8	217.3	2.2	N54W	87N	126	15	S											
	106	5	R			132	23L			344	5	138	23	195.8	8.8	202	46.3						N68W	44N	7	43	R	N89E	82S	264	42	N	
55	72	15	L	74	6R					198	15	196	6	53	3.6	45	8.2	N46W	81S	311	31	D											
	72	15	L			92	40L			198	15	178	40	53	3.6	241.8	25.7						N28W	65N	29	61	R						
	72	15	L					43	21L	198	15	227	21	53	3.6	78.3	17											N12W	72W	177	24	S	
56	134	9	L	113	1L					136	9	157	1	185.7	38.7	195.5	18.1	N75W	71N	66	64	R											
	134	9	L			158	15L			136	9	112	15	185.7	38.7	163.8	58.5						N75E	31N	35	22	R	N52W	58N	118	18	S	
57	65	44	L	80	14L					205	44	190	14	258.1	12.3	227.1	1.5	N44W	88W	319	17	D											
	65	44	L			34	37L			205	44	236	37	258.1	12.3	93.3	7						N5E	83E	193	54	R	N3W	47E	62	44	N	
58	86	33	L	113	26L					184	33	157	26	238.6	17.8	217.5	33.4	N54W	57N	107	26	S											
	86	33	L			72	13L			184	33	198	13	238.6	17.8	51.5	4.9						N38W	86W	313	67	R	N38W	82W	299	73	N	
59	304	8	R	334	18R					146	8	116	18	193.1	30.9	173.2	58.6	N84E	31N	24	29	R											
	304	8	R			296	7L			146	8	334	7	193.1	30.9	187.3	14.8						N84W	76N	318	70	R	N38E	46E	60	27	D	
60	93	30	L	113	36L					177	30	157	36	232.2	20.8	228.4	38.3	N42W	51N	67	51	R											
																							N52W	81N	316	38	D	N3W	53E	9	14	S	
61	80	23	L	63	6L					190	23	207	6	280.2	61.9	263.6	40.5	N8W	50E	47	44	R											XY
	80	23	L			106	9L			190	23	164	9	280.2	61.9	323.5	46.9						N54E	44S	196	30	R	N63W	13E	307	3	N	
62	122	43	L	96	46L					148	43	174	46	24.6	67.1	347.4	84.3	N77E	6S	215	4	R											
	122	43	L			156	42L			148	43	114	42	24.6	67.1	46.3	45						N45W	45W	279	31	S	N25W	40W	286	34	S	
63	299	20	R	295	9R					151	20	155	9	348	52.2	335.5	44	N65E	46S	99	30	D											
	299	20	R			343	36R			151	20	107	36	348	52.2	44.3	37						N46W	53S	289	30	S	N71E	25S	178	25	N	
64	271	43	R	234	49R					179	43	216	49	306	83	198.5	66.8	N72W	23S	3	24	R											
	271	43	R			301	43R			179	43	149	43	306	83	23.7	67.7						N78W	23S	225	22	R						

Continued

65	198	19	L	222	31L			72	19	48	31	55.7	3.5	80.4	1.5	N10E	88W	350	4	S	N47W	63W	273	52	D	N42W	24W	243	27	N	XY
66	301	12	R	278	6R			149	12	172	6	344.7	44.3	311.4	45.5	N40E	45E	49	8	D	N82E	71S	197	69	R	N58W	72N	312	4	N	
67	113	0	R	94	26R			517	0	536	26	329	36.3	308.8	65.8	N38E	25S	165	20	N	N40E	73E	60	49	D	N68W	32S	123	9	N	
68	118	30	L	113	15L			152	30	157	15	357	61	336.2	50.3	N64W	39S	108	29	D	N42W	9W	162	5	N	N88E	66S	255	27	S	
	118	30	L			104	52L	152	30	166	52	357	61	48.2	81																
69	58	43	R	89	28R			32	43	1	28	97	7.1	299.1	12	N28E	77W	40	41	R	N14W	77W	344	16	D	N874E	13S	174	14	N	
	58	43	R			32	40R	32	43	58	40	97	7.1	78.1	13.4																
70	51	42	R	76	34R			39	42	14	34	91.8	8.1	288.4	5.1	N18W	85W	22	39	R	N7W	72W	335	29	D	N8W	88E	160	21	S	
	51	42	R			25	43R	39	42	65	43	91.8	8.1	75.5	18.9																
71	58	34	R	42	31R			32	34	48	31	273.9	1.3	80.4	1.5	N10W	88W	350	13	R	N34E	87E	32	6	S	N18E	75W	211	18	S	
	58	34	R			93	37R	32	34	357	37	273.9	1.3	302.4	3																
72	128	30	L	105	15L			142	30	165	15	9.3	55.3	324.5	52.9	N55S	37S	74	15	D	N84W	70S	181	70	R	N10E	69W	223	46	N	
	128	30	L			150	2L	142	30	120	2L	9.3	55.3	7.4	20.4																
73	207	47	R	203	37R			243	47	247	37	189	49.4	198.6	41.4	N72W	48N	67	38	S	N58W	17E	358	15	N	N28W	21W	331	2	N	
74	170	42	R	158	17R			280	42	292	17	174.1	25.4	2.5	0.4	N2E	89N	90	73	R	N68W	46N	313	21	S	N65E	53S	272	30	D	
	170	42	R			207	36R	280	42	243	36	174.1	25.4	202.4	43.3																
75	164	12	R	185	24R			286	12	265	24	10.1	0.8	197.6	21.3	N74W	69N	334	63	R	N78W	86S	109	67	N	N55E	63N	235	2	N	R
	164	12	R			163	9R	286	12	287	9	10.1	0.8	11.2	3.8																
76	125	48	R	103	3L			325	48	167	3	143.2	12.5	317.5	41.7	N48E	49S	148	48	R	N85E	84S	87	27	R	N12E	85W	256	10	D	
	125	48	R			148	17R	325	48	302	17	143.2	12.5	354.6	5.8																
77	103	24	L	73	43L			167	24	197	43	326	62.1	234.5	76.4	N37W	14E	351	6	R	N56E	44S	144	44	R	N1E	55W	353	11	D	
	103	24	L			108	9L	167	24	162	9	326	62.1	326.2	46.4																
78	56	10	L	75	4L			214	10	195	4	253	41.1	279.6	42.3	N8E	48E	185	5	S	N26W	80E	11	74	R	N75W	42S	249	29	S	
	56	10	L			33	13R	214	10	57	13	253	41.1	244	9.7																
79	309	43	L	348	34L			321	43	282	34	147.8	9	178.8	18.5	N78E	72N	271	11	S	N42E	89N	223	26	D	N16W	73E	23	69	N	
	309	43	L			286	40L	321	43	344	40	147.8	9	132.2	1.1																
80	254	48	L	219	47L			16	48	411	47	109.2	9	86.4	16.5	N8E	73W	352	17	D	N18E	42E	80	39	R	N54E	68S	173	65	N	
	288	42	R	263	8R	304	1R	162	42	187	8	4.1	75.2	289.7	47.6																
81	346	43	R	358	23R			104	43	92	23	53.1	39.5	43.8	18.7	N48W	71S	171	64	R	N88W	31E	265	10	D	N38E	65W	234	28	S	
	346	43	R			306	34R	104	43	144	34	53.1	39.5	12.4	59.3																
82	258	44	R	249	23R			192	44	201	23	241.7	79.9	261	58.4	N8E	31E	93	31	R	N82W	39E	348	38	R	N4E	53W	354	14	S	
	258	44	R			208	48R	192	44	242	48	241.7	79.9	188.1	50.5																
83	91	37	L	96	16L			179	37	174	16	303.5	77	310.3	55.7	N40E	35E	134	35	R	N54W	17N	255	14	S	N85E	23N	327	22	N	
84	75	22	L	99	3L			195	22	171	3	271.7	59.6	312.2	42.4	N42E	48E	187	33	S	N54E	48E	35	43	R	N45W	21N	7	16	N	
	75	22	L			56	10L	195	22	214	10	271.7	59.6	253	41.1																
85	245	0	R	235	16L			205	0	35	16	268.7	35.6	264.8	17.2	N75E	73N	266	36	S	N34E	50E	211	2	S	N24W	54E	23	46	N	
86	60	46	L	65	28L			210	46	205	28	209.7	69.7	249.8	60.9	N21W	30E	118	21	R	N85W	51N	322	46	D	N32W	40N	132	13	N	
	60	46	L			7	50L	210	46	263	50	209.7	69.7	175.9	39.6																
87	42	12	L	72	7L			228	12	198	7	236.8	35.4	274.6	44.4	N5E	46E	7	4	S	N75W	46N	108	8	D	N80W	37N	348	34	N	
88	143	28	R	173	26R			307	28	277	26	164.9	1	187.7	15.4	N74W	74N	286	26	S	N55W	86N	53	10	D	N34W	85N	44	80	N	R
	143	28	R			123	40R	307	28	327	40	164.9	1	144.7	4.6																
89	18	18	L	48	32L			252	18	222	32	211.7	25.2	224.1	54.2	N45W	35N	19	33	R	N85W	75N	283	25	D						
90	207	47	R	203	37R			243	47	247	37	189	49.4	198.6	41.4	N72W	48N	67	38	S	N57W	17N	353	13	N	N38W	88E	236	48	S	
																										N65E	53N	269	28	D	

Location : SBV-5
Rock Type : Calcareous Mudstone

Grains No.	C - Axis Strike (IV)	C - Axis Dip (NS)	C - Axis R/L Dip Direct.	Calcite Twins Ttwin plane (e1) IV	Ttwin plane (e1) NS	Ttwin plane (e2) IV	Ttwin plane (e2) NS	Ttwin plane (e3) IV	Ttwin plane (e3) NS	U-Stage Recalculate C-axis Az	C-axis Plg	Twin Plane Az	Twin Plane Plg	Thin Section Rotation C-axis Az	C-axis Plg	Twin Plane Az	Twin Plane Plg	Twin plane (e1) Twin Plane Az	Twin Plane Plg	Slip Direction Az	Slip Direction Plg	Shear Sense	Twin plane (e2) Twin-untwin Plane Az	Twin-untwin Plane Plg	Slip Direction Az	Slip Direction Plg	Shear Sense	Twin plane (e3) Twin-untwin Plane Az	Twin-untwin Plane Plg	Slip Direction Az	Slip Direction Plg	Shear Sense	Thin Section
1	30	9	L	67	31L					240	9	203	3	98.4	15.2	56.2	14	N34W	76W	148	7	D	N28E	68E	62	55	N	N40E	44W	257	20	S	XZ
2	26	20	L	58	32L					244	20	212	32	93.9	4.4	63.2	10.4	N27W	79W	331	11	D	N8E	62E	82	62	R	N12E	65E	66	62	N	
	26	20	L			356	40L			244	20	274	40	93.9	4.4	276	28.1																
3	34	13	R	53	18R					56	13	37	18	112.3	33.8	100.1	50.5	N10E	39W	324	31	N	N41E	78W	25	54	R	N8E	72W	217	55	S	
	34	13	R			6	12R			56	13	84	12	112.3	33.8	131.1	12.5																
4	64	11	R	43	15L					26	11	227	15	79.8	51.6	84.1	18.5	N8W	72W	283	72	R	N48E	29N	37	8	S	N66W	40S	132	15	D	
5	133	14	R	158	3L					317	14	112	3	330	43.6	323.3	14.1	N44E	75E	72	63	R	N78W	47S	272	10	S	N22E	33E	190	7	D	
6	234	18	L	240	5R					36	18	210	5	99	51.1	73.8	35.6	N17E	54W	196	38	R	N82W	19S	121	5	D	N6W	82E	133	79	R	
	234	18	L			276	24L			36	18	354	24	99	51.1	18.7	71.3																
	234	18	L					203	35R	36	18	247	35	99	51.1	265.6	8.4																
7	330	30	R	296	25R					120	30	154	25	167.4	0.7	11.2	18.8	N79W	71S	112	31	R	N65E	83N	61	24	D	N78E	74S	176	74	N	
	330	30	R			346	24R			120	30	104	24	167.4	0.7	152.9	6.1																
8	136	19	R	116	26L					314	19	154	26	322.2	44.9	11.6	17.9	N78W	72S	266	41	R	N32E	79E	57	65	R	N83W	59S	259	28	S	
	136	19	R			174	10R			314	19	276	10	322.2	44.9	302.4	11.1																
9	246	14	R	271	25R					204	14	179	25	63.1	29.8	35	23	N54W	67W	133	19	D	N12W	81W	336	56	S	N12W	38W	219	34	N	
10	264	8	L	293	9R					6	8	157	9	46.6	55.6	8	34.8	N82W	55S	132	39	R	N5W	45W	330	26	R	N14W	60W	306	30	S	
	264	8	L			236	9L			6	8	34	9	46.6	55.6	87.9	45.5																
11	308	14	L	318	12R					322	14	132	12	335.1	46.9	345.2	20.3	N76E	43S	250	4	R	N78W	27S	118	7	S	N28E	46E	40	15	D	
12	144	0	R	122	9R					306	0	328	9	331.9	25.9	346.3	46.6	N77E	43S	124	36	N	N36E	69S	42	16	D	N84E	84S	248	56	S	
13	125	7	L	96	3R					145	7	354	3	354.1	31.5	26.5	50.6	N64W	39S	135	16	N	N72E	70S	89	39	R	N48E	59S	52	2	D	
	125	7	L			141	9L			145	7	129	9	354.1	31.5	340.7	20.9																
14	134	11	R	116	15R					316	11	334	15	331.9	40.7	348.5	54.9	N78E	35S	117	23	N	N38E	52S	44	7	D	N72E	67S	209	50	R	
15	166	16	R	147	9L					284	16	123	9	302.9	20.9	335.9	17.1	N67E	72S	243	9	S	N12E	44E	154	31	N	N18E	81E	4	58	N	
16	36	4	R	314	11R					54	4	136	11	103.1	28.8	348	23.4	N78E	67S	94	32	D	N68W	52S	125	14	D	N4E	20E	104	21	N	
	36	4	R			279	9R			54	4	171	9	103.1	28.8	24.7	38.3																
17	20	5	L	5	11L					250	5	265	11	108.7	11.2	294.5	3.7	N25E	86E	31	63	R	N8E	33W	296	33	N	N16W	72E	151	34	N	
	20	5	L			58	22R			250	5	32	22	108.7	11.2	99.3	56.6																
18	280	11	R	294	18R					170	11	156	18	23.8	36.2	10.5	26	N80W	65S	123	40	R	N52W	60S	293	28	S	N70W	39S	209	39	N	
19	257	12	L	238	3R					13	12	212	3	60.4	57.9	77.1	36.5	N14W	54W	294	48	R	N86W	28S	108	8	D	N12E	15W	217	7	N	
	257	12	L			285	16L			13	12	345	16	60.4	57.9	5.1	61																
20	356	9	R	324	11R					94	9	126	11	135.4	3	339.6	17.5	N70E	72S	82	34	R	N22E	71W	10	32	D	N52E	54W	303	54	N	
	356	9	R			24	3R			94	9	66	3	135.4	3	111.7	19.7																
21	201	7	R	198	10R					249	7	252	10	106.5	10.5	106.5	6.3	N17E	83W	288	84	R	N26W	53W	319	18	D	N5E	54E	120	53	N	
	201	7	R			248	6R			249	7	202	6	106.5	10.5	64.2	37.9																
22	286	13	L	273	6R					344	13	177	6	5.7	57.8	32	41.9	N58W	49S	261	28	R	N87W	9S	186	9	N	N68E	49S	107	37	D	
23	84	23	L	84	17R					186	23	6	17	42.1	24.8	49.4	64.5	N41W	26W	218	26	N	N74W	86S	98	34	D	N16W	88N	345	41	D	
24	141	17	R	114	20R					309	17	336	20	320	40	345.9	60.1	N78E	29S	109	17	S	N27E	74E	49	54	R	N18E	54E	31	16	D	
	141	17	R			174	17R			309	17	276	17	320	40	297	15.6																
25	328	14	R	303	15R					122	14	147	15	338.5	12.7	0.4	25.4	N89E	65S	103	26	S	N48E	69S	220	17	D	N73E	78N	322	77	N	
26	157	15	L	164	9R					113	15	286	9	332.6	6.2	309.9	17.9	N40E	73E	211	24	D	N54E	70N	325	70	N	N76W	67N	295	28	N	
27	301	6	L	307	3R					329	6	143	3	349.9	44.7	349.6	33.9	N80E	57S	167	57	R	N88W	41S	107	12	S	N68E	41S	231	14	D	
28	230	6	R	254	17L					220	6	16	17	83.4	29.7	69.6	61.5	N20W	29W	273	28	N	N24E	55W	205	3	S	N32W	85W	153	47	D	
	230	6	R			214	14L			220	6	56	14	83.4	29.7	113.1	34.4																
29	226	14	R	247	2R					224	14	203	2	82.2	21	67.4	41.3	N24W	49W	297	37	N	N18W	89W	160	61	D	N18E	72W	15	7	S	
30	306	17	L	318	7R					324	17	132	7	334.1	50.4	341.9	24.3	N73E	66S	191	64	R	N74W	26S	116	5	S	N22E	40E	39	13	D	

Continued

31	238	10	L	254	3R			32	10	196	3	335.8	15.8	314.6	13.9	N56E	77S	57	12	D	N74E	83S	147	48	S	N71E	64S	112	53	N	YZ
32	164	0	R	136	9R			286	0	314	9	59.2	45.6	98.3	39.2	N8E	50W	352	19	R	N53W	29S	271	18	D	N82E	24N	266	10	D	
	164	0	R			180	13R	286	0	270	13	59.2	45.6	36	61																
33	84	8	R	71	1R			6	8	19	1	135.9	0.9	319.8	13.3	N50E	77S	86	69	R	N27E	67W	3	45	D	N34E	64E	170	54	N	
	84	8	R			113	10R	6	8	337	10	135.9	0.9	117.9	23.7																
34	74	0	R	91	2R			16	0	359	2	316.9	11.8	126.8	2.1	N36E	87W	34	50	R	N76E	68S	81	17	S	N29W	72E	333	7	D	
	74	0	R			48	11R	16	0	42	11	316.9	11.8	344.6	21.1																
35	292	2	R	283	3R			158	2	167	3	109.3	14.7	115	7.6	N24E	82W	18	46	S	N16W	60W	335	16	D	N12E	66W	252	60	S	
	292	2	R			327	10R	158	2	123	10	109.3	14.7	74.2	29.9																
36	292	5	R	268	4R			158	5	182	4	107.2	12.6	304.4	4.2	N35E	85E	38	45	R	N6W	61W	335	33	D	N10E	75E	155	66	N	
	292	5	R			318	4R	158	5	132	4	107.2	12.6	86.6	30.2																
37	7	12	R	34	14R			83	12	56	14	27.6	35.6	358.9	25.9	N88E	64S	102	27	D	N45W	74W	296	51	S	N50W	31S	192	28	N	
38	289	10	L	314	8L			341	10	316	8	120.8	20.8	99.4	37.2	N8E	53W	345	28	D	N30E	85E	153	85	R	N24E	85E	187	71	N	
	289	10	L			270	8R	341	10	180	8	120.8	20.8	300	5.3																
39	152	14	R	128	14R			298	14	322	14	85.1	53	110	37.3	N20E	52W	344	38	R	N4W	12W	262	13	N	N34W	53W	180	37	D	
40	126	14	L	109	14L			144	14	161	14	90.4	15.2	102.9	4.2	N13E	86W	10	41	S	N2W	46W	270	47	N	N4E	58W	254	56	N	
	126	14	L			144	8R	144	14	306	8	90.4	15.2	89.4	43.5																
41	243	0	R	258	18R			207	0	192	18	324.8	19.7	300	20.7	N30E	69E	31	4	D	N85E	60S	91	13	S	N65E	87N	252	69	N	
	243	0	R			216	9L	207	0	54	9	324.8	19.7	354.2	29.2																
42	272	23	L	303	27L			358	23	327	27	142.3	16.5	127	41.6	N36E	48W	349	40	R	N36E	82S	206	53	N	N83E	77N	79	12	S	
43	14	0	L	38	4R			256	0	52	4	15.6	46.1	349.2	32.5	N79E	58S	106	37	R	N76W	25W	164	11	R	N52W	61W	280	41	S	
	14	0	L			354	18L	256	0	276	18	15.6	46.1	49.8	65.4																
44	253	17	L	273	7L			17	17	357	7	329.8	0.7	129.2	6.9	N35E	83W	33	14	R	N76E	72S	94	43	S	N76E	74N	272	45	N	
	253	17	L			228	14L	17	17	402	14	329.8	0.7	346.4	18.7																
45	342	8	R	330	20L			108	8	300	20	58.6	37.4	94.2	56.5	N5E	34W	203	13	S	N79E	19S	254	3	D	N74W	55S	116	11	D	
	342	8	R			15	28L	108	8	255	28	58.6	37.4	350	71.4																
46	295	32	R	272	40R			155	32	178	40	266.5	5.1	273.1	24.2	N4E	65E	53	59	R	N3W	74W	250	73	R	N75E	89N	338	13	D	
	295	32	R			308	14R	155	32	142	14	266.5	5.1	88.8	16.4																
47	86	8	L	67	4L			184	8	203	4	302.7	8.3	318.8	19.6	N48E	70E	61	31	S	N23E	63W	325	59	R	N17E	75E	190	17	D	
	86	8	L			118	10R	184	8	332	10	302.7	8.3	114.3	27.4																
48	223	14	L	240	8L			47	14	30	8	350.7	21.4	332.9	16	N64E	74S	69	19	R	N86W	81S	264	49	S	N87E	53S	148	50	N	
49	276	13	R	246	32R			174	13	204	32	292.4	4.3	294.1	37.7	N24E	53E	104	53	R	N89E	60S	93	7	S	N8W	79W	349	25	N	
	276	13	R			31	10R	174	13	59	10	292.4	4.3	359.9	30.8																
50	312	14	L	303	15L			318	14	327	15	106.5	40.1	114.9	34.3	N24E	56W	353	38	R	N20E	41W	270	40	S	N8E	57W	218	38	D	
51	247	10	R	218	18R			203	10	232	18	314.1	23.7	330.9	49.8	N61E	40S	112	33	S	N16E	72W	19	14	D	N60E	88S	245	58	N	
52	183	0	R	154	17R			267	0	296	17	31.5	47.9	85.4	56.6	N7W	34W	348	5	S	N70E	40S	82	9	D	N56W	78S	224	78	R	
53	44	15	R	64	9R			46	15	26	9	350.4	20.1	330.6	12.6	N64W	77S	67	23	R	N73W	80S	283	23	R	N85W	82S	268	44	S	
	44	15	R			23	35R	46	15	67	35	350.4	20.1	17	10.1																
54	242	9	L	264	6L			28	9	6	6	332.1	13.8	314.5	0.5	N46E	89E	46	41	R	N83E	87S	260	32	S	N58E	55S	163	55	N	
55	304	22	L	313	13R			326	22	137	13	120.9	39.5	85.4	20.1	N8W	70W	190	37	R	N58E	77N	44	50	S	N50E	15N	293	14	N	
56	241	14	R	254	18R			209	14	196	18	315.1	30.8	302.6	23.7	N34E	67E	48	32	D	N88E	40S	99	9	S	N58E	67S	222	33	S	
	241	14	R			203	8R	209	14	247	8	315.1	30.8	358.6	50.4																
57	238	18	L	264	18L			32	18	6	18	341.1	9.7	143.4	7.6	N54E	83SN	48	40	R	N72E	54S	151	53	N	N86W	89S	274	21	S	
	238	18	L			221	3R	32	18	229	3	341.1	9.7	341.4	36.5																
58	220	10	L	244	23L			50	10	26	23	351	26.4	340.1	2.2	N70E	87S	76	68	R	N78E	47S	181	46	N	N78W	64S	287	9	S	
	220	10	L			213	6R	50	10	237	6	351	26.4	347.6	43.6																
59	278	0	R	256	11R			172	0	194	11	120.6	5.9	307	17.7	N38E	73E	88	69	R	N6E	76W	360	16	D						
	278	0	R			302	12R	172	0	148	12	120.6	5.9	94.8	14.2																
60	328	8	L	314	24L			302	8	316	24	84.9	45.8	115.5	48.1	N26E	42W	23	3	S	N35W	34S	313	8	D	N36E	66E	98	64	N	
																										N10W	66W	232	65	R	

Continued

61	74	14	R	84	23R			16	14	6	23	233.4	26.4	221.8	18.8	N48W	71N	324	35	D											XY
																					N24W	70W	144	27	S						
																										N38W	51E	57	51	N	
62	72	13	R	68	7R			18	13	22	7	235.7	26.9	241.9	31.7	N28W	59E	0	37	S											
	72	13	R			124	40L	18	13	146	40	235.7	26.9	131.6	64.5						N43E	26S	245	11	D						
																										N43W	62N	132	11	D	
63	298	11	R	310	20L			152	11	320	20	174.3	46.2	177.7	13.1	N88E	76N	21	76	R											
																					N45W	34N	132	2	S						
																										N34E	41W	224	9	D	
64	260	8	R	278	10L			190	8	352	10	231.2	49.1	206.7	31.6	N64W	58N	328	41	R											
	260	8	R			230	17R	190	8	220	17	231.2	49.1	276.4	45						N8E	44E	15	10	S						
																										N10W	56E	142	36	S	
65	288	16	L	240	17R			342	16	210	17	197	24	264.7	50.5	N8W	40E	173	1	S											
	288	16	L			203	40L	342	16	67	40	197	24	83.2	16.1						N8W	73W	182	31	D						
																										N48E	64W	233	9	D	
66	171	6	R	148	10L			279	6	122	10	136.7	1.5	144	28.6	N54E	61N	294	58	N											
	171	6	R			180	19L	279	6	90	19	136.7	1.5	113	14						22E	76W	17	24	D						
																										N21E	82E	198	15	N	
67	208	22	L	176	8L			62	22	94	8	271	0.7	123.6	8.6	N35E	82W	216	13	R											
	208	22	L			228	14R	62	22	222	14	271	0.7	276.1	41.5						N8E	48W	83	49	N						
																										N8W	59E	113	54	N	
68	211	7	R	194	7R			239	7	256	7	286.7	25.6	300.3	14.6	N30E	76E	197	41	R											
																					N22E	48E	96	48	N						
																										N3E	70E	9	23	D	
69	224	14	L	250	4R			46	14	200	4	262.5	15.7	243.7	42.8	N24W	48E	113	36	N											
	224	14	L			188	9R	46	14	262	9	262.5	15.7	306.1	12						N36E	78E	213	10	S						
																										N26W	78W	319	55	N	
70	48	28	R	40	10R			42	28	50	10	252.4	5.2	268.1	17.1	N4W	73E	10	35	S											
	48	28	R			10	14R	42	28	80	10	252.4	5.2	109.3	3.8						N18E	86W	199	12	R						
																										N35W	78E	140	22	D	
71	1	18	L	18	3R			269	18	72	3	317.6	13.9	290.4	9.6	N20E	81E	22	12	D											
	1	18	L			45	24L	269	18	225	24	317.6	13.9	288.2	47.3						N18E	43E	163	28	D						
																										N64E	76N	259	53	N	
72	357	12	L	340	9R			273	12	110	9	316.3	6.9	135	20	N35E	70W	317	70	R											
	357	12	L			32	12L	273	12	238	12	316.3	6.9	289.5	30.1						N20E	60E	180	31	D						
																										N70E	72S	76	19	S	
73	24	13	R	350	20R			66	13	100	20	279.4	5.6	119.4	21.3	N28E	69W	233	46	R											
	24	13	R			44	14R	66	13	46	14	279.4	5.6	262.5	15.7						N8W	75E	163	32	D						
																										N24E	55E	68	14	S	
74	128	0	R	138	1R			322	0	312	1	169.6	31.8	160.4	25.8	N70E	63N	279	38	D											
																					N88E	63N	76	28	S						
																										N9W	47N	352	47	N	
75	124	4	R	148	15R			326	4	302	15	175.8	30.1	160.1	8.6	N70E	82N	53	62	R											
	124	4	R			118	12L	326	4	152	12	175.8	30.1	173.6	47.1						N85E	43N	5	42	N						
																										N65W	67N	107	19	S	
76	88	8	R	88	10L			2	8	182	10	218.4	34	219.2	52	N50W	38N	33	38	N											
	88	8	R			88	12L	2	8	182	12	218.4	34	219.3	54						N53W	35N	37	35	R						
																										N70W	65N	308	32	D	
77	97	9	R	73	4R			353	9	17	4	207.8	32.7	237.1	35.9	N34W	55E	145	42	S											
	97	9	R			123	5L	353	9	327	5	207.8	32.7	177.4	29.6						N87E	60N	275	14	D						
																										N88W	43N	70	21	D	
78	108	11	L	134	12L			162	11	136	12	187.8	50	155.5	38.7	N65E	52N	273	31	D											
																					N40W	39N	126	11	S						
																										N54E	25N	46	4	D	
79	114	0	R	143	9R			336	0	307	9	185.1	37.7	160.7	16.3	N71E	73N	268	45	R											
	114	0	R			108	28L	336	0	162	28	185.1	37.7	174.6	65.6						N85E	25N	15	24	N						
																										N56W	68N	110	35	S	
80	314	18	L	294	13L			316	18	336	13	173.3	13.2	190	25.4	N80W	64N	194	28	S											
	314	18	L			324	4L	316	18	306	4	173.3	13.2	156.9	19.9						N68E	71N	58	22	D						
																										N65E	70N	60	13	D	
81	117	19	R	82	30R			333	19	8	30	189	18.8	223.1	11.7	N28W	79N	130	16	S											
	117	19	R			148	50R	333	19	302	50	189	18.8	0.6	20						N89E	69S	215	65	R						
																										N16E	41E	33	33	N	
82	254	14	L	233	10R			16	14	217	10	233.4	26.4	267.7	40.9	N4W	49E	9	13	S											
																					N74W	54N	102	7	D						
																										N34W	84W	191	81	N	
83	258	6	R	278	12L			12	6	352	12	230.6	35	207	29.6	N63W	62N	210	23	D											
																					N25W	73E	130	54	S						
																										N24W	35E	34	32	N	
84	146	0	R	172	4R			304	0	278	4	152.6	22	134.6	2.4	N45E	88W	228	51	D											
																					N89E	74N	84	21	S						
																										N54E	43N	45	6	N	
85	143	7	R	127	34L			307	7	143	34	159.5	18	139.3	59.2	N50E	31N	352	24	N											
	143	7	R			84	9R	307	7	6	9	159.5	18	223.1	32.8						N47W	57N	131	2	S						
																										N40E	76S	206	44	N	
86	208	26	R	233	35R			242	26	217	35	304.5	37.5	294.3	59.8	N22E	31E	139	29	N											
	208	26	R			167	30R	242	26	283	30	304.5	37.5	335.6	14						N66E	76S	232	45	R						
																										N18E	70E	41	48	D	
87	313	15	L	288	31L			317	15	162	31	172.7	16.3	170.6	68.2	N80E	22N	355	22	N											
																					N40E	77S	212	31	N						
																										N42W	77W	134	30	N	
88	304	24	L	304	9R			146	24	146	9	155.6	54	168.4	41.6	N78E	48N	28	41	R											
	304	24	L			345	22L	326	24	285	22	184.5	11.8	331.6	6.8						N64E	83SN	238	29	R						
																										N81E	22N	315	19	N	
89	178	18	L	164	45L			92	18	106	45	115.2	14.6	100.2	41	N11E	49W	324	41	R											
																					N8W	79E	172	52	N						
																										N8E	81N	54	13	S	
90	166	14	R	150	8R			284	14	300	8	325.7	1.3	154.3	13.2	N64E	76N	266	58	R											
																					N64E	76S	86	57	N						
																										N42E	89S	221	3	D	

Location : BLV-6
Rock Type : Bioclastic Limestone

Grains No.	C - Axis			Calcite Twins						U-Stage Recalculate				Thin Section Rotation				Twin plane (e1)					Twin plane (e2)					Twin plane (e3)					Thin Section
	Strike (IV)	Dip (NS)	R/L Dip Direct.	Ttwin plane (e1)		Ttwin plane (e2)		Ttwin plane (e3)		C-axis		Twin Plane		C-axis		Twin Plane		Twin Plane		Slip Direction		Shear Sense	Twin-untwin Plane		Slip Direction		Shear Sense	Twin-untwin Plane		Slip Direction		Shear Sense	
				IV	NS	IV	NS	IV	NS	Az	Plg	Az	Plg	Az	Plg	Az	Plg	Az	Plg	Az	Plg		Az	Plg	Az	Plg		Az	Plg	Az	Plg		
1	226	14	L	247	10L					44	14	383	10	97.6	27.7	73.9	28.3	N18W	62W	168	8	D	N17E	82W	359	68	N	N24E	46W	239	30	S	XZ
2	70	0	R	63	27R					20	0	207	27	69.2	18.7	252.1	8.9	N63E	83N	59	19	S	N52W	59S	301	15	D	N18W	80E	37	79	N	
	70	0	R			98	9L			20	0	352	9	69.2	18.7	39	28.8																
3	83	15	L	50	27L					187	15	220	27	54.8	4.9	263.7	11.2	N8E	79E	359	28	R	N35W	65W	235	85	N	N38W	53W	238	53	N	
	83	15	L			83	5R			187	15	7	5	54.8	4.9	55.7	24.8																
4	338	40	R	8	47R					112	40	82	47	172.6	30.3	151.5	46	N53E	44N	32	26	D	N18W	81W	278	68	D	N70W	58N	108	3	S	
5	262	28	R	278	30R					188	28	172	30	235.1	8.1	220.9	10.2	N58W	80N	130	3	D	N8E	51W	215	29	R	N31W	84W	160	62	N	
	262	28	R			228	24L			188	28	42	24	235.1	8.1	98.7	37.9																
6	225	40	L	230	14L					45	40	40	14	109.9	52.1	93.4	28.8	N3E	60W	227	51	R	N58E	47N	31	25	S	N24W	16W	312	7	D	
7	221	9	L	251	20L					49	9	19	20	101.3	21.7	71.1	38.7	N19W	51W	324	20	D	N7E	81E	148	75	N	N45E	60W	227	5	S	
8	310	35	R	281	21R					140	35	169	21	194.2	18.9	217.7	1.3	N52W	88S	126	36	S	N68E	86N	261	33	D	N52W	88N	128	35	S	
	310	35	R			333	14R			140	35	117	14	194.2	18.9	167.8	4.4																
9	214	32	L	242	26L					56	32	28	26	117.4	41.3	83.3	43.1	N8W	47W	179	6	D	N32E	74W	339	71	S	N60E	35N	257	17	S	
10	126	10	L	132	7L					144	10	138	7	12.4	6.3	5.9	7.9	N85W	82S	273	12	D	N75W	88S	285	66	N	N74W	78S	119	47	N	
11	102	14	L	124	14L					168	14	146	14	36.3	5.5	15.1	2.8	N75W	87S	106	14	D	N37W	71W	155	31	S	N42W	77W	333	51	N	
	102	14	L			84	2L			168	14	186	2	36.3	5.5	54.3	17.9																
12	68	12	R	83	2R					22	12	7	2	73.1	30.4	55.6	21.8	N34W	67W	159	30	R	N4W	71W	341	43	S	N16W	43W	245	43	N	
13	141	28	R	113	30R					309	28	337	30	345.8	39.2	17.7	47.9	N73W	41S	117	19	S	N45E	44S	221	3	D	N77E	75S	177	76	R	
14	322	40	R	308	5R					128	40	142	5	185.7	26.3	9.4	10.7	N82W	78S	161	77	R	N43W	49E	325	11	N	N54E	53N	53	4	D	
15	274	4	R	284	20L					176	4	346	20	43.8	15.9	31	39.3	N58W	54S	258	42	D	N61W	84N	111	55	N	N20W	79W	338	13	S	
16	272	0	R	294	4R					178	0	156	4	45.9	20	23.3	14.2	N68W	76S	118	19	D	N24W	55W	176	27	R	N30W	87W	328	54	S	
	272	0	R			254	15L			178	0	16	15	45.9	20	66.8	34.1																
17	224	18	L	237	34L					46	18	33	34	101	31.1	92.3	49.7	NB3E	39W	304	35	R	N5W	74W	193	49	D	N32E	65W	23	21	S	
18	123	9	R	156	12R					327	9	294	12	11.4	25.5	336.7	19.3	N68E	71S	74	18	D	N88W	42S	209	39	N	N86E	79S	99	50	R	
19	84	17	L	58	32L					186	17	212	32	53.8	2.9	255.7	14.6	N14W	74E	358	37	R	N46W	65W	274	56	R	N50W	72N	111	47	N	
	84	17	L			94	4R			186	17	356	4	53.8	2.9	43.6	24																
20	48	35	R	81	20R					42	35	9	20	103.6	48.3	59.1	39.7	N32W	50W	170	24	D	N30E	72W	348	64	S	N65E	21N	259	6	S	
21	216	0	L	237	24L					54	0	33	24	103.7	11.6	88.6	40.1	N2W	49W	310	43	R	N34E	88W	32	28	S	N4W	77E	160	52	N	
	216	0	L			195	3R			54	0	255	3	103.7	11.6	122.9	2.3																
22	213	14	L	222	22R					57	14	228	22	111.1	24.1	272.1	8	N3E	82E	168	58	R	N56E	78E	61	52	R	N72E	72N	55	17	S	
	213	14	L			178	11R			57	14	272	11	111.1	24.1	316.1	11																
23	250	22	L	286	38L					20	22	344	38	72.7	40.6	24.6	56.9	N65W	33S	288	4	D	N7W	59W	328	38	R	N26W	82W	184	75	D	
	250	22	L			238	14L			20	22	32	14	72.7	40.6	84.6	30.6																
24	186	14	L	213	34L					84	14	57	34	137.3	15.2	119.5	42.8	N32W	46W	341	37	N	N29E	78E	193	52	N	N78E	79N	77	15	S	
25	186	12	L	208	22L					84	12	62	22	136.5	13.4	119.1	30.1	N30E	60W	6	34	D	N55E	89S	65	35	R	N40E	80E	194	68	N	
	186	12	L			164	6L			84	12	106	6	136.5	13.4	155	0.2																
26	258	18	L	238	34L					12	18	32	34	62.4	37.5	91.1	49.9	N2E	40W	197	13	S	N75W	38S	281	3	D	N15E	48W	12	5	S	
	258	18	L			293	34L			12	18	337	34	62.4	37.5	16.3	51.9					D											
27	268	17	L	232	43L					2	17	38	43	50.4	37	103.6	57	N14E	31W	198	4	S	N65W	41S	276	15	D	N27W	87E	347	77	N	
	268	17	L			288	30L			2	17	342	30	50.4	37	24.1	48.7																
28	268	24	L	295	15L					2	24	335	15	50.6	44	18.9	32.9	N72W	57S	130	29	R	N19E	67W	309	52	S	N18W	20W	216	17	N	
29	193	26	L	214	46L					77	26	56	46	135.3	28.8	126.3	54	N36W	35W	327	34	R	N74W	65N	68	14	S	N26E	79W	218	49	D	
	193	26	L			164	32L			77	26	106	32	135.3	28.8	164.2	24.7																
30	260	0	L	279	21L					10	0	351	21	58.6	19.7	36.9	40.7	N54W	48S	271	34	D	N3W	59W	186	15	S	N42W	82E	123	66	N	
	260	0	L			235	15L			10	0	395	15	58.6	19.7	88.2	30.9																

Continued

31	312	0	L	286	9L					318	0	344	9	48	62	59.1	35.5	N32W	54W	255	53	R
	312	0	L			328	14L			318	0	302	14	48	62	98.3	71.7					
32	305	25	R	334	27L					145	25	296	27	8.8	48	126.4	62.4	N36E	27W	353	20	R
	305	25	R			280	10L			145	25	350	10	8.8	48	59.5	29.5					
33	304	18	R	336	22R					146	18	114	22	19	50.3	327.9	67.6	N58E	22E	228	4	D
	304	18	R			289	12R			146	18	161	12	19	50.3	32.7	38					
34	228	5	R	262	25R					222	5	188	25	222.7	21.9	22.5	10.9	N67W	78S	273	59	R
35	98	18	R	124	8R					352	18	326	8	68.2	26.5	61.4	53.2	N28W	36W	258	36	N
	98	18	R			73	10L			352	18	197	10	68.2	26.5	38	3					
36	32	23	R	7	10L					58	23	263	10	256.3	34.5	206.7	61.3	N62W	29N	102	9	D
	32	23	R			38	14L			58	23	232	14	256.3	34.5	211.6	30.9					
37	174	15	R	194	11R					276	15	256	11	180	69.6	208.9	54.5	N62W	35N	62	30	R
	174	15	R			147	27L			276	15	123	27	180	69.6	341.8	60.2					
38	122	9	R	143	14R					328	9	307	14	62.4	51.1	88.5	68.2	N2W	22W	214	14	N
39	198	9	R	174	11R					252	9	276	11	213.5	51.1	189.1	72.2	N82W	17N	55	14	N
41	68	11	R	58	14L					22	11	212	14	239	2	213.7	11.6	N56W	78N	119	22	D
	68	11	R			103	7L			22	11	167	7	239	2	39.7	32.7					
42	145	0	L	171	12L					125	0	99	12	48	75	276	73.8	N5E	16E	69	15	R
43	135	14	R	161	10R					315	14	289	10	78.5	61.6	143.6	79.9	N60E	10W	239	3	R
	33	10	L	10	25R					237	10	80	25	215.5	36.4	270.9	51.7					
44	257	35	R	280	18L					193	35	350	18	12.8	5.8	68.6	28.4	N22W	62W	165	11	S
	257	35	R			238	8R			193	35	212	8	12.8	5.8	219.8	11.9					
45	343	22	L	318	7L					287	22	312	7	145.5	67.8	66.2	67	N24W	23W	192	14	R
	343	22	L			8	9R			287	22	82	9	145.5	67.8	246.7	60.7					
46	338	18	R	340	9L					112	18	290	9	324.2	71.9	138.3	81	N58E	8W	323	8	R
47	38	5	L	11	21R					232	5	79	21	222.1	31.9	264.7	53.1	N5W	36E	119	33	R
	38	5	L			272	4R			232	5	178	4	222.1	31.9	43.7	22					
48	167	30	R	184	22R					283	30	266	22	150	59.3	183.2	57.9	N87W	31N	75	11	S
	167	30	R			143	9L			283	30	127	9	150	59.3	19.6	70.8					
49	198	1	R	178	18L					252	1	92	18	226.3	52	274.4	64.8	N5E	24E	10	4	R
	198	1	R			222	8R			252	1	228	8	226.3	52	219	27.7					
50	168	37	L	193	27L					102	37	77	27	307.6	52.3	271	48.3	N1E	41E	18	16	D
	168	37	L			153	22L			102	37	117	22	307.6	52.3	334.8	67					
51	281	15	R	300	18L					169	15	330	18	30.7	29.8	74.8	46.7	N16W	42W	262	43	R
52	344	0	R	328	24R					106	0	122	24	228	86	343.1	63.3	N73E	27S	170	28	R
	344	0	R			305	14L			106	0	325	14	228	86	71.5	52.7					
53	298	14	R	314	10L					152	14	316	10	27.6	46.1	69.9	62.3	N18W	27W	175	8	S
54	247	32	R	270	11R					203	32	180	11	195.9	2.5	36.3	19.6	N55W	69S	147	44	R
	247	32	R			218	18R			203	32	232	18	195.9	2.5	207	30.3					
55	123	0	R	132	10R					327	0	318	10	48	53	68.7	60.4	N22W	30W	181	12	S
	123	0	R			84	12L			327	0	186	12	48	53	35.6	13.7					
56	41	15	R	24	10R					49	15	66	10	245	28	242.2	45.1	N28W	45E	76	44	N
57	6	40	L	338	27L					264	40	292	27	165.6	43.5	134.1	62.9	N43E	29W	13	15	D
58	348	24	L	344	14L					282	24	286	14	155.4	64.7	153.7	75.5	N64E	14N	342	14	R
59	214	20	R	190	3L					236	20	80	3	203.8	33.5	233.9	59.9	N36	29E	1	20	R
	214	20	R			208	23R			236	20	242	23	203.8	33.5	198.2	38					
	214	20	R					240	5L	236	20	30	5	203.8	33.5	233.1	10					
60	314	28	R	327	6R					136	28	123	6	117.9	49.2	144	33	N54E	57N	25	37	S
	314	28	R			280	34R			136	28	170	34	117.9	49.2	78.3	73.4					
61	228	14	L	217	2L					42	14	53	2	281.9	36.5	301.4	33.6	N34E	57W	202	13	S
	228	14	L			258	26L			42	14	12	26	281.9	36.5	242.7	42.5					
62	210	0	R	182	10R					240	0	268	10	306.8	28	326.7	5.3	N56E	84S	231	52	R
63	0	15	R	22	4R					90	15	68	4	123.9	5.1	306.2	19.1	N34E	70E	109	70	R
64	282	17	L	263	7R					348	17	187	7	209.5	51.2	256.5	75.3	N15W	15E	12	8	N
	282	17	L			302	27L			348	17	328	27	209.5	51.2	193.4	33.7					
65	232	27	R	201	15L					218	27	69	15	336.8	54.6	296.1	13.7	N26E	75E	53	59	R

N8E	18W	191	2	S	N28E	17W	14	5	N	YZ
N30W	69W	310	44	R	N12E	16E	27	5	N	
N57W	52S	261	41	R	N28E	46W	314	20	S	
N8W	75W	169	17	S	N76W	36N	65	25	D	
N53W	87S	131	43	R	N42W	80W	147	42	D	
N58W	59N	311	18	R	N1E	1E	180	77	D	
N73E	30S	169	30	R	N38E	2	357	1	N	
N59W	45S	140	19	D	N15W	54W	342	6	S	
N74W	58N	329	47	D	N24W	49E	135	23	S	
N50W	57S	270	45	R	N40E	86W	9	4	S	
N68W	41S	187	41	R	N18E	31W	14	2	N	
N1E	37E	180	2	R	N48W	84S	162	79	N	
N50W	77N	317	30	R	N48E	62S	222	11	D	
N23W	29E	106	24	R	N54W	26N	88	18	S	
N16E	38E	68	33	D	N87W	40S	209	37	R	
N46W	67S	218	68	R	N85E	58N	273	10	D	
N68W	19S	164	15	R	N28E	21W	9	9	D	
N52E	61N	15	60	R	N88W	39N	287	13	D	
N65E	22E	98	13	S	N76E	22S	95	8	S	
N78E	54S	79	5	D	N55W	83N	341	79	N	
N19W	36W	250	37	R	N27E	26W	287	26	N	
N77E	46N	91	14	D	N53W	70S	253	66	R	
N64W	60N	346	53	N	54W	59N	349	53	N	
N54W	75S	175	72	R	N18E	46W	353	25	S	
N38W	72N	336	37	D	N8W	69E	158	33	S	
N64E	68N	289	61	D	N68W	49N	98	15	S	
N45E	31N	267	24	D	N83E	30N	46	19	S	
N73W	52N	77	34	D	N37W	80E	132	47	S	
N14W	17W	318	8	S	N28E	15W	298	15	N	XY
N26W	47E	335	1	D	N8W	33E	131	22	N	
N50E	37E	109	34	N	N10E	72E	18	24	D	
N56E	71N	247	27	S	N10E	75W	4	18	D	
N76W	55N	325	45	R	N86E	51N	286	29	D	

Continued

66	294	43	R	273	18R			156	43	177	18	83.8	59.4	172.7	86.5	N75E	3N	79	1	R
	294	43	R			328	38R	156	43	122	38	83.8	59.4	104.9	37.1					
67	218	0	R	194	20R			232	0	256	20	303	35.3	333	19.3	N64E	71S	229	36	R
	218	0	R			243	9R	232	0	207	9	303	35.3	299	61.7					
68	203	9	L	222	3R			67	9	228	3	300.9	18	304.4	40.2	N34E	50E	112	50	R
	203	9	L			174	4R	247	9	276	4	318.9	24.6	143.8	4.3					
69	217	7	R	245	1R			233	7	205	1	311.5	37.1	283.2	59	N12E	31E	160	19	N
70	254	15	L	292	43L			16	15	338	43	253.4	51.6	210.6	23.8	N58W	65N	330	47	R
	254	15	L			250	8L	16	15	20	8	253.4	51.6	265	55.8					
71	304	15	R	314	15R			146	15	136	15	141.3	57.2	137.5	47.9	N48E	41N	304	42	R
	304	15	R			272	40R	146	15	178	40	141.3	57.2	52.5	69.9					
72	118	10	L	117	28R			152	10	333	28	154.2	61.2	198.6	35.4	N72W	55N	69	43	R
	118	10	L			154	6L	152	10	116	6	154.2	61.2	141.3	26.5					
73	216	27	L	198	20L			54	27	72	20	278	19.7	292.8	9	N23E	80E	196	38	S
74	124	24	R	143	20R			326	24	307	20	189.5	34.9	172.4	24.5	N82E	64N	279	32	D
	124	24	R			104	32R	326	24	346	32	189.5	34.9	213.3	36.3					
75	94	20	R	68	18R			356	20	22	18	222.2	49.8	259	46.3	N21W	44E	142	16	S
76	90	27	L	106	36L			180	27	164	36	48	83	85.9	68.7	N6W	20W	280	21	R
	90	27	L			50	46L	180	27	220	46	48	83	5.9	48.3					
77	94	30	R	68	5R			356	30	22	5	223.5	39.9	271.2	56.9	N2E	33E	9	6	S
78	126	14	L	125	1R			324	14	325	1	179	40.9	165.3	49.8	N75E	40N	45	24	S
	126	14	L			100	47L	324	14	170	47	179	40.9	62.5	61.8					
79	328	25	R	313	3R			122	25	137	3	121.1	36.6	154.4	44.8	N64E	44N	248	5	S
	328	25	R			357	8R	122	25	93	8	121.1	36.6	131.5	5.5					
80	338	40	R	345	14R			112	40	105	14	102.5	29.3	129.4	18.6	N38E	70W	30	27	S
	338	40	R			294	34R	112	40	156	34	102.5	29.3	99.7	64.5					
81	258	43	L	276	37L			12	43	354	37	237.7	26	222.3	32.7	N48W	58N	120	19	D
	258	43	L			330	50L	12	43	300	50	237.7	26	194.1	2.3					
82	76	25	L	53	43L			194	25	217	43	341.7	76.1	3.1	51.5	N88W	38S	197	38	R
83	124	12	L	175	23L			146	12	95	23	146.5	56.4	117.7	12.1	N27E	78W	237	65	R
	124	12	L			208	12L	146	12	62	12	146.5	56.4	295.8	21.1					
84	110	15	L	94	6L			160	15	176	6	149.5	70.3	211.9	75.5	N60W	13N	107	4	S
	110	15	L			138	28L	160	15	132	28	149.5	70.3	118	45.7					
85	154	17	L	143	5R			116	17	307	5	129.3	29.6	157.8	32.2	N68E	58N	66	3	R
	154	17	L			182	24L	116	17	88	24	129.3	29.6	114.7	6.3					
86	338	34	L	43	24L			292	34	227	24	177.4	5.8	332.2	46.4	N64E	43S	191	37	R
87	47	14	L	27	10L			223	14	243	10	316.7	48.6	318.7	28.7	N48E	60S	140	61	R
88	202	40	L	254	14L			68	40	16	14	273.3	2.9	254.1	52.5	N16W	37E	103	34	D
89	186	8	R	204	1R			264	8	246	1	323.5	8.3	310.3	22.8	N40E	67E	196	43	S

N65W	71S	269	53	N
N14E	53W	324	47	R
N28E	28E	126	29	N
N54E	85N	266	81	R
N28E	80E	51	66	D
N5W	33E	13	12	S
N36E	20W	168	9	R
N52E	63N	297	63	R
N11E	51E	89	51	N
N57W	54N	121	4	S
N86W	23N	73	10	D
N85W	42S	174	42	R
N88E	49N	279	14	D
N28W	27W	192	19	R
N42E	84N	25	74	R
N10E	25W	285	26	R
N76W	87S	286	34	D
N15E	14W	313	12	N
N27E	69E	157	63	R
N28E	44W	267	40	R
N26E	83W	216	63	R
N28W	80W	323	3	N
N88E	33N	85	5	S
N40W	57W	303	25	N
N47E	79N	18	69	N

N82E	17N	341	17	S
N48E	10W	248	5	N
N28E	24E	128	25	N
N12E	83E	14	26	D
N78E	58S	245	17	S
N21E	69E	169	54	S
N68E	31N	69	1	S
N88W	12S	161	13	N
N8W	78E	358	31	D
N52E	66N	99	37	S
N60W	62N	352	28	R
N57W	8N	45	9	N
N38W	84N	119	79	S
N84E	47N	289	2	S
N3W	43W	352	5	D
N3E	35W	296	33	N
N15W	58E	355	16	S
N11E	30E	66	26	D
N73E	21S	161	17	N
N11E	23W	222	14	D
N15E	44W	350	20	D
N40E	45E	18	21	N
N18E	36E	195	2	D
N54E	78N	237	9	N
N74E	80S	75	5	S

Location : CLV-7
Rock Type : Reddish Limestone

Grains No.	C - Axis			Calcite Twins						U-Stage Recalculate				Thin Section Rotation				Twin plane (e1)					Twin plane (e2)					Twin plane (e3)					Thin Section
	Strike (IV)	Dip (NS)	R/L Dip Direct.	Ttwin plane (e1)		Ttwin plane (e2)		Ttwin plane (e3)		C-axis		Twin Plane		C-axis		Twin Plane		Twin Plane		Slip Direction		Shear Sense	Twin-untwin Plane		Slip Direction		Shear Sense	Twin-untwin Plane		Slip Direction		Shear Sense	
				IV	NS	IV	NS	IV	NS	Az	Plg	Az	Plg	Az	Plg	Az	Plg	Az	Plg	Az	Plg		Az	Plg	Az	Plg		Az	Plg	Az	Plg		
1	30	37	L	5	40L					240	37	265	40	98.9	2.6	287.3	15.3	N18E	75E	46	61	R											XZ
	30	37	L			67	40L			240	37	203	40	98.9	2.6	73.3	16.8						N18W	75W	335	27	D						
																												N18E	72W	221	53	N	
2	36	14	R	55	9R					54	14	35	9	139.5	38	119.6	51.1	N30E	38W	3	20	D											
	36	14	R			9	31R			54	14	81	31	139.5	38	169.1	21.9						N80E	68N	63	36	S						
																												N44E	22N	325	22	N	
3	357	14	L	324	28L					273	14	306	28	314.3	9.5	313.4	43.2	N45E	48E	135	47	N											
	357	14	L			10	10L			273	14	260	10	314.3	9.5	131.3	3.4						N42E	87N	33	70	R						
																												N16E	81W	10	31	N	
4	53	12	L	30	20L					217	12	240	20	100.8	34.9	111.9	13.6	N22E	77	1	57	R											
	53	12	L			84	26L			217	12	186	26	100.8	34.9	61.5	33.7						N28W	56W	159	13	D						
																												N35E	36W	250	25	N	
5	343	25	L	323	35L					287	25	307	35	309.9	26.2	304.1	45.5	N34E	45E	143	43	N											
																							N26E	78E	39	46	D						
																												N60E	72S	231	26	S	
6	143	14	L	182	47L					127	14	88	47	357.9	22.6	187.3	22.8	N84W	68N	337	66	R											
	143	14	L			120	47L			127	14	150	47	357.9	22.6	34.8	8.4						N57W	82S	300	27	S						
																												N75E	32S	190	29	N	
7	134	1	R	116	15R					316	1	334	15	351.4	39.2	351.3	61.8	N82E	28S	170	29	N											
																							N59E	64S	84	39	D						
																												N78W	65S	260	40	S	
8	147	7	R	135	9R					303	7	315	9	336.2	31.9	342	43.1	N74E	46S	142	45	R											
	147	7	R			183	40R			303	7	267	40	336.2	31.9	288	16.6						N18E	74E	26	26	D						
																												N54E	63S	59	13	D	
9	187	9	R	186	9L					263	9	84	9	133.7	1.5	149.8	9.6	N60E	80N	244	26	S											
	187	9	R			157	24L			263	9	113	24	133.7	1.5	357.2	6.1						N86E	84S	87	7	R						
																												N24E	48W	333	41	N	
10	194	18	R	223	40R					256	18	227	40	122.5	2.6	89.4	7.5	N3W	82W	358	10	D											
	194	18	R			157	43R			256	18	293	43	122.5	2.6	291.3	36.1						N78W	53S	289	11	S						
																												N72E	78N	254	10	S	
11	124	26	R	138	11R					326	26	312	11	324.2	59.8	337.6	41.7	N58E	49S	191	43	R											
																							N89W	17S	117	9	S						
																												N19E	37E	45	20	D	
12	48	24	L	74	43L					222	24	196	43	96.5	22.7	67.1	15.6	N76E	74N	73	16	S											
																							N24E	88E	27	53	N						
																												N21E	42W	254	36	N	
13	8	22	L	328	11L					262	22	302	11	302	4.3	331.5	33	N62E	57S	71	12	S											
	8	22	L			16	3L			262	22	254	3	302	4.3	134.2	12.3						N45E	78N	241	54	R						
																												N8E	79E	171	5	D	
14	65	4	R	64	6L					205	4	206	6	94.4	48.4	94	46.2	N5E	44W	270	44	R											
																							N44E	27N	238	7	S						
																												N37W	31W	318	4	N	
15	197	32	R	190	34R					253	32	260	34	289.2	2.9	290.7	8.9	N22E	81E	43	68	R											
	197	32	R			242	46R			253	32	208	46	289.2	2.9	74.3	9.8	N17W	81W	341	18	R	N6E	65E	152	50	N						
																												N13E	88N	13	14	D	
16	293	1	R	266	2R					157	1	184	2	15.6	52	57.9	13.9	N44W	77W	309	55	R											
																							N88W	14N	12	15	N						
																												N58E	74S	79	53	D	
17	128	0	L	113	15L					142	0	157	15	357.6	43	25.6	39.9	N64W	50S	282	15	S											
	128	0	L			162	20L			142	0	108	20	357.6	43	351.3	4.7						N82E	84S	106	81	R						
																												N68E	30S	207	21	N	
18	143	0	L	124	4L					127	0	146	4	345.6	31.4	5.3	43	N86W	47S	118	22	S											
																							N55E	55S	232	3	D						
																												N54E	77S	220	73	R	
19	12	20	L	334	28L					258	20	296	28	121.8	0	310	34.8	N40E	56E	104	54	R											
	12	20	L			36	8R			258	20	54	8	121.8	0	133	35						N42E	55W	281	51	N						
																												N58E	68N	254	31	S	
20	343	16	L	326	22L					287	16	304	22	318.9	22.4	320.1	39.5	N50E	51E	214	19	S											
																							N34E	76E	42	31	D						
21	228	24	R	198	15R					222	24	252	15	96.5	22.7	122.9	7.5	N32E	83W	28	31	S											
	228	24	R			248	32R			222	24	202	32	96.5	22.7	75.4	24.5						N14W	65W	344	3	D						
																												N4E	37W	279	37	N	
22	288	14	R	260	9R					162	14	190	9	30.9	42.7	70.4	49.8	N20W	41W	338	2	S											
																							N79E	40S	258	2	D						
																												N62W	76S	203	76	R	
23	52	12	R	74	1R					38	12	196	1	126.2	50.4	84	55.5	N8E	35W	251	35	R											
																							N36E	66W	308	66	R						
																												N80E	33N	76	3	S	
24	28	20	L	27	12R					242	20	63	12	113.1	12.2	142.2	29.3	N53E	61N	245	24	S											
																							N8W	68W	346	12	D						
																												N28E	71E	94	69	N	
25	58	30	L	45	10L					212	30	225	10	84.8	22.7	109.4	31.1	N18E	58W	209	15	S											
	58	30	L			97	36L			212	30	173	36	84.8	22.7	48.8	23.7						N42W	67W	140	4	D						
																												N30W	55W	318	19	D	
26	284	14	L	293	16L					346	14	337	16	13.1	69.5	353.4	64.7	N84E	27S	117	16	D											
	284	14	L			254	32L			346	14	16	32	13.1	69.5	157.4	76.2						N68E	14N	0	13	R						
																												N54E	42S	104	37	D	
27	258	16	L	276	11L					12	16	354	11	95.8	72.2	37.4	70.2	N54W	19W	157	10	R											
																							N13W	49W	243	47	S						
																												N73E	34N	21	30	D	
28	306	15	L	328	14R					324	15	122	14	341.4	53.7	354.5	18.9	N84E	71S	215	67	R											
	306	15	L			287	6R			324	15	163	6	341.4	53.7	27.8	50.5						N62W	40S	278	16	D						
																												N34W	22S	311	7	S	
29	84	24	R	64	10R					6	24	26	10	98.1	82	110.9	58.6	N22E	31W	300	32	R											
	84	24	R			108	36R			6	24	342	36	98.1	82	298.5	73.8						N28E	16E	113	17	R						
																												N51W	20E	56	12	S	
30	280	15	L	247	17L					350	15	23	17	21.2	72.4	118.4	65.3	N28E	25W	336	21	R											
	280	15	L			298	20L			350	15	332	20	21.2	72.4	340.1	62.8						N70E	28S	112	19	D						
																												N30E	30E	80	23	D	

Continued

31	93	15	L	80	43L					357	15	190	43	310.5	4.9	249.3	21.9	N21W	69E	156	6	D											YZ
	93	15	L			132	23L			357	15	138	23	310.5	4.9	147.5	46.8						N58N	44N	298	40	R						
																												N56E	32W	306	31	N	
32	35	40	R	19	47R					55	40	71	47	296.2	59.9	270.6	67.6	N2E	22E	157	11	D											
																							N88W	44W	93	43	R						
																												N22E	39E	223	5	N	
33	184	35	R	194	12R					266	35	256	12	51.4	24.9	35.1	45.9	N54W	45S	261	35	D											
																							N54W	88S	131	60	D						
																												N14W	69W	342	14	S	
34	54	21	R	68	14R					36	21	22	14	322.3	40.9	323.2	25.8	N54E	65S	148	65	R											
	54	21	R			15	35R			36	21	75	35	322.3	40.9	299.5	76.4						N30E	14S	148	12	D						
																												N32E	43E	201	9	D	
35	34	12	L	20	6R					236	12	70	6	12	36.8	13	59.5	N78W	31S	190	30	D											
																							N80E	66S	99	36	D						
																												N57W	68S	285	38	S	
36	234	18	R	248	20R					216	18	202	20	0.4	19.2	353.4	7.7	N84E	82S	95	61	R											
	234	18	R			205	18R			216	18	245	18	0.4	19.2	25.1	36.3						N65W	53S	133	24	S						
																												N75W	72S	283	7	S	
37	210	20	R	224	21R					240	20	226	21	21.3	32.3	9.9	23.7	N81W	66S	121	41	R											
																							N56W	63S	291	24	S						
																												N74W	44S	212	43	N	
38	216	8	R	202	7L					234	8	68	7	6.8	38.6	8.7	59.1	N84W	31S	182	31	D											
																							N76E	63S	95	33	D						
																												N65W	64S	273	38	S	
39	237	7	L	204	25R					33	7	246	25	336.2	31.9	29.7	30.4	N62W	58S	291	14	S											
																							N11E	36E	184	6	N						
																												N54E	76N	11	70	N	
40	183	18	L	173	4R					87	18	277	4	41.5	77.6	67.4	55.3	N23W	34W	263	34	R											
																							N88E	12N	21	13	N						
																												N75E	28S	132	23	N	
41	66	26	L	73	2R					204	26	17	2	359.4	5.6	331.9	15.7	N64E	75S	236	20	D											
	66	26	L			43	4R			204	26	47	4	359.4	5.6	349.1	41.9						N78E	50S	191	47	D						
																												N87W	67N	339	66	N	
42	224	17	L	240	21R					46	17	210	21	332.8	47.9	358.9	13	N89E	76S	247	58	R											
																							N48W	12S	138	3	R						
																												N16E	61E	39	36	D	
43	23	15	R	21	16R					67	15	69	16	355.4	64.1	356.3	66.2	N84E	23S	154	23	N											
	23	15	R			338	35R			67	15	112	35	355.4	64.1	166	70.8						N78E	20N	358	20	R						
																												N38E	60E	82	51	D	
44	330	21	L	316	43L					300	21	314	43	88.1	31.4	85.8	6.5	N6W	83W	212	81	R											
	330	21	L			2	18L			300	21	268	18	88.1	31.4	52.5	42						N38W	48W	315	8	D						
																												N26W	52W	211	5	S	
45	32	23	L	32	4R					238	23	58	4	21.2	28.7	359.5	50.1	N89W	39S	232	27	D											
	32	23	L			356	24L			238	23	274	24	21.2	28.7	59.5	35.9						N32W	55W	151	3	S						
																												N82W	87S	104	62	N	
46	278	8	R	250	10L					172	8	20	10	148	10.9	326.1	22.2	N54E	67S	168	66	R											
																							N88E	67N	276	18	S						
																												N28E	63W	18	21	D	
47	290	0	L	268	10L					340	0	2	10	134.7	17.2	317.3	6.7	N48E	84E	92	82	R											
																							N65E	61N	259	22	S						
																												N22E	65W	16	14	D	
48	192	14	R	223	14R					258	14	227	14	38.6	44.5	5.5	29.6	N86W	60S	116	31	R											
	192	14	R			170	15R			258	14	280	15	38.6	44.5	68.5	43.9						N24W	47W	329	11	S						
																												N28E	69W	306	49	S	
49	255	18	L	270	12R					15	18	180	12	316	21.5	155.4	6	N64E	83N	59	48	R											
																							N66E	39S	115	32	S						
																												N14E	76N	16	14	D	
50	318	9	R	302	4R					132	9	148	4	125.7	45.5	131.4	29.5	N40E	61N	334	59	R											
																							N55E	34N	263	18	S						
																												N12E	43W	194	2	D	
51	354	13	R	13	20L					96	13	257	20	74.4	72.1	39.4	38.5	N52W	52S	191	48	R											
	354	13	R			328	7L			96	13	302	7	74.4	72.1	100	41.9						N10E	49W	301	47	R						
																												N58W	19N	55	19	N	
52	328	24	L	306	34L					302	24	324	34	88.2	27.9	97.7	8.2	N8E	81W	350	64	R											
																							N14E	47W	231	33	N						
																												N26W	62W	157	4	D	
53	254	28	L	272	4R					376	28	178	4	306.5	26.4	147.5	3.7	N58W	87N	241	51	R											
	254	28	L			242	43L			16	28	388	43	306.5	26.4	292	39.7						N22E	50E	172	33	D						
	254	28	L					303	36L	16	28	327	36	306.5	26.4	98	5											N8E	84W	1	48	R	
54	21	35	R	18	38R					69	35	72	38	303.7	71.6	291.9	73.1	N21E	16E	171	8	R											
	21	35	R			61	22R			69	35	29	22	303.7	71.6	318	35.2						N48E	55E	149	55	R						
																												N34W	25W	274	20	S	
55	44	15	R	43	12L					46	15	227	12	335.4	47	3.9	31.1	N88W	60S	245	38	R											
																							N58E	16S	157	16	N						
																												N40E	61S	69	41	D	
56	198	27	R	227	25L					252	27	43	25	36.4	30.4	320.1	48.3	N48E	41S	60	8	D											
	198	27	R			207	26R			252	27	243	26	36.4	30.4	27.4	28.3						N74W	62S	125	16	D						
	198	27	R					183	12L	252	27	267	12	36.4	30.4	50.6	47.9											N40W	42W	182	31	N	
57	67	13	R	84	14L					23	13	186	14	324.7	26.3	160.1	1.9	N70E	89N	254	66	R											
	67	13	R			64	9R			23	13	26	9	324.7	26.3	330.2	27						N60E	62S	67	13	S						
																												N78E	39S	115	25	S	
58	92	32	R	78	11L					358	32	192	11	295.8	13.8	340.5	4.7	N72E	85S	250	17	S											
	92	32	R			123	13L			358	32	147	13	295.8	13.8	140	34.9						N50E	56N	273	46	R						
																												N70E	40S	94	19	S	
59	275	14	R	268	18L					175	14	2	18	154.8	11.3	310.2	10.6	N40E	80E	210	40	R											
																							N85W	88S	96	21	N						
																												N58E	47N	45	16	D	
60	250	8	R	232	12R					200	8	218	12	342.3	12.9	357	24.7	N88E	65S	105	35	S											
	250	8	R			280	1R			200	8	170	1	342.3	12.9	140.8	9.1						N52E	81N	41	44	R						
																												N54E	72S	230	13	D	
61	314	14	L	344	25L					316	14	286	25	192.1	8	351.1	14	N82E	75S	248	81	R											XY
	314	14	L			304	5L			316	14	326	5	192.1	8	198.7	19.7						N72W	71N	311	48	N						
																												N88W	53N	34	49	N	
62	342	14	L	313	7L					288	14	317	7	347.4	3.4	190.5	14.9	N78W	76N	290	35	R											
	342	14	L			358	22R			288	14	92	22	347.4	3.4	135.2	19.9						N45E	70N	33	30	R						
																												N50E	81N	47	21	S	
63	328	10	L	348	8L					302	10	282	8	177.8	6.3	339.4	1	N68E	89S	250	23	R											
																							N77W	83S	109	39	N						
																												N88W	65N	336	63	N	
64	8	16	L	21	7L					262	16	249	7	326.3	17.8	310.1	16.5	N40E	74E	44	13	D											
	8	16	L			328	3R			262	16	122	3	326.3	17.8	172	18.1						N82E	71N	283	47	R						

Continued

																												N65E	86S	239	60	N
65	178	4	R	214	38R					272	4	236	38	328.7	2.5	318.6	48.9	N50E	42S	156	40	R										
																							N20E	63W	5	27	N					
																												N76W	75N	289	15	D
66	178	18	L	187	11L					92	18	83	11	137.5	16.5	133.5	6.1	N44E	84N	238	69	R										
	178	18	L			142	43L			92	18	128	43	137.5	16.5	149.9	54.7						N60E	36N	308	34	R					
																												N58E	73N	24	4	S
67	43	14	R	46	9L					47	14	224	9	280.6	7	286.9	29.4	N18E	61E	190	12	S										
	43	14	R			68	24R			47	14	22	24	280.6	7	255.1	4.1						N16W	85E	345	7	D					
	43	14	R					18	28R	47	14	72	28	280.6	7	115.7	15.7											N26E	55W	225	51	R
68	356	17	L	334	37L					274	17	296	37	337.1	12.7	5.1	20.3	N84W	70S	100	15	S										
	356	17	L			294	10L			274	17	336	10	337.1	12.7	210.2	17.4						N70W	72N	308	14	D					
																												N38E	69S	211	10	D
69	128	22	R	103	18R					322	22	347	18	200.2	2.3	222.4	11.3	N48W	78N	316	19	S										
	128	22	R			154	14R			322	22	296	14	200.2	2.3	174.3	0.2						N84E	89S	264	5	D					
																												N88W	73N	78	36	D
70	357	27	L	336	24L					273	27	294	24	341.7	21.7	357.2	9.6	N88E	80S	259	42	R										
	357	27	L			23	14L			273	27	247	14	341.7	21.7	311.9	23.5						N42E	67E	42	2	D					
																												N76E	51S	144	50	N
71	189	40	L	218	34L					81	40	52	34	115.7	29.8	97.2	13.2	N8E	77W	199	44	R										
	189	40	L			170	23L			81	40	100	23	115.7	29.8	141.4	24.7						N52E	66N	42	18	S					
																												N84W	80S	207	58	D
72	233	34	L	214	16L					37	34	56	16	85.3	8.8	287.9	1.7	N18E	89E	18	26	R										
																							N10W	58W	281	57	N					
																												N24W	81E	149	42	N
73	290	9	R	316	19L					160	9	314	19	210	36.8	192.1	2.7	N78W	87N	286	65	R										
	290	9	R			281	12L			160	9	349	12	210	36.8	223.7	17.5						N45W	72N	107	55	R					
																												N17W	61E	153	20	S
74	248	2	R	234	14R					202	2	216	14	260.5	29.6	280.6	37	N12E	53E	27	20	S										
	248	2	R			282	4R			202	2	168	4	260.5	29.6	220.6	33.3						N48W	56N	314	4	D					
																												N3W	85W	197	75	N
75	238	22	L	208	28L					32	22	62	28	264.5	3.9	107.7	11.5	N18E	79W	205	31	R										
	238	22	L			253	8R			32	22	197	8	264.5	3.9	256.1	36.4						N14W	53W	102	52	N					
																												N32W	71W	314	39	N
76	220	18	L	188	40L					50	18	82	40	281.8	2.2	116.4	30.2	N25E	60W	255	53	R										
	220	18	L			247	47L			50	18	23	47	281.8	2.2	71.3	18.6						N19W	72W	330	30	R					
																												N45E	76W	230	19	D
77	324	14	R	327	30L					126	14	303	30	170.4	29.6	7.2	11.4	N74W	79S	126	67	R										
	324	14	R			0	14R			126	14	90	14	170.4	29.6	137.9	12.1						N48E	77N	236	33	D					
																												N54W	32N	326	12	N
78	30	25	R	332	18R					60	25	118	18	107.4	8	160.5	29.4	N72E	60N	257	11	S										
	30	25	R			280	10R			60	25	170	10	107.4	8	222.2	39.4						N48W	50N	118	16	S					
																												N38W	60W	318	10	D
79	240	17	R	268	9R					210	17	182	9	274.9	41.9	237.5	39	N32W	51E	340	15	D										
80	240	17	R			226	24R			210	17	224	24	274.9	41.9	295	42.9						N26E	48E	201	3	S					
																												N38E	31E	61	14	S
81	312	36	R	342	24R					318	36	108	24	21.4	12	147.7	29.6	N60E	61N	43	27	R										
	312	36	R			288	9R			318	36	162	9	21.4	12	212.5	37.2						N56W	52N	10	51	R					
																												N8W	77W	356	19	D
82	168	38	R	178	14R					282	38	272	14	355.3	26.8	333.8	11.1	N64E	78S	74	41	D										
																							N73W	76S	276	38	S					
																												N85E	40S	180	39	N
83	224	0	L	217	14L					46	0	53	14	285.1	20.3	286	4.7	N16E	86E	129	86	R										
	224	0	L			198	7L			46	0	72	7	285.1	20.3	305.9	2.7						N37E	87E	215	42	S					
																												N30E	61E	42	23	S
84	237	25	L	217	24L					33	25	53	24	264.6	0.8	102	4.4	N12E	85W	193	15	R										
																							N10W	72E	125	65	N					
																												N16W	76W	326	52	N
85	292	22	L	273	16L					338	22	357	16	214.6	6.1	232	14	N36W	76N	328	25	D										
	292	22	L			314	8R			338	22	136	8	214.6	6.1	183.5	28.5						N85W	62N	77	27	D					
																												N70W	74N	100	32	D
86	355	18	L	2	5R					275	18	88	5	338.4	13.1	140.8	3.3	N52E	87N	48	44	S										
	355	18	L			322	16L			275	18	308	16	338.4	13.1	185.6	3.3						N84W	86N	277	31	R					
																												N8E	84W	269	27	S
87	3	32	R	4	20R					87	32	86	20	125.3	25.9	131.3	15.3	N41E	74N	17	58	R										
																							N43E	54W	263	43	S	N24E	66W	202	2	D
88	168	20	R	179	1R					282	20	271	1	345.3	11.4	326.4	0.4	N56E	90S	236	12	S										
																							N3E	87W	274	34	N					
																												N77E	57S	164	57	N
89	160	31	L	194	25L					110	31	76	25	144.7	36.3	120.5	14.9	N30E	75W	226	48	R										
																							N62W	73N	108	31	S					
																												N50E	22S	159	9	N
90	194	18	R	222	11L					256	18	48	11	322.2	22.5	282.7	9.4	N13E	81E	18	26	D										
																							N78E	81N	268	51	N					
																												N75E	31S	125	25	N
91	138	12	L	118	14R					132	12	332	14	177.5	30.5	207.2	12.6	N63W	78N	107	39	S										
	138	12	L			164	20R			132	12	286	20	177.5	30.5	348.6	9.6						N79E	81S	225	74	R					
																												N1E	27E	2	28	N